



**HAL**  
open science

# Unveiling microbial communities along the polyextreme physicochemical gradients of Dallol and its surroundings (Danakil depression, Afar region, Ethiopia)

Jodie Belilla

► **To cite this version:**

Jodie Belilla. Unveiling microbial communities along the polyextreme physicochemical gradients of Dallol and its surroundings (Danakil depression, Afar region, Ethiopia). Ecosystems. Université Paris-Saclay, 2020. English. NNT : 2020UPASL043 . tel-03121160

**HAL Id: tel-03121160**

**<https://theses.hal.science/tel-03121160>**

Submitted on 9 Feb 2021

**HAL** is a multi-disciplinary open access archive for the deposit and dissemination of scientific research documents, whether they are published or not. The documents may come from teaching and research institutions in France or abroad, or from public or private research centers.

L'archive ouverte pluridisciplinaire **HAL**, est destinée au dépôt et à la diffusion de documents scientifiques de niveau recherche, publiés ou non, émanant des établissements d'enseignement et de recherche français ou étrangers, des laboratoires publics ou privés.

Unveiling microbial communities along the  
polyextreme physicochemical gradients of  
Dallol and its surroundings (Danakil  
depression, Afar region, Ethiopia)

**Thèse de doctorat de l'université Paris-Saclay**

École doctorale n°577 Structure et Dynamique des Systèmes Vivants (SDSV)  
Spécialité de doctorat : Sciences de la vie et de la santé  
Unité de recherche : Université Paris-Saclay, CNRS, AgroParisTech, Ecologie  
Systématique et Evolution (UMR 8079), 91405, Orsay, France  
Référent : Faculté des sciences d'Orsay

**Thèse présentée et soutenue en visioconférence totale,  
le 24/11/2020, par**

**Jodie BELILLA**

**Composition du Jury**

<b>Tamara BASTA-LE BERRE</b> Maître de conférences, Institut de Biologie Intégrative de la Cellule (I2BC), Université Paris-Saclay	Rapportrice
<b>Philippe OGER</b> Directeur de recherche, Microbiologie, Adaptation et Pathogénie (UMR 5240) Lyon 1, INSA Lyon	Rapporteur
<b>Bénédicte MENEZ</b> Professeur, Institut de Physique du Globe de Paris	Présidente
<b>François GUYOT</b> Professeur, Institut de minéralogie, de physique des matériaux et de cosmochimie (UMR 7590) UPMC/CNRS/IRD/MNHN	Rapporteur
<b>Purificación LOPEZ-GARCIA</b> Directrice de recherche, CNRS, Université Paris-Saclay Ecologie Systématique et Evolution (UMR 8079)	Directrice de thèse
<b>David MOREIRA</b> Directeur de recherche, CNRS, Université Paris-Saclay Ecologie Systématique et Evolution (UMR 8079)	Co-Directeur de thèse



## Remerciements

Bien qu'une thèse mette en valeur le nom de son auteur, elle est en réalité le fruit de la collaboration de nombreux chercheurs, ingénieurs et techniciens. Elle n'est portée à son terme que par le soutien indéfectible des proches. Leur dédier des remerciements n'est donc que justice. Les mots que je leur dédie ne sont qu'un pâle reflet de ma gratitude et de ce que je leur dois.

Je remercie en premier lieu mes maîtres de thèse, **Purificación López-García** et **David Moreira**, de m'avoir choisie parmi d'autres candidats au cours d'une rude concurrence et d'avoir placé leur confiance en moi pour porter ce projet. Vous m'avez permis de vivre l'expérience incroyable de deux missions d'échantillonnage dans le site le plus multi-extrême du monde en Ethiopie, ce qui restera pour toujours une des expériences les plus extraordinaires de ma vie. Grâce aux moyens que vous avez mis à disposition sur ce projet, j'ai eu la possibilité de travailler sur de très nombreuses expériences pluridisciplinaires en laboratoire, impliquant des technologies de pointes et des spécialistes de tous horizons, ce qui a été extrêmement enrichissant et nous a permis de porter au plus loin nos connaissances sur Dallol. Vous m'avez également offert de nombreuses opportunités de conférences nationales et internationales afin de communiquer mes résultats, ce qui j'en ai conscience est une grande chance en tant que thésarde. J'ai beaucoup appris au sein de votre équipe, autant scientifiquement parlant que sur le monde de la recherche.

Je ne remercierai jamais assez les membres des missions en Ethiopie que j'ai côtoyé : **Olivier Grunewald** et **Jacques Barthélemy**, pour leur travail dantesque qui a rendu possible les expéditions (avec l'aide de **Luigi Cantamessa**), leur guidance et leur aide précieuse sur place ; **Bernadette Gilbertas**, pour ses coups de main à l'échantillonnage, son beau travail de communication autour de Dallol qui accompagne les clichés et enregistrements d'Olivier (mention spéciale pour m'avoir secourue des sables mouvants !). Vous trois avez également gardé un œil bienveillant sur l'évolution de ma thèse tout au long de ces quatre années, ce qui est très touchant pour moi. Gracias a **José María López-García** por prestarme sus pantalones en el campo cuando el mío se rompió. Tu trabajo con nosotros como geólogo fue muy valiosa. Me animaste mucho durante mi tesis. No olvidaré tu amabilidad. Le Professeur et collaborateur **Ludwig Jardillier** et son humour aussi appréciable que la bière dans le désert du Danakil (c'est-à-dire avec modération), son ardeur à la tâche sur place (notamment pour transporter le matériel très lourd malgré la chaleur), et son aide avec les expériences au cytomètre en flux. **Karim Benzerara**, co-auteur également de mes travaux et tuteur de thèse, dont l'expertise à l'interface entre la géologie et la biologie a été importante aussi bien sur le terrain que pour les analyses au MEB qui ont suivies. Je remercie également les partis financeurs des missions, qui incluent entre autres le CNRS, la fondation Iris et le mécénat de particuliers.

J'éprouve une profonde gratitude pour les autorités Ethiopiennes et notamment les Afars, qui nous ont autorisé à venir travailler sur leur territoire et nous ont prodigué leur aide et leur protection sur place. Je suis attristée de savoir le pays aux prises d'une guerre civile en ce moment, et je ne peux qu'espérer que la paix reviendra et que les gens que nous avons connus seront épargnés du danger.

Je suis également reconnaissante envers les membres de mon comité de thèse pour leur temps et leur attention aux comités annuels. Ceux-ci incluent : **Karim Benzerara** (cité plus haut) ; **Yvan Zivanovic**, pour son regard critique notamment sur la partie bioinformatique ; **Adrienne Kish**, pour son expertise sur les halophiles et qui nous a également permis d'utiliser la sonde d'activité de l'eau en possession de son laboratoire, avec l'aide de son étudiant **Charly Favreau** – une des seules expériences de ma thèse à s'être déroulée parfaitement du 1<sup>er</sup> coup. Les comités ont parfois accueilli des invités importants pour solliciter leur retours, tels que **Ludwig Jardillier** (cité plus haut) et **Ana Gutteriez** (cité plus bas).

Je n'oublie pas les membres du jury de ma thèse, qui m'ont gratifiée de leurs retours, leurs remarques et leurs félicitations très chaleureuses sur ce rapport et l'oral qui ont suivi : **Bénédicte Menez** (dont j'avais déjà de très bons souvenirs en tant qu'enseignante en master), **Tamara Basta-Le Berre**, **François Guyot** et **Philippe Oger**. Je n'aurais pas pu rêver meilleur jury que celui-ci, et j'ai beaucoup appris de la longue discussion que nous avons eue pendant les questions de ma soutenance.

Qu'aurait été la thèse sans les irremplaçables DEEMons ?

Je dois tout ce que j'ai de meilleur au laboratoire à **Paola Bertolino**. Tu as été une excellente formatrice, une collaboratrice irremplaçable mais surtout un pilier moral et une amie précieuse tout au long de cette thèse. Je pourrais même ajouter que tu as été une présence maternelle au laboratoire, et probablement pas seulement pour moi. Je serai à jamais impressionnée par ta force de travail, ton courage et tes valeurs. Tu es pour moi le pivot central de l'équipe et un modèle à suivre. Je garde un excellent souvenir de nos pauses café et des coups que l'on a bus ensemble. Je te souhaite le meilleur pour la suite et j'espère que l'on se reverra souvent, dans le Sud ou à Paris.

Devant un terminal Ubuntu, je dois tout ce que je suis à **Guillaume Reboul**. Aucun de mes articles n'aurait pu voir le jour sans tes secours et tes lumières en bioinformatique, et je sais que je ne suis pas la seule. Je suis heureuse d'avoir pu travailler, collaborer et passer du temps avec toi (notamment nos supers voyages), j'en garderai un très bon souvenir. J'espère qu'on pourra bientôt trinquer à notre parcours, notre amitié et nos diplômes de docteurs bien mérités.

Le bureau 208 a été comme un second foyer, ne serait-ce que par le temps que j'y passais avant que la rédaction ne démarre, mais également parce que l'ambiance y était du tonnerre. Outre Guillaume, c'est donc à ses autres hôtes que je dois tous les bons moments que j'y ai vécu : El gran bromista **Luis Galindo**, a quien debo mis mayores risas. Gracias por tu

constante estímulo durante la tesis. I really will keep precious memories of all your jokes and cheering. La très sainte, douce et omnisciente **Gwendoline David** (puisses-tu nous guider même après la thèse), qui m'a consolée de nombreuses fois lors de mes déboires de thèse... J'espère que tu garderas un bon souvenir de nous malgré le bordel qu'on faisait dans le bureau ! El único postdoctorado que trabajaba en esta oficina antes de ser expulsado por la nueva generación, **Guifré Toledo**. Gracias también por todos los buenos momentos de la tesis, ¡nos vemos pronto en Barcelona! (sorry I couldn't write that in catalan). My excellent friend **Fabian van Beveren**, who also always lent a hand when I was struggling in front of my computer and always found some time to cheer me up in harsh times. I really liked that we spent a lot of time outside work together too ! Also thanks for being my first thesis reviewer. Le très serviable amateur de blagues **Thomas Bacchetta**, à qui on doit avec Luis une grande personnalisation du bureau. Tu as fait un boulot incroyable sur les vidéos, merci infiniment pour ça. J'avoue que tes expériences de « gastronomie » américaine que ne manqueront pas trop, par contre. **Rafael Ponce**, por el tiempo que pasamos juntos en la oficina y las grandes veladas que tuvimos con su amigo Charles. A noter que j'ai beaucoup passé de temps sur les thèses de Rafael et d'**Aurélien Saghāï** avant d'écrire la mienne, vous avez été d'excellent modèles, merci !

En dehors du bureau, il y a évidemment : **Ana Gutteriez**, que es una gran amiga. Me apoyaste mucho y con quien pasé grandes momentos contigo fuera del trabajo (¡gracias de nuevo por descubrir la gastronomía mexicana !). Send loves to **Mikel**, **Sandra** and the cats for me. **Naoji Yubuki**, with whom I spent some lunches and microscope time, and is always doing great job as an actor in our lab videos. **Miguel Iniesto**, un hombre con muchas cualidades humanas, siempre atento a los demás. ¡Tengo grandes recuerdos de Leipzig contigo y los demás! ¡**Jazmin Blaz**, con quien espero algún día volver a las catacumbas! **Feriel Boudarka** and **Brittany Backer**, who at a time shared the flat I was supposed to live in (but was actually not, writing my thesis where the sun is). I really enjoyed the dinners I spent with you and the other flatmates. Mulțumesc **Maria Ciobanu**, toujours amicale et prête à aider même dans les temps difficiles malgré la charge que tu as parfois sur les épaules. Fais attention à ne pas te surmener ! Et évidemment tous les autres membres de l'équipe DEEM : **Laura Eme**, **Philippe** et **Hélène Deschamps**, **Julien Massoni**, pour les bons moments partagés. Je souhaite également honorer les stagiaires qui ont travaillé sur Dallol à mes côtés, à savoir **Corentin Gille**, **Etienne Jeanne**, **Jonathan Huc** et **Ulysse Turquoi**. Ils ont goûté avec moi au sel de Dallol et ont tenu bon (bien joué !), nous avons beaucoup appris tous ensemble. J'ai vraiment beaucoup apprécié de bosser à vos côtés et j'espère garder le contact avec vous. Une petite dédicace également à **Jeanne Chaumont** (avec qui on a passé de supers moments hors du laboratoire) et à **David Boulesteix** qui ont bossé sur des échantillons du Danakil pendant leur stage au laboratoire.

Hors de l'équipe DEEM, je suis redevable également à beaucoup de personnes de l'ESE et de la faculté, que je ne pourrai pas tous citer. Mais voici ceux que j'ai le plus souvent sollicité : **Jane Lecomte**, en sa qualité de directrice de l'ESE qui fait son maximum pour

chapeauter tout le monde et à qui j'ai demandé la signature une bonne centaine de fois ; **Nathalie Leucat** et **Emmanuelle Jestin**, si gentilles et sans qui je ne serai jamais arrivée au bout du labyrinthe administratif relatif au laboratoire ; **Perla Farhat**, avec qui j'ai passé de bons moments à l'ESE et qui m'a également aidée à une répétition de thèse. I wish the best for you and your people in your homeland... **Seïf-Eddine Naâdja**, à qui je souhaite le plus grand courage pour accomplir ce qu'il souhaite. Tu sais que tu peux compter sur moi, et sur beaucoup d'autres personnes, pour t'aider comme on peut dans les épreuves que tu rencontres. **Jacqui Shykoff** pour ses bons conseils sur la rédaction d'articles. **Thimothée Fouqueray** et **Julie Lombard Latune** qui, avec **Gwendoline** et moi, ont été délégués des non-permanents et avec qui nous avons organisé beaucoup d'événements festifs, ainsi qu'aux bénévoles qui ont gravité autour de nous.

Je vous souhaite à tous beaucoup de succès et de bonheur quoi que vous entrepreniez et j'espère que l'on gardera contact et se recroisera, dans ce microcosme qu'est le monde de la recherche, et même (surtout) en dehors !

Au niveau de l'Ecole doctorale SDSV, qui a accordé la bourse de mes trois premières années de thèse, je dois beaucoup à **Pierre Capy** et **Jean-Luc Pernodet** pour leur suivi et à **Sandrine Le Bihan** pour sa réactivité face à tous les casse-têtes administratifs que je lui ai présenté.

Pour la publication de cette thèse, je remercie la reprographie de l'université et la bibliothèque universitaire, notamment **Stéphane Benais**, avec qui j'ai eu le plaisir de faire des cours d'aïkido sous l'enseignement de l'excellent sensei **Didier Michel**.

Ma famille a toujours été et restera à jamais le socle de ma vie. En rendre fiers les membres a été ma plus grande source de persévérance pour parvenir au bout de la thèse. Ils sont beaucoup trop nombreux pour que je les cite tous, je vais nommer ceux que j'ai le plus fréquenté durant ces années de thèse. Je tiens à remercier en tout premier lieu ma mère **Elodie Nguyen**, qui sont en quelque sorte l'auteure de l'auteure, par son rôle de mère. Ma mère m'a toujours poussé à donner le meilleur de moi-même et m'en a surtout toujours donné les moyens. Sans son appui (moral, psychologique, matériel), aucune épreuve de la vie, y compris cette thèse, n'aurait pu être surmontées. Je remercie également mon père **Laurent Belilla**, sa compagne **Rosy** et sa fille **Johanna Auguste** pour les bons moments passés ensemble et leur aide continue au cours de mes études et durant trois premières années de ma thèse. Ma grand-mère **Christiane Belilla**, un modèle sur bien d'aspects, la plus grande géologue et botaniste naturaliste que je connaisse, dont la bonne humeur éclaire toujours les plus sombres journées. Merci à mes cousines : **Melody Sarraf**, qui a toujours été comme une grande sœur complice pour moi et qui vit beaucoup trop loin de moi (reviens !!!) et qui a suivi toutes les étapes de la répétition et de la soutenance ; **Phetmany Kouravongsa**, alias Boubou, notre plus grande cousine, un modèle de dynamisme et de réussite avec qui j'ai passé des supers moments (notamment gustatifs) à Paris et Grenoble depuis des années et qui a suivi les questions de la thèse avec ma mère ; **Thi-Léa Vo**, ma petite cousine/soeur protégée qui

grandit trop vite et inverse un peu trop souvent les rôles, hum... Toi aussi reviens nous voir un peu d'ailleurs ! Au niveau des oncles et tantes, je dois beaucoup à Tonton Hoang (**Hoang Vo**) et Tata La (**Thi-Khamla Nguyen**), qui m'ont toujours considérée comme leur fille m'offrent généreusement le gîte et le couvert (krao niao) quand je passe dans le coin (merci **Thi-Alyssa Vo** de me laisser ta chambre chaque fois, courage pour tes études), tout en essayant de me glisser des enveloppes avec des billets dans mes affaires parce qu'ils ont peur que je manque de quelque chose... merci ! Je pense aussi très fort à Tonton Dith (**Dith Kouravongsa**) et Tata Phet (**Phet Nguyen**) qui me font toujours des petits plats (phô et laab) quand ils savent que je passe à Grenoble, et **Anthony Kouravongsa** qui me fait toujours autant rire et m'introduit à de supers séries et jeux vidéo. Je remercie également Bâ (**Nicole Nguyen**), ma grand-mère maternelle, qui est toujours au petit soin pour me donner des bánh tét ou du chèo bong maison parce qu'elle sait que j'adore ça.

Je n'oublie pas le reste de mes cousins maternels (qui sont plus d'une vingtaine et tous aussi géniaux les uns que les autres) et paternels (mes six petits cousins d'amour que j'aimerais voir plus souvent), mes oncles et tantes encore plus nombreux des deux côtés, mais qui sont trop nombreux pour être listés. J'ai partagé avec eux de nombreuses fêtes durant ces quatre ans de thèse, dont des mariages, de très nombreux repas et soirées endiablées de karaoké, jeux de société et vidéo, films et séries... Ce sont des moments précieux qui m'ont accompagnée et je vous en remercie. Nombreux sont ceux qui se sont dégagés du temps pour les répétitions de thèse (notamment **Amaury Sarraf**), la soutenance de thèse elle-même (notamment **Maëlys Belilla** et **Kim Siratanakoun**), ou bien qui ont regardé la rediffusion. Je suis vraiment heureuse de faire partie de votre famille et je vous remercie pour ce cadeau de tous les jours qui m'a portée dans tous les obstacles de la thèse.

Je souhaite rendre hommage à ceux qui sont partis au cours de ma thèse et qui malheureusement ne verront jamais l'aboutissement de mon travail. Mon grand-père **Gérard Belilla**, qui bien qu'il soit parti de la plus belle façon qu'on pouvait lui souhaiter, c'est-à-dire dans son lit, nous manque beaucoup. Il occupait une place immense à Crémal et dans nos cœurs, et il a laissé un grand vide derrière lui. Mon arrière-grand-père **Jean Sintés**, qui nous a quitté à 102 ans, et qui j'espère m'a transmis quelques-uns de ses gènes ou secrets pour vieillir en bonne santé comme lui. Plus récemment nous a également quitté **Nicole Filippi**, qui était comme ma troisième grand-mère, et avec qui j'aurais aimé fêter la fin de ma thèse (avec toute la famille chtis). Et puis **Isis**, mon amie féline à quatre pattes, qui aura occupé une place dans ma vie du collègue jusqu'à la thèse sans arriver au bout.

Mes amis sont les gardiens de ma santé mentale, les côtoyer m'insuffle de la joie et m'inspire au quotidien. J'ai la chance de les voir si nombreux, d'avoir parfois vécu ou grandi avec eux. Tous les citer, ainsi que leurs exploits ces quatre dernières années, serait impossible.

Je dois tout d'abord parler de mes colocataires, qui ont partagé tant de temps avec moi pendant la thèse, les pires coups durs comme les meilleurs moments de ma vie : **Sophie Jeantet**, tu es clairement la meilleure amie que j'ai jamais eue (dix ans d'amitié, ça ne rajeunit pas). Passer une heure avec toi suffit à recharger toutes les batteries, tellement tu me fais rire.

On est en phase sur beaucoup de choses (la politique, nos goûts...) et ça rend toujours nos conversations intéressantes. Reste comme tu es, tu es parfaite ! **Edwin Nagera**, tu es comme un frère pour moi, et tu es aussi un de mes plus vieux amis (quinze ans d'amitié, c'est dire !). Comme le vin, notre amitié se bonifie avec le temps. On apprend beaucoup et évolue ensemble, j'aime vraiment ça. **Gauthier Arnould**, notre avocat du diable, avec qui on a passé de supers moments en soirée pendant trois années, merci pour les supers souvenirs (fais attention à ne pas te laisser trop bouffer par le travail et donne nous plus de nouvelles !). Vous avez tous fait de notre appartement un foyer où j'ai pu apprécier de vivre et m'amuser, même dans les moments les plus sombres. En coloc, quoi que temporaire, il y a également **Camille Paulet** avec qui j'ai lié d'amitié et qui est toujours disponible pour sortir ou pour papoter, de sujets mondains ou très importants. Je remercie évidemment tous les autres colocs qui ont vécu à Bobillot pour les bons moments que nous y avons tous passé. Cette adresse était vraiment un havre de bonne humeur où je pouvais me ressourcer. Une petite dédicace également à notre voisin **Charles Gatine**, à qui je souhaite le meilleur dans sa vie personnelle et professionnelle, et notamment d'atteindre ses objectifs de développement personnel recherchés.

Hors de la colocation, c'est à mes anciens camarades de master de géoscience **Alexandra Morand** et **Julien Reynes** que je dois le plus. Une fois sa thèse terminée, **Alexandra** a dédié un temps important à me prodiguer des conseils pour terminer la mienne dans les meilleures conditions et m'a également filé un coup de main dans ma lutte contre Word. Et c'est sans compter, bien sûr, les excellents moments de folie partagés ensemble tout au long de ces quatre années. **Julien**, en plus d'être mon Kta-mestre, m'a aussi beaucoup soutenu au long de la thèse et m'a prodigué une aide précieuse pour la préparation de l'oral (aide que j'espère lui avoir rendu convenablement !). En soutien moral, je dois beaucoup **Noé Doquet**, qui possède un fond illimité de gentillesse et de dévotion pour ses amis dont j'ai le plaisir de faire partie (vivement qu'on se revoit et qu'on boive de ton super champagne !), mais aussi **Loris Martin** qui a beaucoup communiqué avec moi pendant les temps difficiles (et a suivi la soutenance de A à Z, merci !). Tous deux font partis de mes plus vieux amis avec **Martin Conreau** (que j'espère revoir également un de ces jours) et **Edwin Nagera**.

Je remercie également nos voisins de la Tour d'Aigues et amis **Eric Bergogne** et **Alice Cochin**, qui m'ont supportée pendant la rédaction et la préparation de l'oral et m'ont permis de souffler régulièrement au travers de goûters et de jeux (merci pour les recharges de gâteaux et de thé !). Une petite dédicace d'ailleurs pour tous nos proches (amis, famille) du Vaucluse avec qui on a partagé tant de supers moments.

Beaucoup d'autres amis avec qui j'ai échangé pendant ces quatre années de thèse pourraient être cités : mes anciens camarades de faculté ou du lycée (voire collègue) pour nos soirées ensemble, nos échanges ou bien vos félicitations touchantes pour le parcours effectué, mes anciens maîtres de sport ou arts martiaux (mention spéciale à **Cyril Edou**, dont l'aide pour la préparation de l'oral et les retours sur ma thèse m'ont beaucoup touchée), mes amis du 13<sup>ème</sup> arrondissement qui m'ont introduite à Paris quand j'ai fraîchement débarqué... ce serait impossible de tous les lister, mais je ne vous ai pas oublié et je vous dis à tous merci !

J'espère passer plus de temps avec vous tous dès que ce sera possible !

J'ai gardé le meilleur pour la fin, puisque je dédie mes derniers mots de remerciements à **Georis Billo**, avec qui je fête en plus de mes quatre années de thèse, dix ans d'amitié dont deux ans d'amour. Le destin a été capricieux avec nous ces dernières années, mais nos efforts communs nous ont permis de nous en sortir plus forts et soudés. Il va sans dire que ta présence, ton soutien et ton aide (notamment pendant la rédaction et la préparation de l'oral) ont été décisifs dans ma réussite personnelle et professionnelle. J'espère que nous fêterons encore de nombreux anniversaires et accomplissements ensemble, et que notre futur sera lui aussi sous le signe de la créativité.





*Sunset view from the Dallol dome © DEEM Team*

## SUMMARY

1. Introduction.....	1
1.1 The journey of discovery of microorganisms and invisible (poly)extremophiles .....	1
1.1.1 From the antique times to the first microscope .....	2
1.1.2 Classifying microorganisms: the first attempts.....	3
1.1.3 Classifying the microorganisms: the birth of molecular biology and the discovery of Archaea .....	5
1.1.4 Screening microbial diversity today .....	8
1.2 Life in extreme environments: implications and limits.....	9
1.2.1 The extremophiles' diversity .....	9
1.2.2 Benefits and perspectives of studying extremophiles .....	11
1.2.3 The unknown limits of (poly)extremophiles .....	14
1.3 The Dallol hydrothermal system and its surroundings: a panel of unique physicochemical gradients on Earth .....	15
1.3.1 Geographical and geological context .....	15
1.3.2 The pH-salinity-temperature gradients of the Dallol dome area .....	19
1.3.2.1 The Dallol dome .....	19
1.3.2.2 Lake Gaet'ale or Yellow Lake.....	22
1.3.2.3 The Black Mountain and the Black Lake .....	23
1.3.2.4 The salt plain .....	23
1.2.3.5 The salt canyons and the cave reservoir .....	24
1.3.2.6 Lake Karum/Assale .....	24
1.2.3.7 The Western Canyons Lakes .....	25
1.2.3.8 Dallol and its surroundings' systems: a resource to explore the limits of life. 26	
2. Objectives.....	35
3. Materials and Methods .....	37
3.1 Chemistry analyses.....	37
3.1.1 Elemental and molecular composition of samples .....	37
3.1.2 Measure and calculation of water activity, chaotropicity and ionic strength .....	39
3.1.2.1 Water activity (aw) .....	39

3.1.2.2 Chaotropicity .....	39
3.1.2.3 Ionic strength .....	41
3.2 From DNA extraction to phylogenetic tree .....	42
3.2.1 DNA purification and 16/18S rRNA gene metabarcoding.....	42
3.2.2 Statistical analyses.....	46
3.2.2.1 Richness (Chao1) .....	46
3.2.2.2 Diversity (Simpson).....	46
3.2.2.3 Evenness.....	46
3.3 Culture approach.....	47
3.4 Microscope observations .....	48
3.4.1 Optical microscope.....	48
3.4.2 Confocal microscope .....	48
3.4.3 Scanning Electronic Microscopy.....	50
3.5 Multiparametric analyses and fluorescent-assisted cell sorting on the cytometer .....	51
4. Unveiling microbial communities of the polyextreme gradients of the Dallol ecosystems	55
4.1 Context and objectives .....	55
4.2 Results .....	56
4.3 Manuscript of article 1 .....	57
5. Detection of (local) biocontamination and biomorphs: how to identify false positives .....	80
5.1 Context and objectives.....	80
5.2 Results .....	81
5.3 Manuscript of article .....	82
5.3.1 Introduction.....	83
5.3.2 Materials and Methods .....	85
5.3.2.1 Sample collection .....	86
5.3.2.2 DNA purification and 16/18S rRNA gene metabarcoding.....	86
5.3.2.3 Electron and epifluorescence microscopy and fluorescence in situ hybridization .....	86
5.3.2.4 DNA degradation tests with Dallol's brine .....	87
5.3.3 Results .....	88
5.3.3.1 The Dallol aerosols are dominated by widespread bacteria but halophile microorganisms likely originating from the surrounding less polyextreme environments are detected.....	88

5.3.3.2 The FISH experiment confirmed an absence of cells in the Dallol dome brine, and in the salt plain sample a potential parasitic association of Halobacteria/Nanohaloarchaeota was discovered.....	91
5.3.3.3 DNA is degraded almost instantly and completely in Dallol's brine.....	93
5.3.4 Discussion.....	95
5.4 Supplementaries .....	101
6. The missing link of the Dallol ecosystems: the Western Canyons Lakes – a permanent, mildly acidic and hypersaline series of ponds .....	105
6.1 Context and objectives.....	105
6.2 Results .....	106
6.3 Manuscript of article .....	108
6.3.1 Introduction.....	108
6.3.2 Results and Discussion .....	112
6.3.3 Materials and methods .....	117
6.3.3.1 Sample collection and in-situ physicochemical parameters measures .....	117
6.3.3.2 Chemical analyses, water activity and salinity estimations.....	119
6.3.3.3 DNA purification and 16S/18S rRNA gene amplification, sequencing and analysis .....	119
6.3.3.4 Scanning electron microscopy (SEM) and elemental mapping .....	119
6.3.4 Supplementaries .....	122
7. Discussion .....	126
7.1 The microbial communities in hypersaline, mildly acidic environments are dominated by a surprisingly wide diversity of Archaea. The closer the physicochemical conditions of an environment are to the limits of life, the higher the proportion of Archaea (especially Nanohaloarchaeota) among prokaryotes. ....	127
7.2 Two physicochemical barriers are limiting for life in the presence of water in the Dallol area: the combination of hyperacidity and hypersalinity (and possibly some sterilizing chemical compounds) and the chaotropicity/water activity/ionic strength values.....	130
7.3 The absence of life in the Dallol dome hydrothermal ponds, the Black Lake and Lake Gaet'ale makes them especially sensitive to biocontamination, though their physicochemical properties may get rid of most of it. ....	132
7.4 Implications of our work in other research fields such as astrobiology and the study of the origin and evolution of life.....	134
8. Conclusion .....	138
Résumé en français .....	139



*The Black Mountain area, view  
from helicopter © DEEM Team*

**INTRODUCTION**

## 1. Introduction

This introduction sets the historical background of the discovery of microorganisms and extremophiles, followed by an up-to-date presentation of (poly)extremophiles. I will explain how their study allows us to better understand the origin and evolution of life on Earth and guide the search of life beyond Earth. The physicochemical conditions near the limits of life will be introduced, together with the microorganisms able to thrive near these limits. The uncertainties remaining about the habitability of some environments will be highlighted and, in the last part of the introduction, I will explain why the Dallol geothermal environments are ideal to investigate potentially new polyextremophiles and explore the unknown limits of life.

### 1.1 The journey of discovery of microorganisms and invisible (poly)extremophiles

Although microorganisms are the smallest forms of life, collectively they constitute the second most important biomass source on Earth behind plants (prokaryotes and protists count together as 15% of the total biomass while plants count as 83% of the total biomass) and their place is probably largely underestimated since endosymbionts and endoparasites are not taken into account in these percentages (Bar-On, Phillips, and Milo 2018). In the absence of microorganisms, multicellular organisms would not have emerged (P. López-García, Eme, and Moreira 2017), and our world would be drastically different, as free oxygen in the atmosphere was first produced by microorganisms (Holland 2002; Guo et al. 2009). Moreover, plants and animals are intimately dependent on microbial activities for recycling key nutrients and degrading organic matter (Bosch and McFall-Ngai 2011; Hassani et al. 2019). Despite their vital role in ecosystems since their appearance on Earth 3.8 or 3.5 billion years ago (Brasier et al. 2002; Whitehouse, Myers, and Fedo 2009), their discovery was late and strewn with obstacles.

The reason for this late discovery lays behind the fact that our understanding of the complexity of nature is limited by what we can perceive with our own senses or the help of technology. It also depends on the accumulated knowledge we possess to interpret findings. Microorganisms being, as their name calls, creatures of microscopic size, our visual acuity is barely sufficient to perceive them (under ideal conditions, the human eye has a spatial resolution of 70  $\mu\text{m}$  at 25 cm distance (Verhoeven 2018)). Although microorganisms have shaped (and still shape) the world as it is today, without the proper tools to observe them they remain invisible to us. This explains why their existence could not be ascertained for a long time.

### 1.1.1 From the antique times to the first microscope

Before we acknowledged the existence of microorganisms, the presence of creatures too small to be seen with the naked eye had been suspected for centuries. The Jain cosmology (which was born in ~V<sup>th</sup> century BC in what is now India which still has worshippers) recognized four main forms of existence: gods, humans, hellish beings, and plants and animals together. The category of animals and plants were subdivided into smaller categories based on their sense-faculties. The lowest of these were the *nigodas*, infinitesimally small organisms, so tiny and undifferentiated they even lacked individual bodies. They were thought to live in clusters, have very short lives and only possess the sense of touch. The *nigodas* were supposed to be all over the place and to inhabit the bodies of plants, animals and people. Jains are willing not to injure living beings and for this purpose, sweet and fermented substances are supposedly forbidden because it is believed that *nigodas* were especially found in them (Singh 2008). Jains would also not kill an animal to eat it. Even if an animal had died a natural death, the dead flesh was considered as breeding for the *nigodas* and was not supposed to be eaten (Jaini 1998). Others ancient cultures developed practices based around microbes long before microbial cells were visualized using a microscope. Circa 400 B.C., the Greek physician Hippocrates wrote about diseases caused by “unwholesome” (e.g. stagnant) waters in comparison with “wholesome” (e.g. streaming) waters (Hippocrates n.d.). Centuries later, the Roman scholar Marcus Terentius Varro (116–27 BC) was among the first people to explicitly write about microscopic creatures in the air. In his books on agriculture, he wrote, talking about where estates shall be built:

*“Note also if there be any swampy ground [...] certain minute animals, invisible to the eye, breed there and, borne by the air, reach inside of the body by the way of the mouth and nose, and cause diseases which are difficult to be rid of.”* (Varro n.d.)

The hypothesis of minute infectious creatures has not been recorded much afterwards. However, the fear of dangerous disease-causing air (“miasma”) and water continued for centuries, especially during pandemics such as the Bubonic plague (XIV<sup>th</sup> century) which caused the end of public baths and later made people avoiding water-based body cleaning for centuries in many countries (Aberth 2016).

It’s only in the XVII<sup>th</sup> century that the hypothesis of the existence of tiny animals, first introduced during Antiquity, appeared again in Western Europe, thanks to the invention and use of a new tool: the optical microscope. Antonie van Leeuwenhoek and one of his contemporaries, Robert Hooke, were the first to record the observation of microorganisms with the use of an optical microscope. Their work confirmed the existence of creatures too small to be seen with the naked eye. Like some of his antique predecessors, Antonie van Leeuwenhoek called them “little animals” or “Animalcula” in his letters (Leeuwenhoek 1705;

Lane 2015) and Robert Hooke introduced the word “cell” (Hooke 1665) (Figure 1).

### 1.1.2 Classifying microorganisms: the first attempts

As soon as they were discovered, microorganisms were more and more recorded. The question of both their role and nature arose. Unlike their multicellular equivalents, microbial morphologies and behaviours are too simple or too difficult to interpret to serve as the basis for a phylogenetically valid taxonomy. The basic organization of life was still largely steeped in the ancient notion that all living entities are either plants or animals.

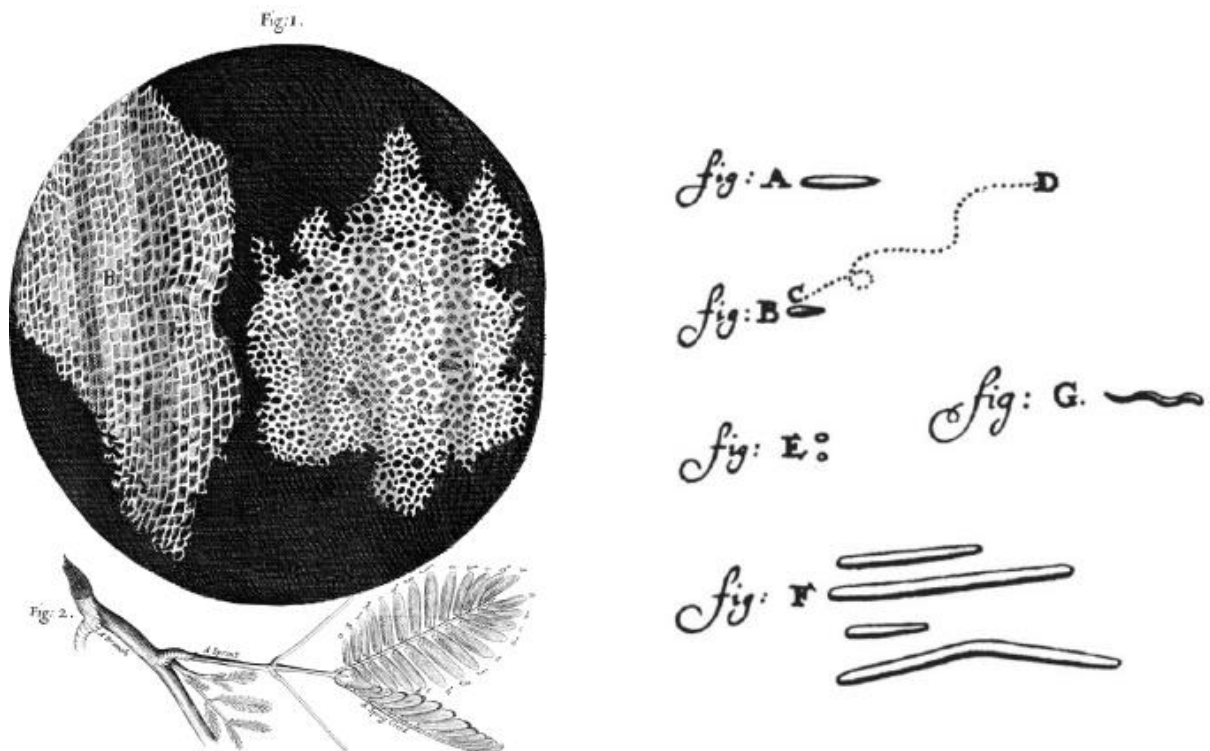


**Figure 1 | Cork and mushroom “cells” by Robert Hooke (left) (Hooke 1665) and Leeuwenhoek’s “animalcula” (right) (Lane 2015) that seem to be bacteria.**

In the XIXth Charles Darwin (and, independently, Alfred Russel Wallace (Wallace 1858)) theorized the evolution of organisms by natural selection, which is set out in detail in his book (Darwin 1859). Ernst Haeckel, who promoted and popularised Darwin’s work in Germany, published his phylogeny-based evolutionary tree, "Monophyletischer Stammbaum der Organismen" in his book "Generelle Morphologie der Organismen" (Haeckel 1866) (Figure 2-a). In this tree, he proposed three major branches being Plantae, Protista (unicellular organisms) and Animalia, challenging the original plant/animal division of the living world.

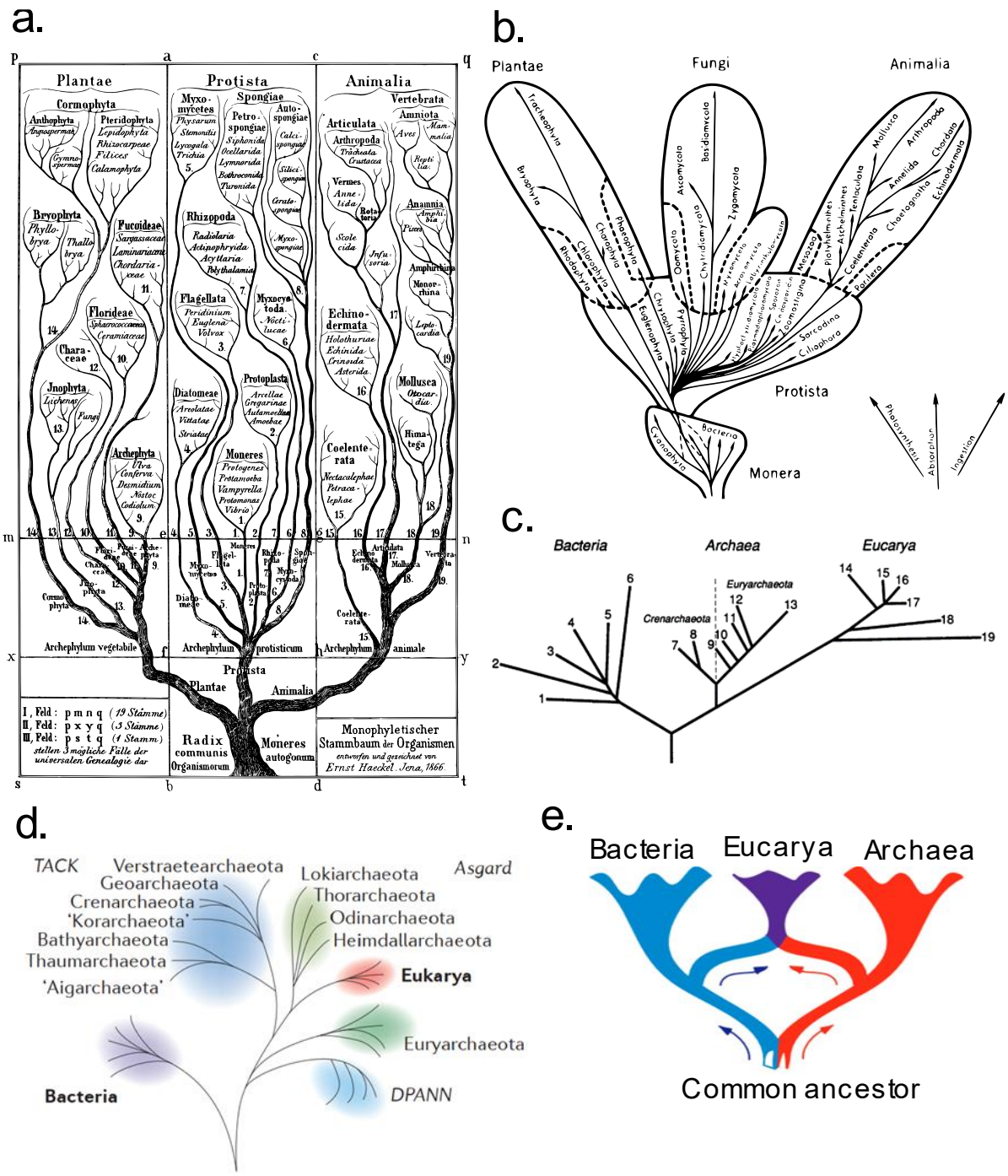


**Figure 2 | Evolution of the tree of life view before and after the Woeseian revolution.** Note that all trees are simplified with the focus on the number, denomination and position of kingdoms or domains. **a.** Haeckel's three branches (Plantae, Protista, Animalia) evolutionary tree (Haeckel 1866). **b.** The five kingdoms model (Plantae, Fungi, Animalia, Protista, Monera) (Whittaker 1969). **c.** The three domains tree (Bacteria, Archaea, Eucarya) (Woese et al. 1990). **d.** The last view of the three domain tree in which Eucarya emerge from within the Archaea, sometimes called the "two domains tree" (Eme et al. 2017) **e.** Another view of the three domains tree which highlight the endosymbiotic origin of eukaryotes, figure modified from López-García and Moreira 1999, see López-García et al (2018) for a detailed tree.

He recognized that the single-celled forms, the protists, did not fit into either category and probably had arisen separately from both animals and plants.

Later in 1938, Copeland split out a fourth main branch, a new kingdom Monera (accommodating bacteria) separated from the Protista (unicellular eukaryotes) (Copeland 1938). The name of "Monera" for unicellular organisms without a nucleus had already been suggested by Haeckel but were attached in his tree within the Protista and did not constitute a kingdom on their own. Whittaker suggested a fifth main branch, for the fungi (Whittaker 1969) (Figure 2-b). The view of the living world was hence divided into Animalia, Plantae, Fungi, Protista and Monera (prokaryotes), and was known as the "five-kingdoms" formulation.

While Haeckel's original proposition and its two more recent refinements did get away with the idea that animal/plant is *the* primary distinction, it left unchallenged the notion that it was *a* primary distinction by representing it at the highest available taxonomic level. By giving the kingdom Monera (prokaryotes) the same taxonomic rank as the Animalia, Plantae, Fungi and Protista, the five-kingdom formulation ignores the fact that the cell structure of Monera (e.g. no nucleus, no organelles) is far different from each of the four other kingdoms, while the four other kingdoms do share similarities (e.g. presence of a nucleus, of organelles such as mitochondria and chloroplasts for Plants). Chatton had codified this distinction with his famous eukaryote-prokaryote proposal, dividing life into these two primary categories. This view of life has coexisted for some time with the five-kingdom scheme, despite their basic incompatibility. The main issue of the eukaryote-prokaryote concept is that it is only based on cytology (Figure 3). The presumption that the eukaryotic organisms form a meaningful phylogenetic unit is a reasonable one, as organisms with this cytology are united by the possession of a set of complex properties that are likely to have been inherited from a common ancestor. The same is not true for prokaryotes, which are united by their lack of the characteristics that define the eukaryotic cell. The definition is consequently a negative one that lacks meaningful phylogenetic information. As the molecular and cytological understandings of cells deepened at a very rapid pace, it became feasible in the 1950s to separate the prokaryotes in different phyla based on their molecular characteristics.

### 1.1.3 Classifying the microorganisms: the birth of molecular biology and the discovery of Archaea

Quickly after their discovery in the XIXth-XXth century, it was rapidly understood that proteins and nucleic acids were universal in living organisms, including microorganisms, though the role of nucleic acids, their structure and their relationship with proteins were not solved yet as the biologist Francis Crick related:

*"Watson [his colleague] said to me, a few years ago, 'The most significant thing about the nucleic acids is that we don't know what they do.' By contrast most significant thing about proteins is that they can do almost anything"* (Crick 1958)

In 1941, Beadle had stated the controversial “one gene – one enzyme” concept, which brought the idea that each gene encodes a single enzyme (Beadle and Tatum 1941). The gene is at this time the Mendelian one (unidentified discrete units of inheritance) and not yet our current understanding of it (a DNA sequence whose series of nucleotide triplets ultimately codes for a series of amino acids forming a polypeptide chain, an enzyme or a nonenzyme protein with an intermediate translation step of DNA to RNA). At this time, many still thought that proteins were produced by other proteins *ad infinitum*.

Light is shed on the synthesis of protein and the role of nucleic acids after one of the major discoveries of the XXth century: the identification of the double-helical structure of DNA in 1953 by Watson and Crick courtesy of the X-ray crystallography work done by Rosalind Franklin and Maurice Wilkins .

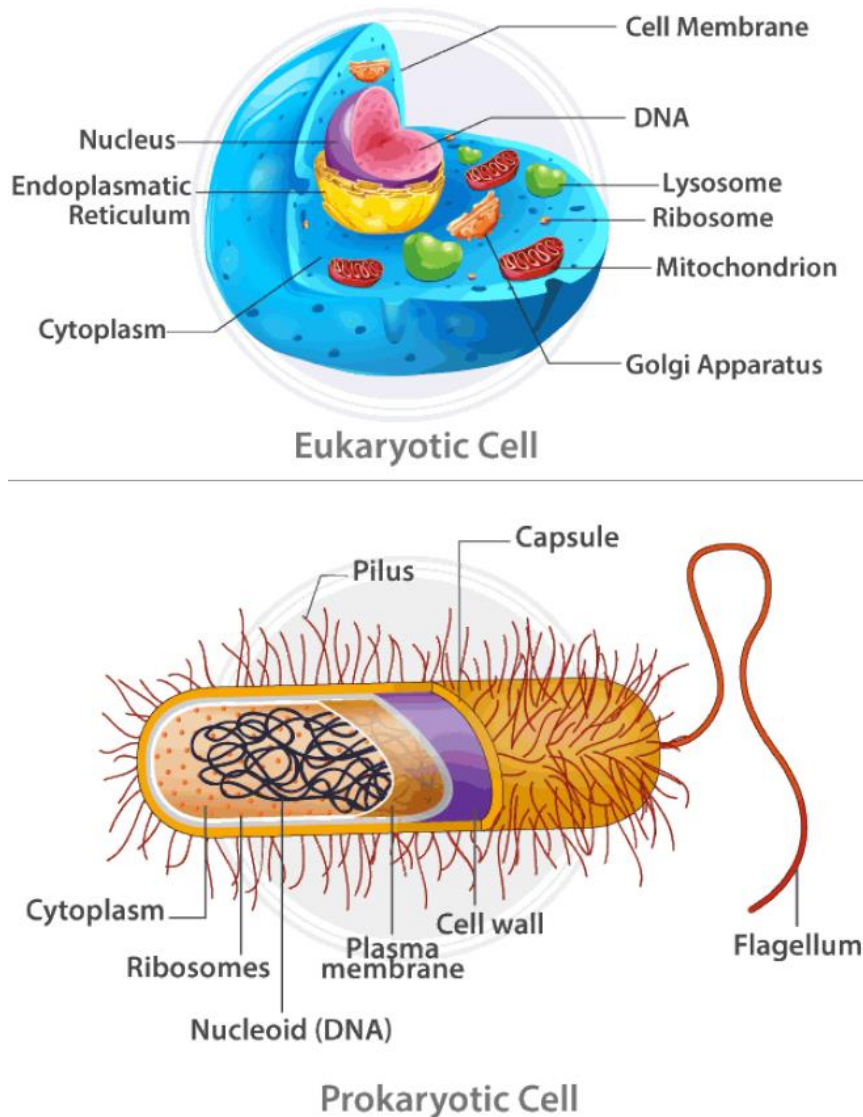


**Figure 3 | Schematic view of an eukaryotic (top) and prokaryotic (bottom) cell and their main characteristics © BUYU'S.**

In 1958, Francis Crick published his Sequence Hypothesis or Central Dogma. It states that:

*"[...] the specificity of a nucleic acid is expressed solely by the sequence of its bases, and that this sequence is a (simple) code for the amino-acid sequence of a particular protein." and  
"[...] the transfer of information from nucleic acid to nucleic acid, or from nucleic acid to protein may be possible, but transfer from protein to protein, or from protein to nucleic acid is impossible." (Crick 1958)*

Further work by Crick and co-workers showed that the genetic code was based on non-overlapping triplets of bases, called codons (Crick et al. 1961), allowing Marshall Warren Nirenberg and his co-workers to decipher the genetic code (Matthaei et al. 1962). These events represent the birth of molecular biology.

As stated in the previous section, before the advent of molecular biology, prokaryotes were regarded as a single group and great emphasis was placed on metabolic and cytological features to characterize them. Instead, in 1965, Emile Zuckerkandl and Linus Pauling proposed to use biomolecules carrying genetic information to work out how prokaryotes were related to each other. As they wrote:

*"[...]the most rational, universal, and informative molecular phylogeny will be built on semantophoretic [DNA, RNA, proteins] molecules alone." (Zuckerkandl and Pauling 1965)*

Which is still the main phylogenetic approach used today. Molecular sequences can reveal evolutionary relationships in a way and to an extent that the classical phenotypic criteria, and even molecular functions, cannot.

In 1977, for the first time, Carl Woese and George E. Fox classify some methanogen prokaryotes separately from bacteria based on 1. lack of peptidoglycan in their cell walls, 2. two unusual coenzymes, 3. results of 16S ribosomal RNA gene sequencing. They explain the choice of the 16S ribosomal gene as a reference by this paragraph:

*"To determine relationships covering the entire spectrum of extant living systems, one optimally needs a molecule of appropriately broad distribution. None of the readily characterized proteins fits this requirement. However, ribosomal RNA does. It is a component of all self-replicating systems; it is readily isolated; and its sequence changes but slowly with time—permitting the detection of relatedness among very distant species"*  
(Woese and Fox 1977)

They called this group the "urkingdom" or the "primary kingdom" of Archaeobacteria from the Ancient Greek ἀρχαῖα, meaning "ancient things" as they were thought to be more primitive than the Eubacteria (meaning "true Bacteria"). On the cytological level, archaeobacteria are prokaryotes (they show none of the defining eukaryotic characteristics),

but on the molecular level they resemble other prokaryotes, the eubacteria, no more than the eukaryotes. To emphasize this difference, Woese, Kandler and Wheelis later proposed reclassifying organisms into three natural domains known as the three-domains system: the Eucarya, the Bacteria and the Archaea (Figure 2-c).

*“For the eubacteria the formal name Bacteria, based upon a traditional common name for the group, is suggested. The term Eucarya derives from that group’s common name and captures its defining cytological characteristic [...]. The archaeobacteria are called Archaea to denote their apparent primitive nature (vis a vis the eukaryotes in particular).”*

(Woese, Kandler, and Wheelis 1990)

Procaryotae (and its synonym Monera) cannot be a phylogenetically valid taxon anymore. This change of view of the tree of life is known as "The Woesian Revolution" and is still supported today, even though it is much more detailed now by the discovery of many other taxa and phyla within the three domains. Also, the root of the Eucarya domain has been moved inside the Archaea (which is sometimes called the two-domains system) (Figure 2-d) (Spang, Caceres, and Ettema 2017; Eme et al. 2017), as eukaryotes are thought to be the result of (multiple) symbioses between a host related to the Asgard archaea and different bacteria (Figure 2-e) (López-García and Moreira 1999; P. López-García, Eme, and Moreira 2017).

#### 1.1.4 Screening microbial diversity today

The discovery of microorganisms not only changed our perception of the evolution of life (as seen in the previous sections) but also of ecosystems, in which they play an important role and are sometimes present when multicellular forms of life are absent, like it is the case in some extreme environments. The first investigations of microorganisms in ecosystems were focused on isolation and characterization of strains using culture-dependent techniques (Bergey, Breed, and Smith 1957). However, it is estimated that less than 1% of the prokaryotes in most environments can be cultured in isolation, although culture methods were improved to try to overcome the issues of strains with stringent growth conditions (Vartoukian, Palmer, and Wade 2010). The advent of molecular methodology (such as the 16S rRNA-based studies) allowed screening microbial diversity without having to isolate and cultivate individuals, which revealed that microbial diversity was much broader than suggested by culture-dependent techniques in all environments. Today, the development of next-generation sequencing technologies allows metagenomic libraries to be rapidly constructed and sequenced. Therefore, the sequences of the 16S rRNA genes or other relevant genes can easily be analysed, providing a more comprehensive view of microbial diversity. Whole genomes can also be reconstructed (from metagenomes or single cells), and (meta)transcriptomics and (meta)proteomics are also used to study the activity and gene expression of microbial communities (Segata et al. 2013). Nevertheless, a thorough knowledge of the physiology (e.g.

physico-chemical boundaries of survival) of organisms in culture is essential to complement genomic or proteomic studies and cannot be replaced by any other approach. Consequently, the combination of improved traditional methods of isolation/cultivation and modern culture-independent techniques may be considered the best approach towards a better understanding of ecosystems.

## 1.2 Life in extreme environments: implications and limits

### 1.2.1 The extremophiles' diversity

The so-called extreme environments evocated in the previous section are characterized by physicochemical parameters values that are unbearable or lethal to most organisms (temperature, salinity, pressure and pH range on Earth can be found in Figure 4). The more extreme an environment is, the more it is expected to be dominated by microorganisms with low levels of diversity until stressors eventually reach levels where no life can thrive (Sharp et al. 2014). New culture-independent technologies such as metagenomics indicate that in fact some of these extreme environments contain a high diversity of microbial species even at maximum levels of stressors (for instance saturated with NaCl salt) (Oren 2015; Ventosa et al. 2015). Extremophiles may be divided into two broad categories: extremophilic organisms which require extreme conditions in order to grow, and extremotolerant organisms which can tolerate extreme conditions that are not optimal for their growth. Extremophiles are classified according to the conditions to which they are adapted. For example:

- Halophiles:

Halophiles are organisms requiring salt (usually NaCl) for growth. Some halophiles (e.g. *Haloquadratum walsbyi*) can thrive at NaCl-salt saturation, like it is the case in saltern crystallizer ponds (Oh et al. 2010) or the Dead Sea (Bodaker et al. 2010). Halophiles are represented by organisms from all three domains of life: Bacteria, Archaea and Eucarya. Prokaryotes are dominant in hypersaline environments, especially Archaea (mainly Halobacteria and Nanohaloarchaeota) whose proportion seems to increase with salinity (Ventosa et al. 2015). Salt composition and concentration have different properties, so organisms adapted to NaCl-rich environments may not thrive if the dominant salt is of different nature (Hallsworth et al. 2007).

- (Hyper)thermophiles:

Thermophiles and hyperthermophiles are organisms growing optimally at high (60°C-80°C) or very high (80°C and more) temperatures, respectively. No hyperthermophile microeukaryotes are known, their upper limit of occurrence being around 60°C (Tansey and Brock 1972; Brock 2001). The highest recorded growth temperature is held by the archaea *Methanopyrus*

*kandleri* strain 116 which seems to be able to grow at 122 °C under specific cultivation conditions (Takai et al. 2008). High-temperature environments are generally associated with volcanic activity, but some can be met in man-made industrial complexes. Natural geothermal areas are widely distributed around the globe, most of them being associated with tectonically active zones at which the movements of the Earth's crust occur.

- Acidophiles:

Organisms growing optimally, or exclusively, in low (acidic) pH environments, and have been sub-divided into moderate (pH optima 3–5) and extreme (pH optima < 3) acidophiles. The majority of acidophiles are prokaryotes, and these comprise a large variety of phylogenetically diverse Bacteria and Archaea, though some single-celled and multicellular eukaryotes are known to grow in highly acidic ponds and streams (Johnson 2009). Archaea from the genus *Picrophilus* include the most acidophilic organisms currently known, with the ability to grow at pH 0.06 (Schleper et al. 1996). Acidic ecosystems are usually located in geothermal areas or associated with ancient mines (Johnson 2009).

- Metallophiles:

Organisms resistant to high metal concentration, usually referring to heavy metals (such as copper, arsenic, iron...). Heavy metals promote highly oxidative environments which can damage biomolecules. Prokaryotes are dominant in heavy metal-rich environments, but microorganisms exhibiting the highest tolerance mainly belong to archaea (Maezato and Blum 2012).

The list goes on. As seen in the above examples, most extremophiles are microorganisms including members of the three domains of life (Bacteria, Archaea, and Eucarya) and a high proportion of them are archaea. Interestingly, extremophiles adapted to the same extreme condition may be broadly dispersed in the phylogenetic tree of life. Considering the high variety of biotopes on Earth, the physiological responses to the environmental extremes can be observed on a gradual scale from tolerance to absolute requirement. In addition, extremophiles are usually polyextremophiles, being adapted to live in habitats where various physicochemical parameters reach extreme values. For example, hot geothermal systems often display a wide range of pH, from acid to alkaline, depending on temperature, water availability, gases and ion concentrations. Low pH facilitates metal solubility in water and therefore acidic water tends to have high concentrations of heavy metals. The two conditions of salinity and alkalinity are also often seen in tandem (Harrison et al. 2013; Merino et al. 2019).

### 1.2.2 Benefits and perspectives of studying extremophiles

With their ability to thrive in conditions that were long thought to be inhospitable for life, extremophiles have never ceased to fascinate researchers and the general public since their discovery. Research on extremophiles has many implications from the point of view of both industrial and basic sciences:

- The origins of life:

The Archaean geological era where the first forms of life have emerged is thought to have been more extreme than today's era such as: anoxic atmosphere, a greater geothermal activity, oceans two to three times saltier than nowadays with a higher concentration of some metals such as arsenic (Knauth 2005; Oremland et al. 2009). Although primitive oceans were long suspected of being alkaline, a recent study suggests that they might have been more acidic and also richer in iron than today's oceans (Albarede et al. 2020). Some modern extreme environments can represent, to some extent, precious analogues of the primitive Earth and can help to better understand what could have been the first life forms and how they adapted to such conditions. In recent and ancient geological records, extremophiles activity has left traces which are called biosignatures. For example, the oldest fossils of microbes are believed to be stromatolites 3.5 billion years old located in modern Australia, even though their biogenicity still needs to be tested (Walter, Buick, and Dunlop 1980; Schopf and Packer 1987; Brasier et al. 2002). Studying modern biosignatures (e.g. biomineralization) and their origin is also essential to interpret the fossil record (Knoll, Canfield, and Konhauser 2012). Since life probably originated in warmer oceans due to the intense hydrothermal activity of the Archaean, it has been long suspected that the primitive forms of life were thermophiles or hyperthermophiles. This theory has been supported by the observation that hyperthermophiles group close to the "universal ancestor" of all organisms on Earth (Di Giulio 2003; P. López-García et al. 2015). For a contrasting point of view, see Catchpole and Forterre (2019). Even though there is no consensus yet about the thermophilic or mesophilic nature of the last common universal ancestor, the study of extremophiles and their ecosystems remains critical for evolutionary studies related to the origins of life. As related in the section 1.1.1.3, the third domain of life, the archaea, was discovered partly due to the first studies of methanogens which are extremophiles (Woese and Fox 1977), with profound consequences for evolutionary biology.

- Limits of life and astrobiology:

The study of extreme environments has become a key area of research for astrobiology. Understanding the biology of extremophiles and their ecosystems permits developing hypotheses regarding the conditions required for the origin and evolution of life elsewhere in the universe. Consequently, extremophiles may be considered as model organisms when

exploring the existence of extra-terrestrial life in other planets and moons of the Solar System and beyond. For example, the microorganisms discovered in ice cores recovered from the depth of the Lake Vostok and other perennially subglacial lakes from Antarctica may serve as models for the search of life on Europa, an ice-covered moon orbiting Jupiter (Karl et al. 1999; Bulat et al. 2011). Microbial ecosystems found in extreme environments like the Atacama Desert, the Antarctic Dry Valleys and the Rio Tinto may be analogous to potential life forms adapted to Martian conditions (Martins et al. 2017) (see Figure 4 for the physicochemical boundaries on Europa and Mars compared to the Earth).

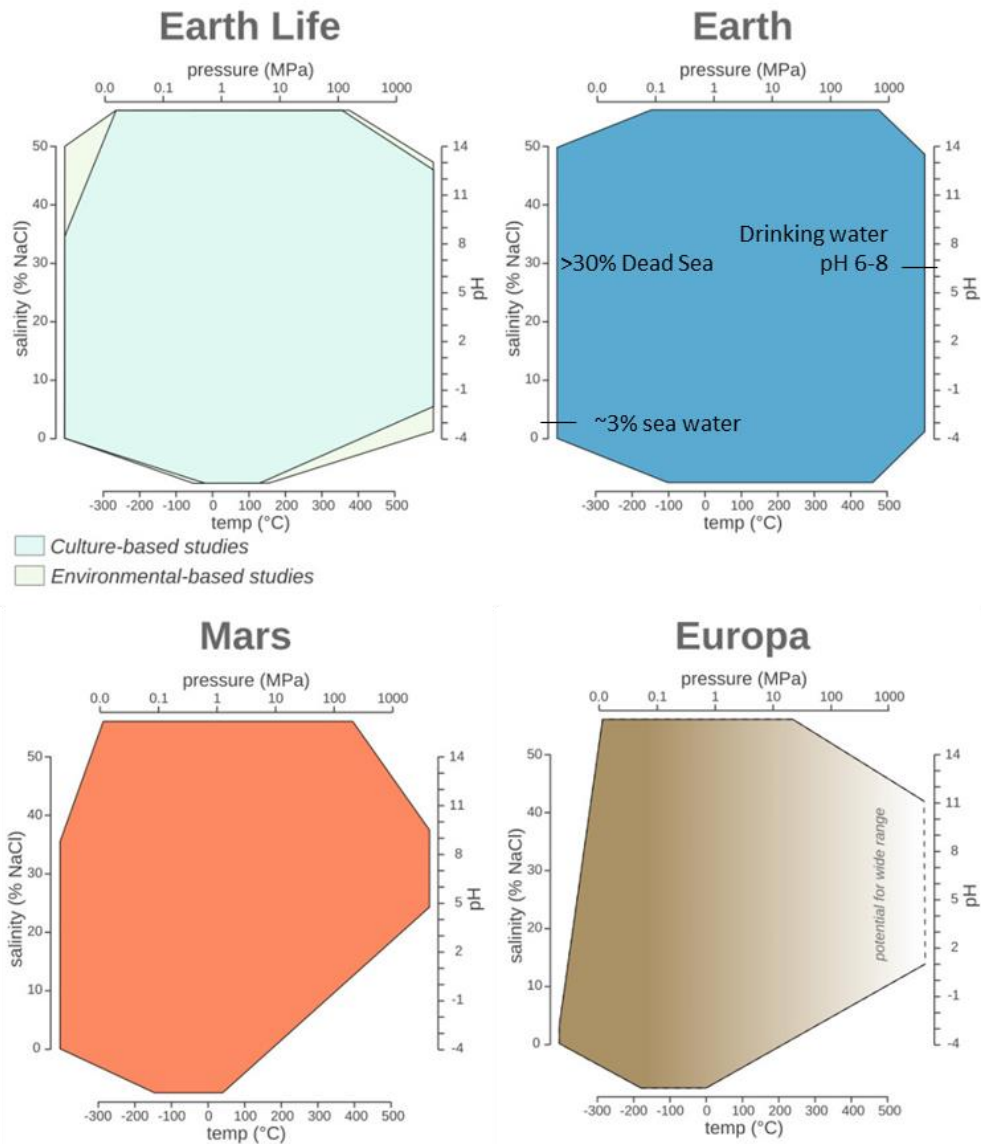


**Figure 4 | The temperature, pressure, pH, and salinity boundaries observed for life on Earth compared to other planetary bodies.** Modified from Merino et al. (2019). Percentage of salt percentage of the sea water and the Dead Sea from Bodaker et al. (2010), pH of drinking water from World Health Organisation (1993).

- Bioremediation:

Bioremediation is a process used to treat contaminated media (e.g. with high heavy metal concentration) including water, soil and subsurface material, by stimulating the growth of microorganisms that will degrade or transform the target pollutants in their environment. Development of bioremediation strategies has motivated detailed studies of archaeal metal resistance to treat heavy metal contamination from mining or industrial waste (Kang et al. 2015; Sara Parwin Banu et al. 2003). Some hyperthermophilic archaea have the capacity to immobilize metals, such as uranium suggesting potential uses for bioremediation of uranium-contaminated groundwater (Finneran, Housewright, and Lovley 2002).

- Biotechnologies and industry:

One of the interests of the study of extremophiles is the potential application of their metabolites and enzymes in biotechnologies. To be able to live in their natural ecosystems, these organisms possess adapted biomolecules and peculiar biochemical pathways which are of great interest for biotechnological purposes. The stability and activity at extreme conditions of such biomolecules make them useful alternatives to more labile molecules. For example, thermostable enzymes from thermophilic microorganisms are important biocatalysts for industrial and biotechnological purposes, given that they can work at temperatures at which mesophilic enzymes would be denatured. The typical case study is the Taq DNA polymerase from *Thermus aquaticus*, purified and isolated from hot springs, which made the development of the PCR amplification technique possible (Saiki et al. 1988).

The extreme acidophiles are a group largely investigated for their ability to withstand high concentrations of heavy metals as this has considerable industrial applications. For example, some microorganisms like *Acidithiobacillus ferrooxidans* or *Ferroplasma acidarmanus* are used in biomining projects (as they accelerate the dissolution of metals) aiming the exploitation of metals such as copper, gold or even uranium (Johnson 2010). Polyextremophiles are of great interest too in the industry for the potential versatility of their biomolecules.

Extremophiles also have the attention of the food industry, for some of them or their biomolecules are relevant to some food transformation processes or, in contrast, are considered a pest as they may overcome the harsh storage conditions (dryness, low water activity associated with high salinity or sugar content, heat shocks or freezing) and spoil the food (Irwin 2020).

The list of fields of interest and applications above is far from exhaustive and continues to expand as our knowledge on extremophiles grows. An understanding of the versatility of life on Earth, as well as the mechanisms that allow some organisms to survive or develop in extreme conditions, will help to gain more insights into those fields.

### 1.2.3 The unknown limits of (poly)extremophiles

Despite the latest advances, we may be still at the beginning of exploring and characterizing the world of extremophiles and their environments. While the microbial communities in saline or acidic environments have been separately characterized many times, little is known about microbial life in environments that are hypersaline and hyperacidic at the same time. These environments would be of particular interest as a source of novel genetic diversity and to improve our understanding of some past ecosystems, such as an ancient (275 – 265 million years old) and widespread saline and acid (pH 0-1) lake and groundwater system in North America (Benison et al. 1998; Benison and Goldstein 2001). In spite of that, microorganisms that can grow simultaneously at low pH (<4) and high salt concentration (30%), and eventually also high temperatures (>40°C), are not known among cultured prokaryotic species (Harrison et al. 2013). One of the reasons may be that hypersaline and hyperacidic environments are rare, making difficult the study of their potential microbial diversity. To the best of our knowledge, only four environmental studies have investigated microbial communities of such ecosystems (Table 1).

**Table 1 | Acid salt lakes and sediments and associated microbial communities**

	Andean Lakes (Chili)	Series of lakes in western Australia	Acid salt lake of western Australia	Lake Magic Australia
Physicochemical parameters	pH 1.5 – 4 Salt concentration probably at saturation (salt flats) Temperature not referenced	pH 3.1 – 4.9 Salinity 4 – 16% Temperature not referenced	pH 3 Salinity 32% Temperature not referenced	<b>Water column:</b> pH 2.3, salinity 30%, 25 °C <b>Groundwater:</b> pH 3.5, salinity 4%, 28 °C <b>Wet sediments:</b> pH 1.7, salinity 26%, 42°C
Main microbial groups detected	<b>Sediments:</b> Actinobacteria, Proteobacteria (β, γ), Firmicutes <b>Water:</b> Proteobacteria (α, γ), Cyanobacteria, Halobacteria, Thermoplasmata	<b>Water:</b> Only 50 sequences (Sanger sequences) including Proteobacteria (α, ε, γ), Actinobacteria, Bacteroidetes. Archaea are not investigated.	<b>Sediments:</b> Proteobacteria (α, β, γ, δ), Actinobacteria, Firmicutes, Planctomycetes. Some Halobacteria are present	<b>Water column:</b> Majority of eucaryotes, almost no archaea <b>Groundwater and wet sediments:</b> Majority of bacteria, little or no archaea
Reference	Escudero et al. 2013	Mormile, Hong and Benison 2009	Johnson et al. 2015	Zaikova et al. 2018

The problem of those scarce studies is that some of them only focus on the sediments of surrounding the lakes (Escudero et al. 2013; Johnson et al. 2015) or mostly focus on the bacterial fraction of the diversity (Mormile, Hong, and Benison 2009; Escudero et al. 2013).

The most complete investigation on the Lake Magic in Australia gives surprising results, showing a dominant fraction of eucaryotes over prokaryotes in the water column and almost no archaea (Zaikova et al. 2018). This is quite at odd with the expected microbial diversity of (hyper)saline or (hyper)acidic environments where archaea are usually dominant, as discussed in section 1.2.1. It also contradicts the little information given on the microbial diversity of the water column of the acid salt lakes of the Central Andean high plateau of Chile. This may be linked to the high seasonal variability stages of Western Australian lakes (flooding, evapoconcentration, desiccation), as the Lake Magic was sampled during evapoconcentration stage and may be much less acidic and salty during the flooding stage. It would also be interesting to know to which extent local contamination (e.g. airborne microbes) may have influenced the dataset.

As we can see, the microbial diversity of hypersaline and acidic environments is still poorly known and no study have yet investigated the ecology of salt-saturated brines with pH below 1.5, leaving us to wonder if such conditions could be limiting for microbial life or not.

### 1.3 The Dallol hydrothermal system and its surroundings: a panel of unique physicochemical gradients on Earth

This section will present the environments I studied during my thesis: a series of ecosystems located in the North of Ethiopia showing a wide array of unique saline-acidity-hot gradients that raised scientific interest due to their life-challenging polyextreme conditions. They represent a natural laboratory to reply to the uncertainties highlighted in the previous section.

#### 1.3.1 Geographical and geological context

The Danakil Depression is a N-S basin of ~72,000 km<sup>2</sup> down to 120 m below sea level, lying at the triple junction between the Nubian, Somalian and the Arabian plates and the Danakil microplate. The triple junction and the rifts (under the Red Sea, the Gulf of Aden and the Main Ethiopian Rifts) are zones associated with a high magmatic and volcanic activity. As a result, several volcanic chains are forming, mainly represented by basaltic shield volcanoes, among them the NNW-SSE Erta Ale range (Hutchinson and Engels 1972; Collet et al. 2000; Chorowicz 2005; Ring 2014; Corti et al. 2015) (Figure 5-a,b).

Categorized as BWh (hot desert climate) according to the Köppen classification, the annual precipitation of the area is very low, usually below 50 mm and up to 144 mm. With the official world record of highest annual mean temperature (34.5°C, Krause and Flood 1997), the Danakil Depression is also one of the hottest places on Earth. In addition, it is characterized by strong hot winds which the local Afar population calls “hahaita-harrur” or “fire-wind” (Aerts and November 2017). Two noticeable escarpments limit the depression: to the west, the

Northern Ethiopian Plateau, of Precambrian and Mesozoic origin, culminates at more than 2000 m of altitude; to the east, the less prominent Danakil Alps sit on a tectonic microplate, the Danakil Block, uprising 500-1000 m above sea level (Collet et al. 2000) (Figure 5-b). The salt plain formed when the northern extremity of an ancient Red Sea arm was closed at the Gulf of Zula (Eritrea) due to the uplift preceding the Alid volcano Quaternary magma flows (Bonatti et al. 1971; Mitchell et al. 1992; Corti et al. 2015). This closure possibly happened during the Pleistocene and left marine reefs at different altitudes (-30 to +90 m), marking ancient shorelines (Bonatti et al. 1971; Hutchinson and Engels 1972; Mitchell et al. 1992) (Figure 5-c). The seawater evaporation in the enclosed depression led to the deposition of a ~2 km thick salt sequence over several thousand years (Bonatti et al. 1971). This thick halite formation is vertically divided into two main sequences: the lower rock salt formation (LRS, Pleistocene to Miocene) and the upper rock salt formation (URS, Pleistocene to Holocene) separated by a potash unit, the Houston Formation, which has been the target of mining exploration since the beginning of the last century (Holmes 1919; Holwerda and Hutchinson 1968; López-García et al. 2020) (Figure 6-a). During the Holocene, the main reliefs continuously eroded and formed alluvial fans fringing the base of the escarpments limiting the depression (Figure 5-c and 6-a). At the same time, a lacustrine system set up in the Danakil Depression in the form of a massive “Lake Afrera” that probably encompassed the present Assale/Karum, Bakili and modern Lake Afrera until it evaporated to its current stage (López-García et al. 2020).

The karstified Jurassic limestones and sandstones that underlay the evaporitic sequence behave as aquifers enabling the infiltration of meteoritic water from the Danakil Alps to the east and the North Ethiopian plateau to the west, *via* the normal faulting and transverse fractures of the rift zone. The presumed depth of this aquifer is around 2 km and at a similar depth may be located a shallow magmatic chamber (Nobile et al. 2012). The magma could have intruded in the potash level. The unique geochemistry of thermal waters in the Dallol dome area, at the Nord of the Danakil Depression, certainly results from the influence of this magma intrusion in the salt unit and its interaction with meteoric groundwater (Figure 6-a).

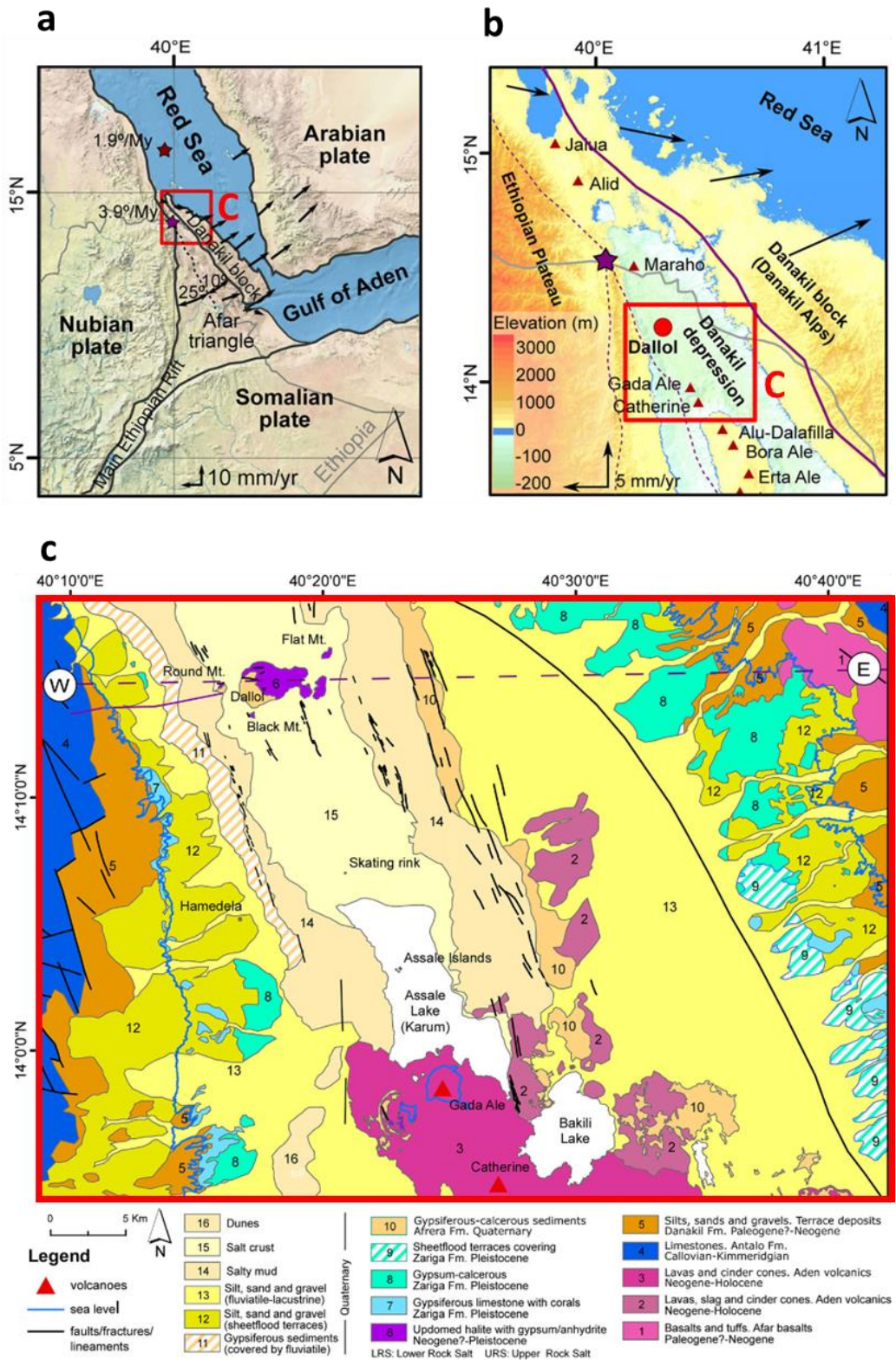


**Figure 5 | Maps of the Danakil depression around the Dallol dome area (Lopez-Garcia et al. 2020).** **a**, The Afar Triangle and the location of the Dallol area. **b**, Elevation of the Danakil depression compared in reference to the sea level. Volcanoes are represented with a triangle shape. The grey line in the border with Eritrea, the dashed lines are tectonic plates limits. **c**, Geological map.

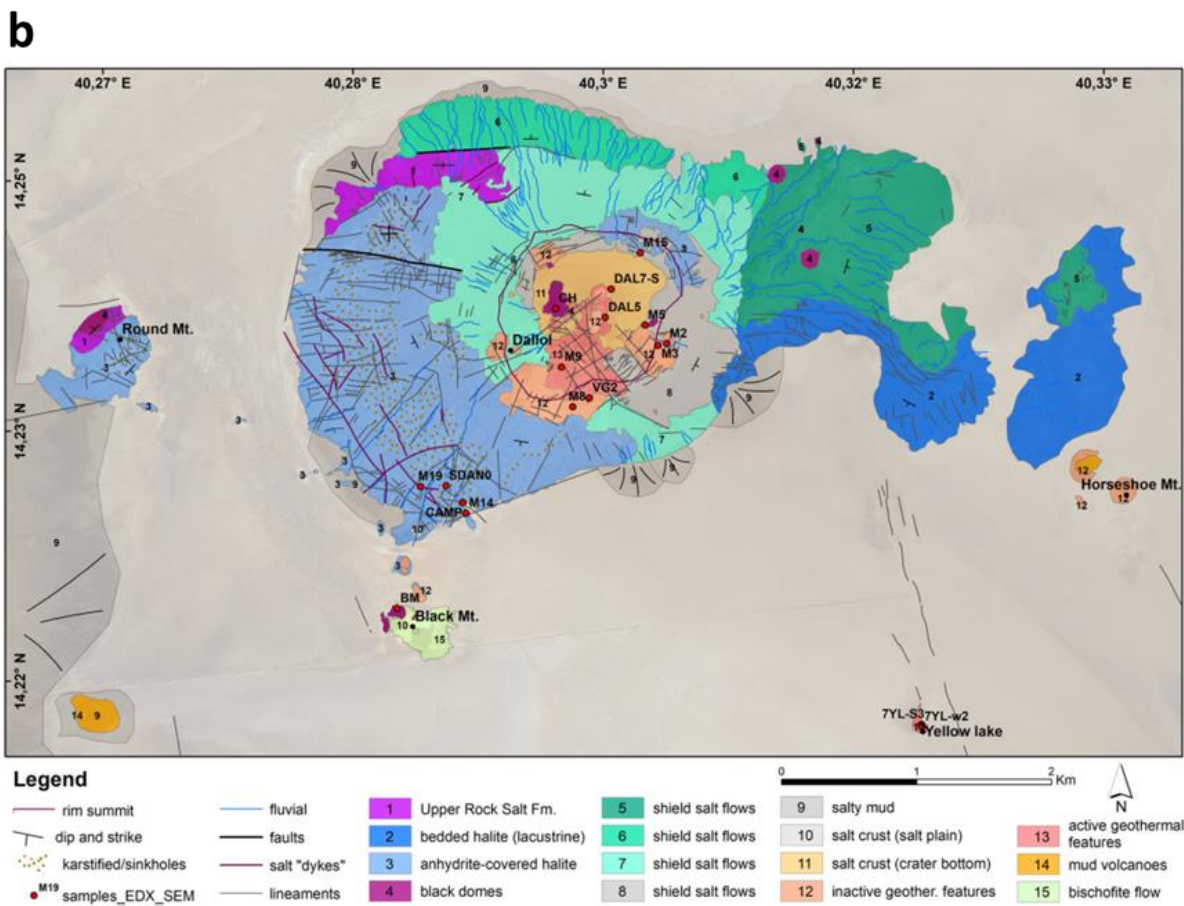
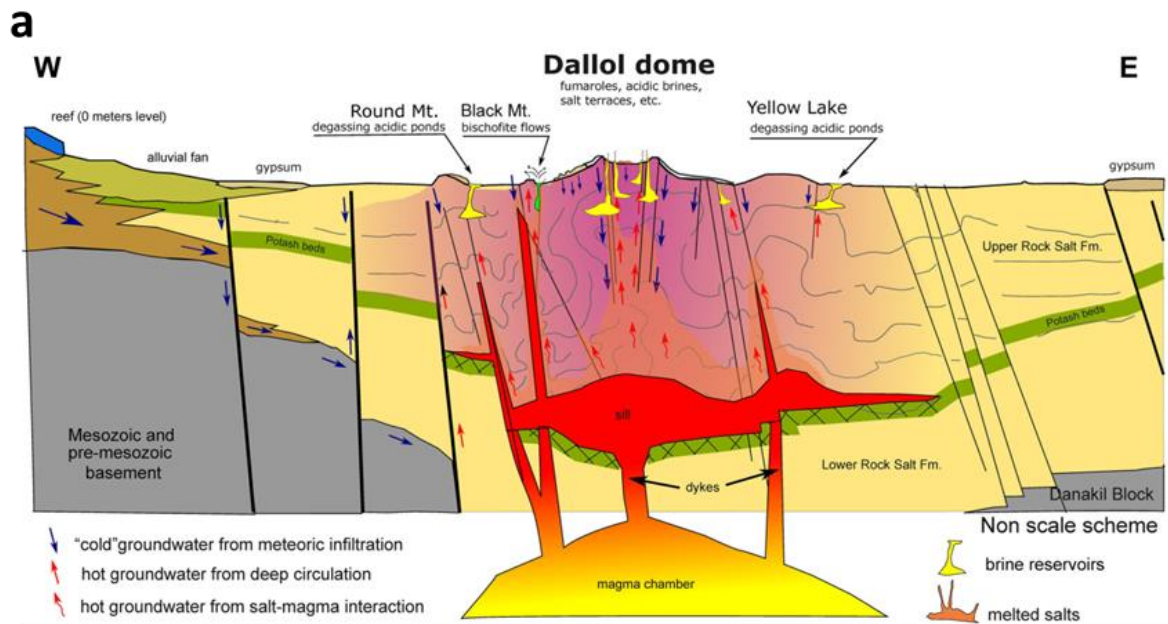


**Figure 6 | The Dallol dome area (Lopez-Garcia et al. 2020). a, Detailed geological map of the Dallol dome and its surroundings. b, Idealized cross section through the Dallol dome.**

### 1.3.2 The pH-salinity-temperature gradients of the Dallol dome area

#### 1.3.2.1 The Dallol dome

The Dallol dome is a complex geothermal structure rising 40 meters on the Danakil Depression, only 13 km south-east of the Eritrea border (Figure 4-b). Although the area is rather dangerous due to the armed conflict between Eritrea and Ethiopia (1998-2018), Dallol has become a tourist destination that attracts thousands of tourists every year (Vereb et al. 2020) under strict security conditions (military surveillance was mandatory until 2018).

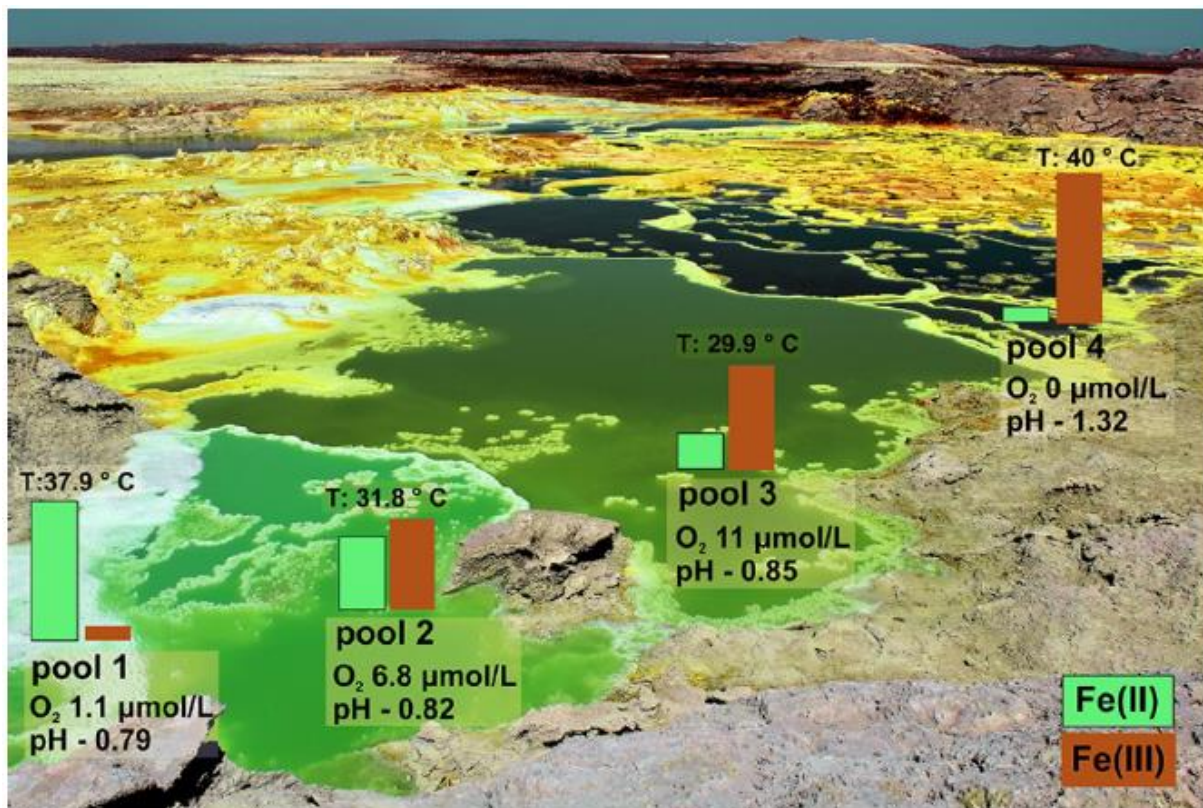


Figure 7 | Fe(II)/Fe(III) ratio, pH, O<sub>2</sub> concentration, and temperature of four successive pools of a typical spring-terrace system (Kotopoulou et al. 2019). Pool 1: Brine pond closest to the source hydrothermal chimney. Pool 4: Brine pond furthest away from the source hydrothermal chimney.

At the origin of this attractiveness is certainly the beautiful colour palette of Dallol's hydrothermal ponds and salt formations (Figure 7, Figure 8-a-c). The springs are discharging boiling (+100°C) oxygen-free, hyperacidic (~0), Fe-rich (up to 150g/L of iron) hydrothermal brines, which are supersaturated with respect to halite as soon as they are in contact with the atmosphere, creating white-coloured small salt cones, big chimneys or pillars up to few meters in height (Kotopoulou et al. 2019; J. M. López-García et al. 2020a). As the water flows

downstream from the springs, a series of self-organized halite terraces retain the brines, turning the turbulent flow into a laminar one. The prevalence of laminar flow in these terraced ponds and the dominance of diffusion over convection enables the discrete display of Dallol's world-renowned stunning colours. The gradual colour variation of the brine, ranging from pale green to dark brown, portrays the oxidation state of iron and the increasing solutes concentration in the hydrothermal fluids as evaporation occurs. The more oxidation and evaporation occur, the more the pH drops and the temperature of the ponds, without being heated by the geothermal activity, increases by a few degrees (Figure 7, Figure 8-a) (Kotopoulou et al. 2019). The amount of organic matter in the dome is practically zero except maybe for some grey spring systems, whose colour may be due to amorphous silica and degraded, partially graphitized, organic matter, both considered as remnants of fossil diatoms trapped in the evaporitic sequence (Figure 8-b,c) (Kotopoulou et al. 2019). The amount of organic matter in the dome water is practically zero. The colour of the solids is white around the springs due to the rapid halite crystallization and further turns to yellowish and then orange and brown as the precipitation of iron oxides takes place (jarosite, akaganeite, hematite). Few nanoparticles of native sulphur and Fe-sulphides are also found dispersed in halite crystals. Life, if present under such conditions, does not play a dominant role in the colour display or the mineral precipitation at Dallol (Kotopoulou et al. 2019).

Although a connection of the surface with the Jurassic aquifers is possible, López-García and his co-workers suggest that most of the brine from the dome likely comes from the infiltration of: (i) direct rainfall over the dome; and/or (ii) rainfall in the Ethiopian plateau and the Danakil alps and periodical flooding on the Danakil Depression (López-García et al. 2020). The evolution of the spring activity may be related to the water table fluctuation in semi-independent underground reservoirs (Carniel, Jolis, and Jones 2010; López-García et al. 2020) (Figure 6-a). The Dallol dome landscape is highly dynamic and can change in a matter of days or weeks (Figure 8-b,c). When the surface of some Dallol area dries out, the geothermal activity can start again as new water supplies feed the depleted reservoirs, and fresh deposits can thus overlay the ancient ones (Kotopoulou et al. 2019; López-García et al. 2020)

A central depression of 1 km in diameter gives the Dallol dome a volcanic crater-like appearance (Holwerda and Hutchinson 1968; López-García et al. 2020) (Figure 6). This volcano-like morphology, coupled with the geothermal activity and location of the dome (on the axis between the Era Ale volcanic ridge in the south and the Maraho, Alid and Jalua volcanoes in the north) has led many authors to refer to this structure as the "Dallol volcano" (e.g. Darrah et al. 2013; Keir et al. 2013; Corti et al. 2015). However, volcanic materials have never been found on the dome or its intermediate surroundings. It has been proposed that the geothermal activity of Dallol probably represents a protovolcanic manifestation related to extensional faulting and magma intrusion in this rift segment, and that Dallol could be referred as a salt-volcano (López-García et al. 2020a), in a wide sense of volcano definition (Borgia et al. 2010). A 100 m structure showing halokinetic and magmatic processes, located 3 km

southwest of the Gada Ale volcano crater, 33 km south of Dallol and close to Lake Karum's south coastline, might be a good analogue of the future Dallol evolution (J. M. López-García et al. 2020a).



**Figure 8 | Pictures of the most polyextreme sites of the Dallol area.** **a**, Drone view of a typical spring-terrace system. The arrow shows the direction of the flow, from the hydrothermal chimneys to the most evaporated/concentrated ponds ©Olivier Grunewald. **b**, Rare grey hydrothermal chimney on the 06/01/2017. **c**, The same hydrothermal chimney as in (**b**), the 11/01/2017. Within few days, the chimney grew ~1m. **d**, Lake Gaet'ale in 2016. **e**, Dead birds found around the Lake Gaet'ale. **f**, The Black Lake in 2019, when its surface temperature was 70°C **g**, The Black Lake in 2017, when its surface temperature was 60°C, with the setup used to sample ~1 m below the surface of the lake (the same setup was used to estimate the depth of the lake). **h**, Bischofite flows next to the Black Lake and the Back Mountain.

Dallol has also been referred as a potential analogue of some Mars regions, as active volcanic environments associated with diffuse hydrothermalism and hydrothermal alteration are reminiscent of past hydrothermal activity on Mars. Salts are considered to be an important component of the regolith on Mars, with the presence of  $(\text{Mg},\text{Na})\text{SO}_4$ ,  $\text{NaCl}$  and other chlorides, and  $(\text{Mg},\text{Ca})\text{CO}_3$ , similar to what can be found on the Dallol dome salt deposits

(Cavalazzi et al. 2019; Clark and Van Hart 1981). The presence of jarosite and iron sulphates is also important on Mars surface as well as on Dallol dome and suggests the potential for locally acidic conditions on Mars (Cockell 2014). Dallol is a natural laboratory for the study of the precipitation of iron minerals and one of the very few present-day sites where we can witness the progressive oxidation of the iron formations, relevant for geochemical processes occurring at early Earth and Martian environments (Kotopoulou et al. 2019).

### *1.3.2.2 Lake Gaet'ale or Yellow Lake*

Lake Gaet'ale, also referred as the Yellow Lake, is situated at 3.8 km southeast of the Dallol crater (Figure 6). Its springs feed a roughly crescent-shaped lake which is about ~60-70 m of diameter. It is not known when the lake was originally formed, but Landsat satellite imagery taken on 6 February 2003 and distributed by Google Earth shows that the lake existed then in quite the same shape and size as at present. It is mentioned as "brine pool" as early as in 1968 in the scientific literature (Holwerda and Hutchinson 1968).

The lake level is about 1-2 m below the level of the surrounding salt flat and between 2016 and 2019 it has evaporated intensively. The hydrothermal springs bubble up powerfully in several small fountains and the water has a distinctive yellow-orange colour (Figure 8-d,e). According to Ahmedela residents (the nearest inhabited village), the spring activity started anew following an earthquake in January 2005 due to a major dyking event (Wright et al. 2006; Nobile et al. 2012; Ayele et al. 2007; Master 2016). After the earthquake, locals said that the geysers fountained up to 3 m high, and lasted this intense for 3 years (Master 2016). Associated with Lake Gaet'ale, a series of smaller ponds with similar features are aligned N-S following the rift East-segment inner fault.

The water temperature is ~40°C with a pH around 1.5 (Belilla et al. 2019) and it releases a strong hydrocarbon smell (Belilla et al. 2019; Gebresilassie, Tsegab, and Kabeto 2011). The lake seems to be undergoing strong evaporation over time as suggested by its ancient shores' lines visible all around its current perimeter. The water has a greasy or oily feel which is likely due to supersaturation in dissolved salts, which precipitate readily on cooling. Lake Gaet'ale was found to be the most saline water (433 g of salt per kg of water) body on earth recorded in front of the Don Juan Pond (403 g of salt per kg of water with 95% CaCl<sub>2</sub> and 1-2% of MgCl<sub>2</sub>) in Antarctica (Pérez and Chebude 2017). The composition of Lake Gaet'ale brine shows the predominance of two main salts: CaCl<sub>2</sub> and MgCl<sub>2</sub> accounting for ~98% of the total dissolved solids with a ratio of Ca:Mg=3.15 (w/w). Traces of K<sup>+</sup> (Ca:K=45.6), Na<sup>+</sup> (Ca:Na=86.7) and NO<sub>3</sub><sup>-</sup> are also detected, as well as Fe(III) complexes which give the water its characteristic yellow colour (Pérez and Chebude 2017). Halite with significant amount of carnallite (and other metal oxides) form most of the salt deposits around the pools (Kotopoulou et al. 2019).

Animals such as birds, insects or arachnids can be found dead by dozens around Lake Gaet'ale. Locals says they witnessed the death of birds in mid-air due to gas release, which is

suspected to be due to CO<sub>2</sub> gas release, potentially a hazard for both animals and visitors (Master 2016).

### *1.3.2.3 The Black Mountain and the Black Lake*

The Black Lake, also known as the Black Pool or Black Water spring, is an active small (15 m diameter, ~10 m depth) geothermal lake located close to the north limit of the Black Mountain (Figure 6). Both are less than a kilometre south from the salt canyons that constitute the eastern flank of the Dallol Dome. The Black Mountain, named after its dark colour, is mainly composed of halite with high content in hematite. These flows frequently preserve an extrusive morphology, evoking those of lava flows. These high viscosity flows often exhibit hexagonal joints indicating retraction after cooling and internal folding (similar formation can be seen on the dome, (Figure 6)). The Black Mountain area exhibits frequent massive bischofite flows (Figure 8-h) coming from several emission centres located close to the southeast Black Mountain limit. This activity and the resulting deposits are the most changing features of the Dallol complex. The Black Mountain and its surroundings display signs of recent explosive activity, as shown by the occurrence of big salt boulders ejected from geothermally active open fissures (for more information about the geology of the Black Mountain, see the source López-García et al. 2020).

The Black Lake (Figure 8-f,g) formed after a phreatic explosion in 1926 (Holwerda and Hutchinson 1968). Its surface temperature is between 60 and 70°C and its pH is between 2.5 and 3.5. The salt concentration of this lake is so high that salt crystallises at its surface before it is blown by the wind, creating beautiful geometrical rims on its surface. When brine is sampled from the lake, the salts dissolved instantly precipitate to almost the top of the bottle (Belilla et al. 2019). These salts are white, suggesting that the dark colour of the lake is mostly due to its depths and very high viscosity, which prevents light to penetrate its surface.

### *1.3.2.4 The salt plain*

The flat bottom of the depression is covered by a salt crust (sometimes called the Assale rock-salt deposit (Binega 2006)) that was formed, as previously mentioned, when the northern extremity of an ancient Red Sea arm was closed and the evaporation of the resulting ancient Afrera Lake that covered most of the Danakil Depression. The salt plain is mainly composed of halite (Binega 2006; López-García et al. 2020). The top few meters of the halite formation is interlayered by mud layers originating from the dissolution, evaporation and re-precipitation of previous salt deposits (Holwerda and Hutchinson 1968), due to flooding episodes and by the displacement of Lake Karum to the north with the intense winds of the depression (López-García et al. 2020). The pH of the salt plain can drop down to 4.2 when there is a local, ephemerally hydrothermal influence (Figure 9-d).

The salt plain has been traditionally exploited for table salt for humans and their cattle consumption for many years and the annual production from the salt mine site is around 35,000 tons (Binega 2006).

#### *1.2.3.5 The salt canyons and the cave reservoir*

During the Dallol dome early evolution, the ancient alkaline “Afrera” Lake still occupied most of the North Danakil basin, extending up to the Dallol area. On what is today the Dallol west flank, bedded gypsum and anhydrite evaporites interlayered with lacustrine silica-rich marls, diatoms-rich white silts and clays are evidence of the “Afrera” lake past presence. The anhydrite-gypsum layers share presence minerals typical of soda lakes (e.g. stevensite or kerolite) (López-García et al. 2020). The halite-gypsum-anhydrite Dallol unit is affected by intense fracturing and karstification, at the origin of the impressive salt canyons landscape. The protective role of less-soluble anhydrite beds on top of halite series results in the formation of the impressive salt canyons’ landscape, punctuated by isolated buttes, pinnacles and demoiselles (López-García et al. 2020) (Figure 9-g).

A brine reservoir (Fig.9-f) can be observed inside the salt canyons. This reservoir, whose level varies from year to year, is salt-saturated with halite and its pH is around 6 (Belilla et al. 2019).

#### *1.3.2.6 Lake Karum/Assale*

Lake Karum, also referenced as Lake Assale, is a permanent, salt-saturated (salinity 30% w/v) and almost neutral (pH ~6) brine lake 30 km south to Dallol, on the northern side of the Erta Ale volcanic chain (Figure 5-b,c). The northern part of the Lake meets the salt plain, while its southern part lies on cooled lava floor and is very inaccessible (Holwerda and Hutchinson 1968) unless with an aircraft. Over the years, the lake experiences significant changes in volume, dependant on the rainfall and runoff from the highland during wet seasons, as supported by a positive correlation between the lake expansion and high precipitation (Nanis and Aly 2020). As previously evoked, the surface area of the lake also changes due to intense winds acting over the flat topography of the depression that can expand the lake further to the North. Stromatolitic gypsum layers are present in Lake Karum, and the underlying bedrock is a bedded halite sequence very similar to the one outcropping in the salt canyons. This bedded halite bedrock is also visible on Lake Karum’s islands (Figure 9-g-i).



**Figure 9 | Pictures of the less polyextreme sites of the Dallol area.** **a**, One of the Western Canyons Lakes. **b**, Another Western Canyons Lake, with the Round Mountain in the background. **c**, Detail of the bubbling surface of one of the Western Canyons Lakes with a sampling bottle for scale. **d**, The hydrothermally influenced salt plain observed in 2016. There was a smell of  $H_2S$  coming from the ground. **e**, Demoiselles in the salt canyons of Dallol dome west flank. **f**, The cave reservoir of the salt canyons. **g**, View from one of the islands of Lake Karum. The top of these islands is covered by ancient stromatolites. **h**, Detail of the stromatolites from the top of Lake Karum's islands. **i**, Modern stromatolites in Lake Karum, with bigger gypsum crystals than the ancient ones. There is no evidence yet of the biogenicity of these stromatolites and no biofilm could be observed.

### 1.2.3.7 The Western Canyons Lakes

Bubbling pools aligned following an E-W direction north of the Round Mountain, 3.5 km west of the Dallol crater (Figure 4-b). Their age and origin are not known, but were already recorded by (Holwerda and Hutchinson 1968) and are visible on Landsat satellite imagery taken in 2003 and distributed by Google Earth in much the same shape and size as at present. Their orange colour reminds the one of Lake Gaet'ale, if a bit browner (Figure 9-a-c). Holwerda and Hutchinson (1968) describe them as pools of salt-saturated brine at ambient temperature in which  $CO_2$  gas is escaping into the atmosphere. An analysis of these brines showed 1.69% KCl, 11.70% NaCl, 6.49%  $MgCl_2$  and 6.45%  $CaCl_2$  w/v (%), as well as minor quantities of

bromine, strontium and boron compounds. They estimate that these lakes are degassing CO<sub>2</sub> and that their water level is related to groundwater level and fluctuate seasonally.

After their first mention in 1968, those lakes fell into oblivion before we visited them again in 2019, where we were able to measure their salinity (~30%) and pH (~5) (see Chapter 6). We named them the Western Canyons Lakes because of their proximity with the canyons of the Round Mountain (at the west of the Dallol dome), but it would be interesting to ask the Afar people if they have named them already.

### 1.2.3.8 Dallol and its surroundings' systems: a resource to explore the limits of life

**Table 2 | Summary of mean temperature, pH and salinity measures of the main sampling areas and their standard deviation.** For more information on the methods, see Materials and Methods and corresponding chapters (chapter 4,5,6).

	Temperature (°C)	pH	Salinity (%)
Dallol Ponds	52.13 ± 31.00	-0.53 ± 0.32	38 ± 9
Lake Gaet'ale (Yellow Lake)	39.20 ± 1.60	1.80 ± 0.20	>50
Black Lake	68.13 ± 7.13	2.92 ± 0.50	76
Western Canyons Lakes	29.56 ± 0.64	4.96 ± 0.10	32 ± 3
Salt canyons cave	25.50 ± 3.50	6.25 ± 0.30	30
Hydrothermally active salt plain	29.3	4.21	20
Lake Karum/Assale	27.18 ± 3.95	6.65 ± 0.08	25 ± 6

As resumed in Table 2, Dallol and its surrounding ecosystems present within a few kilometres range rare polyextreme conditions: different intensities of hypersalinity and acidity with different salt chemistries as suggested by the different water colours. The area is thus perfect to explore the possibility and the limits of life along with the very rare combination of saline-acidity-temperature gradients and discover potential new (poly)extremophiles (see Table 3 for the habitability range of the parameters of interest in Dallol area). Such organisms would be of great interest, as previously mentioned, for biotechnologies, astrobiology or the understanding of similar past environments.

Despite their attractivity, the biology of these environments had never been investigated until recently, since the first fields trips expeditions with microbiologists including ours started in 2016 to the best of our knowledge.

**Table 3 | Known limits of life that may be met in Dallol and its surrounding ecosystems.** Water activity, chaotropy and ionic strength are linked with the chemical composition of solutes. They are further described in the associated articles and in the Materials and Methods chapter.

	<i>Habitability range</i>	<i>References</i>
<i>Temperature</i>	-15°C ↔ 122°C	(Mykytczuk et al. 2013; Takai et al. 2008)
<i>pH</i>	~0 ↔ 11.4	(Schleper et al. 1996; Sturr, Guffanti, and Krulwich 1994)
<i>Salinity (NaCl)</i>	≤350 (g/L)	(Bodaker et al. 2010; Antón et al. 2000)
<i>Water activity</i>	≥0.585	(Stevenson et al. 2017; 2015)
<i>Chaotropy</i>	≤87.3 (kJ/kg)	(Hallsworth et al. 2007)
<i>Ionic strength</i>	≤12.141	(Fox-Powell et al. 2016)

## References

- Aberth, J. 2016. *The Black Death, The Great Mortality of 1348-1350: A Brief History with Documents*. Bedford/St. Martin's. <https://books.google.fr/books?id=vF-ODAEACAAJ>.
- Aerts, Raf, and Eva J. J. November. 2017. "The Dallol Volcano." *Wilderness & Environmental Medicine* 28 (2): 161. <https://doi.org/10/ghb97b>.
- Albarede, Francis, Fanny Thibon, Janne Blichert-Toft, and Harilaos Tsikos. 2020. "Chemical Archeoceanography." *Chemical Geology* 548 (August): 119625. <https://doi.org/10/ghdb8x>.
- Antón, Josefa, Ramón Rosselló-Mora, Francisco Rodríguez-Valera, and Rudolf Amann. 2000. "Extremely Halophilic Bacteria in Crystallizer Ponds from Solar Salterns." *Applied and Environmental Microbiology* 66 (7): 3052–57.
- Ayele, Atalay, Eric Jacques, Mohammed Kassim, Tesfaye Kidane, Ahmed Omar, Stephen Tait, Alexandre Necessian, Jean-Bernard de Chaballier, and Geoffrey King. 2007. "The Volcano–Seismic Crisis in Afar, Ethiopia, Starting September 2005." *Earth and Planetary Science Letters* 255 (1): 177–87. <https://doi.org/10/chhb95>.
- Bar-On, Yinon M., Rob Phillips, and Ron Milo. 2018. "The Biomass Distribution on Earth." *Proceedings of the National Academy of Sciences* 115 (25): 6506–11. <https://doi.org/10/cp29>.
- Beadle, G. W., and E. L. Tatum. 1941. "Genetic Control of Biochemical Reactions in Neurospora." *Proceedings of the National Academy of Sciences* 27 (11): 499–506. <https://doi.org/10/fqh467>.
- Belilla, Jodie, David Moreira, Ludwig Jardillier, Guillaume Reboul, Karim Benzerara, José M. López-García, Paola Bertolino, Ana I. López-Archilla, and Purificación López-García. 2019. "Hyperdiverse Archaea near Life Limits at the Polyextreme Geothermal Dallol Area." *Nature Ecology & Evolution* 3 (11): 1552–61. <https://doi.org/10/ggr3sj>.
- Benison, Kathleen Counter, and Robert H. Goldstein. 2001. "Evaporites and Siliciclastics of the Permian Nippewalla Group of Kansas, USA: A Case for Non-Marine Deposition in Saline Lakes and Saline Pans." *Sedimentology* 48 (1): 165–88. <https://doi.org/10/bz3vxx>.

- Benison, Kathleen Counter, Robert H. Goldstein, Brigitte Wopenka, Robert C. Burruss, and Jill Dill Pasteris. 1998. "Extremely Acid Permian Lakes and Ground Waters in North America." *Nature* 392 (6679): 911–14. <https://doi.org/10/dkgsdm>.
- Bergey, D. H., Robert S. Breed, and Nathan R. Smith. 1957. *Bergey's Manual of Determinative Bacteriology*. 7th ed. Baltimore,: Williams & Wilkins Co.,. <https://www.biodiversitylibrary.org/item/41848>.
- Binega, Yigzaw. 2006. "Chemical Analysis of the Assale (Ethiopia) Rock Salt Deposit." *Bulletin of the Chemical Society of Ethiopia* 20 (2): 319–24. <https://doi.org/10/bd64zf>.
- Bodaker, Idan, Itai Sharon, Marcelino T. Suzuki, Roi Feingersch, Michael Shmoish, Ekaterina Andreishcheva, Mitchell L. Sogin, et al. 2010. "Comparative Community Genomics in the Dead Sea: An Increasingly Extreme Environment." *The ISME Journal* 4 (3): 399–407. <https://doi.org/10/fk6c34>.
- Bonatti, Enrico, Cesare Emiliani, Göte Ostlund, and Harold Rydell. 1971. "Final Desiccation of the Afar Rift, Ethiopia." *Science* 172 (3982): 468–69. <https://doi.org/10/bxh7bs>.
- Borgia, Andrea, Maurice Aubert, Olivier Merle, and Benjamin Van Wyk De Vries. 2010. *What Is a Volcano ?* Special Paper 470. The Geological Society of America. [https://doi.org/10.1130/2010.2470\(01\)](https://doi.org/10.1130/2010.2470(01)).
- Bosch, Thomas C. G., and Margaret J. McFall-Ngai. 2011. "Metaorganisms as the New Frontier." *Zoology* 114 (4): 185–90. <https://doi.org/10/b7b7qf>.
- Brasier, Martin D., Owen R. Green, Andrew P. Jephcoat, Annette K. Kleppe, Martin J. Van Kranendonk, John F. Lindsay, Andrew Steele, and Nathalie V. Grassineau. 2002. "Questioning the Evidence for Earth's Oldest Fossils." *Nature* 416 (6876): 76–81. <https://doi.org/10/d39djh>.
- Brock, Thomas D. 2001. "The Origins of Research on Thermophiles." In *Thermophiles Biodiversity, Ecology, and Evolution*, edited by Anna-Louise Reysenbach, Mary Voytek, and Rocco Mancinelli, 1–9. Boston, MA: Springer US. [https://doi.org/10.1007/978-1-4615-1197-7\\_1](https://doi.org/10.1007/978-1-4615-1197-7_1).
- Bulat, Sergey A., Irina A. Alekhina, Dominique Marie, Jean Martins, and Jean Robert Petit. 2011. "Searching for Life in Extreme Environments Relevant to Jovian's Europa: Lessons from Subglacial Ice Studies at Lake Vostok (East Antarctica)." *Advances in Space Research, Europa Lander: Science Goals and Implementation*, 48 (4): 697–701. <https://doi.org/10/d7m9mj>.
- Carniel, Roberto, Ester Muñoz Jolis, and Josh Jones. 2010. "A Geophysical Multi-Parametric Analysis of Hydrothermal Activity at Dallol, Ethiopia." *Journal of African Earth Sciences, Active Volcanism and Continental Rifting in Africa*, 58 (5): 812–19. <https://doi.org/10/dzv55m>.
- Catchpole, Ryan J., and Patrick Forterre. 2019. "The Evolution of Reverse Gyrase Suggests a Nonhyperthermophilic Last Universal Common Ancestor." *Molecular Biology and Evolution* 36 (12): 2737–47. <https://doi.org/10/ghdcbg>.
- Cavalazzi, B., R. Barbieri, F. Gómez, B. Capaccioni, K. Olsson-Francis, M. Pondrelli, A. P. Rossi, et al. 2019. "The Dallol Geothermal Area, Northern Afar (Ethiopia)-An Exceptional Planetary Field Analog on Earth." *Astrobiology* 19 (4): 553–78. <https://doi.org/10/ggvk97>.
- Chorowicz, Jean. 2005. "The East African Rift System." *Journal of African Earth Sciences, Phanerozoic Evolution of Africa*, 43 (1): 379–410. <https://doi.org/10/fjtt6t>.
- Clark, Benton C., and Daniel C. Van Hart. 1981. "The Salts of Mars." *Icarus* 45 (2): 370–78. <https://doi.org/10/ccj745>.

- Cockell, Charles S. 2014. "Trajectories of Martian Habitability." *Astrobiology* 14 (2): 182–203. <https://doi.org/10/ghdcw4>.
- Collet, B, H Taud, J. F Parrot, F Bonavia, and J Chorowicz. 2000. "A New Kinematic Approach for the Danakil Block Using a Digital Elevation Model Representation." *Tectonophysics* 316 (3): 343–57. <https://doi.org/10/c7b8tz>.
- Copeland, Herbert F. 1938. "The Kingdoms of Organisms." *The Quarterly Review of Biology* 13 (4): 383–420. <https://doi.org/10/bfpdtx>.
- Corti, Giacomo, Ian D. Bastow, Derek Keir, Carolina Pagli, and Elizabeth Baker. 2015. "Rift-Related Morphology of the Afar Depression." In *Landscapes and Landforms of Ethiopia*, edited by Paolo Billi, 251–74. World Geomorphological Landscapes. Dordrecht: Springer Netherlands. [https://doi.org/10.1007/978-94-017-8026-1\\_15](https://doi.org/10.1007/978-94-017-8026-1_15).
- Crick, F. H. 1958. "On Protein Synthesis." *Symposia of the Society for Experimental Biology* 12: 138–63.
- Crick, F. H. C., Leslie Barnett, S. Brenner, and R. J. Watts-Tobin. 1961. "General Nature of the Genetic Code for Proteins." *Nature* 192 (4809): 1227–32. <https://doi.org/10/d3j69t>.
- Darrah, Thomas H., Dario Tedesco, Franco Tassi, Orlando Vaselli, Emilio Cuoco, and Robert J. Poreda. 2013. "Gas Chemistry of the Dallol Region of the Danakil Depression in the Afar Region of the Northern-Most East African Rift." *Chemical Geology, Frontiers in Gas Geochemistry*, 339 (February): 16–29. <https://doi.org/10/f4ssm3>.
- Darwin, Charles, 1809-1882. 1859. *On the Origin of Species by Means of Natural Selection, or Preservation of Favoured Races in the Struggle for Life*. London : John Murray, 1859. <https://search.library.wisc.edu/catalog/9934839413602122>.
- Di Giulio, Massimo. 2003. "The Universal Ancestor and the Ancestor of Bacteria Were Hyperthermophiles." *Journal of Molecular Evolution* 57 (6): 721–30. <https://doi.org/10/cwn8pf>.
- Eme, Laura, Anja Spang, Jonathan Lombard, Courtney W. Stairs, and Thijs J. G. Ettema. 2017. "Archaea and the Origin of Eukaryotes." *Nature Reviews. Microbiology* 15 (12): 711–23. <https://doi.org/10/gc2f7q>.
- Escudero, L., J. Bijman, G. Chong, J. J. Pueyo, and C. Demergasso. 2013. "Geochemistry and Microbiology in an Acidic, High Altitude (4,000 m) Salt Flat — High Andes, Northern Chile." <https://doi.org/10/ghdcg7>.
- Finneran, Kevin T., Meghan E. Housewright, and Derek R. Lovley. 2002. "Multiple Influences of Nitrate on Uranium Solubility during Bioremediation of Uranium-Contaminated Subsurface Sediments." *Environmental Microbiology* 4 (9): 510–16. <https://doi.org/10/bgvpg4>.
- Fox-Powell, Mark G., John E. Hallsworth, Claire R. Cousins, and Charles S. Cockell. 2016. "Ionic Strength Is a Barrier to the Habitability of Mars." *Astrobiology* 16 (6): 427–42. <https://doi.org/10/f8qjhr>.
- Gebresilassie, S., H. Tsegab, and K. Kabeto. 2011. "Preliminary Study on Geology, Mineral Potential and Characteristics of Hot Springs from Dallol Area, Afar Rift, Northeastern Ethiopia: Implications for Natural Resource Exploration." *Momona Ethiopian Journal of Science* 3 (2). <https://doi.org/10/c8th3t>.
- Guo, Qingjun, Harald Strauss, Alan J. Kaufman, Stefan Schröder, Jens Gutzmer, Boswell Wing, Margaret A. Baker, et al. 2009. "Reconstructing Earth's Surface Oxidation across the Archean-Proterozoic Transition." *Geology* 37 (5): 399–402. <https://doi.org/10/djj88v>.

- Haeckel, Ernst, 1834-1919. 1866. *Generelle Morphologie Der Organismen : Allgemeine Grundzüge Der Organischen Formen-Wissenschaft, Mechanisch Begründet Durch Die von Charles Darwin Reformirte Descendenz-Theorie*. Berlin : G. Reimer, 1866. <https://search.library.wisc.edu/catalog/999567599902121>.
- Hallsworth, John E., Michail M. Yakimov, Peter N. Golyshin, Jenny L. M. Gillion, Giuseppe D'Auria, Flavia De Lima Alves, Violetta La Cono, et al. 2007. "Limits of Life in MgCl<sub>2</sub>-Containing Environments: Chaotropy Defines the Window." *Environmental Microbiology* 9 (3): 801–13. <https://doi.org/10/fktqwc>.
- Harrison, Jesse P., Nicolas Gheeraert, Dmitry Tsigelnitskiy, and Charles S. Cockell. 2013. "The Limits for Life under Multiple Extremes." *Trends in Microbiology* 21 (4): 204–12. <https://doi.org/10/f4wgwh>.
- Hassani, M. Amine, Ezgi Özkurt, Heike Seybold, Tal Dagan, and Eva H. Stukenbrock. 2019. "Interactions and Coadaptation in Plant Metaorganisms." *Annual Review of Phytopathology* 57 (1): 483–503. <https://doi.org/10/ghc7xt>.
- Hippocrates. *On Airs, Waters and Places*. Translated by Francis Adam. <https://onemorelibrary.com/index.php/en/books/technology/book/medicine-314/on-air-water-and-places-2425>.
- Holland, Heinrich D. 2002. "Volcanic Gases, Black Smokers, and the Great Oxidation Event." *Geochimica et Cosmochimica Acta* 66 (21): 3811–26. <https://doi.org/10/bzns2c>.
- Holmes, Arthur. 1919. "I.—Non-German Sources of Potash." *Geological Magazine* 6 (8): 340–50. <https://doi.org/10/fqdzp5>.
- Holwerda, James G., and Richard W. Hutchinson. 1968. "Potash-Bearing Evaporites in the Danakil Area, Ethiopia." *Economic Geology* 63 (2): 124–50. <https://doi.org/10/dppvm6>.
- Hooke, Robert (1635-1703) Auteur du texte. 1665. *Micrographia or Some physiological descriptions of minutes bodies made by magnifying glasses : with observations and inquiries thereupon ([Reprod.]) / by R. Hooke,...* <https://gallica.bnf.fr/ark:/12148/bpt6k98770v>.
- Hutchinson, R. W., and G. G. Engels. 1972. "Tectonic Evolution in the Southern Red Sea and Its Possible Significance to Older Rifted Continental Margins." *GSA Bulletin* 83 (10): 2989–3002. <https://doi.org/10/ctgsqc>.
- Irwin, Jane A. 2020. "Chapter 6 - Overview of Extremophiles and Their Food and Medical Applications." In *Physiological and Biotechnological Aspects of Extremophiles*, edited by Richa Salwan and Vivek Sharma, 65–87. Academic Press. <https://doi.org/10.1016/B978-0-12-818322-9.00006-X>.
- Jaini, Padmanabh S. 1998. *The Jaina Path of Purification*. Motilal Banarsidass Publishe.
- Johnson, David. 2009. "Extremophiles: Acidic Environments." In *Encyclopaedia of Microbiology*, 107–26. <https://doi.org/10.1016/B978-012373944-5.00278-9>.
- Johnson, David Barrie. 2010. "The Biogeochemistry of Biomining." In *Geomicrobiology: Molecular and Environmental Perspective*, edited by Larry L. Barton, Martin Mandl, and Alexander Loy, 401–26. Dordrecht: Springer Netherlands. [https://doi.org/10.1007/978-90-481-9204-5\\_19](https://doi.org/10.1007/978-90-481-9204-5_19).
- Johnson, Sarah Stewart, Marc Gerard Chevrette, Bethany L. Ehlmann, and Kathleen Counter Benison. 2015. "Insights from the Metagenome of an Acid Salt Lake: The Role of Biology in an Extreme Depositional Environment." *PLOS ONE* 10 (4): e0122869. <https://doi.org/10/f7j2jj>.

- Kang, Chang-Ho, Soo Ji Oh, YuJin Shin, Sang-Hyun Han, In-Hyun Nam, and Jae-Seong So. 2015. “Bioremediation of Lead by Ureolytic Bacteria Isolated from Soil at Abandoned Metal Mines in South Korea.” *Ecological Engineering* 74 (January): 402–7. <https://doi.org/10/f6wxqb>.
- Karl, D. M., D. F. Bird, K. Björkman, T. Houlihan, R. Shackelford, and L. Tupas. 1999. “Microorganisms in the Accreted Ice of Lake Vostok, Antarctica.” *Science* 286 (5447): 2144–47. <https://doi.org/10/d9x9nh>.
- Keir, Derek, Ian D. Bastow, Carolina Pagli, and Emma L. Chambers. 2013. “The Development of Extension and Magmatism in the Red Sea Rift of Afar.” *Tectonophysics*, The Gulf of Aden rifted margins system : Special Issue dedicated to the YOCMAL project (Young Conjugate Margins Laboratory in the Gulf of Aden), 607 (November): 98–114. <https://doi.org/10/ghdcvf>.
- Knauth, L. Paul. 2005. “Temperature and Salinity History of the Precambrian Ocean: Implications for the Course of Microbial Evolution.” *Palaeogeography, Palaeoclimatology, Palaeoecology*, Geobiology: Objectives, Concept, Perspectives, 219 (1): 53–69. <https://doi.org/10/dncb4c>.
- Knoll, Andrew H., Don E. Canfield, and Kurt O. Konhauser. 2012. *Fundamentals of Geobiology*. John Wiley & Sons.
- Kotopoulou, Electra, Antonio Delgado Huertas, Juan Manuel Garcia-Ruiz, Jose M. Dominguez-Vera, Jose Maria Lopez-Garcia, Isabel Guerra-Tschuschke, and Fernando Rull. 2019. “A Polyextreme Hydrothermal System Controlled by Iron: The Case of Dallol at the Afar Triangle.” *ACS Earth & Space Chemistry* 3 (1): 90–99. <https://doi.org/10/ghdcr4>.
- Krause, Paul F., and Kathleen L. Flood. 1997. “Weather and Climate Extremes.” ARMY TOPOGRAPHIC ENGINEERING CENTER ALEXANDRIA VA. <https://apps.dtic.mil/sti/citations/ADA346058>.
- Lane, Nick. 2015. “The Unseen World: Reflections on Leeuwenhoek (1677) ‘Concerning Little Animals.’” *Philosophical Transactions of the Royal Society B: Biological Sciences* 370 (1666): 20140344. <https://doi.org/10/ghc9rd>.
- Leeuwenhoek, Antoni Van. 1705. “I. A Letter to the Royal Society, from Mr. Anthony Van Leeuwenhoek, F. R. S. Concerning Animalcula on the Roots of Duck-Weed, &c.” *Philosophical Transactions of the Royal Society of London* 24 (295): 1784–93. <https://doi.org/10/bmmr48>.
- López-García, José M., David Moreira, Karim Benzerara, Olivier Grunewald, and Purificación López-García. 2020a. “Origin and Evolution of the Halo-Volcanic Complex of Dallol: Proto-Volcanism in Northern Afar (Ethiopia).” *Frontiers in Earth Science* 7. <https://doi.org/10/ggsr6x>.
- . 2020b. “Origin and Evolution of the Halo-Volcanic Complex of Dallol: Proto-Volcanism in Northern Afar (Ethiopia).” *Frontiers in Earth Science* 7. <https://doi.org/10/ggsr6x>.
- López-García, Purificación, Laura Eme, and David Moreira. 2017. “Symbiosis in Eukaryotic Evolution.” *Journal of Theoretical Biology*, The origin of mitosing cells: 50th anniversary of a classic paper by Lynn Sagan (Margulis), 434 (December): 20–33. <https://doi.org/10/gfb6fk>.
- López-García, Purificación, Yvan Zivanovic, Philippe Deschamps, and David Moreira. 2015. “Bacterial Gene Import and Mesophilic Adaptation in Archaea.” *Nature Reviews Microbiology* 13 (7): 447–56. <https://doi.org/10/gfb6fm>.

- López-García, Purificación, and David Moreira. 1999. "Metabolic Symbiosis at the Origin of Eukaryotes." *Trends in Biochemical Sciences* 24 (3): 88–93. <https://doi.org/10/dzv9kx>.
- Maezato, Yukari, and Paul Blum. 2012. "Survival of the Fittest: Overcoming Oxidative Stress at the Extremes of Acid, Heat and Metal." *Life : Open Access Journal* 2 (3): 229–42. <https://doi.org/10/gchrtf>.
- Martins, Zita, Hervé Cottin, Julia Michelle Kotler, Nathalie Carrasco, Charles S. Cockell, Rosa de la Torre Noetzel, René Demets, et al. 2017. "Earth as a Tool for Astrobiology—A European Perspective." *Space Science Reviews* 209 (1): 43–81. <https://doi.org/10/gbmz2r>.
- Master, Sharad. 2016. "Gaet'ale- a Reactivated Thermal Spring and Potential Tourist Hazard in the Asale Salt Flats, Danakil Depression, Ethiopia." *Journal of Applied Volcanology* 5 (1): 1. <https://doi.org/10/ghdcx2>.
- Matthaei, J. Heinrich, Oliver W. Jones, Robert G. Martin, and Marshall W. Nirenberg. 1962. "CHARACTERISTICS AND COMPOSITION OF RNA CODING UNITS\*." *Proceedings of the National Academy of Sciences of the United States of America* 48 (4): 666–77.
- Merino, Nancy, Heidi S. Aronson, Diana P. Bojanova, Jayme Feyhl-Buska, Michael L. Wong, Shu Zhang, and Donato Giovannelli. 2019. "Living at the Extremes: Extremophiles and the Limits of Life in a Planetary Context." *Frontiers in Microbiology* 10. <https://doi.org/10/gfzhh6>.
- Mitchell, D. J. W., R. B. Allen, W. Salama, and A. Abouzakm. 1992. "Tectonostratigraphic Framework and Hydrocarbon Potential of the Red Sea." *Journal of Petroleum Geology* 15 (s3): 187–210. <https://doi.org/10/cbds4c>.
- Mormile, Melanie R., Bo-Young Hong, and Kathleen C. Benison. 2009. "Molecular Analysis of the Microbial Communities of Mars Analog Lakes in Western Australia." *Astrobiology* 9 (10): 919–30. <https://doi.org/10/d7jds>.
- Mykytczuk, Nadia C S, Simon J Foote, Chris R Omelon, Gordon Southam, Charles W Greer, and Lyle G Whyte. 2013. "Bacterial Growth at –15 °C; Molecular Insights from the Permafrost Bacterium *Planococcus Halocryophilus* Or1." *The ISME Journal* 7 (6): 1211–26. <https://doi.org/10/f463p7>.
- Nanis, Hafid, and Mohamed H. Aly. 2020. "Desegregation of Remote Sensing and GIS to Characterize Fluctuations in the Surface Water Area of Afar Lakes, Ethiopia." *Geocarto International* 35 (9): 976–90. <https://doi.org/10/ghddxk>.
- Nobile, Adriano, Carolina Pagli, Derek Keir, Tim J. Wright, Atalay Ayele, Joel Ruch, and Valerio Acocella. 2012. "Dike-Fault Interaction during the 2004 Dallol Intrusion at the Northern Edge of the Erta Ale Ridge (Afar, Ethiopia)." *Geophysical Research Letters* 39 (19). <https://doi.org/10/ghdcks>.
- Oh, Dickson, Kate Porter, Brendan Russ, David Burns, and Mike Dyll-Smith. 2010. "Diversity of *Haloquadratum* and Other Haloarchaea in Three, Geographically Distant, Australian Saltern Crystallizer Ponds." *Extremophiles* 14 (2): 161–69. <https://doi.org/10/fjhkx3>.
- Oremland, Ronald S., Chad W. Saltikov, Felisa Wolfe-Simon, and John F. Stolz. 2009. "Arsenic in the Evolution of Earth and Extraterrestrial Ecosystems." *Geomicrobiology Journal* 26 (7): 522–36. <https://doi.org/10/cfkxdc>.
- Oren, Aharon. 2015. "Halophilic Microbial Communities and Their Environments." *Current Opinion in Biotechnology, Environmental biotechnology • Energy biotechnology*, 33 (June): 119–24. <https://doi.org/10/f7hkxq>.

- Pérez, Eduardo, and Yonas Chebude. 2017. "Chemical Analysis of Gaet'ale, a Hypersaline Pond in Danakil Depression (Ethiopia): New Record for the Most Saline Water Body on Earth." *Aquatic Geochemistry* 23 (2): 109–17. <https://doi.org/10/ghdczg>.
- Ring, Uwe. 2014. "The East African Rift System." *Austrian Journal of Earth Sciences* 107 (January): 132–46.
- Saiki, R. K., D. H. Gelfand, S. Stoffel, S. J. Scharf, R. Higuchi, G. T. Horn, K. B. Mullis, and H. A. Erlich. 1988. "Primer-Directed Enzymatic Amplification of DNA with a Thermostable DNA Polymerase." *Science* 239 (4839): 487–91. <https://doi.org/10/gfdb23>.
- Sara Parwin Banu, Kamaludeen, K Arunkumar, Avudainayagam Subramanian, and K Ramasamy. 2003. "Bioremediation of Chromium Contaminated Environments." *Indian Journal of Experimental Biology* 41 (October): 972–85.
- Schleper, Christa, Gabriela Puhler, Hans- Peter Klenk, and Wolfram Zillig. 1996. "Picophilus Oshimae and Picophilus Tomdus Fam. Nov., Gen. Nov., Sp. Nov., Two Species of Hyperacidophilic, Thermophilic, Heterotrophic, Aerobic Archaea," *International Journal of Systematic Bacteriology*, 46 (3): 814–16. <https://doi.org/10.1099/00207713-46-3-814>.
- Schopf, J. W., and B. M. Packer. 1987. "Early Archean (3.3-Billion to 3.5-Billion-Year-Old) Microfossils from Warrawoona Group, Australia." *Science (New York, N.Y.)* 237 (July): 70–73. <https://doi.org/10/cnv8vd>.
- Segata, Nicola, Daniela Boernigen, Timothy L Tickle, Xochitl C Morgan, Wendy S Garrett, and Curtis Huttenhower. 2013. "Computational Meta'omics for Microbial Community Studies." *Molecular Systems Biology* 9 (1): 666. <https://doi.org/10/f2pc7m>.
- Sharp, Christine E., Allyson L. Brady, Glen H. Sharp, Stephen E. Grasby, Matthew B. Stott, and Peter F. Dunfield. 2014. "Humboldt's Spa: Microbial Diversity Is Controlled by Temperature in Geothermal Environments." *The ISME Journal* 8 (6): 1166–74. <https://doi.org/10/f56c26>.
- Singh, Upinder. 2008. *A History of Ancient and Early Medieval India: From the Stone Age to the 12th Century*. Pearson Education India.
- Spang, Anja, Eva F. Caceres, and Thijs J. G. Ettema. 2017. "Genomic Exploration of the Diversity, Ecology, and Evolution of the Archaeal Domain of Life." *Science* 357 (6351). <https://doi.org/10/gc2cmq>.
- Stevenson, Andrew, Jonathan A Cray, Jim P Williams, Ricardo Santos, Richa Sahay, Nils Neuenkirchen, Colin D McClure, et al. 2015. "Is There a Common Water-Activity Limit for the Three Domains of Life?" *The ISME Journal* 9 (6): 1333–51. <https://doi.org/10/f7cm86>.
- Stevenson, Andrew, Philip G. Hamill, Callum J. O'Kane, Gerhard Kminek, John D. Rummel, Mary A. Voytek, Jan Dijksterhuis, and John E. Hallsworth. 2017. "Aspergillus Penicillioides Differentiation and Cell Division at 0.585 Water Activity." *Environmental Microbiology* 19 (2): 687–97. <https://doi.org/10/f9n7kk>.
- Sturr, M G, A A Guffanti, and T A Krulwich. 1994. "Growth and Bioenergetics of Alkaliphilic Bacillus Firmus OF4 in Continuous Culture at High PH." *Journal of Bacteriology* 176 (11): 3111–16.
- Takai, Ken, Kentaro Nakamura, Tomohiro Toki, Urumu Tsunogai, Masayuki Miyazaki, Junichi Miyazaki, Hisako Hirayama, Satoshi Nakagawa, Takuro Nunoura, and Koki Horikoshi. 2008. "Cell Proliferation at 122°C and Isotopically Heavy CH<sub>4</sub> Production by a Hyperthermophilic Methanogen under High-Pressure Cultivation." *Proceedings of the National Academy of Sciences* 105 (31): 10949–54. <https://doi.org/10/crqvsn>.

- Tansey, Michael R., and Thomas D. Brock. 1972. "The Upper Temperature Limit for Eukaryotic Organisms." *Proceedings of the National Academy of Sciences* 69 (9): 2426–28. <https://doi.org/10/ffj4k3>.
- Varro, Marcus Terentius. 1912. *Varro on Farming = M. Terenti Varronis Rerum Rusticarum Libri Tres*. Translated by Lloyd Storr-Best. London : Bell. <http://archive.org/details/varroonfarmingmt00varr>.
- Vartoukian, Sonia R., Richard M. Palmer, and William G. Wade. 2010. "Strategies for Culture of 'Unculturable' Bacteria." *FEMS Microbiology Letters* 309 (1): 1–7. <https://doi.org/10/dkrnfp>.
- Ventosa, Antonio, Rafael R. de la Haba, Cristina Sánchez-Porro, and R. Thane Papke. 2015. "Microbial Diversity of Hypersaline Environments: A Metagenomic Approach." *Current Opinion in Microbiology* 25 (June): 80–87. <https://doi.org/10/ghdbwb>.
- Vereb, Viktor, Benjamin van Wyk de Vries, Miruts Hagos, and Dávid Karátson. 2020. "Geoheritage and Resilience of Dallol and the Northern Danakil Depression in Ethiopia." *Geoheritage* 12 (4): 82. <https://doi.org/10/ghdcrz>.
- Verhoeven, Geert. 2018. "Resolving Some Spatial Resolution Issues – Part 1: Between Line Pairs and Sampling Distance" 57 (October): 25–34. <https://doi.org/10/ghc8zw>.
- Wallace, Alfred Russel. 1858. "Contributions to the Theory of Natural Selection: A Series of Essays," 1858. <https://doi.org/10.1017/CBO9780511693106>.
- Walter, M. R., R. Buick, and J. S. R. Dunlop. 1980. "Stromatolites 3,400–3,500 Myr Old from the North Pole Area, Western Australia." *Nature* 284 (5755): 443–45. <https://doi.org/10/dqqhk2>.
- Whitehouse, M., J. S. Myers, and C. M. Fedo. 2009. "The Akilia Controversy: Field, Structural and Geochronological Evidence Questions Interpretations of >3.8 Ga Life in SW Greenland." *Journal of the Geological Society*. <https://doi.org/10/cbh92h>.
- Whittaker, R. H. 1969. "New Concepts of Kingdoms of Organisms." *Science* 163 (3863): 150–60. <https://doi.org/10/bg85q2>.
- Woese, C. R., O. Kandler, and M. L. Wheelis. 1990. "Towards a Natural System of Organisms: Proposal for the Domains Archaea, Bacteria, and Eucarya." *Proceedings of the National Academy of Sciences of the United States of America* 87 (12): 4576–79. <https://doi.org/10/b7s3gv>.
- Woese, Carl R., and George E. Fox. 1977. "Phylogenetic Structure of the Prokaryotic Domain: The Primary Kingdoms." *Proceedings of the National Academy of Sciences* 74 (11): 5088–90. <https://doi.org/10/ft974h>.
- World Health Organisation. 1993. *Guidelines for Drinking-Water Quality*. World Health Organization.
- Wright, Tim J., Cindy Ebinger, Juliet Biggs, Atalay Ayele, Gezahegn Yirgu, Derek Keir, and Anna Stork. 2006. "Magma-Maintained Rift Segmentation at Continental Rupture in the 2005 Afar Dyking Episode." *Nature* 442 (7100): 291–94. <https://doi.org/10/d5x7x5>.
- Zaikova, Elena, Kathleen C. Benison, Melanie R. Mormile, and Sarah Stewart Johnson. 2018. "Microbial Communities and Their Predicted Metabolic Functions in a Desiccating Acid Salt Lake." *Extremophiles: Life Under Extreme Conditions* 22 (3): 367–79. <https://doi.org/10/gc9w84>.
- Zuckermandl, Emile, and Linus Pauling. 1965. "Molecules as Documents of Evolutionary History." *Journal of Theoretical Biology* 8 (2): 357–66. <https://doi.org/10/cwxpst>.





*The Yellow Lake bubbling surface*  
© DEEM Team

**OBJECTIVES**

## 2. Objectives

As presented in the Introduction, little is known about microbial life in hypersaline, hyperacidic and hot environments. The scarcity of their natural occurrence may be at fault, but it also raises questions about the possibility for microbial life to adapt to those combined conditions when they tend to be more extreme. The Dallol hydrothermal system and its surroundings, with their broad gradients of temperature, salinity and pH with *a priori* different chemical compositions within only a few kilometres of radius, are the ideal places to investigate those rare, potential polyextremophiles.

My thesis work is articulated around three big questions to which we attempt to reply:

### **1. Can we detect microbial life all along the physicochemical gradients of Dallol and its surroundings (especially in the most polyextreme environments)?**

The less polyextreme places of Dallol surroundings in regard of temperature, acidity or salinity are Lake Karum, the salt plain, the cave reservoir (sections 1.3.2.4 to 1.3.2.6). Even though the microbial communities of these sites have never been investigated to our knowledge, we expect their conditions to be favourable to the development of halophile organisms, like it is the case in solar salterns of the Dead Sea (section 1.2.1). They'll constitute, in a sense, natural positive controls for our investigation protocol. On the other hand, we are not sure how the microbial communities will be shaped with the increase of salinity, pH and/or temperature. We expect that we may reach the physicochemical limits of life in some environments and, in this is the case, our goal would be to define those limits more precisely.

### **2. As inhospitable environments are especially sensitive to biocontamination during sampling and analyses, how can we guaranty that the microorganisms detected are endogenous or exogenous?**

If some brines are so multi-extreme that there is possibly no life in them, it is likely that biocontamination, even if minor, will become a major issue for the interpretation of our results. This is true for DNA contamination, but we expect that the risk of confusion with abiotic biomorphs during microscope observations may increase too. One of the main objectives of this work is also to propose a rigorous protocol based on cross-analysis and thoughtful utilization of positive/negative controls for each experiment. This should help to assess if DNA is local or not and if cell-like features are likely to be microbes or abiotic biomorphs. Such a protocol could be applied for similar extreme environments on Earth or beyond.

**3. What kind of microbial communities are found in the environments where the presence of endogenous life was confirmed and how do they change along with the progressively more extreme physicochemical conditions?**

When it is assessed which environment do harbour adapted microorganisms, we can finally describe the microbial diversity using both molecular biology methods (with the construction of 16S/18S rRNA phylogenetical tree) and microscope observations to characterize it. The chemical analyses and physicochemical measures can then be correlated with the microbial communities' change, making it possible to see what are the most polyextreme organisms selected over the salinity-hypersalinity-temperature gradients. Our last goal is to propose selection mechanisms behind those communities change that could be tested in the future with metagenomics, metatranscriptomics or metaproteomics analyses.





*The Black Lake surface and  
bischophite crystallization*

© DEEM Team

**MATERIALS AND METHODS**

## 3. Materials and Methods

Although every subproject had its particularities, the methodological approach we used to reply to the questions asked in the previous chapter is similar in all our studies. This chapter describes the different methodologies and/or technologies we used to give an overview of their purpose and functioning. For a detailed description of the methodology (e.g. brand names of tools, kits, exact list of samples), see the materials and methods section of the corresponding article chapter (chapter 4, 5, 6).

Our team collected samples in the Danakil depression during three expeditions: in January 2016, 2017 and 2019, plus two samples collected for us in 2018 by our collaborator Olivier Grunewald. I took part in the 2017 and 2019 field missions. In total, 235 samples (bottled brine samples, solids, filters) were collected from 95 sampling spots and studied for this manuscript. They mainly come from six areas: the Dallol hydrothermal ponds, Lake Gaet'ale, the Black Lake, the salt canyons and their cave reservoir, the salt plain, the Western Canyons Lakes, and Lake Karum (see chapter 1 for pictures and descriptions).

I took part to all experiments and data treatment, except the elemental and molecular composition analyses and the sequencing that were entrusted to specialized laboratories.

### 3.1 Chemistry analyses

#### 3.1.1 Elemental and molecular composition of samples

Describing the chemistry of a sample is a crucial step to discern the correlations between microorganisms and their environment. *Ex situ* chemical analyses were done on either rock/salt samples or 0.2  $\mu\text{m}$  prefiltered brine samples by the SIDI service of the Universidad Autónoma de Madrid. They included:

- **Inductively coupled plasma mass spectrometry (ICP-MS):** Mass spectrometry is an analytical technique that measures the mass-to-charge ratio of ions. ICP-MS is a type of mass spectrometry that uses a plasma supplied by electric currents (produced by electromagnetic induction) to ionize the sample. It atomizes the sample and creates atomic and small polyatomic ions, which are then detected. This technique was used on liquid samples. The elements H, He, C, N, O, F, S, Cl, Ar, Br and I cannot be adequately quantified due to technique limitation. The result per element is in mg/L.
- **Total Reflection X-ray Fluorescence (TXRF):** X-ray fluorescence analyses are based on the property of atoms excited by an external source (here, X-ray light) to release this energy by emitting X-ray radiation in fluorescence characteristic of each atom (Figure 10). Total reflection X-ray fluorescence makes use of the fact that, at very low glancing

angles, the high background that would generally occur due to scattering from the liquid sample support is absent. We used this technique mainly to recover the concentration of the elements S and Cl. The result is in mg/L.

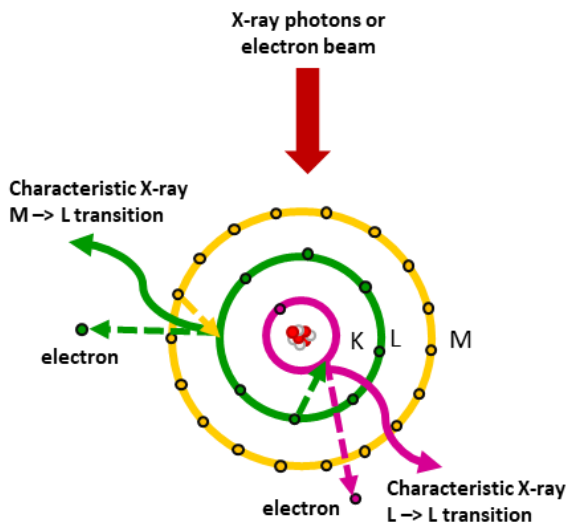


**Figure 10 | Interaction between (X-ray) photons or electron beam with an atom.** When particles (electrons or photons) collide with a tightly bound inner-shell electron with energy higher than the binding, they may eject it and create an unstable vacancy, causing the atom to shift from a fundamental state to an excited one. An outer shell electron transition will fill this vacancy, emitting an X-ray equal to the difference in binding energies of the outer and inner electron shell that are “characteristic” of the atom.

about the 3D distribution and density of electrons within the crystal. From this electron density, the mean positions of the atoms in the crystal can be determined, as well as their chemical bonds and various other information. We used this technique to determine the chemical composition of our salts/rocks.

Coupled all together, those techniques help to infer the chemical composition of the different brines. The salts dissolved can also be assessed based on the stoichiometry of the different elements in addition to the crystallized salts identified.

- **Gas chromatography:** Chromatography is a physical method that separate compounds in a column using two phases, one mobile phase (usually an inert gas in the case of gas chromatography) in which the compounds (called solutes) circulate and one stationary phase (e.g. silica layer). The function of the stationary phase is to cause a phenomenon of chromatographic retention with the different solutes. The more affinity the compound has with the stationary phase, the longer it will take to leave the column. This retention time is used to identify the components of each sample. We used gas chromatography for organic molecules detection and identification.

- **X-ray crystallography (XRC):** XRC is used to determine the atomic and molecular structure of a crystal. The crystalline structure causes a beam of incident X-rays to diffract into many specific directions. The angles and intensities of these diffracted beams give information

### 3.1.2 Measure and calculation of water activity, chaotropy and ionic strength

Considering the extreme salinity and the different chemical composition suggested by the intense colours of some environments, we decided to evaluate the habitability of Dallol and its surrounding environments through three parameters: water activity, chaotropy and ionic strength.

#### 3.1.2.1 Water activity (*aw*)

The water activity (*aw*) is the ratio of the partial vapour pressure of water above a sample to the partial vapour pressure of pure water at the same temperature and pressure (Figure 11). Water activity can display values between 0 (when no water is available in the sample) and 1 (for pure water). A water activity of 0.80 means the vapour pressure is 80% of that of pure water. Water activity should not be mistaken with moisture content, which is the total content of water and does not consider the “(un)availability” of water molecules imprisoned in the sample or already interacting with components. Since no active microorganisms have been reported under 0.585 of water activity, it is considered as the lower limit for microbial life (Stevenson et al. 2015; 2017). On the opposite, substances with higher water activity tend to support more microorganisms (Labuza 1977). We measured water activity of our samples using a probe that measures the partial vapour pressure of the sample in a closed chamber and compares it to the partial vapour pressure of water in the same conditions.

#### 3.1.2.2 Chaotropy

Chaotropy describes the entropic disordering of lipid bilayers and other biomacromolecules which is caused by substances (ion mixtures, aromatics, other solutes...) dissolved in water. It is opposed to kosmotropy, which favours biomacromolecules stability. It is measured in kJ/kg. The experimental method to quantify the chaotropy/kosmotropy potential of a substance was proposed by Cray et al. (2013) with the use of a 1.5% agar (or gelatine) with a fraction of the substance of interest diluted in the solution (Figure 12). The agar in this protocol is used as a proxy for biomolecules. If the substance dissolved in the 1.5% agar solution causes it to gelify at a lower temperature than it would with a pure water solution (<43°C), it means this substance is chaotropic. Conversely, if it causes the 1.5% agar solution to gelify at a higher temperature (>43°C), it means this substance favours agar polymerisation and is kosmotropic. The relation between the substance fraction in the solution and the agar gel point temperature is approximatively linear (Hallsworth, Heim, and Timmis 2003), though the slope may be different from one chaotropic/kosmotropic agent to another. Knowing that the heat capacity of a 1.5% agar gel is 4.15 kJ kg<sup>-1</sup> °C<sup>-1</sup>, it is possible to find the chaotropy/kosmotropy value of the substance.

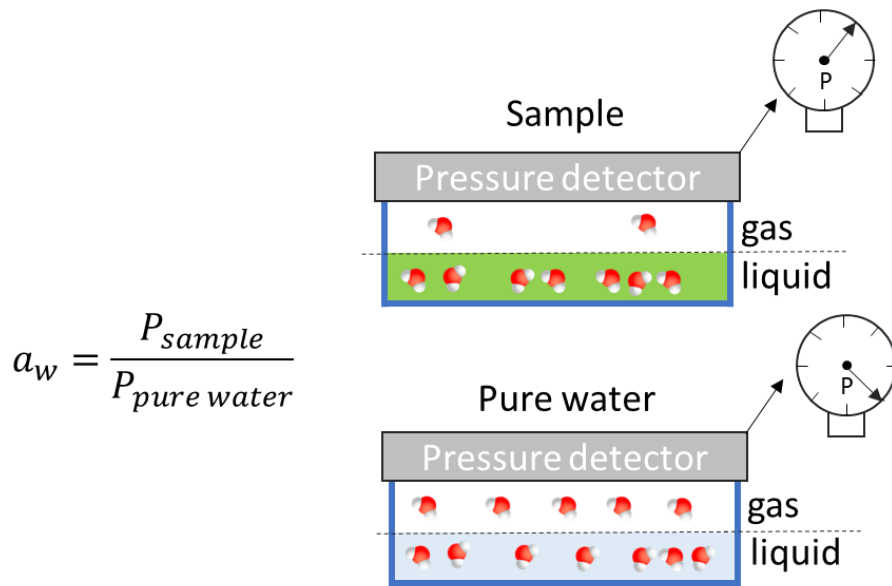


**Figure 11 | Water activity formula and representation of the measuring device.**

**P: partial vapour pressure.** When a sample is placed in a closed container, water molecules with enough energy will escape in the headspace in the form of water vapour, exerting pressure on the top and sides of the container. The more water molecules in the headspace and the faster those molecules are moving, the higher the vapour pressure. The vapour molecules are in a dynamic equilibrium with the liquid water and the overall pressure in the container stays constant while this exchange occurs. Vapour pressure of the sample is the same basic concept. In a sample, fewer water molecules can escape into the headspace compared to the pure water setting, because they interact with components of the sample. The partial vapour pressure of the sample divided by the partial vapour pressure of pure water is the water activity.

Due to the interactions between CaCl<sub>2</sub> and agar, gelatine is recommended instead of agar to analyse solutions that contain this salt (Cray et al. 2013). However, we couldn't find the heat capacity of gelatine in the literature, we thus performed the experiments with both agar and gelatine to estimate the relation between the two and assessed it was linear. Thus, measuring the 1.5% gelatine gel point temperature of a CaCl<sub>2</sub>-rich sample, we could determine the equivalent temperature it would have reached in agar and then calculate its chaotropicity/kosmotropicity value.

The transition point between liquid to solid state of agar or gelatine is determined using a spectrometer (Figure 12). Samples were put in a heated water bath equipped with a thermometer prior to spectrometry measures to monitor their temperature. For samples for which we had elemental composition data but no more liquid available, we estimated their chaotropicity/kosmotropicity through calculations based on their salt composition and

concentration and the known chaotropicity/kosmotropicity of those salts (using measures from Cray et al. (2013)).

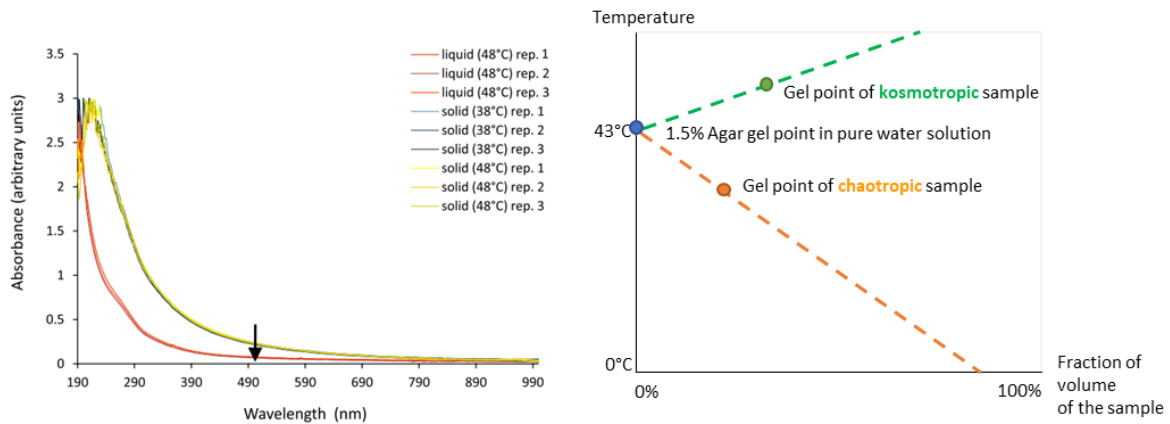


**Figure 12 | The liquid to solid transition of agar with pure water and chaotropic/kosmotropic solution.** On the left graph, the difference of absorbance of liquid (48°C) and solid (38°C) 1.5% (w/v) agar gel (figure from Cray et al. 2013). A visible wavelength of 500 nm (black arrow) was selected for monitoring assays to avoid interference with readings from aromatic solutes absorbing in the ultraviolet range, and to keep absorbance readings below 0.5 in order to maintain accuracy. Furthermore, the spectra for solid agar remained consistent even when the temperature of the gel was elevated from 38 to 48°C, indicating that these absorbance readings were not temperature-sensitive. On the right graph are plotted the gel point temperature of 1.5% agar gel with pure water and with a theoretical chaotropic or kosmotropic sample. Dashed lines represent the linear relationship between the fraction of volume of the sample and its chaotropic or kosmotropic effect on the agar solution.

### 3.1.2.3 Ionic strength

The ionic strength of a solution is a measure of the concentration of ions in that solution. Ionic strength can be expressed in mol/L solution. It is calculated as follows:

$$I = \frac{1}{2} \sum_{i=1}^n c_i z_i^2$$

Where one half is because we are including both cations and anions,  $c_i$  is the molar concentration of ion (M, mol/L),  $z_i$  is the charge number of that ion, and the sum is taken over all ions in the solution.

Due to a complex dependency on charge interactions in biological molecules, high ionic strength can perturb native structure and function. High charge density is capable of inducing

deformations in biomolecules such as nucleic acids and proteins (Baumann et al. 1997; Baldwin 1996). It was hypothesized that ionic strength may play a role in defining the window for habitability even when other parameters such as water activity are permissive (Fox-Powell et al. 2016), which is why we also take it into account in our study.

## 3.2 From DNA extraction to phylogenetic tree

### 3.2.1 DNA purification and 16/18S rRNA gene metabarcoding

DNA extraction of samples was done using Power Soil DNA Isolation Kit and occasionally using Arcturus PicoPure DNA Isolation kit. In the Power Soil kit, the cell lysis occurs by mechanical and chemical methods followed by purifying steps supposed to precipitate non-DNA organic and inorganic material that may reduce DNA purity and inhibit downstream DNA applications. In the last step, total genomic DNA is captured on a silica membrane. DNA is then washed and eluted from the membrane. This procedure provides very pure DNA from a chemically complex sample, though its main drawback is the potential DNA loss at the different steps especially the final one. On the other hand, PicoPure provides a fast and easy genomic DNA extraction procedure that can only be done on cell pellets in our case. The extraction occurs chemically with a Proteinase K solution. After heat-deactivation of the enzyme, the DNA will be ready-to-use for downstream experiments. Since there is no purification step, this method is ideal for samples with few cells where maximum DNA recovery is critical, if the initial cell pellet is “clean” enough.

PCR is a method widely used to make millions to billions of copies (amplicons) of a specific region of a DNA strand. The region of interest for us was the 16S or 18S rRNA gene, which is often used in phylogenetic studies as it is highly conserved between different species of bacteria and archaea (for 16S) and eukaryotes (for 18S) but also has hypervariable regions that can vary significantly between different taxonomic groups (Yang, Wang, and Qian 2016), helping to identify them. This region of interest is targeted using short DNA molecules called primers that are complementary to the 3' end of both complementary strands of the target region. The list of primers used in our study is given in Table 4. For more details about PCR steps, see Figure 13. For our experiments, we used 35 repeated thermal cycles and 50 to 55 °C of annealing temperature depending of the stringency wanted (lower temperature facilitates hybridization between primers and single-stranded DNA but also increases chances of imperfect bindings).

Long amplicons (~900 base pairs or bp, up to ~1400 when merged) were isolated from each other and amplified separately with cloning methods and then sequenced using Sanger sequencing. Though the longest the sequence, the more information we have, this method is time-consuming and only a total of few hundred sequences were obtained this way. Shorter amplicons (~250 when merged) were sequenced with high throughput sequencing method

using Illumina MiSeq technology, producing thousands of reads of the sequences. Though those amplicons are less informative than the longer ones, the number of sequences obtained gives a better coverage of the sample diversity and relative abundances of each taxon. Complementary reads are cleaned and merged and undergo different steps (Figure 14-A) before they are clustered into Operational Taxonomic Units (OTUs, which is a pragmatic proxy for species) based on the similarity of their 16S/18S rRNA gene sequence. We clustered our sequences based on OTUs with a minimum threshold of 95% similarity, which is considered the genus level. OTUs are then compared to database sequences with BLAST algorithms. The BLAST's best-hits, the long Sanger sequences and some additional reference organisms are used to construct a phylogenetic tree. Short Illumina OTUs are then placed on this reference tree using phylogenetic placement. The final tree is then used for interpretation.

The pipeline used to construct the phylogenetic trees is detailed in Figure 14-B.

**Table 4 | Forward and reverse primers used in this study for targeting 16S/18S rRNA genes during PCR and their nucleotides sequences.**

Forward primer	Sequence	16S/18S Target
21F	5'-TTCCGGTTGATCCTGCCGGA	Archaea
27F	5'-AGAGTTTGATCCTGGCTCAG	Bacteria
82F	5'-GGTTACCTTGTTACGACTT	Eukaryotes
Ar109F	5'-ACKGCTGCTCAGTAACACGT	Archaea
U340F	5'-CCTACGGGRBGCASCAG	Archaea/Bacteria
U515F	5'-GTGCCAGCMGCCGCGGTAA	Archaea/Bacteria
EK565F	5'-GCAGTTAAAAAGCTCGTAGT	Eukaryotes
Reverse primer	Sequence	16S/18S Target
1492R	5'-GGTTACCTTGTTACGACTT	Archaea/Bacteria
1520R	5'-CYGCAGGTTACCTAC	Eukaryotes
U806R	5'-GTGCCAGCMGCCGCGGTAA	Archaea/Bacteria
1134-R-UNonMet	5'-TTTAAGTTTCAGCCTTGCG	Eukaryotes

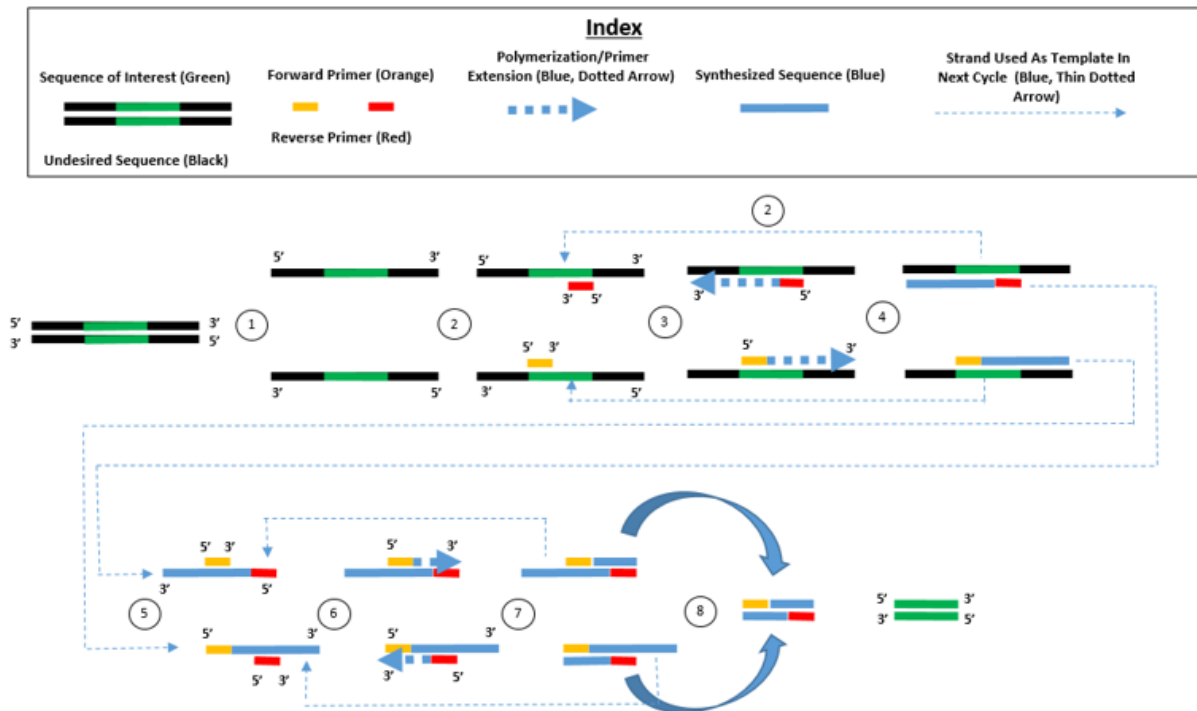


**Figure 13 | Polymerase Chain Reaction steps (Credit: Mwt4fd).**

1. The DNA double helix is melted apart with a temperature above 90 °C: its strands separate.
2. The temperature is decreased to slightly below the melting temperature of both the primers being used (annealing temperature). Both primers bind to the available DNA strands.
3. Polymerization (extension of the complementary strand) occurs thanks to the polymerase enzyme in the 5' to 3' direction for each strand. Temperature = 75 °C
- 4-5. The previously polymerized strands act as a template for the other primers for the next cycle.
6. Polymerisation occurs again. After the 1<sup>st</sup> cycle, only the sequence of interest is amplified.
- 7-8. Cycle repeats and more amplicons of the interest region are produced.

The copies of this target region are exponentially amplified in a series of cycles of temperature changes (thermal cycles), the amplification process is limited by the amount of available substrates (primers, single nucleotides, polymerase) for the reaction.

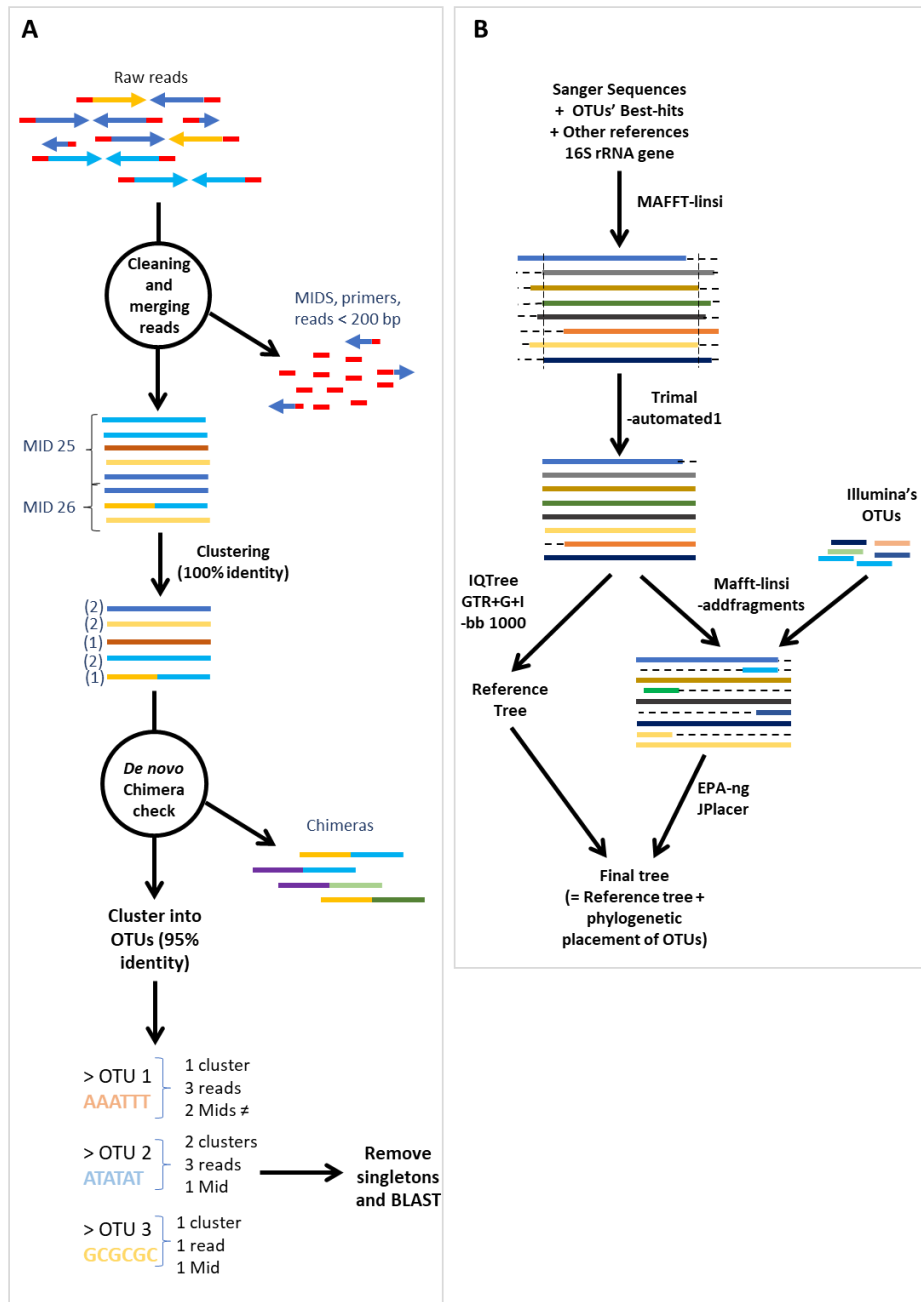


**Figure 14 | Data treatment of 16S rRNA gene sequences from raw reads to phylogenetic trees. A,** Metabarcoding raw reads contain multiplex identifiers (MIDs) to tell apart amplicons from several independent samples. After the sequence's original sample has been identified, MIDs are removed, along with sequences that don't fit minimum size criterion. The reads are merged before being clustered with 100% identity (dereplication step). Chimeric sequences are removed (contaminant DNA sequences originating from multiple sequences). In the next step, the 100% identity clusters are clustered again into OTUs with 95% identity. OTUs containing a single cleaned merged read (singleton) are removed from analysis. Remaining OTUs are compared to databases (BLAST). **B,** Long sequences (Sanger sequences, best hits and other reference sequences) are aligned together with MAFFT and trimmed, then used as a template for the reference tree. Illumina's OTUs are aligned to the reference alignment prior to infer their phylogenetic placement on the reference tree using EPA-ng and Jplacer.

### 3.2.2 Statistical analyses

Different indices were used to characterize communities' structure, based on the abundance of OTUs in each sample in and around Dallol. All these analyses were done using R software (R Core Team, 2013) and the R-package "vegan" (version 2.0-10; Oksanen et al. 2012).

#### 3.2.2.1 Richness (Chao1)

The richness of a sample corresponds to the total number of species present. The Chao1 index is based on the abundance of rare OTUs to calculate the theoretical richness of the sample and thus makes it possible to estimate the extent to which the number of OTUs observed is representative of the total number of OTUs (Chao 1984). This S-index is calculated with the following formula:

$$S = S_{obs} + \frac{n_1(n_1 - 1)}{2(n_2 + 1)}$$

where  $S_{obs}$  is the number of observed OTUs,  $n_1$  is the number of OTUs with a single sequence and  $n_2$  is the number of OTUs with two sequences. The Chao1 index was calculated with the function "estimateR".

#### 3.2.2.2 Diversity (Simpson)

Sample diversity was calculated using Simpson's index, which is the probability that two randomly drawn sequences belong to two different OTUs (Simpson 1949). Its value  $D'$  is between 0 and 1 and is calculated using the following formula:

$$D' = 1 - \sum_{i=1}^S f_i^2$$

where  $f_i$  is the frequency of the OTUs in the sample. Thus, the closer the value of  $D'$  is to 1, the more diverse a sample is.

#### 3.2.2.3 Evenness

Finally, the calculation of the Pielou equitability index makes it possible to determine whether the OTUs in a sample are present in relatively equal proportions or whether the sample is dominated by a small number of abundant OTUs (Pielou 1966). It is calculated with the formula:

$$e = \frac{-\sum_{i=1}^{S'} f_i \ln(f_i)}{\ln(S_{obs})}$$

where  $S_{obs}$  is the number of observed OTUs,  $f_i$  the frequency of OTUs in the sample and  $S'$  the integer part of  $S$ . The evenness  $e$  value is constrained between 0 and 1. The less evenness in communities between the species (and the presence of a dominant species), the lower the value, and vis versa.

### 3.3 Culture approach

Our culture approach was designed for two attempts:

- 1) Enrich biomass of some environments that may have very low cell concentration by providing a slightly less aggressive and more nutritive environment
- 2) Isolate some microorganisms into axenic cultures.

We designed a culture medium based on a compromise of the chemistry data of Dallol and surroundings environments (Table 5).

**Table 5 | Culture media composition.**

Medium	Component	Final volume 1L
All	NaCl	234 g
"	KCl	6 g
"	(NH <sub>4</sub> ) <sub>2</sub> SO <sub>4</sub>	1 g
"	MgSO <sub>4</sub> * 7H <sub>2</sub> O	30.5 g
"	MgCL <sub>2</sub> * 6H <sub>2</sub> O	19.5 g
"	CaCl <sub>2</sub> * 2H <sub>2</sub> O	1.10 g
SALT-YE	Yeast extract	0.2 g
SALT-Thio	Thiosulfate	0.5 g
SALT-H+B	Benzoate (solid)	0.610 g
"	Hexadecane (liquid)	5 mM=1.46 mL

**Added after autoclave:**

Medium	Component	Final volume 1L
All except with pH≈1.5	FeCl <sub>3</sub> * 6 H <sub>2</sub> O	0.167 g
"	Trace minerals (L1)	1 mL
"	K <sub>2</sub> HPO <sub>4</sub> 10%	10 mL
To acidify	HCl 34%	Variable
For pH≈1.5	FeCl <sub>3</sub> * 6 H <sub>2</sub> O	11.68 g
"	Trace minerals (L1)	10 mL
"	K <sub>2</sub> HPO <sub>4</sub> 10%	10 mL

There were four types of incubation conditions:

- Room temperature with a white light cycle
- 37°C in the dark
- 50°C with a white light cycle
- 70°C in the dark

## 3.4 Microscope observations

### 3.4.1 Optical microscope

The optical microscope was used to check microorganisms' presence in cultures and brine samples. Two sources of light were used for this purpose:

- A visible light source that illuminates the sample from below. The contrast of the particles and microorganisms with their natural colours are seen this way.
- A mercury-vapour lamp that illuminates the sample from above. The illumination light is filtered to select only the wavelength range of interest (Figure 15). This lamp is used for fluorescence microscopy since it requires intense, near-monochromatic illumination that widespread light sources cannot provide. The sample may be naturally fluorescent (e.g. pigments like chlorophyll or bacteriorhodopsin may be fluorescent when excited by some wavelength) or it can be made fluorescent by fluorophores. For our epifluorescence observations, we used the DNA dye SYTO9. We also did fluorescent in situ hybridization (FISH, Figure 16) experiments using CY3-Narc1214 probe supposed to target nanohaloarchaeota and the DNA dye SYBRGold. The results of the FISH experiment were also observed using the confocal microscope.

### 3.4.2 Confocal microscope

The confocal microscope is a special type of fluorescence microscope (Figure 15). Two pinhole apertures (or diaphragms) are positioned at confocal positions. The light beam is focused by the first pinhole on only a small part of the sample. If fluorophores are present, they emit light which is then filtered by the dichroic mirror and the filter. The second pinhole positioned in the focal plane selects only the light coming from the targeted point of the sample. The objective thus collects only this light. The surface of the sample is then scanned by moving either the sample or the light beam. This allows reconstructing a 2D image at a given height. One can then move vertically to obtain images at different heights. A 3D image of the sample can then be reconstructed using the proper software, though we didn't use that

specificity. The higher stability of the confocal microscope compared to a classical optical microscope also contribute obtaining better resolution images.

When two or more fluorochromes are simultaneously excited in a specimen, it cannot be avoided that several fluorescence signals are recorded in a detection channel and can no longer be separated in the image. Sequential scanning is an advantageous tool when detecting multiple fluorophores as it will enhance the image quality (avoiding crosstalk) by recording in sequential order instead of simultaneous acquisition.

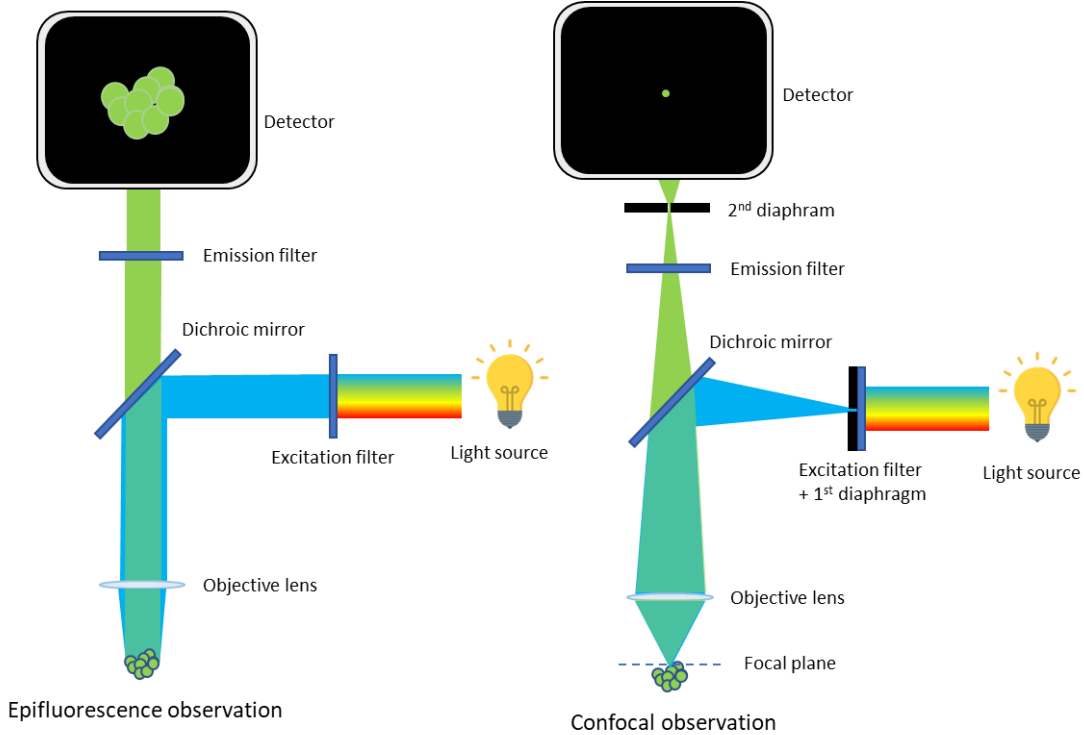


**Figure 15 | Schematic assemblies of an epifluorescence microscope (left) and a confocal microscope (right)**

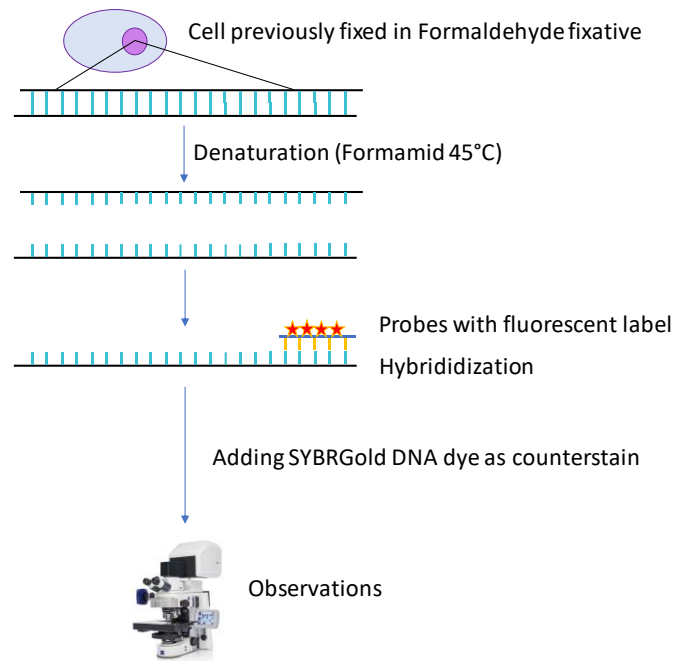


**Figure 16 | Simplified scheme of the principle of fluorescent in situ hybridization (FISH).** FISH is a molecular cytogenetic technique that uses fluorescent probes that bind to only those parts of a nucleic acid sequence with a high degree of sequence complementarity. It is used to detect and localize the presence or absence of specific DNA sequences in cells. FISH works by exploiting the ability of one DNA strand to hybridise (bind) specifically to another DNA strand.

### 3.4.3 Scanning Electronic Microscopy

The SEM uses an electron beam instead of a photon beam for the optical microscope. Due to the very narrow electron beam, its magnification resolution is about 250 times the magnification limit of the best light microscopes. Samples are previously vacuum-dried and coated with a conductive material (carbon in our case) to make them electrically conductive. The signals used to produce an image result from interactions of the electron beam with atoms at various depths within the sample (Figure 17). Various types of signals are produced including:

- Secondary electrons (SE): their very low energies (approximately 50 eV) limit their mean free path in solid matter. Consequently, they can only escape from the top few nanometres of the surface of a sample. The signal from SE tends to be highly localized at the point of impact of the primary electron beam, making it possible to use them to collect images of the sample's surface with a resolution of ~1 nm.
- Reflected or back-scattered electrons (BSE): which are beam electrons that are reflected from the sample by elastic scattering. They emerge from deeper locations within the specimen and, consequently, the resolution of BSE images is less than SE images. However, BSE are often used in analytical SEM, along with the spectra made

from the characteristic X-rays, because the intensity of the BSE signal is strongly related to the atomic number ( $Z$ ) of the specimen. BSE images can provide information about the distribution, but not the identity, of the different elements in the sample. In samples predominantly composed of light elements, such as biological specimens, BSE imaging can image organic objects which would otherwise be difficult or impossible to detect in SE images

- Characteristic X-rays: the electron beam removes an inner shell electron from the sample, causing a higher-energy electron to fill the shell and release energy like previously shown in Figure 10. The energy or wavelength of these characteristic X-rays can be measured by energy-dispersive X-ray spectroscopy (called EDS) and used to identify and measure the abundance of elements in the sample and map their distribution.

We used the SEM to see if we could identify cells on filters of Dallol brines, cultures and particles sorted with the flow cytometer (see next section). The BSE images and the chemical data (including chemical maps) collected with the EDS helped to distinguish organic features from mineral phases, and to identify some mineral particles.

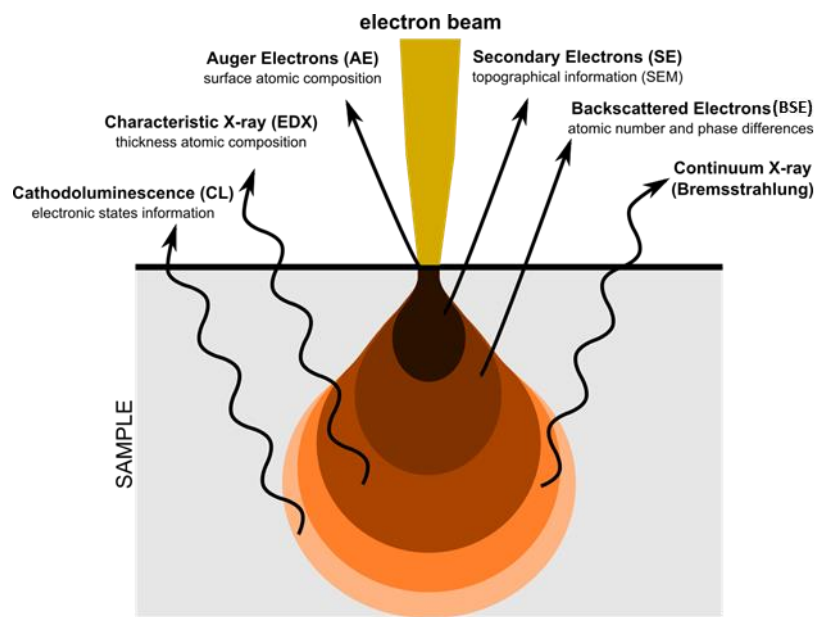


**Figure 17 | Interactions between the electron beam and the sample in the scanning electron microscope (Autor not found).**

### 3.5 Multiparametric analyses and fluorescent-assisted cell sorting on the cytometer

Flow cytometry is a technique in which particles (hopefully cells) suspended in a buffered solution are counted as they pass through the beam of a laser (Figure 18-A). Particles are diluted, and the flow rate of the suspension carefully controlled. Light detectors positioned around the flow cell can then detect any perturbation of the laser beam as a particle in the

liquid passes through, which allows the multiparametric analysis (MPA) of the flow cytometry data. This data can include:

- Particle size: The path of light through a given particle depends of its size and internal composition. As light interacts with the particle, it deviates from its initial direction. This is known as scattering. In our case, we only focused on forward scatter, detected as the changes of light intensity. The degree of forward scatter being proportional to the particle surface area lit, it gives information about its size.
- Particle fluorescence: Different wavelengths of excitation can be chosen depending on the equipment. If the particle hit gets excited by photons, the light it emits in return will be detected. The fluorescence of a particle may be natural (like it is the case for some minerals or cell pigments) or induced (DNA dyes/fluorophores).

Since the nature of the detected particles is uncertain at this stage, they are called “events”. To assess if particles in our samples were cells or inorganic particles (e.g. salts), we chose to use DNA dyes. In order to assess which DNA dye would be the most unlikely to fix on an inorganic particle, we analysed the event distribution of a blank, a sterile hypersaline medium used for the cultures. We compared the event distribution in this blank with and without different DNA dyes. We chose for our experiment the two dyes (SYTO13, DRAQ5) that led to the least change of fluorescence in the control. The fluorescence background range was also estimated thanks to this test.

We analysed the event distribution of the samples with and without the DNA dyes. If no change is detected between the two tests, it suggests there is no DNA in the particles (Figure 18-B). If on the opposite more events are detected above background, it suggests that some particles are cells with DNA.

In order to better identify events detected above background, we used a technique called FACS (Fluorescence activated cell sorting). Droplets containing particles with a fluorescence greater than the background were sorted into a collection tube with electrostatic means (Figure 18-A).

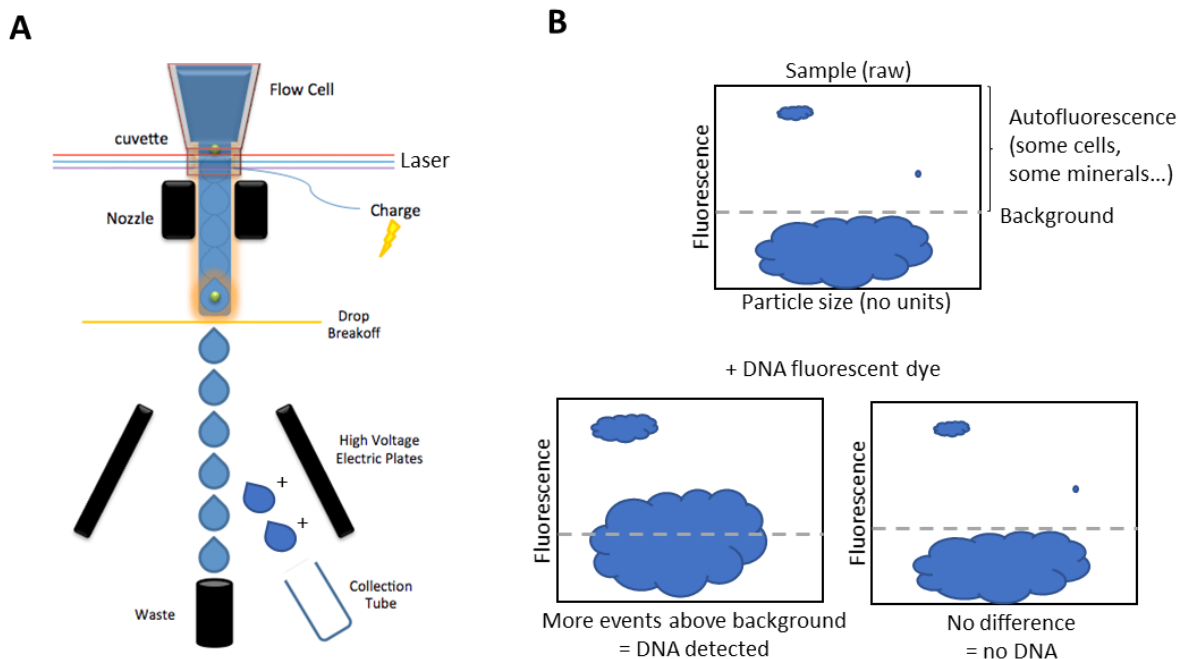


**Figure 18 | The flow cytometer analysis.** **A**, Schematic view of the end of the flow cell. The sample is diluted in an ultraclean buffered saline solution in order to make the particles/cells of the sample flow at a certain rate. Light detectors collect light changes (scattering, fluorescence) when the particle gets hit by the laser and transmit it to the computer. In order to sort the particles with fluorescent-assisted-cell-sorting, a set of criteria (a “sorting gate”) needs to be established which divided the cells/particles into discrete groups. The flow stream is broken into a series of discrete drops through vibration, with each drop containing a single cell/particle. Depending on the characteristics of the cell, each drop is given a charge, and charged plates are used to divert the drops to the collection vessel. If the particle is not of interest, it does not get charged and just ends its course in the waste bin. **B**, Schematic graphs that could be obtained from the multiparametric analysis on the flow cytometer. The events distribution is represented by the blue clouds.

## References

- Baldwin, R. L. 1996. “How Hofmeister Ion Interactions Affect Protein Stability.” *Biophysical Journal* 71 (4): 2056–63. <https://doi.org/10/d2qpc5>.
- Baumann, Christoph G., Steven B. Smith, Victor A. Bloomfield, and Carlos Bustamante. 1997. “Ionic Effects on the Elasticity of Single DNA Molecules.” *Proceedings of the National Academy of Sciences* 94 (12): 6185–90. <https://doi.org/10/cwvq2j>.
- Chao, Anne. 1984. “Nonparametric Estimation of the Number of Classes in a Population.” *Scandinavian Journal of Statistics* 11 (4): 265–70.
- Cray, Jonathan A., John T. Russell, David J. Timson, Rekha S. Singhal, and John E. Hallsworth. 2013. “A Universal Measure of Chaotropicity and Kosmotropicity.” *Environmental Microbiology* 15 (1): 287–96. <https://doi.org/10/ggddmj>.

- Fox-Powell, Mark G., John E. Hallsworth, Claire R. Cousins, and Charles S. Cockell. 2016. "Ionic Strength Is a Barrier to the Habitability of Mars." *Astrobiology* 16 (6): 427–42. <https://doi.org/10/f8qjhr>.
- Hallsworth, John E., Sabina Heim, and Kenneth N. Timmis. 2003. "Chaotropic Solutes Cause Water Stress in *Pseudomonas Putida*." *Environmental Microbiology* 5 (12): 1270–80. <https://doi.org/10/db2s9s>.
- Labuza, Theodore P. 1977. "The Properties of Water in Relationship to Water Binding in Foods: A Review<sup>1,2</sup>." *Journal of Food Processing and Preservation* 1 (2): 167–90. <https://doi.org/10/btdpxk>.
- Pielou, E. C. 1966. "The Measurement of Diversity in Different Types of Biological Collections." *Journal of Theoretical Biology* 13 (December): 131–44. <https://doi.org/10/fqtpwp>.
- Oksanen, J., Blanchet, G., Kindt, R., Legendre, P., O'hara, R. B., Simpson, G. L., et al. (2011). *Vegan: Community Ecology Package*. R Package Version 1.17-9. Available at: <http://CRAN.R-project.org/package=vegan>
- Simpson, E. H. 1949. "Measurement of Diversity." *Nature* 163 (4148): 688–688. <https://doi.org/10/c6c7h8>.
- Stevenson, Andrew, Jonathan A Cray, Jim P Williams, Ricardo Santos, Richa Sahay, Nils Neuenkirchen, Colin D McClure, et al. 2015. "Is There a Common Water-Activity Limit for the Three Domains of Life?" *The ISME Journal* 9 (6): 1333–51. <https://doi.org/10/f7cm86>.
- Stevenson, Andrew, Philip G. Hamill, Callum J. O'Kane, Gerhard Kminek, John D. Rummel, Mary A. Voytek, Jan Dijksterhuis, and John E. Hallsworth. 2017. "Aspergillus Penicillioides Differentiation and Cell Division at 0.585 Water Activity." *Environmental Microbiology* 19 (2): 687–97. <https://doi.org/10/f9n7kk>.
- R Development Core Team (2013). *R: A Language and Environment for Statistical Computing*. Vienna: R Foundation for Statistical Computing.
- Yang, Bo, Yong Wang, and Pei-Yuan Qian. 2016. "Sensitivity and Correlation of Hypervariable Regions in 16S rRNA Genes in Phylogenetic Analysis." *BMC Bioinformatics* 17 (March). <https://doi.org/10/ggsnzp>.





*The Dallol hydrothermal ponds and chimneys © DEEM Team*

ARTICLE 1

## 4. Unveiling microbial communities of the polyextreme gradients of the Dallol ecosystems

### 4.1 Context and objectives

Even though high throughput sequencing technologies have led to new understandings of extremophiles, little is known about some polyextremophiles such as the ones adapted to both hypersaline and hyperacidic conditions. Two hypotheses could explain that: either the scarcity of their natural occurrence makes them difficult to study, or there is a biological incompatibility to this combination of extremes.

Dallol ecosystems represent ones of the few known hyperacidic and hypersaline water bodies on Earth and, to our knowledge, it holds the most extreme combination of those parameters. The hydrothermal chimneys and closed ponds even show high temperature (60-110 °C). Even more interestingly, within a few kilometres range, the different ecosystems of Dallol and its surroundings hydrothermal lakes are characterized by a wide array of polyextreme physicochemical parameters (temperature, pH, salinity and different salt compositions), making them ideal sampling places to investigate the limits of life and potential different (new) microbial communities. At the time of the first expedition of our team (January 2016), very little is known about the chemical composition of those different places and there is still no microbial study in process.

To investigate the presence/absence of microorganisms and characterize them along those unique gradients, we established the following objectives:

- 1. Collect a high number of different types of sample** (filters, cell-traps, salts...) **to have the deepest analysis possible of each ecosystem.**
- 2. Run a battery of cross-analyses to confirm or not the presence of cells/DNA in the samples and construct a phylogenetic tree of Archaea and Bacteria based on 16S rRNA gene.** These analyses include: 16/18S rRNA gene sequencing, construction of diversity histograms and bacterial/archaeal phylogenetic trees, microscope observations (optical and SEM), flow cytometry (MPA and FACS) and attempts of microbial enrichment and isolation by the mean of cultures.
- 3. Correlate the presence/absence of life and microbial communities' patterns with their environments' physicochemical parameters and chemical composition.** The goal is to try to assess what are the shaping or limiting factors of the populations observed. Some parameters (pH, temperature, salinity) are measured *in situ* with a multi-probe or a refractometer. Complementary measures are done back from field to refine the salinity values, identify their chemical composition and evaluate the chaotropicity, water activity, ionic force induced.

## 4.2 Results

Two multidisciplinary expeditions with our team members were held in January 2016 and 2017. We collected 183 samples from over 63 places. These samples include 0.2µm pore-sized filters fixed in ethanol, brine in glass bottles and solid samples. In the less polyextreme sites (the salt plain, the Lake Karum and the cave reservoir) a high diversity of halophile microorganisms was found. Archaea were dominant (90% on average) compared to Bacteria (10%). Within the Archaea, the main phyla were Halobacteria (56-84% of total prokaryotic reads) and Nanohaloarchaeota (1-15% total prokaryotic reads). In contrast, amplicons were obtained only after a semi-nested PCR for the most polyextreme samples (from the Dallol hydrothermal dome, Lake Gaet'ale and the Black Lake), attesting the very low DNA concentration in the samples to begin with. As the sequences were related to OTUs found in the less polyextreme places despite drastically harsher conditions, it was highly doubtful they would be endogenous organisms. Those results were consistent with observations from cross-analyses. The results of this study are resumed in Table 6.

**Table 6 | Summary of the results of each type of analysis per site.** Green background: detection of a high diversity of halophiles. Orange background: local microbial contamination (dispersion) suspected. Red background: no traces of life detected.

	Salt Plain Cave reservoir Lake Karum (Assale)	Dallol hydrothermal ponds	Lake Gaet'ale (Yellow Lake)	Black Lake
Microscope (optical, SEM)	Cells observed, sometimes with (bio?)mineralization	No cells observed but biomorphs	No cells observed but biomorphs	No cells observed
Sequencing (Sanger, Illumina) and analyses	90% Archaea 10% Bacteria	Hard to amplify, airborne dispersal suspected	Hard to amplify, airborne dispersal suspected	Nothing detected
Flow cytometry (MPA and FACS)	DNA detected and cells sorted successfully	No DNA detected; no cells sorted	No DNA detected; no cells sorted	Not tested (viscosity too high)
Cultures (enrichment and isolation)	Enrichment succeeded; 1 isolation succeeded	No growth	No growth	No growth

The principal component analysis of elemental composition (Figure 19) shows that Lake Gaet'ale and the Black lake are characterized by high concentration of Mg and Ca salts, probably causing their estimated low water activity, high chaotropicity and ionic strength. We assess that those extreme values of water activity, chaotropicity and ionic strength are the reason behind the absence of life in these two environments. The Dallol dome brines, on the opposite, are characterized by high concentration of NaCl salt which is kosmotropic. Despite their high content in iron salts, their water activity, chaotropicity and ionic strength remain within the estimated range of habitable parameters. We interpret that the combination of hypersalinity (average 40%) and hyperacidity (negative pH) constitute the major barrier for

life in these ponds, even though we cannot exclude that their combination with other compounds (e.g. the high content of metals) also play a role in their sterility.

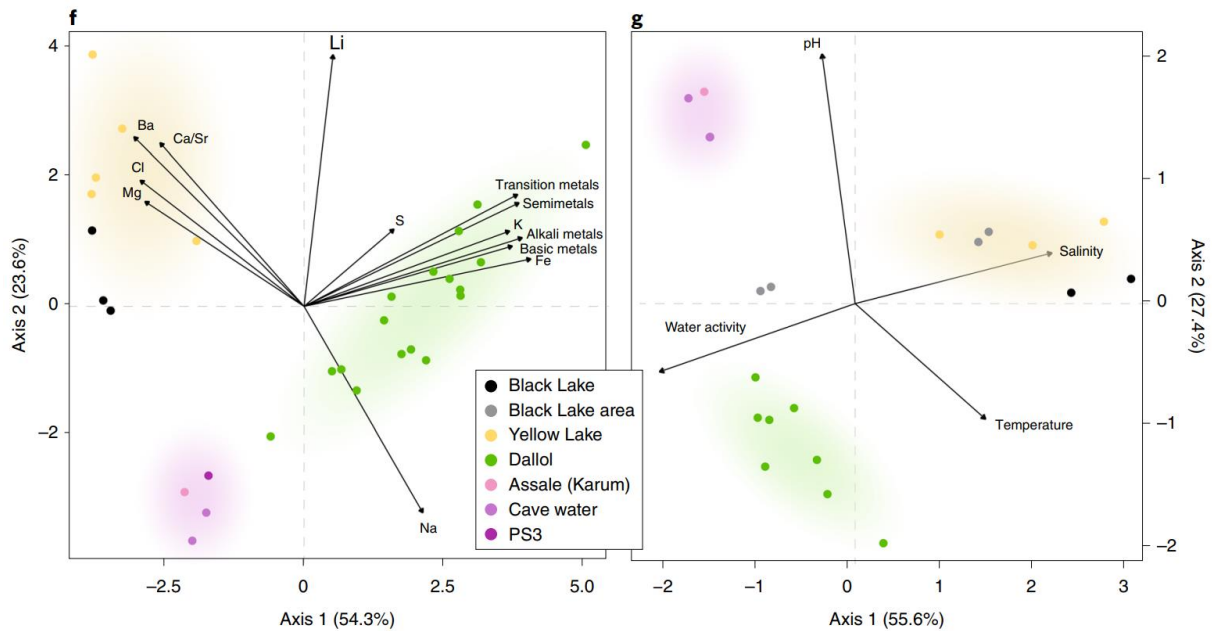


**Figure 19 | Principal component analyses of the Dallol area liquid samples according to their chemical composition (left) and they potentially life-limiting physicochemical parameters (right).** The only samples where life could be detected with confidence are the salt plain, the cave reservoir and Lake Assale (Karum).

### 4.3 Manuscript of article 1

Article published in *Nature Ecology and Evolution* (see next page).

# Hyperdiverse archaea near life limits at the polyextreme geothermal Dallol area

Jodie Belilla<sup>1</sup>, David Moreira<sup>1</sup>, Ludwig Jardillier<sup>1</sup>, Guillaume Reboul<sup>1</sup>, Karim Benzerara<sup>2</sup>, José M. López-García<sup>3</sup>, Paola Bertolino<sup>1</sup>, Ana I. López-Archilla<sup>4</sup> and Purificación López-García<sup>1\*</sup>

**Microbial life has adapted to various individual extreme conditions; yet, organisms simultaneously adapted to very low pH, high salt and high temperature are unknown. We combined environmental 16S/18S ribosomal RNA gene metabarcoding, cultural approaches, fluorescence-activated cell sorting, scanning electron microscopy and chemical analyses to study samples along such unique polyextreme gradients in the Dallol–Danakil area in Ethiopia. We identified two physicochemical barriers to life in the presence of surface liquid water defined by (1) high chaotropicity–low water activity in Mg<sup>2+</sup>/Ca<sup>2+</sup>-dominated brines and (2) hyperacidity–salt combinations (pH ~0/NaCl-dominated salt saturation). When detected, life was dominated by highly diverse ultrasmall archaea that were widely distributed across phyla with and without previously known halophilic members. We hypothesize that a high cytoplasmic K<sup>+</sup>-level was an original archaeal adaptation to hyperthermophily, subsequently exapted during several transitions to extreme halophily. We detect active silica encrustment/fossilization of cells but also abiotic biomorphs of varied chemistry. Our work helps circumscribing habitability and calls for cautionary interpretations of morphological biosignatures on Earth and beyond.**

Microbial life has adapted to so-called extreme values of temperature, pH or salinity, but also to several polyextreme, for example hot acidic or salty alkaline, ecosystems<sup>1,2</sup>. Various microbial lineages have been identified in acidic brines in the pH range 1.5–4.5, for example in Western Australia<sup>3,4</sup> and Chile<sup>5</sup>. However, although some acidophilic archaea thrive at pH ~0 (*Picrophilus oshimae* grows at optimal pH 0.7)<sup>6</sup> and many halophilic archaea live in hypersaline systems (>30% weight/volume; NaCl-saturation conditions), organisms that adapted simultaneously to very low pH (<1) and high salt, and eventually also high temperatures, are not known among cultured prokaryotic species<sup>1</sup>. Are molecular adaptations to these combinations incompatible or are (hot) hyperacidic hypersaline environments simply rare and unexplored? The Dallol geothermal dome and its surroundings (Danakil Depression, Afar, Ethiopia) allow this question to be addressed by offering unique polyextreme gradients combining high salt content (33 to >50%; either Mg<sup>2+</sup>/Ca<sup>2+</sup> or Na<sup>+</sup>/Fe<sup>2+/3+</sup>-rich), high temperature (25 to 110 °C) and low pH (≤−1.5 to 6.0).

Dallol is an uplifted (~40 m) dome structure located in the north of the Danakil Depression (~120 m below sea level). The Danakil Depression is a 200-km-long basin within the Afar Rift at the junction between the Nubian, Somalian and Arabian Plates<sup>6</sup>. Lying only 30 km north of the hypersaline, hydrothermally influenced Lake Assale (Karum) and the Erta Ale volcanic range, Dallol does not display volcanic outcrops but intense degassing and hydrothermalism. These activities are observed on the salt dome and the adjacent Black Mountain and Yellow Lake (Gaet'Ale) areas<sup>6,7</sup> (Fig. 1a,b). Gas and fluid isotopic measurements indicate that meteoritic waters, notably infiltrating from the high Ethiopian plateau (>2,500 m), interact with an underlying geothermal reservoir (280–370 °C)<sup>7,8</sup>. Further interaction of those fluids with the 1-km thick marine evaporites filling the Danakil Depression results in unique combinations

of polyextreme conditions and salt chemistries<sup>6,7,9,10</sup>, which have led some authors to consider Dallol as a Mars analogue<sup>11</sup>.

Here, we use environmental 16S/18S ribosomal RNA gene metabarcoding, cultural approaches, fluorescence-activated cell sorting (FACS) and scanning electron microscopy (SEM) combined with chemical analyses to explore microbial occurrence, diversity and potential fossilization along Dallol–Danakil polyextreme gradients<sup>12–15</sup>.

## Results and discussion

To investigate the distribution and, eventually, type of microbial life along those polyextreme gradients, we analysed a large variety of brine and mineral samples collected mainly from two field expeditions (January 2016 and 2017; a few additional samples were collected in 2018) in four major zones (Fig. 1 and Extended Data Figs. 1–3). The first zone corresponded to the hypersaline (37–42%) hyperacidic (pH between ~0 and −1; values down to pH −1.6 were measured on highly concentrated and oxidized brines on site) and sometimes hot (up to 108 °C) colourful ponds at the top of the Dallol dome (Fig. 1c and Extended Data Figs. 1a, 2a–h and 3). The second zone consisted of the salt canyons located at the southwestern extremity of the Dallol dome and the Black Mountain area, which includes the Black Lake (Fig. 1b,d and Extended Data Figs. 1b,c and 2l–q). Brine samples collected in a cave reservoir (Gt samples) and in ephemeral pools with varying degrees of geothermal influence at the dome base (PS/PS3 samples) were hypersaline (~35%), with moderate temperature (~30 °C) and acidity (pH ~4–6). By contrast, pools located near the small (~15 m diameter), extremely hypersaline (>70%), hot (~70 °C) and acidic (pH ~3) Black Lake were slightly more acidic (pH ~3), warmer (40 °C) and hypersaline (35–60%) than the dome-base pools (PSBL samples; Extended Data Fig. 3). The third zone corresponded to the Yellow Lake and neighbouring ponds (Fig. 1e and Extended Data Figs. 1d and 2i–k), which

<sup>1</sup>Ecologie Systématique Evolution, CNRS, Université Paris-Sud, Université Paris-Saclay, AgroParisTech, Orsay, France. <sup>2</sup>Institut de Minéralogie, de Physique des Matériaux et de Cosmochimie, CNRS, Sorbonne Université, Muséum National d'Histoire Naturelle, Paris, France. <sup>3</sup>Instituto Geológico y Minero de España, Palma de Mallorca, Spain. <sup>4</sup>Departamento de Ecología, Universidad Autónoma de Madrid, Madrid, Spain. \*e-mail: [puri.lopez@u-psud.fr](mailto:puri.lopez@u-psud.fr)

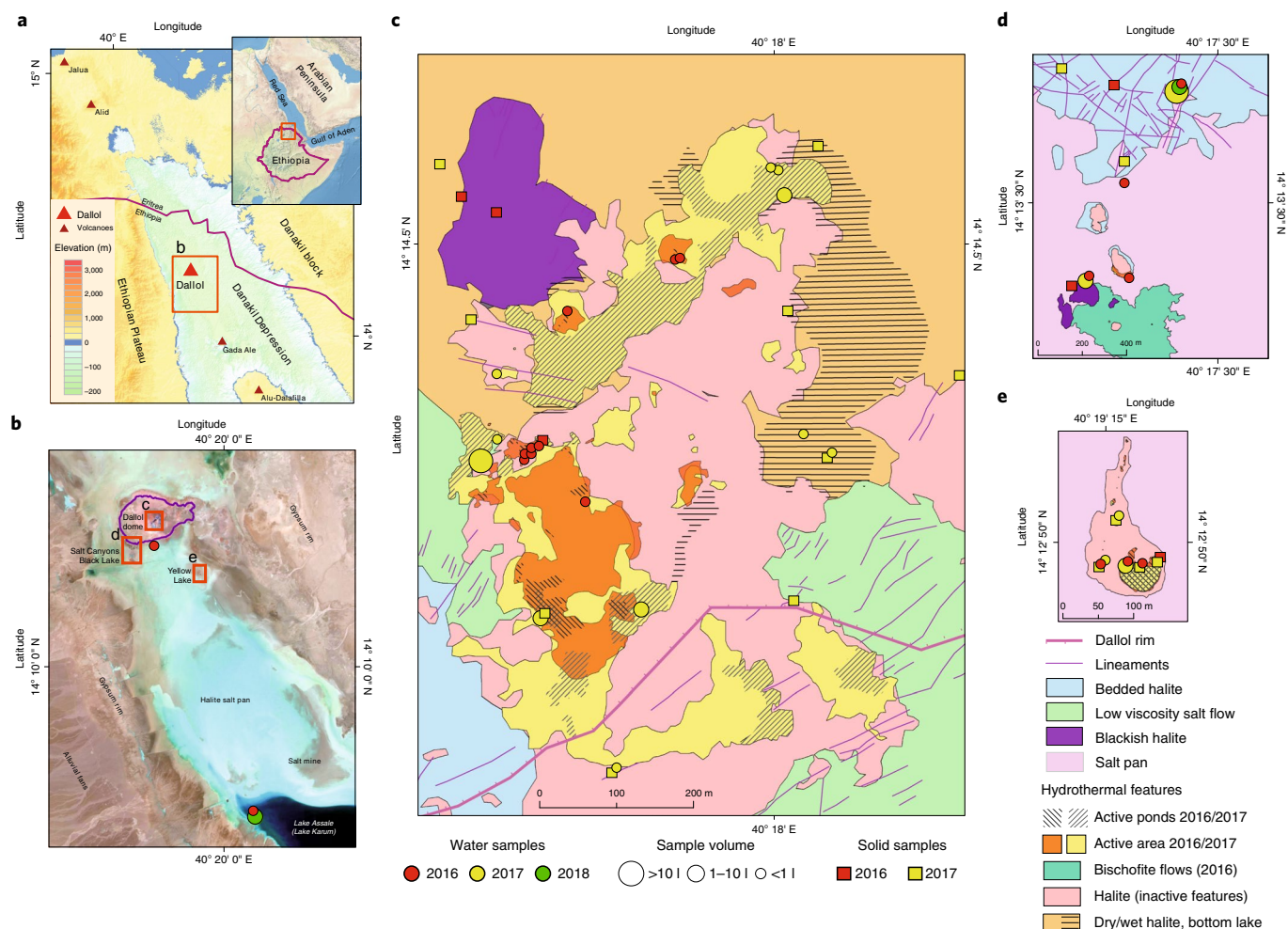


**Fig. 1 | Overview of sampling sites at the polyextreme geothermal field of Dallol and its surroundings in the Danakil Depression, Ethiopia.** **a**, Location of the Dallol dome area in the Danakil Depression following the alignment of the Erta Ale volcanic range (Gada Ale, Alu-Dalafilla), Northern Ethiopia. **b**, Closer view of the sampling zones in the Dallol area and Lake Assale or Karum (satellite image from Copernicus Sentinel 1; 19 January 2017). **c–e**, Geological maps showing the sampling sites at the Dallol dome summit (**c**), west salt canyons and Black Mountain, including the Black Lake (**d**) and Yellow Lake (Gaet’Ale) zone (**e**). Squares (solid samples) and circles (liquid samples) indicate the nature of the collected samples. The colour indicates the collection date (red, 2016; yellow, 2017; green, 2018). The size of circle is proportional to the collected brine volume for analyses. Specific sample names are indicated in the aerial view shown in Extended Data Fig. 1.

were acidic (pH ~1.8), warm (~40°C) and extremely hypersaline<sup>16</sup> (≥50%). The Yellow Lake actively bubbles and emits toxic gases for animals, as illustrated by the presence of numerous dead birds. The gas phase includes light hydrocarbons<sup>8</sup>. The fourth zone consisted of the hypersaline (36%), almost neutral (pH ~6.5), Lake Assale (Fig. 1b and Extended Data Fig. 2r), which we used as a milder, yet extreme Danakil system for comparison. In contrast to a continuous degassing activity, the hydrothermal manifestations were highly dynamic, particularly on the dome and the Black Mountain area. The area affected by hydrothermal activity in January 2017 was much more extensive than the previous year (Fig. 1 and Extended Data Fig. 1). Dallol chimneys and hyperacidic ponds can appear and desiccate in a matter of days or weeks, generating a variety of evaporitic crystalline structures observable in situ<sup>17</sup>. Similarly, very active and occasionally explosive (salt ‘bombs’) hydrothermal activity that was characterized by hot (110°C), slightly acidic (pH ~4.4) black hypersaline fluids was detected in the Black Mountain area in 2016 (‘Little Dallol’; sample BL6-01; Extended Data Figs. 1b and 2l) but not in the following years. Active bischofite flows<sup>6,7,18</sup> (116°C) were also observed in the Black Mountain area in 2016 but not in 2017.

To assess potential correlations between microbial life and local chemistry, we analysed the chemical composition of representative samples used in parallel for microbial diversity analyses (see Methods). Our results revealed three major types of solution chemistry depending on the dominant elements (Fig. 2f and Extended Data Fig. 4a). In agreement with recent observations, Dallol ponds were characterized by NaCl-supersaturated brines that were highly enriched in iron with different oxidation states, which explained the colour variation<sup>17</sup>. Potassium and sulfur were also abundant (Supplementary Table 1). By contrast, samples from the salt canyons and plain near Dallol and Lake Assale were NaCl-dominated with a much lower iron content, and the Yellow and Black lakes and associated ponds had very high Mg<sup>2+</sup> and Ca<sup>2+</sup> concentrations (Supplementary Table 1). Many aromatic compounds were identified, particularly in Dallol and Yellow Lake fluids (Supplementary Table 2). High chaotropicity associated with Mg<sub>2</sub>Cl-rich brines, high ionic strength and low water activity (*a<sub>w</sub>*) is thought to be a limiting factor for life<sup>12,13,19,20</sup>. We therefore determined these parameters in representative samples (Extended Data Fig. 5). Based on our experimental measures and theoretical calculations from dominant

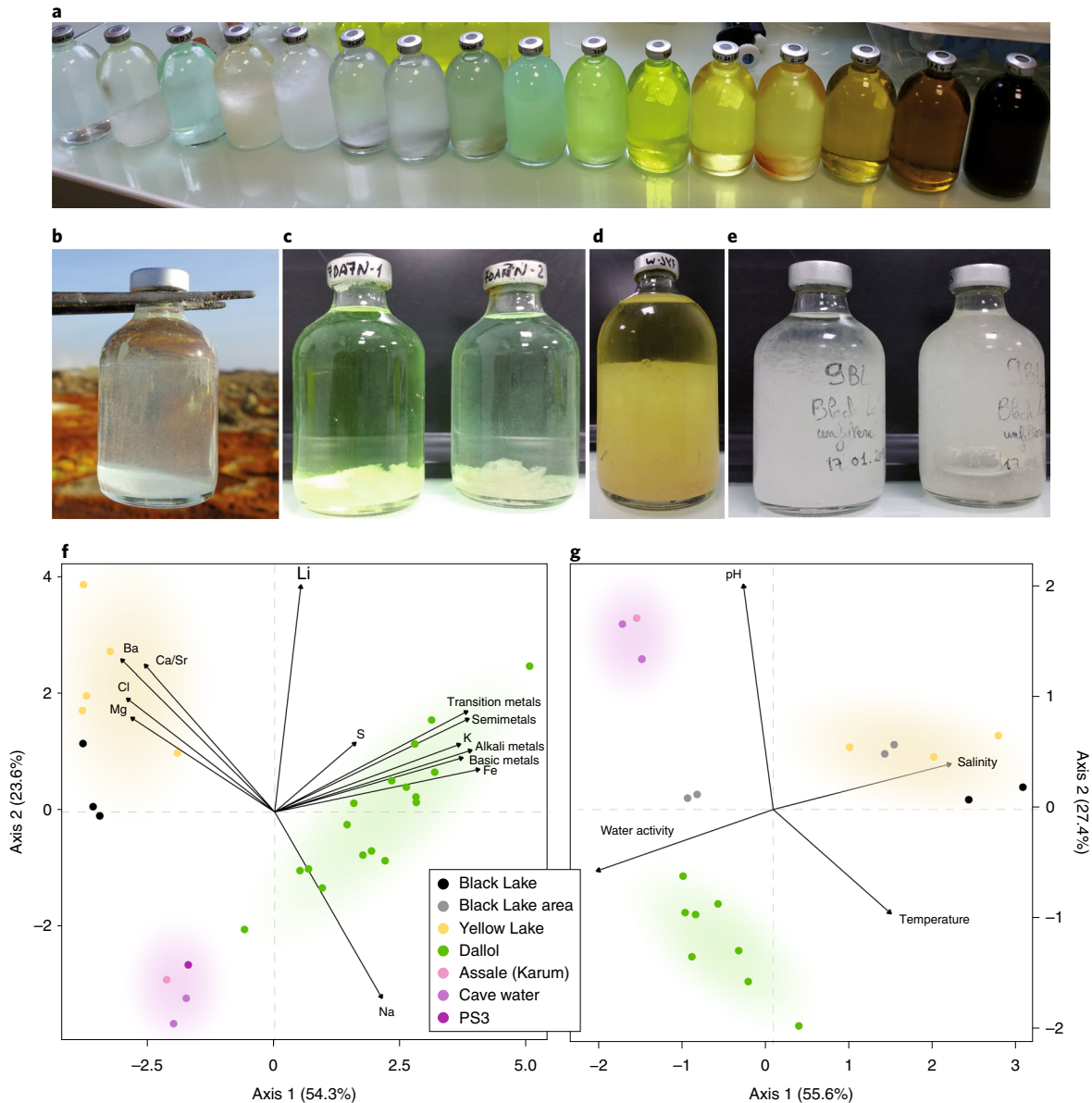


**Fig. 2 | Physicochemical features of liquid samples from the Dallol area.** **a**, Examples of colours displayed by the different samples analysed in this study, reflecting different chemistries and oxidation states. **b–e**, Examples of salt-oversaturated samples. Immediate (seconds) precipitation of halite crystals as water from a hot spring (108 °C) cools down upon collection (**b**), salt precipitates forming after storage at -8 °C in water collected from Dallol hyperacidic ponds (**c**), Yellow Lake (**d**) and Black Lake (**e**). **f**, PCA of 29 samples according to their chemical composition (see Supplementary Table 2). Transition metals, Cr, Mo, Mn, Sc, Zn, V, U, Ce, La, Cu; semimetals, As, B, Sb, Si; alkali metals, Rb, Cs; basic metals, Tl, Al, Ga, Sh. Some elements are highlighted out of these groups owing to their high relative abundance or to their distant placement. A PCA showing all individual metal variables can be seen in Supplementary Fig. 3a. **g**, PCA of 21 samples and key potentially life-limiting physicochemical parameters in the Dallol area (temperature, pH, salinity, water activity). Water activity and salinity-related parameters are provided in Extended Data Fig. 5. Coloured zones in PCA analyses highlight the groups of samples corresponding to the three major chemical zones identified in this study.

salts, only samples in the Yellow and Black Lake areas displayed life-limiting chaotropy and  $a_w$  values according to established limits<sup>12,13,19,20</sup>. A principal component analysis (PCA) showed that the sampled environments were distributed in three major groups depending on solution chemistry, pH and temperature: Black and Yellow Lake samples, anticorrelating with  $a_w$ ; Dallol dome samples, mostly correlating with  $a_w$  but anticorrelating with pH; and Dallol canyon cave reservoir (Gt samples) and Lake Assale, correlating with  $a_w$  and pH (Fig. 2g). These results are consistent with those obtained with analysis of variance and subsequent post-hoc analysis, which show significant differences between the three major

chemical zones (coloured areas in Fig. 2f,g) among them for the variables tested (Supplementary Table 4).

To ascertain the occurrence and diversity of microbial life along these physicochemical gradients, we purified DNA from a broad selection of brine samples (0.2–30  $\mu\text{m}$  size fraction) and solid samples (gypsum and halite-rich salt crusts, compacted sediment and soil-like samples; Extended Data Fig. 3). We carried out 16S/18S rRNA gene-based diversity studies by high-throughput short-amplicon sequencing (metabarcoding approach) but also sequenced almost-full length genes from clone libraries, providing local reference sequences for more accurate phylogenetic

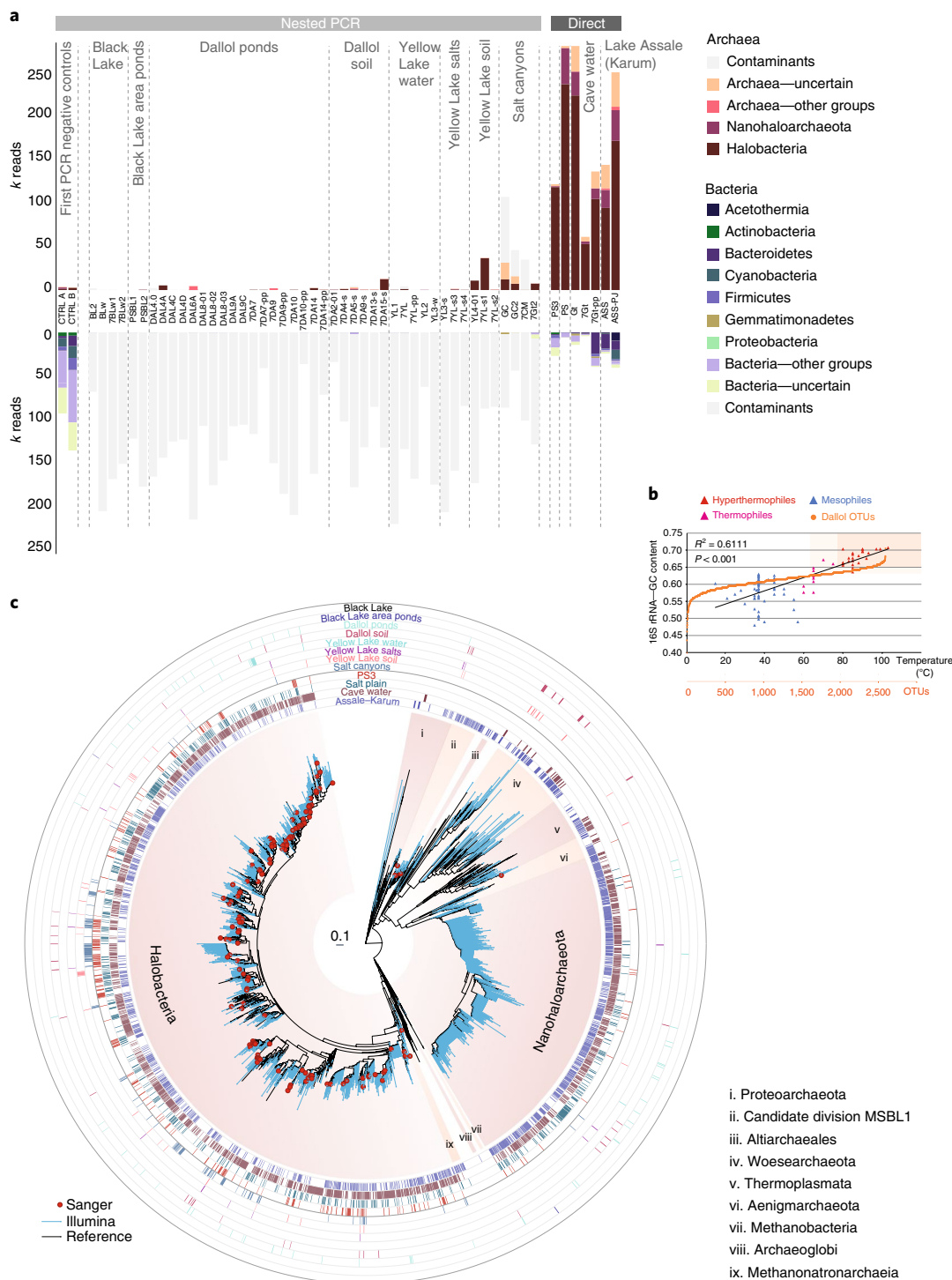


**Fig. 3 | Distribution and diversity of prokaryotes in samples from the Dallol dome and surrounding areas based on 16S rRNA gene metabarcoding data.** **a**, Histograms showing the presence/absence and abundance of amplicon reads of archaea (upper) and bacteria (lower) obtained with universal prokaryotic primers. Samples yielding amplicons directly (negative PCR controls were negative) are shown on the right (direct). Samples for which amplicons were only obtained after nested PCR, all of which also yielded amplicons in ‘negative’ controls, are displayed on the left (nested PCR). Sequences identified in the ‘negative’ controls, considered as contaminants, are shaded in light grey in the corresponding Dallol samples. The phylogenetic affiliation of dominant archaeal and bacterial groups is colour coded. For details, see Supplementary Table 5. k reads, thousand reads. The names of the different samples are provided on the x axis. **b**, GC content of archaeal OTUs plotted on a graph showing the positive correlation of GC content (for the same 16S rRNA region) and growth temperature of diverse described archaeal species. **c**, Phylogenetic tree of archaeal 16S rRNA gene sequences showing the phylogenetic placement of archaeal OTUs identified in the different environmental samples (full tree provided in Supplementary Data 1). Sequences derived from metabarcoding studies are represented with blue branches (Illumina sequences); those derived from cloning and Sanger sequencing of environmental samples, cultures and FACS-sorted cells are labelled with a red dot. Reference sequences are in black. Concentric circles around the tree indicate the presence/absence of the corresponding OTUs in different groups of samples (groups shown in (a)).

analyses (see Methods). Despite intensive PCR efforts and extensive sampling in Dallol polyextreme ponds, including pools that were active in two consecutive years (Extended Data Fig. 1) to minimize ephemeral system-derived effects, we only amplified 16S/18S rRNA genes from Dallol canyon cave water, the dome-base geothermally influenced salt plain and Lake Assale, but never from the Dallol dome or Black/Yellow lakes (Fig. 3a). To check whether this resulted from excessively low DNA amounts in those samples (although relatively large volumes were filtered), we carried out seminested PCR reactions using, as templates, potential amplicons produced during the first PCR–amplification reaction, including the first PCR negative controls. Almost all samples produced amplicons in seminested PCR reactions, including the first PCR blanks (Fig. 3a). Metabarcoding analysis revealed that amplicons from direct PCR reactions (PS/PS3, Gt, Assale) were largely dominated by archaeal sequences (>85%) grouping in diverse and abundant operational taxonomic units (OTUs) (Extended Data Fig. 6). By contrast, amplicons derived from Dallol ponds, Black and Yellow lakes and also first PCR ‘negative’ controls were dominated by bacterial sequences. Most of them were related to well-known molecular biology kit and laboratory contaminants<sup>21,22</sup>, whilst others were human-related bacteria probably introduced during intensive afar and tourist daily visits to the site. A few archaeal sequences might also result from aerosol cross-contamination, despite extensive laboratory precautions (see Methods). After the removal of contaminant sequences (grey bars in Fig. 3a, and Supplementary Table 5), only rare OTUs encompassing few reads (mostly archaeal) could be associated with Dallol dome or Yellow Lake brines, which we interpret as dispersal forms (dusty wind is frequent in the area). Slightly higher abundances of archaeal OTUs were identified in ‘soil’ samples, that is samples retrieved from salty consolidated mud or crusts where dust brought by the wind from the surrounding plateaux accumulates and starts constituting a proto-soil (with incipient microbial communities; for example, Extended Data Fig. 2i). Therefore, although we cannot exclude the presence of active life in these ‘soil’ samples, our results strongly suggest that active microbial life is absent from polyextreme Dallol ponds and the Black and Yellow lakes.

By contrast, PS/PS3, Gt and Assale samples harboured extremely diverse archaea (2,653 OTU conservatively determined at 95% identity, that is genus level) that virtually spanned the known archaeal diversity (Fig. 3, Extended Data Fig. 6 and Supplementary Table 5). Around half of that diversity belonged to Halobacteria, and an additional quarter to the Nanohaloarchaeota<sup>23</sup>. The rest of archaea distributed in lineages typically present in hypersaline environments, for example, the Methanonatronoarchaeia<sup>24,25</sup> and Candidate Division MSBL1, which is thought to encompass methanogens<sup>26</sup> and/or sugar-fermentors<sup>27</sup>. However, they also included other archaeal groups not specifically associated with salty systems (although they can sometimes be detected in hypersaline settings, for example some Thermoplasmata or Woesearchaeota). These included Thermoplasmata and Archaeoglobi within Euryarchaeota, Woesearchaeota

and other lineages (Aenigmarchaeota, Altiarchaeales) usually grouped as DPANN<sup>28–30</sup>, and Thaumarchaeota and Crenarchaeota (Sulfolobales) within the TACK/Proteoarchaeota<sup>31</sup> (Fig. 3a and Supplementary Table 5). In addition, because rRNA GC content correlates with growth temperature, around 27% and 6% of archaeal OTUs were inferred to correspond to thermophilic and hyperthermophilic organisms, respectively (see Methods; Fig. 3b). As previously observed<sup>23,28,29</sup>, common archaeal primers for near-full 16S rRNA genes (Fig. 3c, red dots) failed to amplify Nanohaloarchaeota and other divergent DPANN lineages. These probably encompass ectosymbionts or parasites<sup>28–30,32</sup>. Given their relative abundance and co-occurrence in these and other ecosystems, it is tempting to suggest that Nanohaloarchaeota are (ecto)symbionts of Halobacteria, and Woesearchaeota could potentially be associated with *Thermoplasma*-like archaea. Although much less abundant, bacteria belonging to diverse phyla, including CPR (Candidate Phyla Radiation) lineages, were also present in these samples (710 OTUs; Extended Data Figs. 6 and 7 and Supplementary Table 5). In addition to typical extreme halophilic genera (for example, *Salinibacter*, Bacteroidetes), one Deltaproteobacteria group and two divergent bacterial clades were overrepresented in Dallol canyon Gt samples. Eukaryotes, which were less abundant and diverse, were present in Lake Assale and occasionally in the salt plain and Gt. They were dominated by halophilic *Dunaliella* algae (Extended Data Fig. 8 and Supplementary Table 6).

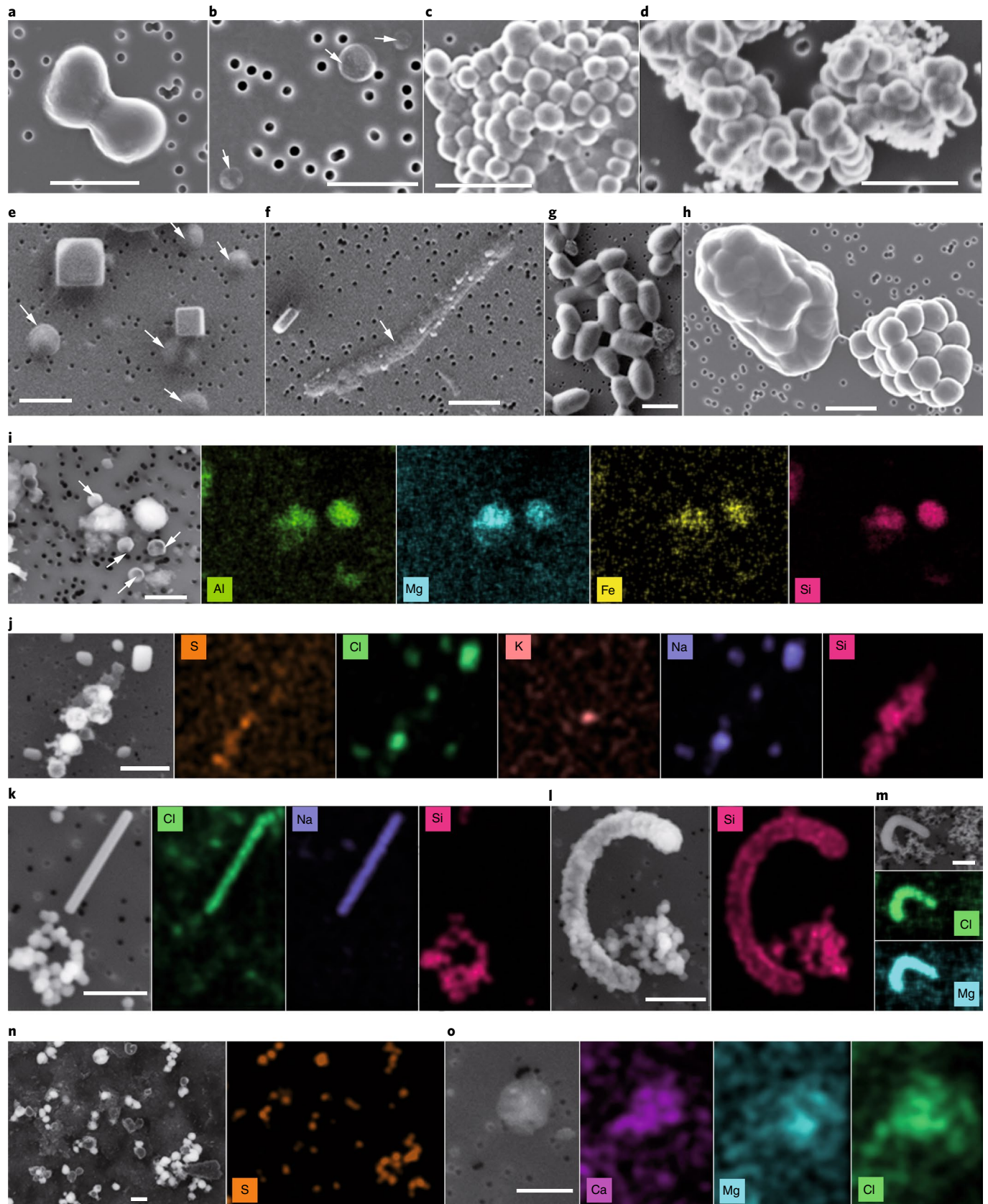
Consistent with metabarcoding results, and despite the use of various culture media and growth conditions mimicking local environments (see Methods), cultural approaches did not yield enrichments for the Dallol dome, Black Lake and Yellow Lake samples. We obtained enrichments from the canyon cave (Gt/7Gt) and salt plain (PS/PS3) samples in most culture media (except in benzoate/hexadecane) and tested conditions (except at 70 °C in the dark). However, all attempts to isolate microorganisms at pH <3 from these enrichments failed. The most acidophilic isolate obtained from serial dilutions (PS3-A1) only grew at 37 °C and optimal pH 5.5 (range pH 3–7). Its 16S rRNA gene was 98.5% identical to that of *Halarchaeum rubridurum* MH1-16-3 (NR\_112764), an acidophilic haloarchaeon growing at pH 4.0–6.5 (ref. <sup>33</sup>).

In agreement with metabarcoding and culture-derived observations, multiparametric fluorescence analysis showed no DNA fluorescence above background for Dallol and Yellow Lake samples (Extended Data Fig. 9). Because optical and SEM observations suggested that indigenous cells were unusually small, we applied FACS to samples from the different Dallol environments (Extended Data Fig. 3), followed by systematic SEM analysis of sorted events. Despite some samples showed no difference in fluorescence after incubation with DNA dyes, we sorted all events above background limit (as defined in Extended Data Fig. 9a). We only detected cells in Dallol cave water and salt plain samples, but not in Dallol dome ponds or Yellow Lake samples (Extended Data Fig. 9). Consistent with this, after DNA purification of FACS-sorted particles, 16S rRNA gene amplicons could only be obtained from different cave

**Fig. 4 | SEM pictures and chemical maps of cells and abiotic biomorphs identified in samples from the Dallol region. a–h**, SEM pictures of cells (a–c, e–h) and abiotic biomorphs (d). FACS-sorted dividing cells from sample PS (hydrated salt pan between the Dallol dome base and the Black Lake) (a); FACS-sorted ultrasmall cells from 7Gt samples (cave water reservoir, Dallol canyons) (b); FACS-sorted colony of ultrasmall cells from sample PS (note cytoplasmic bridges between cells) (c); FACS-sorted abiotic silica biomorphs from the Dallol pond 7DA9 (note the similar shape and morphology compared to cells in c) (d); cocci and halite crystals in 8Gt samples (cave water) (e); long rod in 8Gt (f); FACS-sorted cells from Gt samples (g) and FACS-sorted colonies from sample PS (note the bridge between one naked colony and one colony covered by an exopolymeric-like matrix) (h). **i–o**, SEM images and associated chemical maps of cells and biomorphs. Colour intensity provides semiquantitative information of the mapped elements. Small cocci and amorphous Al–Mg–Fe-rich silicate minerals from Gt (i); NaCl crystals and S–Si rich abiotic biomorphs from Dallol pond sample 7DA7 (j); NaCl crystal and Si biomorphs (k); Si-encrusted cell and Si biomorphs in sample 8Ass (Lake Assale) (l); Mg–Cl biomorph in sample BLPS\_04 (Black Lake area pond) (m); S-rich biomorphs in Dallol pond 7DA9 (n) and Ca–Mg–Cl biomorph in YL-w2 (Yellow Lake pond) (o). SEM photographs were taken using In Lens or AsB detectors. For additional images and SEM details, see Supplementary Figs. 1 and 2. White arrows indicate cells difficult to recognize due to their small size and/or flattened aspect, which may result from sample preparation and/or high vacuum conditions within the SEM. Scale bars, 1 μm.

and salt plain samples but not from Dallol dome or Yellow Lake samples. Cell counts estimated from FACS for the cave and salt plain samples were low (average  $3.1 \times 10^4$  cells  $\text{ml}^{-1}$  and  $5.3 \times 10^4$  cells  $\text{ml}^{-1}$  for the cave and PS samples, respectively). Sorted cells were usually

small to ultrasmall (down to  $0.25\text{--}0.3\ \mu\text{m}$  diameter; Fig. 4). In PS samples, some of these small cells formed colonies (Extended Data Fig. 9 and Fig. 4c), which were sometimes surrounded by an exopolymeric matrix cover (Fig. 4h). The presence of cytoplasmic



bridges and/or potential cell fusions (Extended Data Fig. 9 and Fig. 4c) suggest that they might be archaeal colonies<sup>34</sup>.

FACS-sorted fluorescent particles in Dallol pond samples appeared to correspond exclusively to salt crystals or cell-sized amorphous minerals morphologically resembling cells, that is biomorphs<sup>35,36</sup> (for example, Fig. 4d compared with Fig. 4c). This prompted us to carry out a more systematic search for abiotic biomorphs in our samples. SEM observations coupled with chemical mapping by energy-dispersive X-ray spectrometry (EDXS) showed a variety of cocci-like biomorph structures of diverse elemental compositions. Many of them were Si biomorphs (Dallol ponds, Yellow Lake and Assale Lake), but we also detected Fe–Al silicates (Gt), S or S-rich biomorphs (Dallol ponds), and Ca or Mg chlorides (Yellow Lake, BLPS samples) (Fig. 4, Extended Data Fig. 10 and Supplementary Figs. 1 and 2). We also observed Si-encrusted rod-shaped cells in Lake Assale samples (Fig. 4l). Therefore, silica-rounded precipitates represent ultrasmall cell-like biomorphs in samples with no detectable life but they contribute to cell encrustment and potential fossilization when life is present.

Our work has three major implications. First, by studying the microbial distribution along gradients of polyextreme conditions in the geothermal area of Dallol and its surroundings in the Danakil Depression, we identify two major physicochemical barriers that prevent life from thriving in the presence of liquid water on Earth and, potentially, elsewhere<sup>14</sup>, despite the presence of liquid water at the surface of a planet being a widely accepted criterion for habitability. In line with previous studies<sup>12,13,19,20</sup>, one barrier is imposed by high chaotricity and low  $a_w$ , which are associated with high Mg<sup>2+</sup>-brines in the Black Lake and Yellow Lake areas. The second barrier seems to be imposed by the hyperacid–hypersaline combinations found in the Dallol dome ponds (pH ~0; salt >35%), regardless of temperature. This suggests that molecular adaptations to simultaneous very low pH and high salt extremes are incompatible beyond those limits. In principle, more acidic proteins, intracellular K<sup>+</sup> accumulation ('salt-in' strategy) or internal positive membrane potential generated by cations or H<sup>+</sup>/cation antiporters serve both acidophilic and halophilic adaptations<sup>37–39</sup>. However, membrane stability/function problems and/or high external Cl<sup>−</sup> concentrations that induce H<sup>+</sup> and cation (K<sup>+</sup>/Na<sup>+</sup>) import, potentially disrupting membrane bioenergetics<sup>38</sup>, might be deleterious under these conditions. We cannot exclude other explanations linked to the presence of several stressors, such as high metal content or an increased susceptibility to the presence of local chaotropic salts in the Dallol hyperacidic ponds even if measured chaotricity values are relatively low (−31 to +19 kJ kg<sup>−1</sup>) compared to the established limit for life (87.3 kJ kg<sup>−1</sup>)<sup>12,13,20</sup> (Extended Data Fig. 6). Future studies should help to identify the molecular barriers limiting the adaptation of life to this combination of extremes. Second, although extreme environments are usually low-diversity systems, we identify exceptionally diverse and abundant archaea spanning known major taxa in hypersaline, mildly acidic systems near life-limiting conditions. A wide archaeal (and to a lesser extent, bacterial) diversity seems consistent with suggestions that NaCl-dominated brines are not as extreme as previously thought<sup>40</sup> and, with recent observations that the mixing of meteoric and geothermal fluids leads to hyperdiverse communities<sup>41</sup>. Nonetheless, life under high salt conditions requires extensive molecular adaptations<sup>12,13,19,40</sup>, which might seem at odds with several independent adaptations to extreme halophily across archaea. Among those adaptations, the intracellular accumulation of K<sup>+</sup> ('salt-in' strategy), together with the corresponding adaptation of intracellular proteins to function under those conditions, has been crucial. Based on the observation that the deepest archaeal branches correspond to (hyper)thermophilic lineages<sup>42</sup> and that nonhalophilic hyperthermophilic archaea accumulate high intracellular K<sup>+</sup> (1.1–3 M) for protein thermoprotection<sup>43,44</sup> (thermoacidophiles also need K<sup>+</sup> for pH homeostasis<sup>38</sup>), we hypothesize that intracellular K<sup>+</sup>

accumulation is an ancestral archaeal trait linked to thermophilic adaptation that has been independently exapted in different taxa for adaptation to hypersaline habitats. Finally, the extensive occurrence of abiotic, mostly Si-rich, biomorphs mimicking the simple shape and size of ultrasmall cells in the hydrothermally influenced Dallol settings reinforces the equivocal nature of morphological 'microfossils'<sup>35</sup> and calls for the combination of several biosignatures before claiming the presence of life on the early Earth and beyond.

## Methods

**Sampling and measurement of physicochemical parameters on site.** Samples were collected during two field trips in January 2016 and January 2017 (when air temperature rarely exceeded 40–45 °C); a few additional samples were collected in January 2018 (Fig. 1 and Extended Data Figs. 1 and 3). All sampling points and mapping data were georeferenced using a Trimble handheld global positioning system (Juno SB series) equipped with Environmental Systems Research Institute software ArcPad 10. Cartography of hydrogeothermal activity areas was generated using Environmental Systems Research Institute GIS ArcMap mapping software ArcGIS 10.1 over georeferenced Phantom-4 drone images taken by O. Grunewald during field campaigns, which was compared with and updated previous local geological cartography<sup>7</sup>. Samples were collected from three major areas at the Dallol dome and its vicinity (Fig. 1b): (1) the top of the Dallol dome, consisting of various hydrothermal pools with diverse degrees of oxidation (Fig. 1c); (2) the Black Mountain area (Fig. 1d), including the Black Lake and surrounding bischofite flows and the southwestern salt canyons, which contain water reservoirs often influenced by the geothermal activity; and (3) the Yellow Lake (Gae'Ale) area (Fig. 1e). We also collected samples from the hypersaline Lake Assale (Karum), located a few kilometres to the south in the Danakil Depression (Fig. 1b). Physicochemical parameters (Fig. 3) were measured in situ with a YSI Professional Series Plus multiparameter probe (pH, temperature, dissolved oxygen, redox potential) up to 70 °C and a Hanna HI93530 temperature probe (working range −200/1,000 °C) and a Hanna HI991001 pH probe (working pH range −2.00/16.00) at higher temperatures. Salinity was measured in situ with a refractometer on 1/10 dilutions in MilliQ water. Brine samples for chemical analyses were collected in 50-ml glass bottles after prefiltration through 0.22- $\mu$ m pore-diameter filters; bottles were filled to the top and sealed with rubber stoppers to prevent the (further) oxidation of reduced fluids. Solid and water samples for microbial diversity analyses and culturing assays were collected under aseptic conditions to prevent contamination (gloves, sterile forceps and containers). Samples for culture assays were kept at room temperature. Salts and mineral fragments for DNA-based analyses were conditioned in Falcon tubes and fixed with absolute ethanol. Water samples (volumes for each sample are indicated in Supplementary Table 1) were filtered through 30- $\mu$ m pore-diameter filters to remove large particles and sequentially filtered either through 0.22- $\mu$ m pore-diameter filters (Whatman) or 0.2- $\mu$ m pore-size cell-trap units (MEM-TEQ Ventures). Filters or cell-trap concentrates retaining 0.2–30  $\mu$ m particles were fixed in 2-ml cryotubes with absolute ethanol (>80% final concentration). Back in the laboratory, ethanol-fixed samples were stored at −20 °C until use.

## Chemical analyses, salinity, chaotricity, ionic strength and water activity.

The chemical composition of solid and 0.2- $\mu$ m prefiltered liquid samples was analysed at SIDI Service (Servicio Interdepartamental de Investigación, Universidad Autónoma de Madrid). Major and trace elements in liquid samples were analysed by total reflection X-ray fluorescence with a TXRF-8030c FEI spectrometer and inductively coupled plasma–mass spectrometry using a Perkin–Elmer NexION 300XX instrument. Ions were analysed using a Dionex DX-600 ion chromatography system. Organic molecules were characterized using a Varian HPLC–diode array detector/FL/LS liquid chromatograph. Crystalline phases in solid samples were characterized by X-ray diffraction using a X'Pert PRO Theta/Theta diffractometer (Panalytical) and identified by comparison with the International Centre for Diffraction Data PDF-4+ database using the High Score Plus software (Malvern Panalytical <https://www.malvernpanalytical.com/es/products/category/software/x-ray-diffraction-software/highscore-with-plus-option>). Inorganic data are provided in Supplementary Table 1 and organic and ionic chemistry data in Supplementary Tables 2 and 3, respectively. Salinity (weight/volume, expressed in percentage throughout the manuscript) was measured in triplicates (and up to six times) by weighing the total solids after heat-drying 1-ml aliquots in ceramic crucibles at 120 °C for at least 24 h. Chaotricity was measured according to the temperature of gelation of ultrapure gelatin (for Ca-rich samples) and agar (rest of samples) and determined using the spectrometric assay developed by Cray et al.<sup>45</sup> (Extended Data Fig. 5). Chaotricity was also calculated according to Cray and coworkers<sup>46</sup> based on the abundance of dominant Na, K, Mg, Ca and Fe cations and, on the ground that Cl is the dominant anion, assuming they essentially form chlorine salts (NaCl, KCl, MgCl<sub>2</sub>, CaCl<sub>2</sub> and FeCl<sub>2</sub>). Ionic strength was calculated according to Fox-Powell et al.<sup>47</sup>. Water activity was measured on 10-ml unfiltered aliquots at room temperature (25 °C) using a HC2-AW probe and HP23-AW-A indicator (Rotronic AG) calibrated at 23 °C using the

AwQuick acquisition mode (error per measure 0.0027). From a strict biological perspective, these water activity measurements are not sufficiently accurate and need to be considered as indicative because cells can be sensitive to a 0.001 water activity change<sup>48</sup>. However, the measurements follow the same trend as shown by the other related parameters measured experimentally (salinity, chaotropy). We used R-software<sup>49</sup> packages FactoMineR<sup>50</sup> and factoextra<sup>51</sup> to carry out a PCA of samples, chemical and physicochemical parameters (Fig. 2 and Extended Data Fig. 4). Differences between the groups of samples belonging to the same physicochemical zone that segregated in the PCA were tested using the one-way analysis of variance module of IBM SPSS Statistics 24 software. The significance of differences among groups and with the measured parameters were checked by a post-hoc comparison using the Bonferroni test.

**DNA purification and 16S/18S rRNA gene metabarcoding.** DNA from filters, cell-trap concentrates and grinded solid samples was purified using the Power Soil DNA Isolation Kit (MoBio) under an ultraviolet-irradiated Erlab CaptairBio DNA/RNA PCR Workstation. Before DNA purification, filters were cut into small pieces with a sterile scalpel and the ethanol remaining in cryotubes was filtered through 0.2 µm pore-diameter filters and processed in the same way. Ethanol-fixed cell-trap concentrates were centrifuged for 10 min at 13,000 r.p.m. and the pellet resuspended in the first kit buffer. Samples were rehydrated for at least 2 h at 4 °C in the kit resuspension buffer. We used the Arcturus PicoPure DNA Isolation kit (Applied Biosystems; samples labelled pp) for a selection of cell-trap concentrates, FACS-sorted cells and for monitoring potential culture enrichments. DNA was resuspended in 10 mM Tris-HCl buffer, pH 8.0 and stored at -20 °C. Bacterial and archaeal 16S rRNA gene fragments of approximately 290 bp encompassing the V4 hypervariable region were amplified with PCR using U515F (5'-GTGCCAGCAGCGCCGGTAA) and U806R (5'-GGACTACVSGGGTATCTAAT) primers. PCR reactions were conducted in 25 µl, using 1.5 mM MgCl<sub>2</sub>, 0.2 mM of each dNTP (PCR Nucleotide Mix, Promega), 0.1 µM of each primer, 1–5 µl of purified 'DNA' and 1 unit of the hot-start Taq Platinum polymerase (Invitrogen). GoTaq (Promega) was also used when amplicons were not detected, but did not yield better results. Amplification reactions were performed for 35 cycles (94 °C for 15 s, 50–55 °C for 30 s and 72 °C for 90 s), after a 2 min-denaturation step at 94 °C and before a final extension at 72 °C for 10 min. Amplicons were visualized after gel electrophoresis and staining with ultrasensitive GelRed nucleic acid gel (Biotium) on an ultraviolet-light transilluminator. When direct PCR reactions failed to yield amplicons after several assays, PCR conditions and using increasing amounts of input potential DNA, we carried out seminested reactions. For seminested reactions, we used those same primers for PCR amplification but we used as input potential DNA 1 µl of PCR products, from a first amplification reaction performed with universal prokaryotic primers U340F (5'-CCTACGGGRRGCASCAG) and U806R, including the negative controls from the first PCR reaction. Eukaryotic 18S rRNA gene fragments that included the V4 hypervariable region were amplified using primers EK-565F (5'-GCAGTTAAAAGCTCGTAGT) and 18S-EUK-1134-R-UNonMet (5'-TTTAAGTTTCAGCCTTGCG). Primers were tagged with different molecular identifiers (MID) to allow multiplexing and subsequent sequence sorting. Amplicons from at least five independent PCR products for each sample were pooled together and then purified using the QIAquick PCR purification kit (Qiagen). Whenever seminested PCR reactions yielded amplicons, seminested reactions using first PCR negative controls as the input also yielded amplicons (second PCR controls did not yield amplicons). Products of these positive 'negative' controls were pooled in two control sets (1 and 2) and sequenced along with the rest of amplicons. DNA concentrations were measured using Qubit dsDNA HS assays (Invitrogen). Equivalent amplicon amounts obtained for 54 samples (including controls) were multiplexed and sequenced using paired-end (2 × 300 bp) MiSeq Illumina technology (Eurofins Genomics). In parallel, we tried to amplify near-complete 16S/18S rRNA gene fragments (~1,400–1,500 bp) using combinations of forward archaea-specific primers (21F, 5'-TTCCGGTTGATCCTGCCGGA; Ar109F, 5'-ACKGCTGCTCAGTAACACGT) and bacteria-specific primers (27F, 5'-AGAGTTTGATCCTGGCTCAG) with the prokaryotic reverse primer 1492R (5'-GGTTACCTTGTACGACTT) and eukaryotic primers 82F (5'-GAACTGCGAATGGCTC) and 1520R (5'-CYGAGGTTACCACTAC). When amplified, DNA fragments were cloned using TopoTA cloning (Invitrogen) and clone inserts were Sanger-sequenced to yield longer reference sequences. Forward and reverse Sanger sequences were quality controlled and merged using Codon Code Aligner (<http://www.codoncode.com/aligner/>).

**Sequence treatment and phylogenetic analyses.** Paired-end reads were merged and treated using a combination of existing software to check quality, eliminate primers and MID, and to remove potential chimeras. Sequence statistics are given in Extended Data Fig. 6. Briefly, read merging was determined with FLASH<sup>52</sup>; primers and MID, trimmed with cutadapt<sup>53</sup>; and clean merged reads dereplicated using vsearch<sup>54</sup> with the `uchime_denovo` option to eliminate potential chimeras. The resulting dereplicated clean merged reads were used to define OTUs at 95% identity cut-off using CD-HIT-EST<sup>55</sup>. This cut-off offered (1) a reasonable operational approximation to the genus-level diversity while producing

a manageable number of OTUs to be included in phylogenetic trees (see below) and (2) a conservative identification of potential contaminants in our seminested PCR-derived datasets. Diversity (Simpson), richness (Chao1) and evenness indices were determined using R-package 'vegan' (Supplementary Table 5). OTUs were assigned to known taxonomic groups based on similarity with sequences of a local database, including sequences from cultured organisms and environmental surveys retrieved from SILVA128 (ref. <sup>56</sup>) and PR2v4 (ref. <sup>57</sup>). The taxonomic assignment of bacteria and archaea was refined by phylogenetic placement of OTU representative sequences in reference phylogenetic trees. To build these trees, we used Mafft-linsi v.7.38 (ref. <sup>58</sup>) to produce alignments of near full-length archaeal and bacterial 16S rRNA gene sequences comprising Sanger sequences from our gene libraries (144 archaeal and 91 bacterial) and selected references for major identified taxa plus the closest blast-hits to our OTUs (702 archaea and 2,922 bacterial). Poorly aligned regions were removed using TrimAl<sup>59</sup>. Maximum likelihood phylogenetic trees were constructed with IQ-TREE<sup>60</sup> using the general time reversible (GTR) model of sequence evolution with a gamma law and taking into account invariable sites (GTR + G + I). Node support was estimated by ultrafast bootstrapping as implemented in IQ-TREE. Shorter OTU representative sequences (2,653 archaeal and 710 bacterial) were added to the reference alignment using MAFFT (accurate-linsi 'addfragments' option). This final alignment was split into two files (references and OTUs) before using the EPA-ng tool (<https://github.com/Pbdas/epa-ng>) to place OTUs in the reference trees reconstructed with IQ-TREE. The `jplace` files generated by EPA-ng were transformed into newick tree files with the `genesis` library (<https://github.com/lczech/genesis>). Tree visualization and ring addition were done with GraphLan<sup>61</sup>. To determine whether our OTUs might correspond to thermophilic species, we plotted the GC content of the 16S rRNA gene region used for metabarcoding analyses of a selection of 88 described archaeal species with optimal growth temperatures ranging from 15 to 103 °C. These included representatives of all Halobacteria genera because they are often characterized by high GC content. A regression analysis confirmed the occurrence of a positive correlation<sup>62</sup> between rRNA GC content and optimal growth temperature for this shorter 16S rRNA gene amplified region (Fig. 3b). We then plotted the GC content of our archaeal OTUs on the same graph. Dots corresponding to Halobacteria genera remain out of the dark shadowed area in Fig. 3b.

**Cultures.** Parallel culture attempts were carried out in two different laboratories (Orsay and Madrid). We used several culture media derived from a classical halophile base mineral growth medium<sup>63</sup> containing NaCl (234 g l<sup>-1</sup>), KCl (6 g l<sup>-1</sup>), NH<sub>4</sub>Cl (0.5 g l<sup>-1</sup>), K<sub>2</sub>HPO<sub>4</sub> (0.5 g l<sup>-1</sup>), (NH<sub>4</sub>)<sub>2</sub>SO<sub>4</sub> (1 g l<sup>-1</sup>), MgSO<sub>4</sub>·7H<sub>2</sub>O (30.5 g l<sup>-1</sup>), MnCl<sub>2</sub>·7H<sub>2</sub>O (19.5 g l<sup>-1</sup>), CaCl<sub>2</sub>·6H<sub>2</sub>O (1.1 g l<sup>-1</sup>) and Na<sub>2</sub>CO<sub>3</sub> (0.2 g l<sup>-1</sup>). The pH was adjusted to 4 and 2 with 10 N H<sub>2</sub>SO<sub>4</sub>. The autoclaved medium was amended with filter-sterilized cyanocobalamin (1 µM final concentration) and 5 ml of an autoclaved CaCl<sub>2</sub>·6H<sub>2</sub>O 1 M stock solution. Our medium MDH2 contained yeast extract (1 g l<sup>-1</sup>) and glucose (0.5 g l<sup>-1</sup>). The MDSH1 medium had only two-thirds of each base medium salt concentration plus FeCl<sub>3</sub> (0.1 g l<sup>-1</sup>) and 10 ml<sup>-1</sup> of Allen's trace solution. It was supplemented with three energy sources (prepared in 10 ml distilled water at pH 2 and sterilized by filtration): yeast extract (1 g l<sup>-1</sup>) and glucose (0.5 g l<sup>-1</sup>) (MDSH1-org medium); Na<sub>2</sub>S<sub>2</sub>O<sub>3</sub> (5 g l<sup>-1</sup>) (MDSH1-thio medium) and FeSO<sub>4</sub>·7H<sub>2</sub>O (30 g l<sup>-1</sup>) (MDSH1-Fe medium). Medium MDSH2 mimicked more closely some Dallol salts as it also contained FeCl<sub>3</sub> (0.1 g l<sup>-1</sup>), MnCl<sub>2</sub>·4H<sub>2</sub>O (0.7 g l<sup>-1</sup>), CuSO<sub>4</sub> (0.02 g l<sup>-1</sup>), ZnSO<sub>4</sub>·7H<sub>2</sub>O (0.05 g l<sup>-1</sup>) and LiCl (0.2 g l<sup>-1</sup>). It also contained 10 ml<sup>-1</sup> of Allen's trace solution combined with the same energy sources used for MDSH1, yielding media MDSH2-org, MDSH2-thio and MDSH2-Fe. For enrichment cultures, we added 0.1 ml liquid samples to 5 ml medium at pH 2 and 4 and incubated at 37 °C, 50 °C and 70 °C in 10-ml sterile glass tubes depending on the original sample temperatures. Three additional variants of the base salt medium, which was supplemented with FeCl<sub>3</sub> and trace minerals, contained 0.2 g l<sup>-1</sup> yeast extract (SALT-YE), 0.5 g l<sup>-1</sup> thiosulfate (SALT-THIO) or 0.6 g l<sup>-1</sup> benzoate and 5 mM hexadecane (SALT-BH). The pH of these media was adjusted with 34% HCl to pH 1.5 for Dallol and Black Lake samples, and to pH 3.5 for Yellow Lake, PS3 and PSBL samples. We added 1 ml of sample to 4 ml of medium and incubated it at 45 °C in light conditions and at 37 °C and 70 °C in dark conditions. We also tried cultures in anaerobic conditions. Potential growth was monitored by optical microscopy and, for some samples, SEM. In the rare cases where enrichments were obtained, we attempted isolation by serial dilutions.

**Flow cytometry and FACS.** The presence of cell/particle populations above background levels in Dallol samples was assessed with a flow-cytometer cell-sorter FACSAriaIII (Becton Dickinson). Several DNA dyes were tested for lowest background signal in forward scatter (FSC) red (695 ± 20 nm) and green (530 ± 15 nm) fluorescence (Extended Data Fig. 9a) using sterile SALT-YE medium as blank. DRAQ5 and SYTO13 (ThermoFisher) were retained and used at 5 µM final concentration to stain samples in the dark at room temperature for 1 h. Cell-trap concentrated samples were diluted at 20% with 0.1-µm filtered and autoclaved MilliQ water. The FACSAriaIII was set at purity sort mode triggering on the forward scatter (FSC). Fluorescent target cells/particles were gated based on the FSC and red or green fluorescence (Extended Data Fig. 9b) and flow-sorted at a rate of 1–1,000 particles s<sup>-1</sup>. Sorting was conducted using the FACS Diva software (Becton Dickinson) and figures were produced using FCSEXPRESS 6 software

(De Novo Software). Sorted cells/particles were subsequently observed by SEM for characterization. Minimum and maximum cell abundances were estimated based on the number of sorted particles, duration of sorting and minimal (10  $\mu\text{l min}^{-1}$ ) and maximal (80  $\mu\text{l min}^{-1}$ ) flow rates of the FACSARIA (Becton Dickinson FACSARIA manual).

**SEM and elemental analysis.** SEM analyses were carried out on natural samples, FACS-sorted cells/particles and a selection of culture attempts. Liquid samples were deposited onto 0.1  $\mu\text{m}$  pore-diameter filters (Whatman) under a mild vacuum aspiration regime and briefly rinsed with 0.1- $\mu\text{m}$  filtered and autoclaved MilliQ water under the same vacuum regime. Filters were allowed to dry and sputtered with carbon prior to SEM observations. A Zeiss ultra55 field emission gun SEM was used for the SEM analyses. Secondary electron images were acquired using an In Lens detector at an accelerating voltage of 2.0 kV and a working distance of  $\sim 7.5$  mm. Backscattered electron images were acquired for chemical mapping using an angle selective backscattered detector at an accelerating voltage of 15 kV and a working distance of  $\sim 7.5$  mm. Elemental maps were generated from hyperspectral images (HyperMap) by EDXS using an EDS QUANTAX detector. EDXS data were analysed using the ESPRIT software package (Bruker).

**Reporting Summary.** Further information on research design is available in the Nature Research Reporting Summary linked to this article.

### Data availability

Sanger sequences have been deposited in GenBank (National Center for Biotechnology Information) with accession numbers MK894601–MK894820 and Illumina sequences in GenBank Short Read Archive with BioProject number PRJNA541281.

Received: 30 May 2019; Accepted: 16 September 2019;

Published online: 28 October 2019

### References

- Harrison, J. P., Gheeraert, N., Tsigelnitskiy, D. & Cockell, C. S. The limits for life under multiple extremes. *Trends Microbiol.* **21**, 204–212 (2013).
- Merino, N. et al. Living at the extremes: extremophiles and the limits of life in a planetary context. *Front. Microbiol.* **10**, 1785 (2019).
- Johnson, S. S., Chevrette, M. G., Ehlmann, B. L. & Benison, K. C. Insights from the metagenome of an acid salt lake: the role of biology in an extreme depositional environment. *PLoS ONE* **10**, e0122869 (2015).
- Zaikova, E., Benison, K. C., Mormile, M. R. & Johnson, S. S. Microbial communities and their predicted metabolic functions in a desiccating acid salt lake. *Extremophiles* **22**, 367–379 (2018).
- Futterer, O. et al. Genome sequence of *Picrophilus torridus* and its implications for life around pH 0. *Proc. Natl Acad. Sci. USA* **101**, 9091–9096 (2004).
- Varet, J. in *Geology of Afar (East Africa). Regional Geology Reviews* (eds Oberhänsli, R. et al.) Ch. 7 (Springer, 2018).
- Franzson, H., Helgadóttir, H. M. & Óskarsson, F. Surface exploration and first conceptual model of the Dallol geothermal area, northern Afar, Ethiopia. In *Proc. World Geothermal Congress* (2015).
- Darrah, T. H. et al. Gas chemistry of the Dallol region of the Danakil Depression in the Afar region of the northern-most East African Rift. *Chem. Geol.* **339**, 16–29 (2013).
- Holwerda, J. G. & Hutchinson, R. W. Potash-bearing evaporites in the Danakil area, Ethiopia. *Econ. Geol.* **63**, 124–150 (1968).
- Warren, J. K. *Danakil Potash, Ethiopia: Beds of Kainite/Carnallite, Part 2 of 4* (SaltWork Consultants, 2015).
- Cavalazzi, B. et al. The Dallol geothermal area, northern Afar (Ethiopia): an exceptional planetary field analog on Earth. *Astrobiology* **19**, 553–578 (2019).
- Hallsworth, J. E. et al. Limits of life in  $\text{MgCl}_2$ -containing environments: chaotropy defines the window. *Environ. Microbiol.* **9**, 801–813 (2007).
- Stevenson, A. et al. Is there a common water-activity limit for the three domains of life? *ISME J.* **9**, 1333–1351 (2015).
- McKay, C. P. Requirements and limits for life in the context of exoplanets. *Proc. Natl Acad. Sci. USA* **111**, 12628–12633 (2014).
- Moissl-Eichinger, C., Cockell, C. & Rettberg, P. Venturing into new realms? Microorganisms in space. *FEMS Microbiol. Rev.* **40**, 722–737 (2016).
- Pérez, E. & Chebude, Y. Chemical analysis of Gaet'Alé, a hypersaline pond in Danakil Depression (Ethiopia): new record for the most saline water body on Earth. *Aquat. Geochem.* **23**, 109–117 (2017).
- Kotopoulou, E. et al. A polyextreme hydrothermal system controlled by iron: the case of Dallol at the Afar triangle. *ACS Earth Space Chem.* **3**, 90–99 (2019).
- Warren, J. K. *Danakil Potash, Ethiopia: Is the Present Geology the Key? Part 1 of 4* (SaltWork Consultants, 2015).
- Tosca, N. J., Knoll, A. H. & McLennan, S. M. Water activity and the challenge for life on early Mars. *Science* **320**, 1204–1207 (2008).
- Stevenson, A. et al. *Aspergillus penicillioideus* differentiation and cell division at 0.585 water activity. *Environ. Microbiol.* **19**, 687–697 (2017).
- Sheik, C. S. et al. Identification and removal of contaminant sequences from ribosomal gene databases: lessons from the census of deep life. *Front. Microbiol.* **9**, 840 (2018).
- Weyrich, L. S. et al. Laboratory contamination over time during low-biomass sample analysis. *Mol. Ecol. Resour.* **19**, 982–996 (2019).
- Narasimgarao, P. et al. De novo metagenomic assembly reveals abundant novel major lineage of archaea in hypersaline microbial communities. *ISME J.* **6**, 81–93 (2012).
- Sorokin, D. Y. et al. Discovery of extremely halophilic, methyl-reducing euryarchaea provides insights into the evolutionary origin of methanogenesis. *Nat. Microbiol.* **2**, 17081 (2017).
- Sorokin, D. Y. et al. *Methanonatronarchaeum thermophilum* gen. nov., sp. nov. and 'Candidatus Methanohalarchaeum thermophilum', extremely halo(natrono)philic methyl-reducing methanogens from hypersaline lakes comprising a new euryarchaeal class *Methanonatronarchaeia* classis nov. *Int. J. Syst. Evol. Microbiol.* **68**, 2199–2208 (2018).
- Borin, S. et al. Sulfur cycling and methanogenesis primarily drive microbial colonization of the highly sulfidic Urania deep hypersaline basin. *Proc. Natl Acad. Sci. USA* **106**, 9151–9156 (2009).
- Mwirichia, R. et al. Metabolic traits of an uncultured archaeal lineage—MSBL1—from brine pools of the red sea. *Sci. Rep.* **6**, 19181 (2016).
- Castelle, C. J. et al. Biosynthetic capacity, metabolic variety and unusual biology in the CPR and DPANN radiations. *Nat. Rev. Microbiol.* **16**, 629–645 (2018).
- Castelle, C. J. & Banfield, J. F. Major new microbial groups expand diversity and alter our understanding of the tree of life. *Cell* **172**, 1181–1197 (2018).
- Dombrowski, N., Lee, J. H., Williams, T. A., Offre, P. & Spang, A. Genomic diversity, lifestyles and evolutionary origins of DPANN archaea. *FEMS Microbiol. Lett.* **366**, fnz008 (2019).
- Petitjean, C., Deschamps, P., Lopez-Garcia, P. & Moreira, D. Rooting the domain archaea by phylogenomic analysis supports the foundation of the new kingdom proteoarchaeota. *Genome Biol. Evol.* **7**, 191–204 (2014).
- Golyshina, O. V. et al. 'ARMAN' archaea depend on association with euryarchaeal host in culture and in situ. *Nat. Commun.* **8**, 60 (2017).
- Minegishi, H. et al. Acidophilic haloarchaeal strains are isolated from various solar salts. *Saline Syst.* **4**, 16 (2008).
- Naor, A. & Gophna, U. Cell fusion and hybrids in archaea: prospects for genome shuffling and accelerated strain development for biotechnology. *Bioengineered* **4**, 126–129 (2013).
- Garcia-Ruiz, J. M. et al. Self-assembled silica-carbonate structures and detection of ancient microfossils. *Science* **302**, 1194–1197 (2003).
- Garcia-Ruiz, J. M., Melero-Garcia, E. & Hyde, S. T. Morphogenesis of self-assembled nanocrystalline materials of barium carbonate and silica. *Science* **323**, 362–365 (2009).
- Slonczewski, J. L., Fujisawa, M., Dopson, M. & Krulwich, T. A. Cytoplasmic pH measurement and homeostasis in bacteria and Archaea. *Adv. Micro. Physiol.* **55**, 1–79 (2009).
- Buetti-Dinh, A., Dethlefsen, O., Friedman, R. & Dopson, M. Transcriptomic analysis reveals how a lack of potassium ions increases *Sulfolobus acidocaldarius* sensitivity to pH changes. *Microbiology* **162**, 1422–1434 (2016).
- Gunde-Cimerman, N., Plemenitas, A. & Oren, A. Strategies of adaptation of microorganisms of the three domains of life to high salt concentrations. *FEMS Microbiol. Rev.* **42**, 353–375 (2018).
- Lee, C. J. D. et al. NaCl-saturated brines are thermodynamically moderate, rather than extreme, microbial habitats. *FEMS Microbiol. Rev.* **42**, 672–693 (2018).
- Colman, D. R., Lindsay, M. R. & Boyd, E. S. Mixing of meteoric and geothermal fluids supports hyperdiverse chemosynthetic hydrothermal communities. *Nat. Commun.* **10**, 681 (2019).
- López-García, P., Zivanovic, Y., Deschamps, P. & Moreira, D. Bacterial gene import and mesophilic adaptation in Archaea. *Nat. Rev. Microbiol.* **13**, 447–456 (2015).
- Hensel, R. & König, H. Thermoadaptation of methanogenic bacteria by intracellular ion concentration. *FEMS Microbiol. Lett.* **49**, 75–79 (1988).
- Shima, S., Thauer, R. K. & Ermler, U. Hyperthermophilic and salt-dependent formyltransferase from *Methanopyrus kandleri*. *Biochem. Soc. Trans.* **32**, 269–272 (2004).
- Cray, J. A., Russell, J. T., Timson, D. J., Singhal, R. S. & Hallsworth, J. E. A universal measure of chaotropy and kosmotropy. *Environ. Microbiol.* **15**, 287–296 (2013).
- Cray, J. A. et al. Chaotropy: a key factor in product tolerance of biofuel-producing microorganisms. *Curr. Opin. Biotechnol.* **33**, 228–259 (2015).
- Fox-Powell, M. G., Hallsworth, J. E., Cousins, C. R. & Cockell, C. S. Ionic strength is a barrier to the habitability of Mars. *Astrobiology* **16**, 427–442 (2016).
- Stevenson, A. et al. Multiplication of microbes below 0.690 water activity: implications for terrestrial and extraterrestrial life. *Environ. Microbiol.* **17**, 257–277 (2015).

49. R Development Core Team *R: A Language and Environment for Statistical Computing* (R Foundation for Statistical Computing, 2017).
50. Lê, S., Josse, J. & Husson, F. FactoMineR: an R package for multivariate analysis. *J. Stat. Softw.* **25**, 1–18 (2008).
51. Kassambara, A. & Mundt, F. factoextra: extract and visualize the results of multivariate data analyses. <https://CRAN.R-project.org/package=factoextra> (2017).
52. Magoc, T. & Salzberg, S. L. FLASH: fast length adjustment of short reads to improve genome assemblies. *Bioinformatics* **27**, 2957–2963 (2011).
53. Martin, M. Cutadapt removes adapter sequences from high-throughput sequencing reads. *EMBnet. J.* **17**, 10–12 (2011).
54. Rognes, T., Flouri, T., Nichols, B., Quince, C. & Mahe, F. VSEARCH: a versatile open source tool for metagenomics. *PeerJ* **4**, e2584 (2016).
55. Fu, L., Niu, B., Zhu, Z., Wu, S. & Li, W. CD-HIT: accelerated for clustering the next-generation sequencing data. *Bioinformatics* **28**, 3150–3152 (2012).
56. Quast, C. et al. The SILVA ribosomal RNA gene database project: improved data processing and web-based tools. *Nucleic Acids Res.* **41**, D590–D596 (2013).
57. Guillou, L. et al. The protist ribosomal reference database (PR2): a catalog of unicellular eukaryote small sub-unit rRNA sequences with curated taxonomy. *Nucleic Acids Res.* **41**, D597–D604 (2013).
58. Katoh, K. & Standley, D. M. MAFFT multiple sequence alignment software version 7: improvements in performance and usability. *Mol. Biol. Evol.* **30**, 772–780 (2013).
59. Capella-Gutierrez, S., Silla-Martinez, J. M. & Gabaldon, T. trimAl: a tool for automated alignment trimming in large-scale phylogenetic analyses. *Bioinformatics* **25**, 1972–1973 (2009).
60. Nguyen, L. T., Schmidt, H. A., von Haeseler, A. & Minh, B. Q. IQ-TREE: a fast and effective stochastic algorithm for estimating maximum-likelihood phylogenies. *Mol. Biol. Evol.* **32**, 268–274 (2015).
61. Asnicar, F., Weingart, G., Tickle, T. L., Huttenhower, C. & Segata, N. Compact graphical representation of phylogenetic data and metadata with GraPhlAn. *PeerJ* **3**, e1029 (2015).
62. Wang, H. C., Xia, X. & Hickey, D. Thermal adaptation of the small subunit ribosomal RNA gene: a comparative study. *J. Mol. Evol.* **63**, 120–126 (2006).
63. Rodriguez-Valera, F., Ruiz-Berraquero, F. & Ramos-Cormenzana, A. Behaviour of mixed populations of halophilic bacteria in continuous cultures. *Can. J. Microbiol.* **26**, 1259–1263 (1980).

## Acknowledgements

We are grateful to O. Grunewald for co-organizing the Dallol expeditions, documenting field research and providing drone images, and also to Jean-Marie Hullot (in memoriam), Françoise Brenckmann and the Fondation Iris for funding the first field

trip. We thank L. Cantamessa for the in situ logistics and discussions about local history. We acknowledge M. Tafari (Mekelle University), A. A. Aliyu and the Afar authorities for local assistance, as well as the Ethiopian army and the Afar police for providing security. We thank J. Barthélémy, E. Kotopoulou and J. Garcia-Ruiz for help and discussions during field trips. We thank H. Timpano and the UNICELL platform for cell sorting; A. Gutiérrez-Preciado for bioinformatic assistance; A. Kish and C. Faveau for allowing us to measure water activity of selected samples at the Muséum National d'Histoire Naturelle; E. Viollier for discussion on chemical analyses; C. Gille for help with cultures; G. Billo for script help to treat SEM pictures; and J. T. Diaz and P. T. Sanz for advice on statistical analyses. This research was funded by the French CNRS (National Center for Scientific Research) basic annual funding, the CNRS programme TELLUS INTERRVIE and the European Research Council (ERC) under the European Union's Seventh Framework Programme (ERC grant no. 322669 to P.L.-G.). We thank the European COST Action TD1308 Origins for funding a short stay of A.I.L.-A. in Orsay. J.B. was financed by the French Ministry of National Education, Research and Technology.

## Author contributions

P.L.-G. and D.M. designed and supervised the research. P.L.-G. organized the scientific expeditions. J.B., P.L.-G., D.M., L.J. and J.M.L.-G. collected samples and took measurements in situ. J.B., P.L.-G. and P.B. carried out molecular biology analyses. J.B., A.I.L.-A. and D.M. performed culture, chemistry analyses and water–salt related measurements. A.I.L.-A. and J.B. performed statistical analyses. J.B., G.R. and D.M. analysed metabarcoding data. K.B. performed SEM and EDX analyses. J.M.L.-G. mapped geothermal activity and georeferenced all samples. L.J. and J.B. performed FACS-derived analyses. P.L.-G. and J.B. wrote the manuscript. All authors read and commented on the manuscript.

## Competing interests

The authors declare no competing interests.

## Additional information

**Extended data** is available for this paper at <https://doi.org/10.1038/s41559-019-1005-0>.

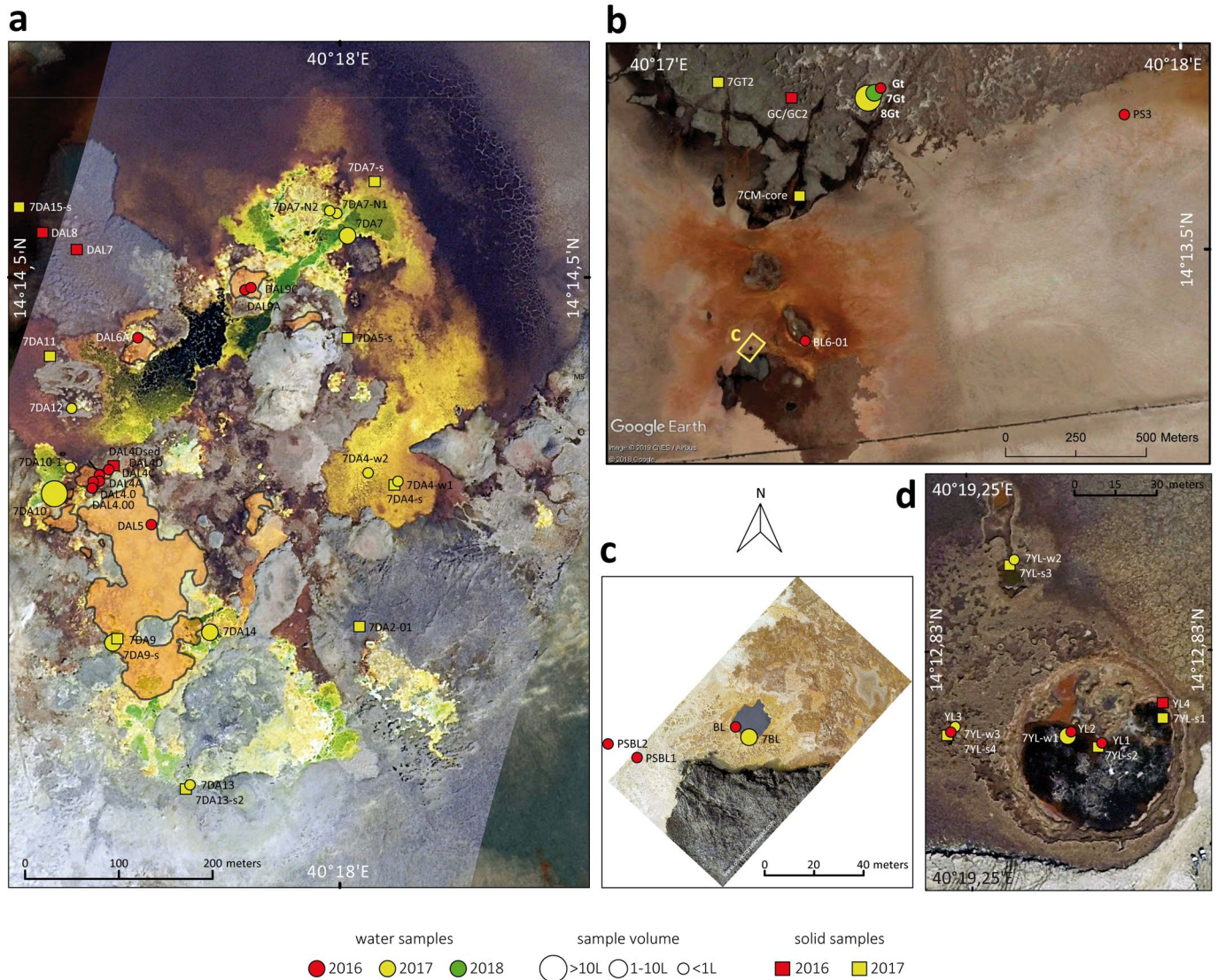
**Supplementary information** is available for this paper at <https://doi.org/10.1038/s41559-019-1005-0>.

**Correspondence and requests for materials** should be addressed to P.L.-G.

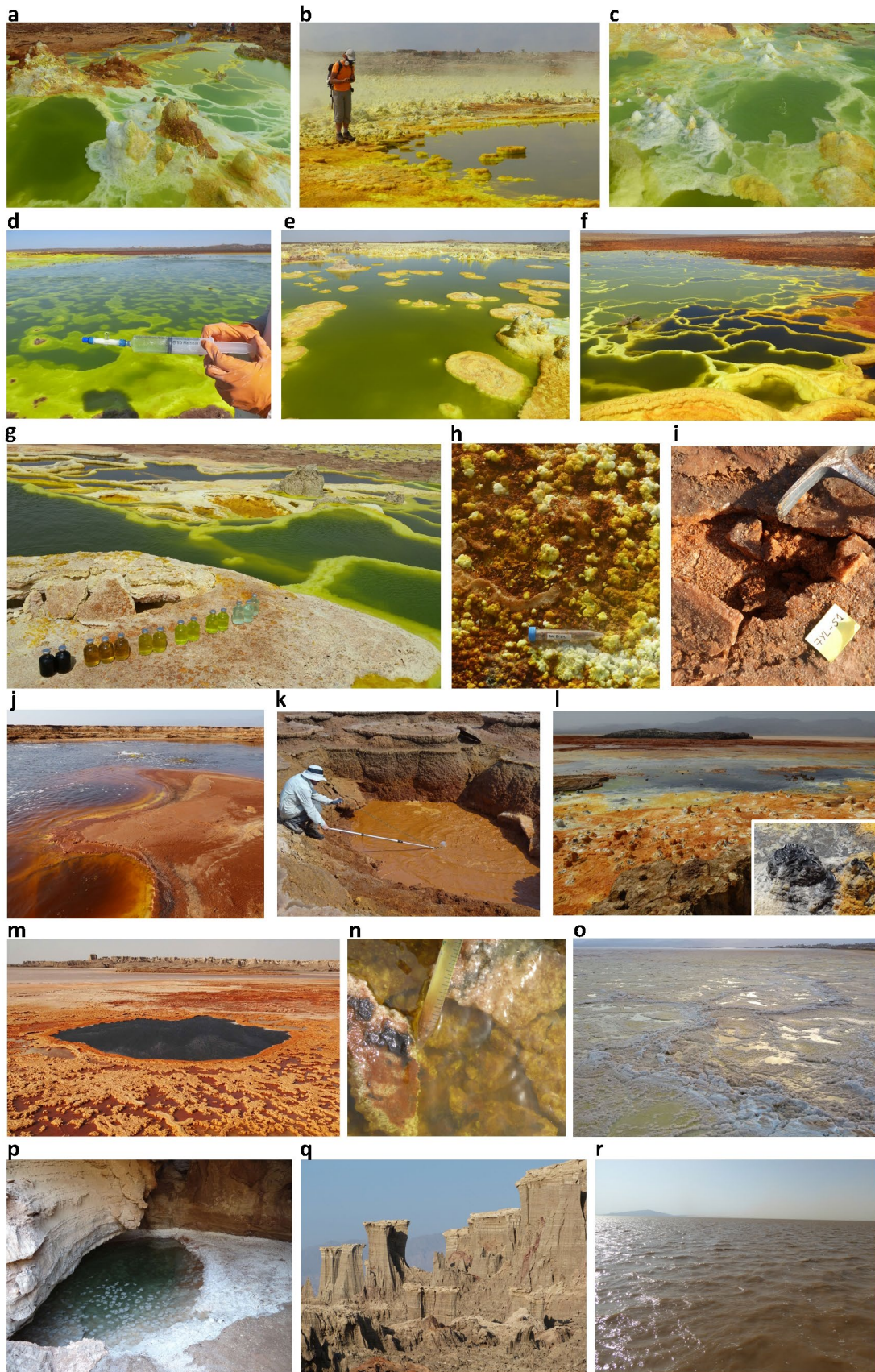
**Reprints and permissions information** is available at [www.nature.com/reprints](http://www.nature.com/reprints).

**Publisher's note** Springer Nature remains neutral with regard to jurisdictional claims in published maps and institutional affiliations.

© The Author(s), under exclusive licence to Springer Nature Limited 2019



**Extended Data Fig. 1 | Aerial view of the main sampling sites in the Dallol area.** **a**, Dallol dome summit showing the acidic green-yellow-brown coloured hydrothermal ponds and active degassing areas during our 2017 sampling trip; the orange-shaded area shows the active hydrothermal zone in January 2016. **b**, Dallol West salt canyons and Black Mountain area. **c**, Black Lake. **d**, Yellow Lake and surroundings. Names of samples and sampling sites are indicated. The size of circles is proportional to the water volume collected or filtered for subsequent analyses. Aerial photographs were taken from a drone by O. Grunewald, except b, which is a Google Earth aerial image (09/03/2016) obtained by the Sentinel satellite (ESA Copernicus program) provided by Image © 2019 CNES/Airbus.

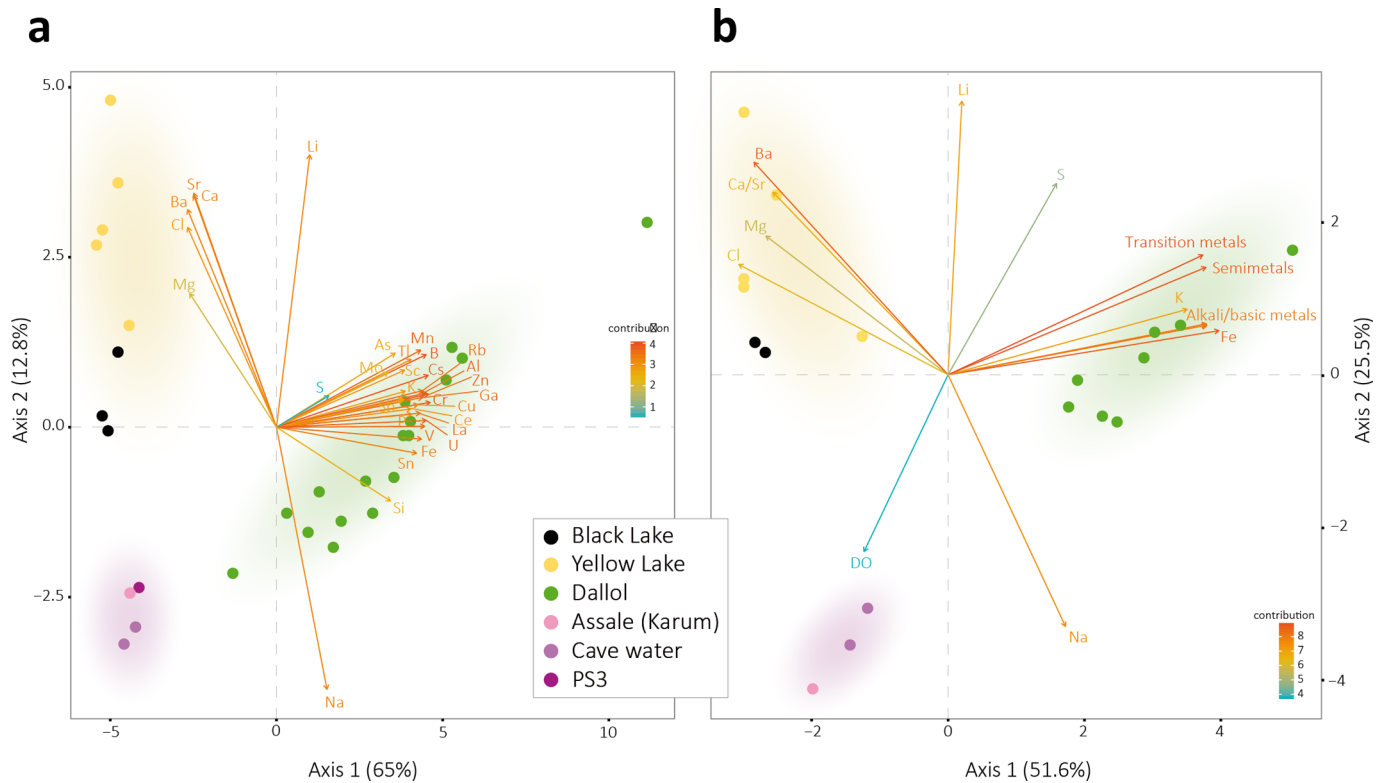


Extended Data Fig. 2 | see figure caption on next page.

**Extended Data Fig. 2 | Views of different sampling sites in the Dallol dome and surroundings in the Danakil Depression.** **a**, DAL4 sampling site ponds; **b**, DAL5 pond and active degassing area; **c**, active hydrothermal springs in DAL9 ponds; **d**, in situ cell-trap filtration at the 7DA7 sampling area; **e**, 7DA9 sampling site; **f**, 7DA10 ponds showing increasingly darker and brownish colours along the oxidation gradient; **g**, water samples from the different 7DA10 ponds; **h**, DAL8 mineral precipitates; **i**, 'proto-soil'-like salt crust (7YL-S1) near the Yellow Lake; **j**, Yellow Lake showing active degassing; **k**, YL3, salt-mud volcano in the Yellow Lake area; **l**, 'Little Dallol' hydrothermal very active area in 2016 on the way to the Black Mountain (in the distance; inlet, chimney emitting hydrocarbon-rich fluids at 110 °C); **m**, Black Lake; **n**, PSBL2 (Black Lake area ponds); **o**, wet salt plain, influenced by hydrothermal activity, corresponding to PS3 sample area; **p**, the cave in the salt canyons where Gt, 7Gt and 8Gt samples were collected; **q**, salt canyons; **r**, Assale (Karum) lake. Sample names starting by 7 indicate collection in 2017. Pictures from all other samples/sampling sites were taken during the 2016 expedition.

Color of ponds or solid samples	Sample name	Coordinates	Collection date	Brief description	Sample type / volume		Physicochemical parameters										Type of analyses						
					Solid	Liquid (ml)	0.2-30 µm fraction (ml) <sup>a</sup>	Temp (°C)	pH	DO (%)	DO (mg/l)	ORP (mV)	Refractometry inferred salinity (%)	Salinity - Total Solids (g/l) ± 10	Chemistry	Cloning/Sanger seq.	Meta-barcoding	Culture assays <sup>b</sup>	SEM/EDS	FACS			
<b>Dalol hydrothermal ponds</b>																							
	DAL4.00	14.23916N 40.297059E	16.01.2016	Hydrothermal fluid from a salt chimney feeding cascading ponds along redox gradient site DAL4		50	1000	108.0	n.d.	n.d.	n.d.	n.d.	30.0	375.40 ± 10.06	X	X							
	DAL4.0	14.23923N 40.29707E	17.01.2016	Warm whitish green pond in the redox pond series DAL4		50	1000	46.3	-0.43	0.55	0.03	328.95	21.0	373.29 ± 4.83	X	X	X	X	Y	X			
	DAL4A	14.23921N 40.29713E	17.01.2016	Bright green pond in the redox pond series DAL4		50	1000	30.5	-0.53	3.05	0.26	366.8	22.0	n.d.	X	X	X	Y	X				
	DAL4C	14.23967N 40.29744E	16.01.2016	Brownish green pond in the redox pond series DAL4			1000	31.6	-0.95	1	0.08	384.05	21.5	n.d.	X	X	X	Y	X				
	DAL4D	14.23934N 40.29738E	16.01.2016	Dark brown pond along an oxidation gradient, DAL4 site		50	1000	31.0	-0.72	1.4	0.11	381.55	n.d.	405.32 ± 19.6	X	X	X	X	Y	X			
	DAL4D-SED	14.23934N 40.29738E	16.01.2016	Yellow salt front forming pond wall	X			n.a.	n.a.	n.a.	n.a.	n.a.	n.a.	n.a.	X	X							
	DAL 5	14.23869N 40.29776E	17.01.2016	Yellow water from one big Dalol pond		50		42.6	-0.93	3.4	0.19	373.3	40	386.84 ± 6.18							Y		
	DAL6A	14.24085N 40.29756E	18.01.2016	Fluid from a salt chimney feeding various ponds along an oxidation gradient, site DAL6		50	1000	108.4	-0.65	n.d.	n.d.	n.d.	n.d.	424.51 ± 38.22	X	X	X	X	Y				
	DAL 7	14.242343N 40.296798E	18.01.2016	Sulfur-colored mineral precipitates on "chocolate formation"	X			n.a.	n.a.	n.a.	n.a.	n.a.	n.a.	n.a.							Y		
	DAL8-01	14.24217N 40.29635E	20.01.2016	Yellow, potentially sulfur-rich precipitates	X			n.a.	n.a.	n.a.	n.a.	n.a.	n.a.	n.a.		X	X	Y					
	DAL8-02	14.24217N 40.29635E	20.01.2016	Golden, potentially sulfur-rich salt precipitates	X			n.a.	n.a.	n.a.	n.a.	n.a.	n.a.	n.a.		X	X						
	DAL8-03	14.24217N 40.29635E	20.01.2016	Brown, potentially sulfur-rich salt precipitates	X			n.a.	n.a.	n.a.	n.a.	n.a.	n.a.	n.a.		X	X						
	DAL9A	14.241504N 40.298836E	21.01.2016	Large light green bubbling pond with various hydrothermal sources; site DAL9		50	650	37.9	-0.27	n.d.	n.d.	n.d.	n.d.	n.d.	X	X	X	X	Y				
	DAL9C	14.24151N 40.298874E	21.01.2016	Smaller deep green hydrothermal pond at the DAL9 site		50	750	56.0	-0.20	n.d.	n.d.	n.d.	n.d.	n.d.	X	X	X						
	7DA2-Q1	14.241275N 40.300633E	06.01.2017	Grey cauliflower-like mineral precipitates	X			n.a.	n.a.	n.a.	n.a.	n.a.	n.a.	n.a.		X	X						
	7DA4-w1	14.239465N 40.300419E	10.01.2017	Yellow-brownish water from a drying pond formed by yellow-colored salt		100		27.9	-0.73	3.8	0.13	416.1	44	446.07 ± 11.41	X								
	7DA4-w2	14.239892N 40.300106E	10.01.2017	Slightly lighter water from the same kind of pool as 7DA4-w1		100		27.0	-0.72	2.9	0.09	420.1	40	371.77 ± 2.11	X								
	7DA4-s	14.239465N 40.300419E	10.01.2017	Fresh, yellow cauliflower-like mineral precipitates near 7DA4-w2	X			n.a.	n.a.	n.a.	n.a.	n.a.	n.a.	n.a.		X	X						
	7DA5-s	14.240908N 40.300119E	10.01.2017	Brown (oxidized), fluid-impregnated cauliflower-like mineral precipitates	X			n.a.	n.a.	n.a.	n.a.	n.a.	n.a.	n.a.		X	X						
	7DA7	14.24219N 40.300102E	07.01.2017	Water from an active green large pond fed by multiple hydrothermal springs		500	3000	19.7	-0.55	4.1	0.16	371.9	47	429.6 ± 12.89		X	X	X	X	X	X		
	7DA7-s	14.2428N 40.300494E	10.01.2017	Brown salt crust East to 7DA7 active site on a drying pond covering a layer of wet yellow salt	X			n.a.	n.a.	n.a.	n.a.	n.a.	n.a.	n.a.									
	7DA7N-1	14.242381N 40.299992E	10.01.2017	Bluish hot pond on the northern terrace feeding 7DA7		50		44.6	-0.33	5.7	0.16	271.2	40.0	404.13 ± 20.16	X						Y		
	7DA7N-2	14.242381N 40.299992E	10.01.2017	Hotter, greenish pond adjacent to 7DA7N-1		50		68.0	n.d.	n.d.	n.d.	n.d.	37.0	411.1 ± 0.57	X								
	7DA9	14.241528N 40.29884E	08.01.2017	Large pond in active degassing area with many white-yellowish chimneys and salt neuphars		500	6000	31.9	-0.34	5.5	0.16	369	43	379.03 ± 17.18	X	X	X	X	X	X			
	7DA9-s	14.241528N 40.29884E	08.01.2017	Centrifugal round-shaped salt and sulfur formations in a dry pond next to 7DA9	X			n.a.	n.a.	n.a.	n.a.	n.a.	n.a.	n.a.		X	X						
	7DA10	14.23908N 40.29698E	09.01.2017	Upper green pond in a well-manicured terrace system along an oxidation gradient		100	14700	55.2	-0.08	2.2	0.05	321.8	35.0	366.83 ± 7.71	X	X	X						
	7DA10-1	14.23908N 40.29698E	09.01.2017	Highly evaporated, dark brown pond, lower in the 7DA10 terrace system		100		33.4	n.d.	n.d.	n.d.	n.d.	70	n.d.	X						Y		
	7DA12	14.240136N 40.29675E	10.01.2017	Active chimney (nearby 2016 site DAL6)		100		108.3	0.47	n.d.	n.d.	n.d.	43.0	385.48 ± 21.18	X								
	7DA13-w1	14.235495N 40.298135E	11.01.2017	Hydrothermal fluid from big grey active chimney		100		103.6	n.d.	n.d.	n.d.	n.d.	35.0	342.50 ± 18.87	X								
	7DA13-s2	14.235495N 40.298135E	11.01.2017	Grey, hard salt fragments at the bottom of chimney 7DA13	X			n.a.	n.a.	n.a.	n.a.	n.a.	n.a.	n.a.		X	X						
	7DA14	14.237398N 40.29842E	12.01.2017	Central pond in active group of geothermal ponds. Green color		50	675	39.7	-0.51	2.4	0.15	382	40	338.90 ± 8.17	X	X	X						
	7DA15-s	14.242142N 40.297727E	13.01.2017	Green/yellow sediment near the "chocolate formation" CH-F	X			n.a.	n.a.	n.a.	n.a.	n.a.	n.a.	n.a.		X	X						
<b>Yellow Lake (Gaet'Ale)</b>																							
	YL1	14.213574N 40.32128E	19.01.2016	Yellow Lake bubbling water, yellow-orange color, silty texture, smell of organics-containing gas	X	50	400	40.6	1.88	6.6	0.37	447.1	>50	724.40 ± 5.77	X	X	X	X	Y	X			
	YL2	14.213648N 40.321188E	19.01.2016	Yellow Lake bubbling water - nearby spot (few meters away)		50	400	39.5	1.88	5.4	0.35	419.3	51.0	677.60 ± 2.24	X	X	X	Y					
	YL3-O1-w	14.213588N 40.320748E	19.01.2016	Water from salt/sediment volcano			400	37.1	n.d.	n.d.	n.d.	n.d.	>50	761.59 ± 69.51		X	X	Y	X				
	YL3-O1-s	14.213588N 40.320748E	19.01.2016	Salty deposits from bubbling salt/sediment volcano - reddish color	X			37.1	n.a.	n.a.	n.a.	n.a.	n.a.	n.a.		X	X						
	YL4-O1	14.213588N 40.321482E	19.01.2016	Salt crust on top of sediment at the further upper rim of Yellow Lake	X			n.a.	n.a.	n.a.	n.a.	n.a.	n.a.	n.a.		X	X						
	7YL-w1	14.213574N 40.32128E	12.01.2017	Water from the Yellow Lake		150	5000	37.4	1.52	11.5	0.63	462.2	>50	944.60 ± 60.38	X					X	X		
	7YL-w2	14.213648N 40.321188E	12.01.2017	Water from a mid-sized pond near the Yellow Lake, strong smell of organics, dead birds		200		33.8	2.40	4.4	0.20	310.3	70	683.80 ± 80.61	X					X			X
	7YL-w3	14.213588N 40.320748E	12.01.2017	Water from salt mud volcano (YL3 in 2016)		100		35.9	1.37	5.1	0.32	349.3	80	n.d.	X					X			
	7YL-s1	14.213574N 40.32128E	12.01.2017	Salt crust from dried area in Yellow Lake	X			n.a.	n.a.	n.a.	n.a.	n.a.	n.a.	n.a.		X	X						
	7YL-s2	14.213648N 40.321188E	12.01.2017	Pinkish salt forming ripple marks on the rim of the Yellow Lake	X			n.a.	n.a.	n.a.	n.a.	n.a.	n.a.	n.a.		X	X						
	7YL-s3	14.213588N 40.320748E	12.01.2017	Salt fragments from rim of 7YL-w2	X			n.a.	n.a.	n.a.	n.a.	n.a.	n.a.	n.a.		X	X						
	7YL-s4	14.2136083N 40.3212611E	12.01.2017	Reddish salt/sediment from salt mud volcano	X			n.a.	n.a.	n.a.	n.a.	n.a.	n.a.	n.a.		X	X						
<b>Black Lake and surroundings</b>																							
	PSBL1	14.221732N 40.28582E	19.01.2016	Reddish salt and water from pond close to Black Lake		50		40.6	2.63	n.a.	n.a.	n.a.	62.0	643.40 ± 22.20		X	X	X	XY				
	PSBL2	14.221738N 40.285713E	19.01.2016	Yellowish salt and water from pond close to Black Lake		50		40.6	2.50	n.a.	n.a.	n.a.	58.0	620.4		X	X	X	XY				
	PSBL3	14.22173N 40.28582E	19.01.2016	Orange salt and water from pond between Black Lake and camp site		50		n.d.	n.d.	n.a.	n.a.	n.a.	34.0	344.40 ± 10.77						XY	X		
	PSBL4	14.22173N 40.28582E	22.01.2016	Warm red pond with acid emissions		50		40.0	3.50	n.a.	n.a.	n.a.	38.0	366.67 ± 9.63						X	X		
	BL2	14.221842N 40.286173E	19.01.2016	Black Lake bischoffite-enriched water, very high viscosity		25		n.a.	n.a.	n.a.	n.a.	n.a.	n.a.	n.d.		X							
	BL2 / BL1-O2 / BL-w	14.22182N 40.286208E	19.01.2016	Black Lake bischoffite-enriched water, very high viscosity		50	150	70.6	3.50	n.a.	n.a.	n.a.	n.a.	819.83 ± 181.88	X	X	X	Y					
	BL6-O1	14.22211N 40.28805E	24.01.2016	Black fluid from chimney in very active young geothermal formation, black dome area		15		110.0	4.40				n.d.	n.d.							Y		
	7BL-w1	14.22182N 40.286208E	10.01.2017	Black Lake bischoffite-enriched water from surface		150		60.1	2.57	2.8	0.11	226.9	76	718.94 ± 17.94	X				X	X			
	7BL-w2	14.22182N 40.286208E	10.01.2017	Black Lake bischoffite-enriched water, 3 m depth		100		n.a.	n.a.	n.a.	n.a.	n.a.	n.a.	n.d.	X					X	Y		
<b>Salt plain at Dalol dome base</b>																							
	PS	14.2250194N 40.288900E	19.01.2016	Salt pan fragment between the Dalol dome and Black Lake, rehydrated with sterile spring water	X	100	30	n.a.	n.a.	n.a.	n.a.	n.a.	n.a.	n.a.		X	X	X	X	X	X		
	PS3	14.22512N 40.297955E	19.01.2016	Water from salt shallow, hydrothermally influenced, pond at the dome base		150	950	29.3	4.21	n.d.	n.d.	n.d.	20.0	352.64 ± 10.78	X	X	X	XY	X				
<b>Lake Assale (Lake Karum)</b>																							
	Ass	14.089567N 40.348583E	23.01.2016	Water from Lake Assale (Karum), overflowed towards the North of the Danakil Depression			8000	26.2	6.68	53													

**Extended Data Fig. 3 | List and description of samples from the Dallol area analysed in this study and type of analyses performed.** DO, dissolved oxygen; ORP, oxido-reduction potential; SEM-/EDXS, scanning electron microscopy/energy-dispersive x-ray spectrometry; FACS, fluorescence-activated cell sorting analysis; n.a., not applicable; n.d. not determined. Refractometry-derived salinity refers to the percentage (w/v) of local salt composition (see Supplementary Tables 1 and 3 for elementary and ionic analyses) measured in situ. Salinity was also directly measured by weighting the total solids (dry weight experimentally measured in triplicates; SD, standard deviation).



**Extended Data Fig. 4 | Principal Component Analyses (PCA) of Dallol area sampling sites as a function of physicochemical parameters.** PCA of 29 samples according to their chemical composition; only relatively abundant elements (see Supplementary Table 1) are included in the analysis. A summary of this analysis is shown in Fig. 2f. **b**, PCA including the same variables as Fig. 2f but additionally including dissolved oxygen (DO). Measured parameters on site can be found in Extended Data Fig. 3. Coloured zones in PCA analyses correspond to the three major chemical zones identified in this study.

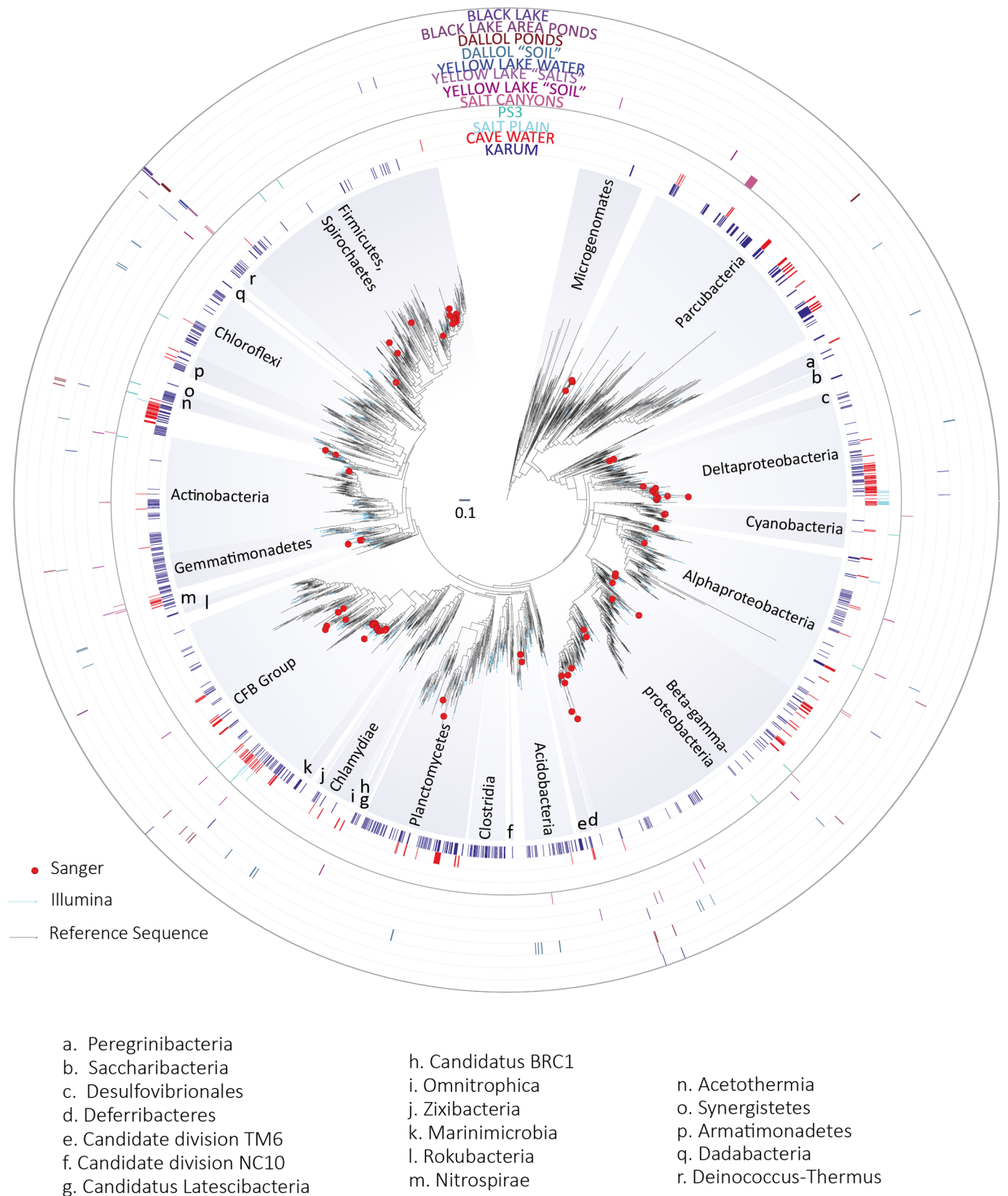
		Measured chaotropy (kJ/kg)	Calculated chaotropy (kJ/kg)	Ionic strength (mol/L)	Water activity (a <sub>w</sub> )
	Life threshold*	≤87.3		≤12.141	≥0.585
	Gt		n.d	n.d	0.728
Cave water	7Gt	-18.3	-23.80	4.751	0.729
	8Gt	-57.5	-56.65	6.873	0.731
Lake Assale	8Ass	n.d.	7.10	7.274	0.718
Geothermally influenced Salt Plain	PS3	n.d.	24.09	7.138	n.d
	DAL 4.00	-21.7	-17.87	6.104	0.719
	DAL 4.0	n.d.	-18.71	7.307	n.d
	DAL 4A	n.d.	-9.61	6.346	n.d
	DAL 4D	n.d.	2.14	7.104	n.d
	DAL 6A	n.d.	-23.97	7.203	n.d
	DAL 9A	n.d.	-7.77	7.529	n.d
	DAL 9C	n.d.	-16.15	8.349	n.d
	7DAL4-W1	19.3	40.44	6.314	0.667
Dallol dome hydrothermal pools	7DAL4-W2	8.3	14.28	5.383	0.698
	7DAL7	8.8	19.64	5.989	0.694
	7DAL-N1	9.2	20.84	6.472	0.694
	7DAL-N2	11.5	11.01	5.940	0.698
	7DAL9	-8.2	2.95	5.176	0.708
	7DAL10	2.1	-7.46	5.037	0.714
	7DAL10-1	n.d	n.d	n.d	0.580
	7DAL12	-31.2	-20.57	5.793	n.d
	7DAL13-W1	-24.8	-20.13	4.785	0.723
	7DAL14	-11.7	7.54	5.307	0.748
	PSBL1	108.3	n.d	n.d	0.334
Black Lake area pools	PSBL2	93.5	n.d	n.d	0.345
	PSBL3	63.4	n.d	n.d	0.722
	PSBL4	61.8	n.d	n.d	0.711
	BL	288.3	354.19	19.155	0.319
Black Lake	7BL-W1	198.5	259.41	14.206	0.322
	7BL-W2	201.3	268.89	14.721	n.d
	YL1	n.d.	492.06	19.141	n.d
	YL2	n.d	574.04	22.085	n.d
Yellow Lake	YL3	231.8	n.d	n.d	0.319
	7YL-W1	320.8	495.01	18.446	0.261
	7YL-W2	308.2	328.92	13.796	0.467
	7YL-W3	n.d.	466.64	17.609	n.d

\* Data from Hallsworth et al (2007) and Stevenson et al (2015 and 2017)

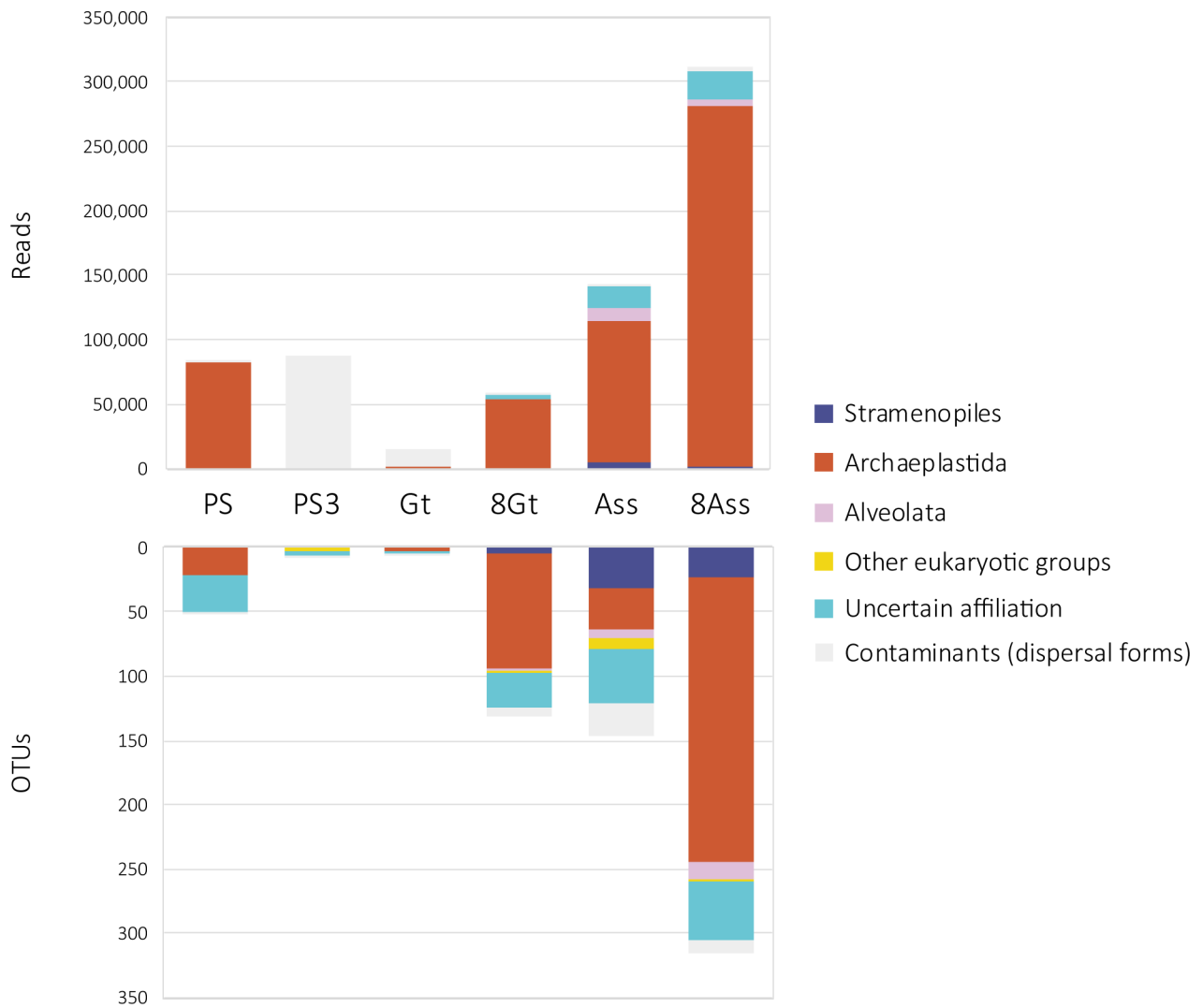
**Extended Data Fig. 5 | Chaotropy, ionic strength and water activity for a selection of samples of the Dallol area.** Chaotropy was measured experimentally (see Methods) and also calculated, together with ionic strength values were from dominant Na, K, Mg, Ca, Fe chemistry data; water activity values were measured using a probe (see Methods). Known limits for life for each parameter are listed at the top of the table. Samples beyond that threshold for one or more of those parameters are shaded in grey.

Sample name	Initial No. of merged reads	No. of high quality reads	No. of retained reads after chimera check	No. of retained reads after removing contaminants*	No. archaeal reads	No. OTUs	Diversity (Simpson index)	Evenness	Richness (Chao1) (s.e.)	No. of bacterial reads	No. OTUs	Diversity (Simpson index)	Evenness	Richness (Chao1) (s.e.)
<b>Prokaryotic sequences</b>														
					<b>Archaea</b>					<b>Bacteria</b>				
DAL4.0	169949	169648	165257	4	3	2	0.44	0.92	2 (0)	1	1	0.00	NA	1 (0)
DAL4A	152469	152298	146065	5023	5023	2	0.00	0.01	2 (0)	0	0	1.00	0.00	0 (NA)
DAL4C	126853	126665	123020	0	0	0	1.00	0.00	0 (NA)	0	0	1.00	0.00	0 (NA)
DAL4D	125034	124804	120619	0	0	0	1.00	0.00	0 (NA)	0	0	1.00	0.00	0 (NA)
DAL6A	234168	233935	224050	4314	4303	21	0.03	0.03	35 (11)	11	4	0.45	0.64	7 (4)
DAL8-01	113894	112383	108675	6	0	0	1.00	0.00	0 (NA)	6	2	0.28	0.65	2 (0)
DAL8-02	182460	176331	172030	2	0	0	1.00	0.00	0 (NA)	2	2	0.50	1.00	3 (2)
DAL8-03	154815	151700	148869	41	0	0	1.00	0.00	0 (NA)	41	4	0.34	0.49	4 (0)
DAL9A	132758	131862	126420	2	0	0	1.00	0.00	0 (NA)	2	2	0.50	1.00	3 (2)
DAL9C	107108	106589	104746	0	0	0	1.00	0.00	0 (NA)	0	0	1.00	0.00	0 (NA)
7DA7	133151	132970	128002	1	1	1	0.00	NA	1 (0)	0	0	1.00	0.00	0 (NA)
7DA7-pp	42089	42043	41253	2	2	2	0.50	1.00	3 (2)	0	0	1.00	0.00	0 (NA)
7DA9	158516	158249	152576	1821	1	1	0.00	NA	1 (0)	0	0	1.00	0.00	0 (NA)
7DA9-pp	217467	217096	192709	2	0	0	1.00	0.00	0 (NA)	2	1	0.00	NA	1 (0)
7DA10	213263	212784	205528	1	1	1	0.00	NA	1 (0)	0	0	1.00	0.00	0 (NA)
7DA10-pp	44566	44540	40224	62	0	0	1.00	0.00	0 (NA)	62	2	0.03	0.12	2 (0)
7DA14	168809	168500	162187	2096	2094	5	0.01	0.02	5 (0)	2	2	0.50	1.00	3 (2)
7DA14-pp	82248	82170	71068	471	345	30	0.94	0.89	32 (3)	126	7	0.69	0.72	7 (0)
7DA2-01	33880	33832	33711	45	31	5	0.68	0.82	5 (0)	14	7	0.83	0.94	9 (3)
7DA4-s	103418	103261	102476	1492	1490	13	0.81	0.69	15 (3)	2	2	0.50	1.00	3 (2)
7DA5-s	184910	184641	180701	5243	3208	22	0.91	0.82	32 (10)	2035	19	0.84	0.78	19 (0)
7DA9-s	130399	130259	129730	261	212	8	0.72	0.70	9 (1)	49	1	0.00	NA	1 (0)
7DA13-s	100425	100280	99550	298	298	7	0.66	0.67	7 (0)	0	0	1.00	0.00	0 (NA)
7DA15-s	143741	143552	142694	12589	12460	11	0.06	0.08	11 (0)	129	2	0.48	0.97	2 (0)
YL1	226774	226389	217444	42	1	1	0.00	NA	1 (0)	41	4	0.30	0.43	5 (2)
7YL	178284	177903	172455	1770	1302	13	0.57	0.47	13 (0)	468	7	0.74	0.76	7 (0)
7YL-pp	65597	65556	62547	0	0	0	1.00	0.00	0 (NA)	0	0	1.00	0.00	0 (NA)
YL2	153107	152918	144028	2	2	1	0.00	NA	1 (0)	0	0	1.00	0.00	0 (NA)
YL3-01w	188511	188312	172260	126	0	0	1.00	0.00	0 (NA)	126	3	0.03	0.08	4 (2)
YL3-01s	232822	232611	210691	3	0	0	1.00	0.00	0 (NA)	3	2	0.44	0.92	2 (0)
7YL-s3	158645	158488	157145	979	898	15	0.86	0.83	15 (0)	81	4	0.07	0.14	7 (4)
7YL-s4	86468	86366	85180	207	157	4	0.60	0.76	4 (0)	50	2	0.08	0.24	2 (0)
YL4.01	200889	200588	191536	10711	10691	2	0.00	0.00	2 (0)	20	3	0.27	0.47	3 (0)
7YL-s1	124032	123877	122505	36177	36016	39	0.79	0.50	39 (0)	161	6	0.79	0.91	6 (0)
7YL-s2	85188	85072	84444	668	547	10	0.75	0.70	10 (0)	121	5	0.71	0.83	5 (0)
BL2	76395	76209	73977	12	0	0	1.00	0.00	0 (NA)	12	6	0.78	0.91	8 (3)
BLw	227966	227636	218708	0	0	0	1.00	0.00	0 (NA)	0	0	1.00	0.00	0 (NA)
7BLw1	177297	177131	171404	3	0	0	1.00	0.00	0 (NA)	3	1	0.00	NA	1 (0)
7BLw2	158986	158630	151304	1	0	0	1.00	0.00	0 (NA)	1	1	0.00	NA	1 (0)
PSBL1	127518	127100	124137	8	0	0	1.00	0.00	0 (NA)	8	4	0.66	0.88	5 (1)
PSBL2	181312	180562	177286	5	3	2	0.44	0.92	2 (0)	2	1	0.00	NA	1 (0)
PS3	150482	149968	146028	146028	118980	291	0.88	0.56	313 (7)	26537	123	0.96	0.56	138 (11)
PS	304190	303656	282495	282495	274013	602	0.94	0.51	701 (22)	5893	39	0.30	0.51	50 (8)
ASS	173226	172959	165299	165299	140633	1013	0.94	0.59	1190 (33)	23963	496	0.69	0.59	544 (13)
ASS-PJ	314682	314213	288299	288299	244551	1349	0.94	0.57	1441 (18)	39873	859	0.88	0.57	912 (12)
GT	303592	303083	288086	288086	274039	656	0.87	0.53	755 (25)	14047	173	0.91	0.53	193 (11)
7GT	71483	71368	64143	64143	59788	524	0.95	0.57	735 (46)	4353	147	0.92	0.57	201 (22)
7GT-pp	235497	235111	172010	172010	132967	1495	0.97	0.57	1565 (13)	39039	227	0.77	0.57	253 (10)
GC	198582	198288	189428	32807	30700	68	0.71	0.40	80 (7)	2107	2	0.00	0.01	2 (0)
GC2	94053	93926	87922	16162	15575	64	0.83	0.50	71 (5)	587	1	0.00	NA	1 (0)
7Cmcore	135254	135086	133629	202	136	16	0.55	0.50	19 (3)	66	1	0.00	NA	1 (0)
7Gt2	150640	150409	138429	14250	7334	33	0.64	0.43	36 (4)	6916	18	0.64	0.48	19 (1)
NEGATIVE CONTROL A	106471	105571	96569	94348	2876	19	0.69	0.49	26 (7)	91472	351	0.97	0.69	461 (36)
NEGATIVE CONTROL B	149421	148866	140175	135739	2782	16	0.83	0.72	17 (2)	132957	484	0.97	0.72	555 (20)
<b>Eukaryotic sequences</b>														
8Ass	320243	319549	312333	307451		306	0.68	0.25	308 (2)					
Ass	148963	148396	142049	140678		122	0.65	0.31	136 (7)					
PS	83526	83207	82325	82316		50	0.06	0.04	55 (4)					
PS3	87971	87459	86745	54		6	0.36	0.46	6 (0)					
Gt	15063	14998	14883	1795		4	0.25	0.34	4 (0)					
8Gt	57995	57773	56359	56269		125	0.56	0.23	125 (0)					

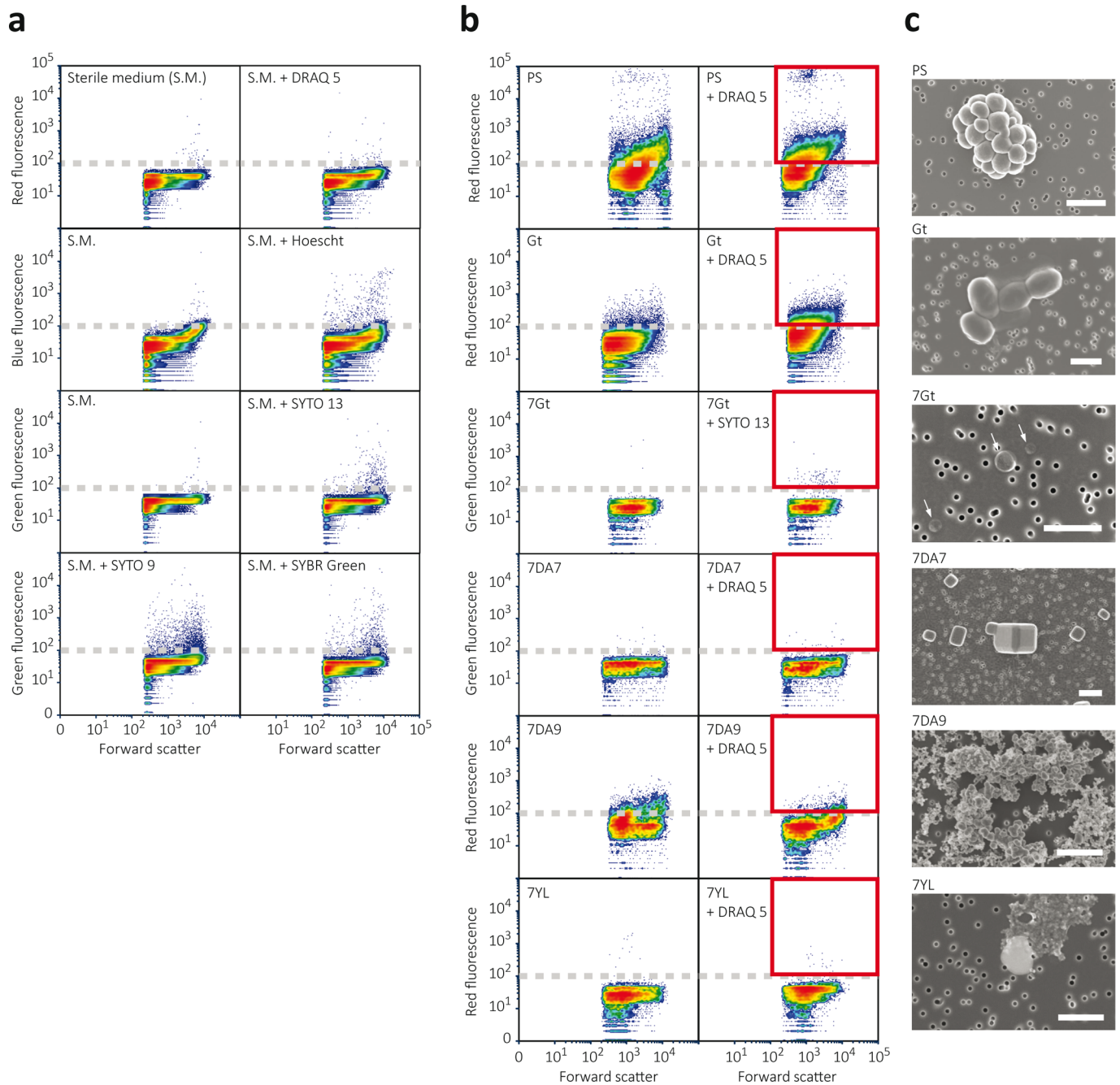
**Extended Data Fig. 6 | Sequence data and diversity measurements.** \*Contaminant sequences included sequences identified in negative controls and/or high similarity to human-associated bacteria; s.e., standard error. Eventual mitochondrial and chloroplast 16S rRNA gene sequences were also removed at this step.



**Extended Data Fig. 7 | Phylogenetic tree of bacterial 16S rRNA gene sequences showing the phylogenetic placement of OTUs identified in the different Dallol area samples.** Sequences derived from metabarcoding studies are represented by blue lines (Illumina sequences); those derived from cloning and Sanger sequencing of environmental samples, cultures and FACS-sorted cells are labelled with a red dot. Reference sequences are in black. Concentric circles around the tree indicate the presence/absence of the corresponding OTUs in different groups of samples (groups shown in Fig. 3a). Only sequences not deemed contaminant (see Supplementary Table 5) were included in the tree. The full tree is provided as Supplementary Data 1.



**Extended Data Fig. 8 | Eukaryotic presence, diversity and relative abundance in Dallol area samples.** Histogram showing the phylogenetic affiliation and abundance of 18S rRNA gene amplicon reads of eukaryotes (upper panel) obtained with universal eukaryotic primers and the associated OTU diversity (lower panel). Only a few samples yielded amplicons; negative PCR controls were always negative. Sequences corresponding to macroscopic plants and fungi (probably derived from pollen or spores) were considered contaminant (light grey). The phylogenetic affiliation of dominant eukaryotic groups is colour-coded.



**Extended Data Fig. 9 | Multiparametric fluorescence analyses and fluorescence-activated cell sorting (FACS) analyses of representative Dallol area samples. a**, effect of DNA fluorescent dyes on background fluorescence emission; natural (sterile medium-only) and DNA dye-induced fluorescence in the sterile hypersaline SALT-YE medium used to dilute/sort Dallol samples. Fluorescence is plotted against the size of the analysed particles (forward scatter); events concentration is colour-coded, red being high concentration and blue, low concentration. DRAQ5 and SYTO13 introduced less background and were chosen for FACS of natural samples. The approximate background threshold (ca.  $10^2$ ) is indicated by a broken grey line. **b**, multiparametric fluorescence analyses of different Dallol samples before (left panels) and after (right panels) adding fluorescent DNA dyes. Events (particles) above background (red squares) were FACS-sorted and filtered on 0.1  $\mu\text{m}$  pore-size filters prior to SEM observations. **c**, SEM photographs showing examples of sorted particles. Cells are observed in samples PS, Gt and 7Gt; halite crystals in 7DA7 and amorphous mineral particles in 7DA9 and 7YL. Arrows indicate ultrasmall cells. The scale bar is 1  $\mu\text{m}$ .

Site	Samples	Mineral phases	
		Typical 'crystals'	Abiotic 'Biomorphs'
Cave water	Gt2016, 7Gt, 8Gt_1	Si, Ca sulfate, Fe-K sulfate, Al-Mg Fe oxides, Fe and Ca oxides	Fe-Al silicates
Lake Assale (Karum)	8Ass_2, 8Ass_3, 8Ass_4, 8Ass_6, 8Ass_7, 8Ass_8	NaCl, Na-K-Mg chloride	Si biomorphs (and encrustment)
Dallol dome (ponds)	Dal4.0, 7DA7_07, DAL4D, 7DA9-P1, 7CA9_P1_3, 7DA7_04, 7DA7_05, 7DA7_06, 7DA9_P1_2, 7DA9_P1_5, 7DA9_P3_10, 7DA9_P3_12	NaCl, Na-K-Mg chloride, Fe-K oxides, Ti oxides	Sulfur biomorphs, <b>Si biomorphs</b> , S- rich Na-K silicates, locally S-rich Si biomorphs, <b>Fe phosphates</b> , Fe-K phosphate, Si biomorphs – enriched in Fe, Mg, K and locally S
Yellow lake	YL1-03_4, 7YL_4, YL1- 03_5, 7YL_6	Fe chloride, Mg chloride	Si, CaCl <sub>2</sub> , Ca phosphate
Black lake area (ponds)	BLPS_05_5	Mg-Fe-K chloride	Mg chloride

**Extended Data Fig. 10 | Mineral phases observed by SEM-EDX in precipitates of typical abiotic morphology and 'biomorphs'.** Biomorphs correspond to rounded-shaped crystalline morphs resembling cell structures (cocci, rods) and compatible with cellular sizes. Observed dominant phases are highlighted in bold.



*An abandoned mining camp at the top of the Dallol dome © DEEM Team*

**ARTICLE 2**

## 5. Detection of (local) biocontamination and biomorphs: how to identify false positives

### 5.1 Context and objectives

As we have seen in the previous chapter, 16S rRNA gene PCR amplicons were difficult to obtain from Dallol, Lake Gaet'ale and the Black Lake (and we couldn't obtain 18S rRNA gene amplicons from those sites). The amplicons from seminested PCR, when cleaned from the contaminant sequences, were very similar to haloarchaeal or nanohaloarchaeal amplicons obtained from nearby hypersaline (and slightly acidic) sites (e.g. the salt plain), leading us to think they were airborne-dispersal from the surroundings (local contamination).

To test this hypothesis of local contamination through the wind, we established the following objectives:

1. **Collect bioaerosols on filters** (passively or with active pumping) **at the Dallol dome and the campsite at its base. Assess the microbial diversity of those bioaerosols using 16S/18S rRNA gene metabarcoding** as we previously did (Belilla et al. 2019).
2. **Observe filters of Dallol's brine and dissolved Dallol's salts in comparison with a positive control** (the salt plain) **through the SEM and FISH** to see if we can detect cells that we couldn't detect previously.
3. **Compare our results with our previous findings** (Belilla et al. 2019) and the ones of another study (Gómez et al. 2019) claiming that a polyextreme nanohaloarchaea thrive in Dallol's brine.
4. **Estimate if airborne cells falling to the ponds disaggregate with their content and how fast the degradation occurs.** In the case of confirmed microbial dispersal, the degradation of imported exogenic cells would explain why it is very difficult to amplify DNA from Dallol despite the possibly strong airborne dispersal. Three different experiments were set for this: 1) the comparison of DNA concentration on filters with or without having been in contact with Dallol's brine; 2) the observation of cells' induced fluorescence with DNA dye with or without Dallol's brine diluted in the solution; and 3) the DNA extraction and amplification from cell pellets with or without contact with Dallol's brine.

## 5.2 Results

DNA extraction and metabarcoding analysis of bioaerosols showed that they contained a majority of Bacteria (99%) and very few Archaea (1%), which included Halobacteria and Nanohaloarchaeota (Figure 20). This repartition strongly reminds what was found in Dallol ponds in our first study before we got rid of PCR contaminants (Belilla et al. 2019). Archaeal OTUs of bioaerosols were very similar to OTUs from the salt plain and Lake Karum, which supports the idea that they can be transported from those places through the wind. During the FISH experiment, no traces of cells were detected on Dallol filters while interesting cell associations that could correspond to a parasitic interaction between nanohaloarchaea and haloarchaea were observed on the control samples from the salt plain.

In places with already established microbial communities, airborne dispersal may be negligible, but in places with very little or no biomass, as Dallol, its influence may be greater. Nevertheless, our initial work showed that it is very difficult to amplify DNA from Dallol ponds. We showed in our experiments that the cells' content is disrupted almost instantly in the Dallol ponds. We hypothesize that the combination of high salinity and acidity of Dallol's brine is at the origin of this degradation, but it is possible that other chemical compounds (e.g. heavy metals, potential presence of perchlorate) also play a role.

Altogether, these results support the absence of endemic microorganisms in the Dallol ponds (and, by extent, in Lake Gaet'ale and the Black Lake) and highlights the importance of controlling bioaerosols in extreme environments and the thoughtful use of controls during experiments to avoid interpretation bias.

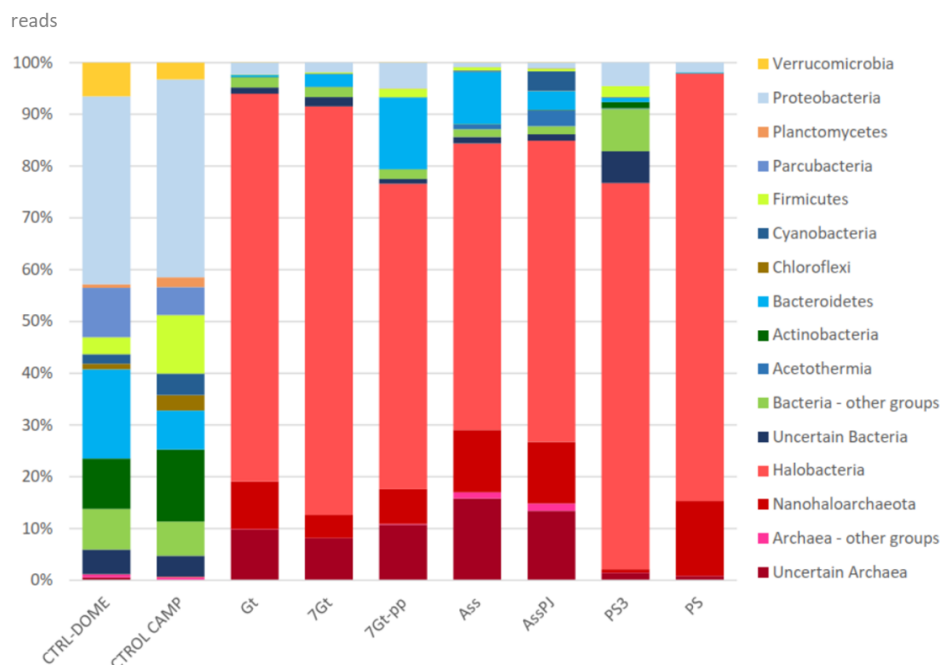


**Figure 20 | Histogram showing the presence/absence and relative abundance of amplicon reads of archaea and bacteria obtained with universal prokaryotic primers. Phyla that were representing <1% for the total reads have been put in categories “bacteria – other groups” or “archaea – other groups”. Uncertain phyla are the one for which the first-hit is ≤90% identical to the OTU. For samples names' details, see Table 7.**

## 5.3 Manuscript of article

*Article status: in preparation*

### **Provisional titles:**

- Strong microbial airborne dispersal and biomorphs as confounding factors for life detection in the polyextreme brines of Dallol
- Rapid DNA degradation counteracts intense airborne microbial contamination in the lifeless polyextreme brines of Dallol

**Authors:** Jodie Belilla<sup>1</sup>, David Moreira<sup>1</sup>, Karim Benzerara<sup>2</sup>, Emmanuelle Gérard<sup>3</sup>, Purificación López-García<sup>1</sup>

1. Ecologie Systématique Evolution, CNRS, Université Paris-Sud, Université Paris-Saclay, AgroParisTech, Orsay, France.

2. Institut de Minéralogie, de Physique des Matériaux et de Cosmochimie, CNRS, Sorbonne Université, Muséum National d'Histoire Naturelle, Paris, France.

3. Institut de Physique du Globe de Paris, CNRS, Université Paris Diderot, Paris, France

### **Abstract**

The Dallol hydrothermal system and its surrounding salt desert harbour unique gradients of polyextreme physicochemical parameters (hypersalinity, hyperacidity, high temperature) and different salt compositions. Only a few OTUs have been detected so far in the most polyextreme systems of these gradients using 16S rRNA gene metabarcoding, and they were very similar to the OTUs that could be found in hypersaline-only environments. Here, we tested the hypothesis that the OTUs found in Dallol correspond to airborne contaminants from the less extreme surroundings. Using dust traps, we collected and analysed the microbial diversity of the airborne particles from the Dallol dome and its base and show that halophiles typical from hypersaline environments such as the salt plain are transported through the air (including Halobacteria and Nanohaloarchaeota), consistently with our hypothesis. Despite this substantial airborne dispersal, DNA remains very difficult to amplify in the most polyextreme environments and the fluorescent in situ hybridization (FISH) experiments showed no trace of cells in the hydrothermal brine pools. Our results suggest that Dallol's brine destroys cells' content. Besides their extreme acidity and salinity, the presence of chaotropic and sterilizing chemical compounds (such as perchlorate) may be involved in this rapid degradation. Our study highlights the critical need for positive and negative controls when working with sterile or low-biomass samples, as it is the case in extreme environments and other celestial bodies.

### 5.3.1 Introduction

The last decades of research on extremophilic microorganisms have continuously pushed further the known limits of life. Extremophiles can survive at temperature between  $-15^{\circ}\text{C}$  (Mykytczuk et al. 2013) and  $122^{\circ}\text{C}$  (Takai et al. 2008), pH between  $\sim 0$  (Schleper et al. 1996) and 11.4 (Sturr, Guffanti, et Krulwich 1994) and salinity around 350 g/L in NaCl-dominated environments (Bodaker et al. 2010; Antón et al. 2000) – which is approximatively the saturation value for this salt. Although most extreme environments are characterized by several coexisting stressors, it is currently not well understood how combinations of these factors limit the presence of life (Harrison et al. 2013), in part because some of these combinations are only met in places that are rare or difficult to access. This is the case, for example, for naturally occurring hyperacidic and hypersaline brines. Besides, the study of these systems can be specially challenging because of i) their very low biomass, and thus a high potential for field or laboratory (Weyrich et al. 2019) contamination, and ii) their unusual physicochemical properties to which classical experimental approaches may not be designed, potentially leading to hardly predictable biases. One example is the Don Juan Pond, a  $\text{CaCl}_2$ -rich brine in Antarctica where the presence of planktonic microbial life is debated: Cameron, Morelli, et Randall (1972) have shown that previous findings claiming the presence of life could be aerial microbial contamination. Likewise, Samarkin et al. (2010) assess that the *in situ*  $\text{N}_2\text{O}$  fluxes which were thought to be associated with microbial activity in fact have an abiotic origin. Another controversial example is the Discovery deep brine (Red Sea), where the  $\text{MgCl}_2$  concentration increases with depth to almost saturation. DNA traces are detectable almost all along this gradient, whereas RNA traces become undetectable after a certain depth/ $\text{MgCl}_2$  concentration (2.3M) (Hallsworth et al. 2007). Based on experiments showing that DNA is better preserved than RNA in  $\text{MgCl}_2$  and that no cultivation was successful at more than 2.3 M  $\text{MgCl}_2$  without chaotropic salt compensation, Hallsworth et al. (2007) argued that there is no active life after this concentration limit and that the DNA detected comes from dead cells from upper levels. When endemic biomass is low or inexistent, it can easily be overwhelmed by exogenic import, especially if the conditions are favourable to its preservation. Thus, the discrimination between autochthonous and allochthonous microorganisms is crucial.

The Dallol dome and its surroundings, in the North of the Danakil Depression of Ethiopia, include unique hydrothermal systems located in the middle of a vast salt plain in a volcanically active area at the junction of three tectonic plates (López-García et al. 2020). The interaction of underground salt-saturated fluids with a magma chamber are at the origin of the many hot springs and brine reservoirs with different chemistry and extensive physicochemical gradients, with a pH  $< 0$  to 6.5, a salinity range of 20-75%, and a temperature up to  $110^{\circ}\text{C}$ , and high  $\text{Na}^+/\text{K}^+$  or  $\text{Ca}^{2+}/\text{Mg}^{2+}$  concentrations (Belilla et al. 2019; López-García et al. 2020). During three field campaigns, we extensively sampled this area and characterized its microbial diversity using 16S/18S rRNA gene metabarcoding (Belilla et al. 2019). We found surprisingly diverse Archaea (dominated by Halobacteria and Nanohaloarchaeota) in the less polyextreme places (Lake Karum, the salt canyons' cave reservoir, and the -slightly

hydrothermally active- salt plain). By contrast, we did not find any reliable trace of life in the most polyextreme brines (the Dallol dome, Lake Gaet'ale, and the Black Lake) or, given their extremely low abundance and their similarity with known halophiles, interpreted the few OTUs found there as airborne contamination from the less extreme surroundings (Belilla et al. 2019). In the present article, we have tested our hypothesis of airborne contamination by analysing the microbial diversity in aerosols collected on the Dallol dome and surroundings. Our analysis also includes the comparison of filters from one Dallol pond (brine sample and dissolved salts) and from the salt plain using fluorescent in situ hybridization (FISH) and correlates the epifluorescence observations with scanning electron microscopy images. While testing the validity of the aerial contamination assessment, we also wanted to understand why, if it was occurring, the DNA of exogenic cells was not easily detectable. We hypothesized that Dallol brine polyextreme conditions might destroy most of falling cells' DNA and designed different experiments to see if this was likely and how fast this reaction might occur.

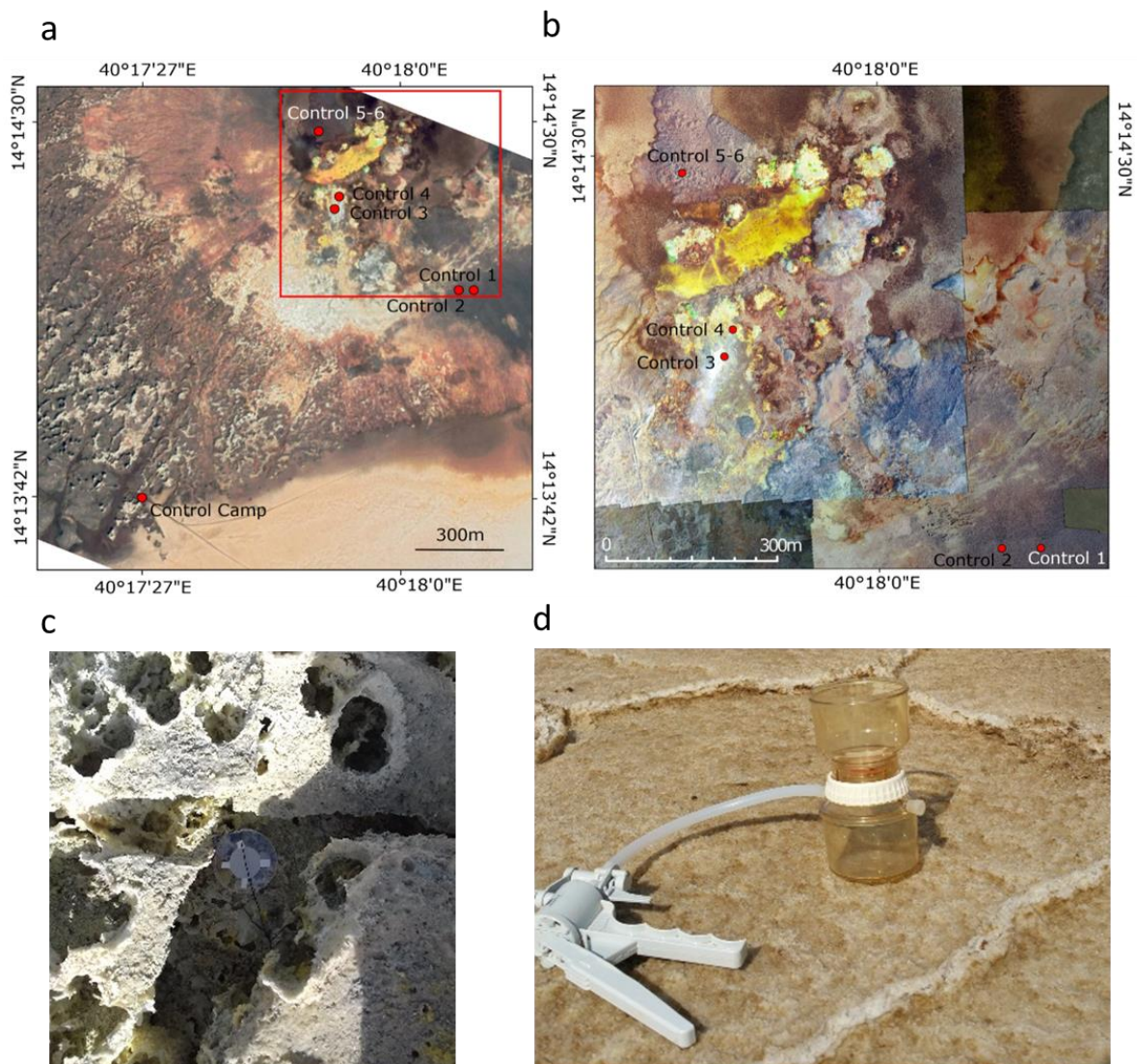


**Figure 21 | Bioaerosols collection systems and localisation.** **a**, Sampling sites of bioaerosol control samples georeferenced (Google satellite picture from 26/02/2019). **b**, Detail of the dome samples location by Phantom-4 drone images © Olivier Grunewald. **c**, Passive collecting system (here filter n°4). **d**, Active collecting system in the campsite.

**Table 7 | List and description of samples from Dallol area analysed in this study and type of analyses performed.** ORP: redox potential; Refractometry-derived salinity refers to the percentage (w/v) of local salt composition measured in situ. Salinity was also directly measured in our last study by weighting the total solids (see Belilla et al. (2019) for method).

	Coordinates	Collection date	Brief description	Color	Temp (°C)	pH	Physicochemical parameters			
							ORP (mV)	Refractometry inferred salinity (%)	Salinity - TS (g/l) ±SD	
<b>Controls</b>										
SPA spring water	/	18.01.2019	Water used on site to clean our material		n.a		n.a	n.a	n.a	n.a
CTRL-CAMP	14°13'42.30"N 40°17'26.76"E	15.01.2019- 25.01.2019	Aerosols actively pumped in the camp site at the base of Dallol's dome	/	n.d	n.d	n.d	n.d	n.d	n.d
CTRL-DOME-1	14°14'7.41"N 40°18'7.08"E	15.01.2019- 19.01.2019	Aerosols passively collected on filter at the top of the dome (close to the tourist's path)	/	n.d	n.d	n.d	n.d	n.d	n.d
CTRL-DOME-2	14°14'7.41"N 40°18'9.33"E	15.01.2019- 19.01.2019	Aerosols passively collected on filter at the top of the dome (close to the tourist's path)	/	n.d	n.d	n.d	n.d	n.d	n.d
CTRL-DOME-3	14°14'18.45"N 40°17'50.90"E	15.01.2019- 19.01.2019	Aerosols passively collected on filter at the top of the dome (very close of fumaroles)		n.d	n.d	n.d	n.d	n.d	n.d
CTRL-DOME-4	14°14'20.00"N 40°17'51.40"E	15.01.2019- 19.01.2019	Aerosols passively collected on filter at the top of the dome (a bit further from the fumaroles than n°3)		n.d	n.d	n.d	n.d	n.d	n.d
CTRL-DOME-5	14°14'29.00"N 40°17'48.49"E	15.01.2019- 19.01.2019	Aerosols passively collected on filter at the top of the dome (in the "Chocolate formation")	/	n.d	n.d	n.d	n.d	n.d	n.d
CTRL-DOME-6	14°14'29.00"N 40°17'48.49"E	15.01.2019- 19.01.2019	Aerosols passively collected on filter at the top of the dome (in the "Chocolate formation")	/	n.d	n.d	n.d	n.d	n.d	n.d
<b>Assale/Karum lake</b>										
9ASS	14° 31'3.13"N 40°22'51.97"E	23.01.2019	Water from Lake Assale (Karum), island in the middle-west of the lake		30.60	6.70	184.30	29.00	302.27 ± 4.76	
8ASS	14.089567N 40.348583E	15.01.2018	Water from Lake Assale (Karum), overflowed towards the North of the Danakil Depression		22.0	6.54	221	31	363.15 ± 11.51	
Ass	14.089567N 40.348583E	23.01.2016	Water from Lake Assale (Karum), overflowed towards the North of the Danakil Depression		26.2	6.68	97.7	20.0	360.72 ± 11.52	
<b>Salt canyon's cave brine</b>										
9GT	14.229704N 40.289952E	15.01.2019	Cave hypersaline water reservoir at the salt canyons, West Dallol dome		25.50	5.94	240.30	30.00	325.27 ± 5.46	
8GT	14.229704N 40.289952E	16.01.2018	Cave hypersaline water reservoir at the salt canyons, West Dallol dome		22.0	6.54	262.1	30	330.82 ± 10.78	
7GT	14.229704N 40.289952E	11.01.2017	Cave hypersaline water reservoir at the salt canyons, West Dallol dome		29.0	6.27	117.2	30	323.87 ± 19.39	
GT	14.229704N 40.289952E	18.01.2016	Cave hypersaline water reservoir at the salt canyons, West Dallol dome		n.d	n.d	n.d	30	n.d	
<b>Dallol hydrothermal ponds</b>										
PS	14.2250194N 40.2899000E	19.01.2016	Salt pan fragment between the Dallol dome and Black Lake, rehydrated with sterile spring water		n.a	n.a	n.a	n.a	n.a	
PS3	14.22912N 40.297935E	19.01.2016	Water from salt shallow, hydrothermally influenced, pond at the dome base		29.3	4.21	n.d	20.0	352.64 ± 10.78	
<b>Dallol hydrothermal ponds</b>										
DAL4-s	14.23916N 40.297059E	17.01.2016	Yellow salt crust from inside the closest pond of a chimney hydrated with sterile milliQ water in the lab		n.d	n.d	n.d	n.d	n.d	
7DA9	14.241528N 40.29884E	08.01.2017	Large pond in active degassing area with many white-yellowish chimneys and salt meniscaps		31.9	-0.34	369	43	379.03 ± 17.18	
7DA13-w1	14.235495N 40.298135E	11.01.2017	Hydrothermal fluid from big grey active chimney		103.6	n.d	n.d	35.0	342.50 ± 18.87	
7DA13-w2		11.01.2017	Closest pond from 7DA13-w1 with darker grey shade		50.2	0.43	323.8	35	n.a	

\* it was originally green but it became oxidized since the bottle was opened

### 5.3.2 Materials and Methods

#### 5.3.2.1 Sample collection

Dallol's brine and aerosol samples were collected in January 2019 (when air temperature rarely exceeded 40-45°C). All sampling points and mapping data were georeferenced using a Trimble® handheld GPS (Juno SB series) equipped with ESRI software ArcPad® 10. Location of the different sampling sites can be seen in Figure 21. Sampling was carried out under the most possible aseptic conditions to prevent contamination. Liquid samples were filtered *in situ* through 0.22 µm pore-diameter Millipore filters. Aerosols were collected both 1) passively on the Dallol dome, using 0.22 µm pore-diameter filters taped onto an open Petri dish, positioned in pairs in three different areas for five days, and 2) actively in the campsite at the base of the dome (Figure 21, Supplementary Figure 1), by concentrating air particles on a 0.22 µm pore-diameter filter using a manual pump during 2-3 hours per day for 11 days. Additionally, we filtered the bottled spring water (Spa-natural™) that we used to clean our material in the field to check if it could be an additional vector of contamination. Brine and water filters were then fixed in 2 mL cryotubes with absolute ethanol (>80% final concentration). Aerosol filters were stored dry in Petri dishes at -20°C prior use. 50 mL glass bottles of brine samples were collected for chemical analyses, microscope observation and DNA degradation experiment. Physicochemical parameters of brines were measured the same way as in (Belilla et al. 2019). The coordinates and physicochemical parameters data of the samples in this study are summarized in Table 7. Back in the laboratory, brine and ethanol-fixed samples were stored respectively at 4 and -20°C until further use.

#### 5.3.2.2 DNA purification and 16/18S rRNA gene metabarcoding

DNA purification from filters, concentration measurement, PCR, metabarcoding data treatment and tree visualisation were performed as previously described (Belilla et al. 2019). DNA extractions from the six bioaerosols filters of the Dallol dome were all pooled on the same column of the last extraction step to increase the concentration of DNA. No nested PCRs were needed to obtain 16S/18S rRNA gene amplicons filters.

#### 5.3.2.3 Electron and epifluorescence microscopy and fluorescence *in situ* hybridization

Sample processing for Scanning Electron Microscopy (SEM) and elemental chemical mapping were done as previously described (Belilla et al. 2019). For fluorescence *in situ* hybridization (FISH), we used the CY3-labeled Nanohaloarchaeota-specific probe Narc1214 (Narasingarao et al. 2012). We followed Gómez et al. (2019) FISH protocol to compare our results, except we included more controls including: 1) a Nanohaloarchaeota positive control from the salt plain; 2) a blank filter negative control; 3) hybridization and autofluorescence controls (see below for details). We also did not prefilter particles >0.45 µm because

nanohaloarchaea are known to live attached as epibionts of bigger cells (Narasingarao et al. 2012), and were already detected in high quantity in the salt plain without this prefiltration step (Belilla et al. 2019). Instead, we prefiltered through 20 or 50  $\mu\text{m}$  to get rid of big mineral particles before filtering a few mL of brine on 0.2  $\mu\text{m}$  filters. We then deposited 2-3 mL of formaldehyde 4% (methanol free, ultra-pure; Polysciences, Inc., Warrington, PA, USA) on the filters for  $\sim$ 1 hour, rinsed them with 1X PBS and vacuum-dried for few seconds. The filters were then put into sterile Petri dishes and stored at 4  $^{\circ}\text{C}$  until hybridization. Just before starting hybridization, filters were dried again at 45  $^{\circ}\text{C}$  before being cut in three pieces: 1) for hybridization with CY3-Narc1214 (Eurofins genomics), 2) for hybridization with the CY3-Non-Eub (ThermoFisher Scientific, Waltham, Massachusetts, USA) probe to check the hybridization specificity (Sunde et al. 2003; Amann, Ludwig, et Schleifer 1995), 3) for a control without probe to check the autofluorescence. A drop of 20  $\mu\text{L}$  of hybridizing solution (NaCl 5 M 180  $\mu\text{L}$ , Tris 1M pH 8.1 20  $\mu\text{L}$ , formamide 30% 300  $\mu\text{L}$ , Milli-Q water 499  $\mu\text{L}$ , SDS 10% 1  $\mu\text{L}$ ) including 50 ng of probe was put on the filters. Hybridizations were done at 45 $^{\circ}\text{C}$  for 90 minutes in a homogenized atmosphere. Filters were rinsed for 15 mins in 50 mL rinsing solution (NaCl 5 M 1.02 mL, Tris-HCl 1 M pH8 1 M, completed with EDTA 0.5 M pH 8, preheated at 48 $^{\circ}\text{C}$ ). They were then dried on Kimtech paper. 50  $\mu\text{L}$  of 1X SYBR Gold (Eurofins genomics) was deposited on the surface of the filters and incubated for 15 minutes in the dark at room temperature before they were rinsed gently in Milli-Q water and dried again on Kimtech paper. The filters were then mounted between two glass slides with a drop of Citifluor (glycerol mountant solution from Emgrid). Filters were first observed at the Institut de Physique du Globe de Paris using under an Olympus BX51 epifluorescence microscope using specific light-filters (U-MNIB3: excitation 470-495, emission 510F and U-MWIG3: excitation 530-550, emission 575F). After that, they were examined under an Olympus FluoView FV1000 confocal laser scanning microscope with a spectral resolution of 2 nm and a spatial resolution of 0.2  $\mu\text{m}$ . Observations were carried out with an oil immersion UPLSAPO 60XO objective (Olympus; x60 magnification, numerical aperture = 1.35). Fluorescence images were taken with sequential excitation at wavelengths of 405, 488 and 543 nm by collecting the emitted fluorescence between 25–475, 500–530 and 560–660 nm, respectively.

All solutions used in this protocol were 0.2  $\mu\text{m}$ -filtered and autoclaved, all dilutions were done using DNA-free water.

#### 5.3.2.4 DNA degradation tests with Dallol's brine

Different tests were carried out to measure the cell and DNA-degradation potential of the Dallol hyperacidic and hypersaline brine:

- 1) Epifluorescence optical microscopy observation of SYTO<sup>TM</sup> 9 (ThermoFisher) DNA-labelled cultures (*Escherichia coli*, *Halobacterium salinarum*) and natural samples (the salt plain, the salt canyons's cave reservoir, and Lake Karum) mixed or not with Dallol's brine (1/3 of final volume). The pH of the mixed solution was always  $\leq 0$ . Culture media and pure brine of Dallol were also observed as controls.

- 2) PCR amplification of 16S rRNA genes of cultures (*E. coli*, *H. salinarum*, *Haloferax denitrificans*) and some natural samples (the salt plain, Lake Karum) before and after mix with a solution mimicking the Dallol brine conditions (ATTC Medium 112 supplemented with 25% NaCl and acidified with HCl, with a final pH  $\leq 0$ ). In some tests acidity was neutralised right after mix by adding either 2:3 of TE solution (1:2 EDTA 0.5M pH 9, 1:2 Tris 10 mM pH 8) or TE+ solution (1:2 EDTA 0.5M pH 9, 1:2 Tris 1M pH 8) to raise the pH from  $\leq 0$  to 5-6 or 7-8, respectively. After homogenisation, the tubes were centrifuged 10 mins at 12500 rpm and the supernatant was discarded. The pellets were resuspended in Tris (10 mM, pH8). Tubes were heat-shocked by freezing them at  $-20^{\circ}\text{C}$  for a few hours and then dipping them in  $42^{\circ}\text{C}$  water for 20 seconds. They were subsequently microwaved (3x10 seconds 700W) to be sure to break-up the cells for PCR. We used archaea-specific primers (21F, 5'-TTCCGGTTGATCCTGCCGGA; Ar109F, 5'-ACKGCTGCTCAGTAACACGT) and bacteria-specific primers (27F, 5'-AGAGTTTATCCTGGCTCAG) with the prokaryotic reverse primer 1492R (5'-GGTTACCTTGTTACGACTT). Amplification reactions were performed for 35 cycles ( $94^{\circ}\text{C}$  for 15 s,  $50\text{--}55^{\circ}\text{C}$  for 30 s and  $72^{\circ}\text{C}$  for 90 s), after a 2 min-denaturation step at  $94^{\circ}\text{C}$  and before a final extension. Amplicons were visualized after gel electrophoresis and staining with ultrasensitive GelRed nucleic acid gel (Biotium) on an ultraviolet light transilluminator.
- 3) DNA concentration measures before and after contact with Dallol's brine: in a first step, we filtered fixed volumes of cultures (*E. coli*, *H. salinarum*) and one natural sample (Salt Plain) on  $0.2\ \mu\text{m}$  pore-diameter sized filters, rinsed them with 2 mL of Milli-Q water and extracted DNA with the Power Soil DNA Isolation Kit (MoBio, Carlsbad, CA, USA). In a second step, we repeated the experiments but adding 500  $\mu\text{L}$  of Dallol's brine on the surface of the filters before rinsing them with 2 mL of sterile Milli-Q water to stop potential reactions. DNA concentrations were measured using Qubit dsDNA HS assays (Invitrogen). The pH during the different experiments was measured using either pH paper 0-6.

### 5.3.3 Results

#### 5.3.3.1 The Dallol aerosols are dominated by widespread bacteria but halophile microorganisms likely originating from the surrounding less polyextreme environments are detected

We carried out 16S/18S rRNA metabarcoding analyses to study the microbial diversity of the aerosols collected on the Dallol dome and the campsite close to it (Figure 21) and compared it with data from hypersaline and mildly acidic sites around Dallol: the salt plain (samples PS and PS3), the salt canyons' cave reservoir (samples 9Gt, 8Gt, 7Gt, and Gt) and Lake Karum/Assale (samples Ass and 9Ass) (Table 7) (Belilla et al. 2019). The bioaerosols and the hypersaline brines exhibited considerable differences in their microbial communities' structure since the prokaryotic fraction of the bioaerosols was almost exclusively (99%)

composed of Bacteria, in sharp contrast with the hypersaline brines that were mostly dominated by Archaea (77-98% of total prokaryotes) (Figure 22, Supplementary Figure 2). A large part of the bacterial fraction in the bioaerosols corresponded to groups common in soil environments (such as Verrucomicrobia, Proteobacteria, Acidobacteria and Actinobacteria) (Köberl et al. 2020), as well as part of the eukaryotic fraction which was composed of land plants and land fungi (Supplementary Figure 3). Some eukaryotic organisms even seemed to originate from the sea, as for example some radiolarians were also detected (Anderson 2001). Nevertheless, despite these strong differences, aerosols also shared several OTUs with the salt plain, the cave and Lake Karum, including Archaea (Halobacteria and Nanohaloarchaeota) and some Cyanobacteria. In fact, phylogenetic analysis showed that the Nanohaloarchaeota and Halobacteria OTUs from the aerosols branched among OTUs previously observed in the Dallol surroundings (Figure 23). That was also the case for the Nanohaloarchaeota OTU found by Gomez et al. (2019) in a Dallol pond, closely related to sequences from Lake Karum and the cave's brine and to the sequence EU869371 from the Sidi Ameer Salt Lake (Algeria).

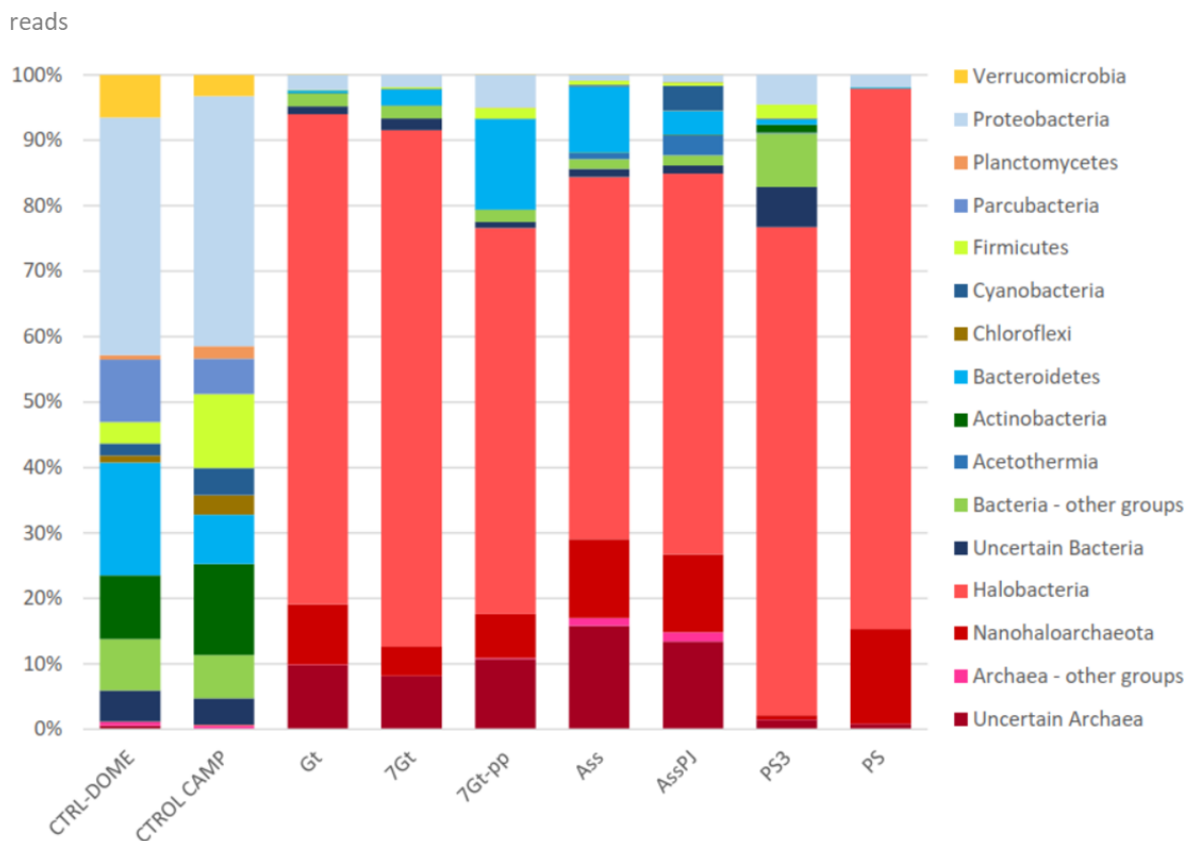


**Figure 22 | Histogram showing the presence/absence and relative abundance of amplicon reads of archaea and bacteria obtained with universal prokaryotic primers.** Phyla that were representing <1% of the total reads have been put in categories “bacteria – other groups” or “archaea – other groups”. Uncertain phyla are the one for which the first-hit is  $\leq 90\%$  identical to the OTU. For samples names' reference see Table 7.

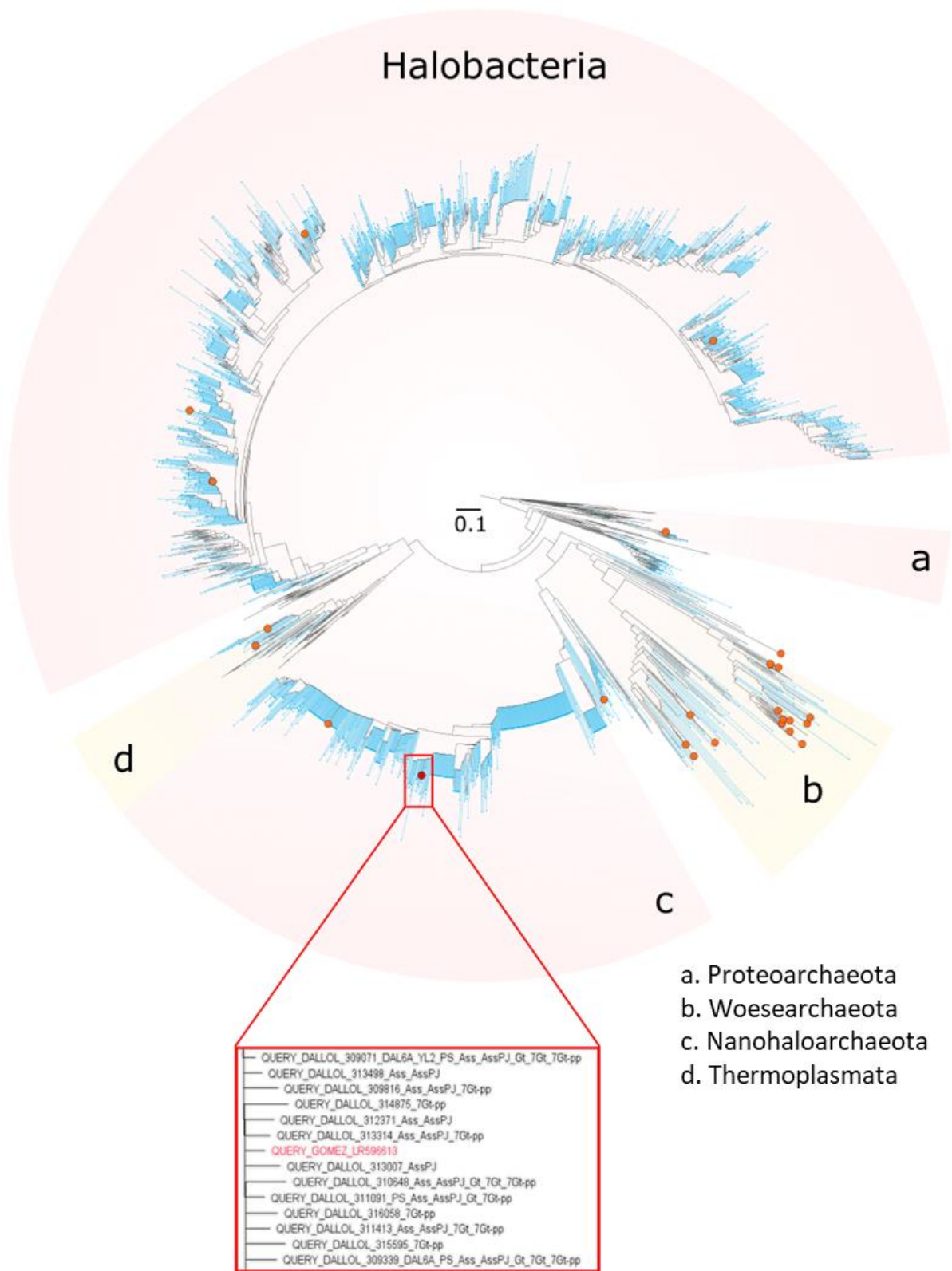


**Figure 23 | Phylogenetic tree of archaeal 16S rRNA gene sequences.** Black lines/leaves: reference sequences and best-hits. Blue lines/leaves: Illumina OTUs from Belilla et al. (2019), also called QUERY\_DALLOL in the zoomed section of the tree. Orange dots: archaeal OTUs from the bioaerosols of Dallol dome and our campsite. Red dot: Gomez et al. (2019) Nanohaloarchaea, also represented in red in the zoomed section of the tree.

5.3.3.2 The FISH experiment confirmed an absence of cells in the Dallol dome brine, and in the salt plain sample a potential parasitic association of Halobacteria/Nanohaloarchaeota was discovered

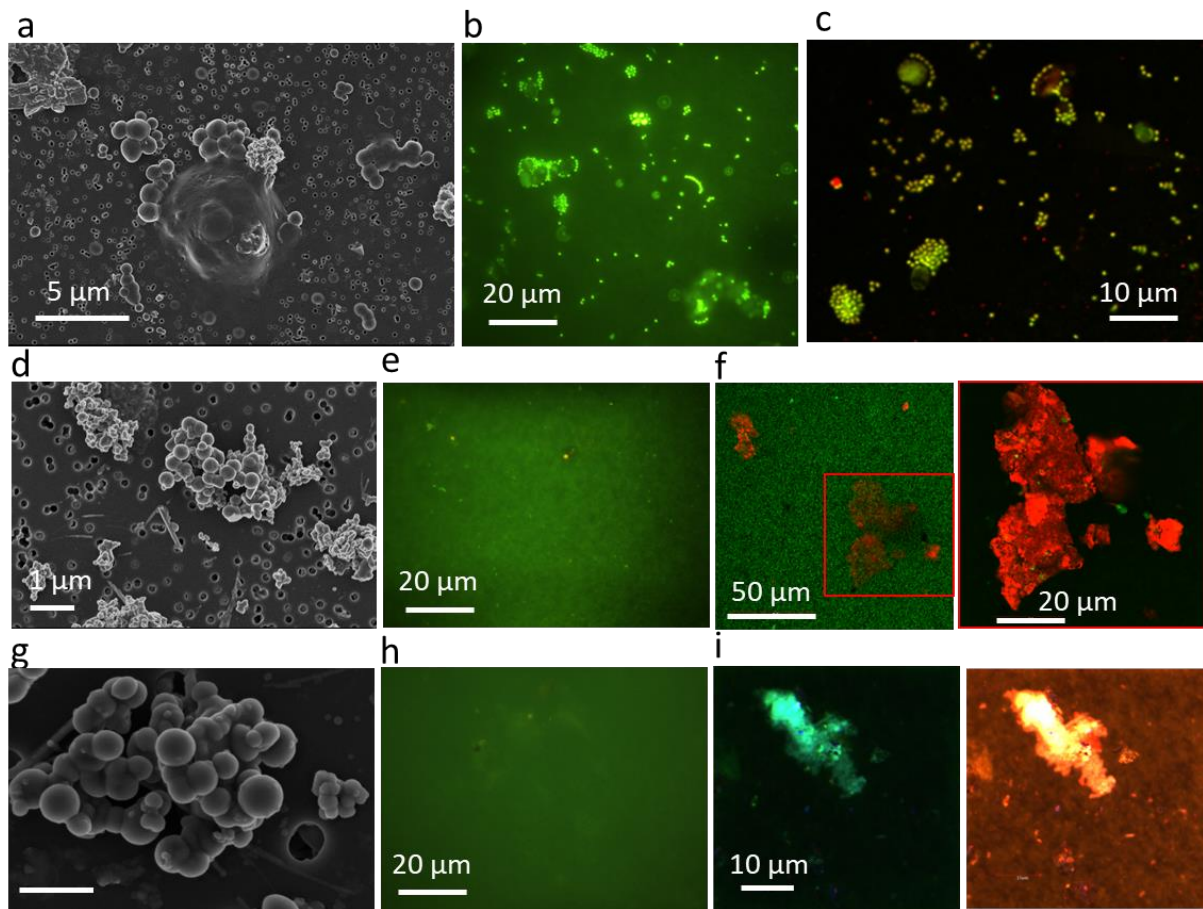


**Figure 24 | The salt plain (PS) cells and Dallol biomorphs through scanning electron microscopy (SEM) epifluorescence observations (optical microscope, confocal laser scanning) on filters.** On the optical microscope pictures, only SYBR Gold wavelength is excited. On the confocal microscope pictures, both SYBR Gold and CY3-Narc1214 are excited. SYBR Gold: green, CY3-Narc1214: red. **a**, SEM image of PS cocci. Two morphologies are visible: ~5 μm ones, and <1 μm ones. The little cells tend to be associated with the bigger one. **b**, Same filter as **(a)** through the optical microscope. **c**, Same filter as **(a)** through the confocal microscope. **d**, SEM image of 7DA13-w1 nanococci-like biomorphs. **e**, Same filter as **(d)** through the optical microscope. **f**, Same filter as **(d)** through the confocal microscope with the same camera parameters as **(c)**, and a zoomed section (red square) with different camera parameters. **g**, SEM image of DAL4 nanococci-like biomorphs. **h**, Same filter as **(g)** through the optical microscope. **i**, Same filter as **(e)** through the confocal microscope with the same camera settings as **(c)** (left) and without sequential scanning (right).

We applied a FISH protocol close to the one Gomez et al. (2019) employed to analyse their Dallol sample in order to be able to compare our respective results. Accordingly to this protocol, we used the CY3-labeled Nanohaloarchaeota-specific probe Narc1214 (Narasingarao et al. 2012) and SYBR Gold to reveal Nanohaloarchaeota and cells' DNA respectively. We added to the procedure Non-Eub controls (Amann, Ludwig, et Schleifer 1995; Sunde et al. 2003). We used as a positive control a salt plain's filter (PS), where the presence of Nanohaloarchaeota has been previously reported (Belilla et al. 2019), and only after tested

the Dallol brine and dissolved salts cell's presence. Observations of PS filter revealed two cell's phenotypes: small ( $<1\ \mu\text{m}$ ) coccoid cells attached to bigger ( $\sim 5\ \mu\text{m}$ ) cells (Figure 24-a-c, Figure 25), the two being visible at the SYBR Gold excitation wavelength though the bigger cells had a weaker signal. Given the density of these cells and the known microbial composition of PS, we suppose those two phenotypes are associated with Halobacteria (for the big ones) and Nanohaloarchaeota (for the little ones), and their relationship could be parasitic since the biggest cells seem depleted in DNA. These cells all showed autofluorescence at the CY3 excitation wavelength, with no difference in intensity even if the cells had been in contact with the probe CY3-Narc1214 (or with the hybridization control probe Non-Eub). Moreover, some particles autofluorescent under CY3 excitation wavelength were not fluorescent with the SYBR Gold colouration (supplementary figures with all hybridization controls are not shown in this manuscript but may be added to the final version of the paper).

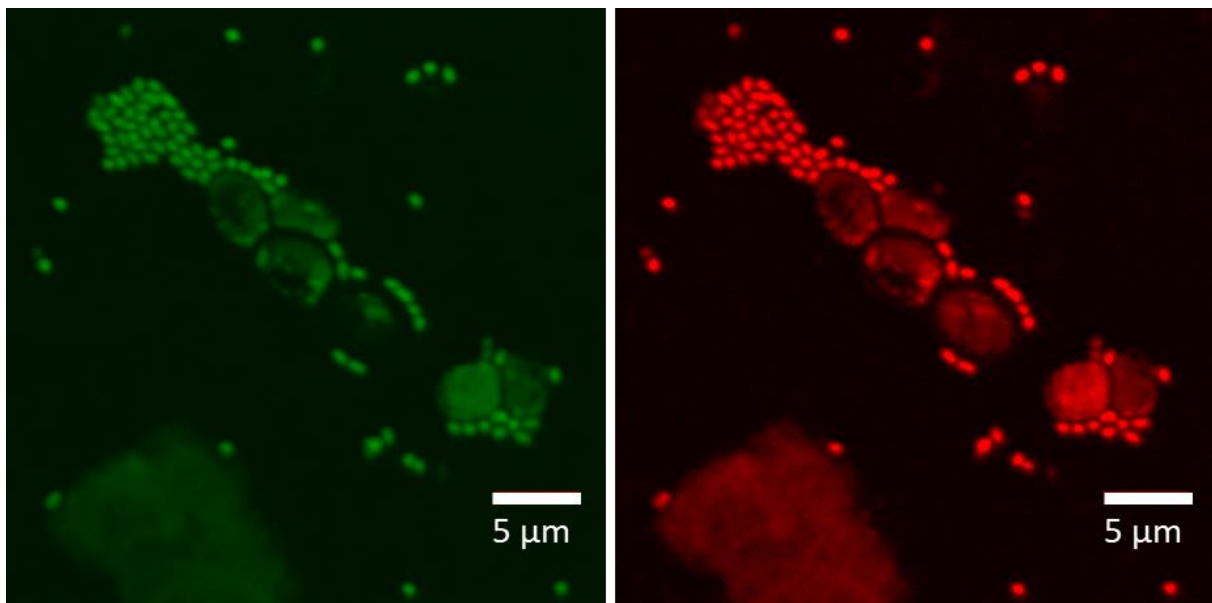


**Figure 25 | Salt plain (PS) cells epifluorescence observations through the confocal microscope.** Left: SYBR Gold in green. Right: CY3-Narc1214 in red.

We then applied the same protocol to analyse two samples of the hyperacidic hypersaline Dallol dome brine, 7DA13-w1 and DAL4, using as a reference the settings we used to observe cells in PS. Despite the abundant presence of biomorphs particles in both samples as observed on the SEM images, we did not observe any signal after SYBR Gold staining (Figure 24-d-i). Likewise, we did not observe any signal after hybridization with the Narc1214 and Non-Eub probes. Using different image acquisition settings than for PS, we could see few particles fluorescent at the SYBR Gold or CY3 excitation wavelengths, but most of the time they were not correlated (Figure 24-f). Only when we forced the image acquisition by taking off the sequential acquisition of the confocal microscope or by changing camera parameters, we could observe more fluorescent particles and more correlation between SYBR Gold and CY3 (Figure 24-i,f).

We studied the same samples under Scanning Electron Microscopy (SEM), which allows the determination of chemical composition by Energy Dispersive X-Ray (EDX) analysis. The small and big cells of sample PS were easily visible (Figure 24-a, Figure 26-A). We also observed many cell-like small particles in the brine samples 7DA13-w1 and DAL4 (Figure 24-d,g, Figure 26-B). However, whereas the EDX analysis did not reveal the presence of significant amounts of heavy elements in the cells of PS (in agreement with their C-based organic nature), the cell-like particles in the brines were very rich in amorphous silica, sulphur and, in the case of DAL4, also sulphur-rich minerals (Figure 26), indicating that they are most likely biomorphs (cell-shaped mineral particles).

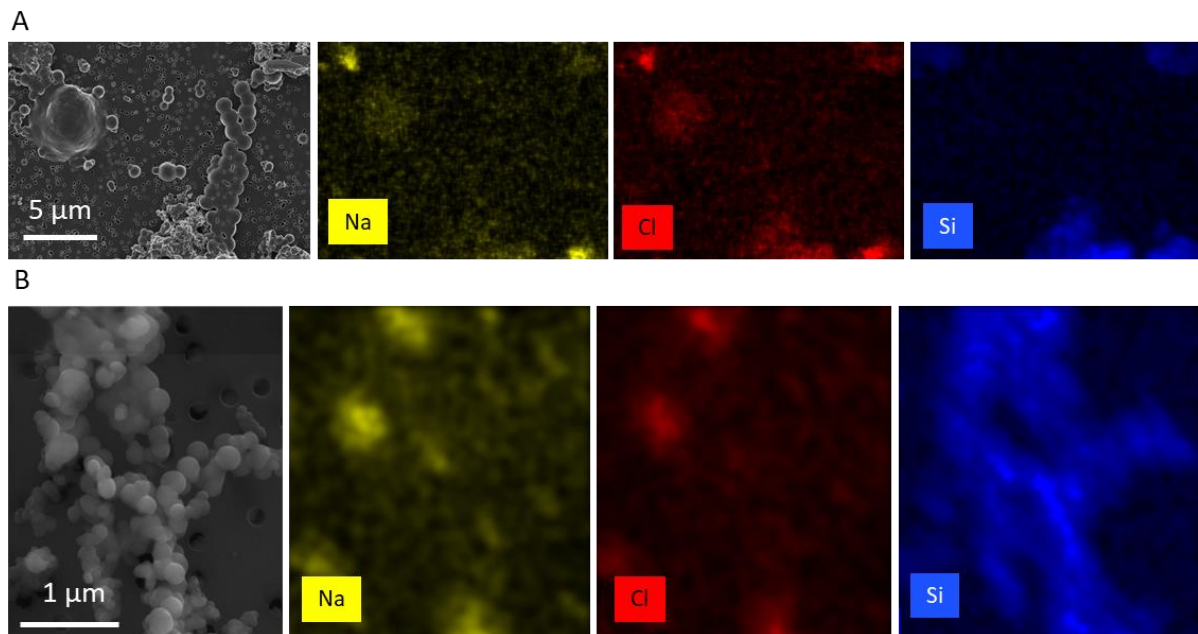


**Figure 26 | Salt plain (PS) cells and Dallol biomorphs through scanning electron microscopy (SEM) with associated chemical maps.** The colour intensity provides semiquantitative information of the mapped elements. **A**, PS cocci. Two morphologies are visible: ~5 µm ones, and <1 µm ones. Some little cells seem associated with the bigger one. **B**, 7DA13-w1 cocci-like silicates biomorphs.

### 5.3.3.3 DNA is degraded almost instantly and completely in Dallol's brine

We carried out several experiments to test if the hyperacidic and hypersaline water of Dallol has the capacity to degrade DNA using both natural samples from less extreme places around Dallol (salt plain, salt canyons' cave, and Lake Karum, all harbouring a wide microbial diversity dominated by halophilic archaea Belilla et al. 2019) and cultures of bacterial (*Escherichia coli*) and haloarchaeal (*Halobacterium salinarum* and *Haloferax denitrificans*) species. They were analysed before and after mixing with the Dallol brine by i) epifluorescence microscopy observation, ii) DNA extraction and quantification, and iii) PCR amplification of 16S rRNA genes (see Methods for details).

While fluorescent cells were clearly visible after colouration with the fluorescent DNA stain SYTO9 in all samples and cultures, the fluorescence disappeared instantly and completely for most of them after addition of Dallol's brine (Figure 27-A, Supplementary Figure 4).

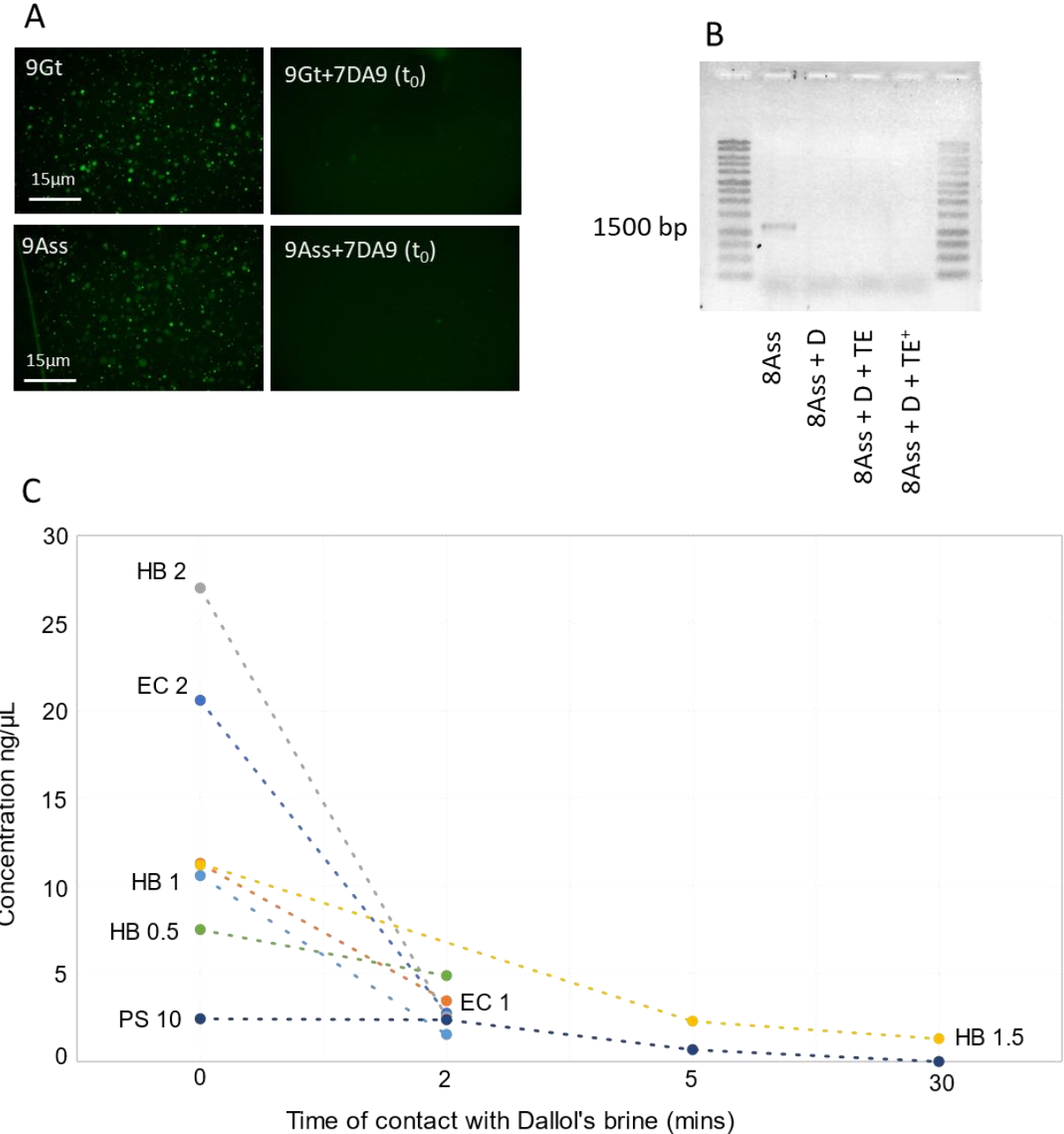


**Figure 27 | Test of the DNA-degrading potential of Dallol's brine.** **A**, SYTO9 epifluorescence of 9Gt and 8Ass before and right after (t<sub>0</sub>) adding 1:3 7DA9. The scale was estimated with a hemocytometer. **B**, 16S rRNA gene amplifying test on cell pellets. From left to right: positive control (cell pellet only), cell pellet in contact with acidified (pH~0) hypersaline medium (D), cell pellet in contact with D but the acidity have been neutralized with TE or TE<sup>+</sup> solutions (see Mat et Mat). Contact with D only last an instant (for vortex and centrifugation). All supernatant has been removed and pellets diluted in DNA buffer before PCR. **C**, DNA concentration on filters for different cultures (and the salt plain sample PS) before and after contact with 7DA9. The number next to the names are the volume (mL) of culture or sample filtered. HB: *Halobacterium salinarum*; EC: *Escherichia coli*

When the sample was rich in mineral particles, fluorescent particles could still be seen after contact with 7DA9 though usually they did not have a cell shape and corresponded most likely to minerals. Likewise, we did not obtain any 16S rRNA gene amplicon from the samples or cultures after brief incubation in Dallol brine, even when the acidic pH was neutralized as fast as possible (Figure 27-B, Supplementary Figure 5). Finally, we observed a dramatic instantaneous decrease of DNA concentration (by a factor of two to six) in biomass concentrated on filters immediately after contact with the Dallol brine (Figure 27-C), with final concentrations always  $\leq 5$  ng/ $\mu$ L, close to the detection limit of our instrument.

#### 5.3.4 Discussion

In a recent study, we showed that the polyextreme hydrothermal system of Dallol contained extremely low or non-existent biomass (Belilla et al. 2019). The 16S/18S rRNA metabarcoding analyses revealed a surprising dominance of non-extremophilic bacteria, in sharp contrast with the archaea-dominated communities found in the moderately acidic-hypersaline systems around Dallol (salt plain, salt canyons' cave, Lake Karum). Using appropriate controls, we explained these unexpected results by demonstrating that most of the bacterial diversity supposedly associated to the Dallol brines actually corresponded to laboratory contaminants (from DNA extraction kits, PCR reagents, etc.), a recurrent observation in studies of low-biomass samples (Weyrich et al. 2019). We also detected bacterial OTUs typical from soil or from human or plant microbiomes, which we interpreted as airborne contaminants coming from non-extreme regions or deposited by the people visiting the area. We concluded that the polyextreme Dallol brines constitute a unique case of liquid water devoid of microbial life on the surface of our planet (Belilla et al. 2019). This conclusion was at odds with a study that claimed to have found one nanohaloarchaeal species in a Dallol pond using metabarcoding and FISH approaches (Gómez et al. 2019).

Here, we have explored the impact that short- and long-distance airborne microorganisms may have on the contamination of the Dallol pools. To collect these microorganisms, we deployed dust traps on three spots of the dome and we also actively filtered the air in the campsite at the base of the dome during our last expedition in January 2019. 16S/18S rRNA gene metabarcoding analysis of these samples revealed that they were largely dominated by bacteria, in contrast with the less extreme sites around Dallol, which host microbial communities dominated by archaea (Figure 22). This result suggests that most airborne organisms on the Dallol dome are transported from long distance since the neighbouring area is mostly inhabited by halophilic archaea (both halobacteria and nanohaloarchaea). The presence of plant sequences in the 18S rRNA metabarcoding data provides an obvious example of long-distance transport: no plant grows on the dome or on the salt-saturated surroundings, so that these sequences most likely derived from airborne pollen coming from distant places where vegetation thrives. Another example is the detection of typical marine microorganisms (e.g. radiolarians), Dallol being located at more than 70 km

from the Red Sea, the closest marine area. These results show that microorganisms can be transported from tens to hundreds of kilometres into Dallol. This is not surprising since Dallol and the whole Danakil Depression are subjected to a ceaseless blowing hot wind, which the local Afar population calls “hahaita-harrur” or “fire-wind” (Aerts et November 2017). Dallol is located in the middle of the Danakil Depression, which is surrounded by high mountains (the Danakil Alps on the East and the Ethiopian Plateau on the West), from where the wind might bring dust, pollen and diverse microorganisms. In addition, despite its remoteness, Dallol is a touristic spot that attracts thousands of visitors from all over the world every year, which may represent additional sources of long-distance microbial contamination.

Even if long-distance airborne microorganisms (mostly bacteria) dominate the aerosols on the dome, we also detect several OTUs that most likely represent short-distance contamination, which can also be explained by wind and/or human-associated transport. These OTUs, in particular halophilic archaea, are also present in the salt plain, the salt canyons’ cave or Lake Karum (Figure 23). That is also the case for the single nanohaloarchaeal OTU found by Gomez et al. (2019) in a hyperacidic Dallol pool, very similar to several of the OTUs that we found in less extreme places around the Dallol dome (Figure 23). This similarity raised doubts about its actual origin (they did not provide any information about the taxonomic affiliation of the rest of OTUs that they discarded, despite they represented most of their sequences). Using a FISH protocol close to theirs and adding a positive control (PS) we could tell that cells are auto fluorescent in the CY3 excitation signal, making it impossible to know if the hybridization was successful or not. Nevertheless, association of cells that could be haloarchaea and nanohaloarchaea were detected on the PS filters, either during the FISH or the SEM experiment. On the opposite, no cells could be detected in the Dallol samples, except if distancing the observation settings of those from the control (Figure 24). Moreover, the objects that they observed with SEM strongly resembled some nanominerals that precipitate abundantly in the Dallol hyperacidic pools, such as jarosite (Kotopoulou et al. 2019) and silicate (Belilla et al. 2019) spherules. Close association to larger cells that have been described for the Nanohaloarchaeota (Narasingarao et al. 2012; Hamm et al. 2019). In fact, there is growing evidence that Nanohaloarchaeota depend on other organisms for their growth (Hamm et al. 2019; Cono et al. 2019) and based on the DNA fluorescence differences, we hypothesize here that this interaction could be parasitic in the case of PS sample. In that sense, it is also surprising that Gomez et al. only reported a nanohaloarchaeal OTU but not any suitable host. Considering these caveats and our analysis of the Dallol aerosols, we conclude that the most parsimonious explanation for detection of non-extremophile or known halophiles in the hyperacidic hypersaline pond is contamination from one of the numerous hyperdiverse ecosystems close to Dallol (through the wind and potentially the human activity).

These results may seem paradoxical because whereas we unveiled a large microbial diversity in the aerosols, the Dallol brine samples did not appear to contain life. Moreover, it was much easier to amplify 16S and 18S rRNA genes from the aerosols (a single PCR was

enough) than from the brine pools (semi nested PCRs were necessary). Why it was not equally easy to detect by PCR all the aerosol-transported biomass that is continuously falling into the brines? We hypothesize that the reason might be a very active DNA destruction process occurring in the brine. Our experiments confirm this hypothesis as we measured an almost instantaneous disappearance of DNA in cells incubated in Dallol brine (Figure 27). This was the case even for several haloarchaeal species despite their adaptation to salt-saturated conditions, which suggests that the hyperacidity of the Dallol brine is the main factor leading to DNA destruction. Indeed, depurination of DNA under acidic conditions has been known for a long time (Tamm, Hodes, et Chargaff 1952; Hevesi et al. 1972), though most likely it had never been studied under the extremely low pH values (<0) typical of the Dallol brine. Nevertheless, the high salinity and the complex and poorly-known chemistry of the Dallol brine probably also play a role, for example through the abundant presence of chaotropic salts (e.g. FeCl<sub>2</sub>, FeCl<sub>3</sub>, MgSO<sub>4</sub>) (Belilla et al. 2019; Kotopoulou et al. 2019) that can disrupt biomolecules (Hallsworth et al. 2007) and facilitate the passage of the acidic brine through the cell membrane to DNA. It has recently been shown that another chaotropic salt, sodium perchlorate, is formed under high UV irradiation of NaCl in presence of silica (Carrier et Kounaves 2015). These conditions are prevalent in Dallol, so the presence of this chaotropic agent would be likely increase the cell destructing capacity of Dallol's brine. Moreover, Dallol has been proposed as a suitable terrestrial analogue to study the potential presence of life on Mars since this planet possesses extensive acidic evaporitic areas (Cavalazzi et al. 2019) where perchlorate is suspected to form (Carrier et Kounaves 2015). However, this study shows that the brine of Dallol do not only lack life, but its unique combination of hyperacidity, hypersalinity and high concentration of chaotropic salts actively destroys all contaminant life. These similarities with Mars may explain why life, or even complex organic matter, has not been found on the Red Planet (Kerr 2013).

In this work, we have shown that the aerosols over the polyextreme site of Dallol contain a wide diversity of microorganisms. This diversity is dominated by non-extremophilic bacteria coming from very distant places but also encompasses some halophilic microorganisms, mostly archaea, transported from the less extreme areas around Dallol. The abundant airborne microbial contamination detected casts doubts about the validity of the recent claims about the presence of life in the hyperacidic hypersaline brine of Dallol based on PCR amplification of 16S rRNA genes and microscopy observation (Gómez et al. 2019). We provide support to the alternative conclusion that these results are due to local contamination and the presence of numerous minerals with cell-like morphologies (biomorphs). We cannot exclude, in fact, that the Dallol brine might destroy the totality of exogenous DNA, and that all that can be detected afterwards are cells from the material contaminated on site or cross-contamination with other samples. Rather than being a refuge for life, our experiments show that the Dallol brine have the unusual capacity to destroy cells and DNA exceedingly fast, most likely due to the combination of extreme acidity and salinity with a high concentration of various chaotropic salts. The Dallol dome remains a unique example on Earth of surface liquid

water devoid of life. This work illustrates the importance of adequate controls to work with low biomass, or even sterile, samples.

### Acknowledgements:

We are grateful to Olivier Grunewald for co-organizing the Dallol expeditions, documenting field research and providing drone images and to the Fondation Iris and Frederic Paulsen for funding field trips. We thank Luigi Cantamessa for the *in situ* logistics, and Dr. Makonen Tafari (Mekelle University), Abdul Ahmed Aliyu and the Afar authorities for local assistance as well as the Afar police for providing security. We thank Jacques Barthélémy for help during the field trips. We thank Paola Bertolino, Jonathan Huc and Ulysse Tuquoi for help with the experiments and Maria Ciobanu for advice. We thank Guillaume Reboul, Ana Gutierrez and Fabian van Beveren for help with the sequence treatment. This work was supported by the CNRS programs 'TELLUS INTERRVIE' and 'EC2CO' and the European Research Council under the European Union's Seventh Framework Program (ERC Grant Agreement 322669 to P.L.-G.).

### References

- Aerts, R., et Eva J. J. November. 2017. « The Dallol Volcano. » *Wilderness & environmental medicine*. <https://doi.org/10/ghb97b>.
- Amann, R I, W Ludwig, et K H Schleifer. 1995. « Phylogenetic identification and in situ detection of individual microbial cells without cultivation. » *Microbiological Reviews* 59 (1): 143-69.
- Anderson, O. R. 2001. « Protozoa, Radiolarians\* ». In *Encyclopedia of Ocean Sciences (Second Edition)*, édité par John H. Steele, 613-17. Oxford: Academic Press. <https://doi.org/10.1016/B978-012374473-9.00193-4>.
- Antón, Josefa, Ramón Rosselló-Mora, Francisco Rodríguez-Valera, et Rudolf Amann. 2000. « Extremely Halophilic Bacteria in Crystallizer Ponds from Solar Salterns ». *Applied and Environmental Microbiology* 66 (7): 3052-57.
- Bodaker, Idan, Itai Sharon, Marcelino T. Suzuki, Roi Feingersch, Michael Shmoish, Ekaterina Andreishcheva, Mitchell L. Sogin, et al. 2010. « Comparative Community Genomics in the Dead Sea: An Increasingly Extreme Environment ». *The ISME Journal* 4 (3): 399-407. <https://doi.org/10/fk6c34>.
- Cameron, R.E, F.A Morelli, et L.P Randall. 1972. « Aerial, Aquatic, and Soil Microbiology of Don Juan Pond, Antarctica ». *Antartic Journal of the United States* 7 (6): 254-58.
- Carrier, Brandi L., et Samuel P. Kounaves. 2015. « The Origins of Perchlorate in the Martian Soil ». *Geophysical Research Letters* 42 (10): 3739-45. <https://doi.org/10/f7hcpn>.
- Cavalazzi, B., R. Barbieri, F. Gómez, B. Capaccioni, K. Olsson-Francis, M. Pondrelli, A. P. Rossi, et al. 2019. « The Dallol Geothermal Area, Northern Afar (Ethiopia)-An Exceptional Planetary Field Analog on Earth ». *Astrobiology* 19 (4): 553-78. <https://doi.org/10/ggvk97>.
- Cono, Violetta La, Enzo Messina, Manfred Rohde, Erika Arcadi, Sergio Ciordia, Francesca Crisafi, Renata Denaro, et al. 2019. « Differential Polysaccharide Utilization Is the Basis for a Nanohaloarchaeon: Haloarchaeon Symbiosis ». *BioRxiv*, octobre, 794461. <https://doi.org/10/ghdpj5>.
- Gómez, Felipe, Barbara Cavalazzi, Nuria Rodríguez, Ricardo Amils, Gian Gabriele Ori, Karen Olsson-Francis, Cristina Escudero, Jose M. Martínez, et Hagos Miruts. 2019. « Ultra-Small Microorganisms in the Polyextreme Conditions of the Dallol Volcano, Northern Afar, Ethiopia ». *Scientific Reports* 9 (1): 1-9. <https://doi.org/10/gf2756>.

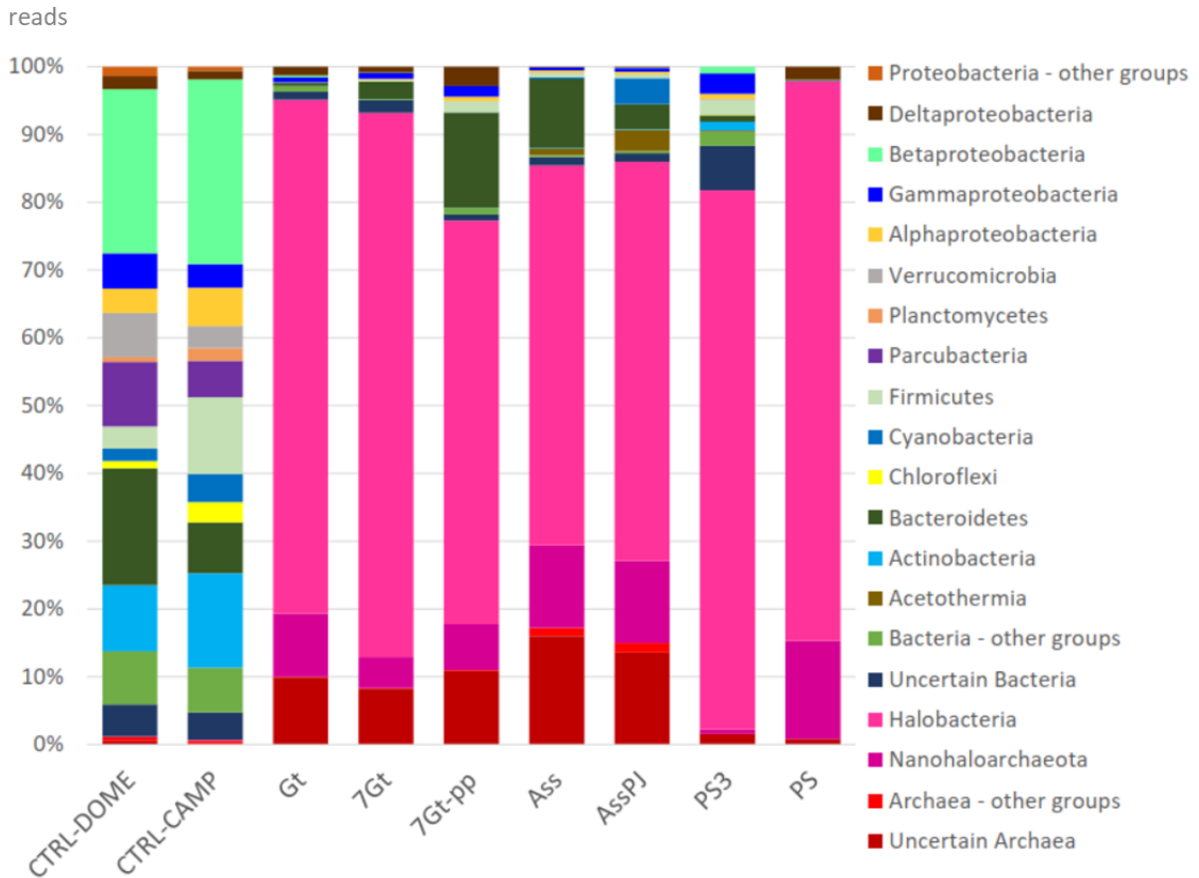
- Hallsworth, John E., Michail M. Yakimov, Peter N. Golyshin, Jenny L. M. Gillion, Giuseppe D'Auria, Flavia De Lima Alves, Violetta La Cono, et al. 2007. « Limits of Life in MgCl<sub>2</sub>-Containing Environments: Chaotropicity Defines the Window ». *Environmental Microbiology* 9 (3): 801-13. <https://doi.org/10/fktqwc>.
- Hamm, Joshua, Susanne Erdmann, Emiley Eloë-Fadrosch, Allegra Angeloni, Ling Zhong, Christopher Brownlee, Timothy Williams, et al. 2019. « Unexpected host dependency of Antarctic Nanohaloarchaeota ». *Proceedings of the National Academy of Sciences* 116 (juin). <https://doi.org/10/gf4ggj>.
- Harrison, Jesse P., Nicolas Gheeraert, Dmitry Tsigelnitskiy, et Charles S. Cockell. 2013. « The Limits for Life under Multiple Extremes ». *Trends in Microbiology* 21 (4): 204-12. <https://doi.org/10/f4wgwh>.
- Hevesi, L., E. Wolfson-Davidson, J. B. Nagy, O. B. Nagy, et A. Bruylants. 1972. « Contribution to the mechanism of the acid-catalyzed hydrolysis of purine nucleosides ». *Journal of the American Chemical Society* 94 (13): 4715-20. <https://doi.org/10/cwwqd3>.
- Kerr, Richard A. 2013. « Pesky Perchlorates All Over Mars ». *Science* 340 (6129): 138-138. <https://doi.org/10/ghdpj9>.
- Köberl, Martina, Philipp Wagner, Henry Müller, Robert Matzer, Hans Unterfrauner, Tomislav Cernava, et Gabriele Berg. 2020. « Unraveling the Complexity of Soil Microbiomes in a Large-Scale Study Subjected to Different Agricultural Management in Styria ». *Frontiers in Microbiology* 11. <https://doi.org/10/ghqnht>.
- Kotopoulou, Electra, Antonio Delgado Huertas, Juan Manuel Garcia-Ruiz, Jose M. Dominguez-Vera, Jose Maria Lopez-Garcia, Isabel Guerra-Tschuschke, et Fernando Rull. 2019. « A Polyextreme Hydrothermal System Controlled by Iron: The Case of Dallol at the Afar Triangle ». *ACS Earth & Space Chemistry* 3 (1): 90-99. <https://doi.org/10/ghdcr4>.
9. López-García JM, Moreira D, Benzerara K, Grunewald O, López-García P. Origin and Evolution of the Halo-Volcanic Complex of Dallol: Proto-Volcanism in Northern Afar (Ethiopia). *Front Earth Sci* [Internet]. 2020 [cité 23 avr 2020];7. Disponible sur: <https://www.frontiersin.org/articles/10.3389/feart.2019.00351/full>
- Mykytczuk, Nadia C S, Simon J Foote, Chris R Omelon, Gordon Southam, Charles W Greer, et Lyle G Whyte. 2013. « Bacterial growth at -15 °C; molecular insights from the permafrost bacterium *Planococcus halocryophilus* Or1 ». *The ISME Journal* 7 (6): 1211-26. <https://doi.org/10/f463p7>.
- Narasingarao, Priya, Sheila Podell, Juan A. Ugalde, Céline Brochier-Armanet, Joanne B. Emerson, Jochen J. Brocks, Karla B. Heidelberg, Jillian F. Banfield, et Eric E. Allen. 2012. « De Novo Metagenomic Assembly Reveals Abundant Novel Major Lineage of Archaea in Hypersaline Microbial Communities ». *The ISME Journal* 6 (1): 81-93. <https://doi.org/10/bmkzrz>.
- Samarkin, Vladimir A., Michael T. Madigan, Marshall W. Bowles, Karen L. Casciotti, John C. Priscu, Christopher P. McKay, et Samantha B. Joye. 2010. « Abiotic Nitrous Oxide Emission from the Hypersaline Don Juan Pond in Antarctica ». *Nature Geoscience* 3 (5): 341-44. <https://doi.org/10/bchns8>.
- Schleper, Christa, Gabriela Puhler, Hans- Peter Klenk, et Wolfram Zillig. 1996. « *Picrophilus* Oshimae and *Picrophilus* Tomdus Fam. Nov., Gen. Nov., Sp. Nov., Two Species of Hyperacidophilic, Thermophilic, Heterotrophic, Aerobic Archaea », *International Journal of Systematic Bacteriology*, 46 (3): 814-16. <https://doi.org/10.1099/00207713-46-3-814>.
- Sturr, M G, A A Guffanti, et T A Krulwich. 1994. « Growth and bioenergetics of alkaliphilic *Bacillus firmus* OF4 in continuous culture at high pH. » *Journal of Bacteriology* 176 (11): 3111-16.
- Sunde, Pia T., Ingar Olsen, Ulf B. Göbel, Dirk Theegarten, Sascha Winter, Gilberto J. Debelian, Leif Tronstad, et Annette Moter. 2003. « Fluorescence in Situ Hybridization (FISH) for Direct Visualization of Bacteria in Periapical Lesions of Asymptomatic Root-Filled Teeth ». *Microbiology (Reading, England)* 149 (Pt 5): 1095-1102. <https://doi.org/10/csw48s>.
- Takai, Ken, Kentaro Nakamura, Tomohiro Toki, Urumu Tsunogai, Masayuki Miyazaki, Junichi Miyazaki, Hisako Hirayama, Satoshi Nakagawa, Takuro Nunoura, et Koki Horikoshi. 2008. « Cell Proliferation at 122°C and Isotopically Heavy CH<sub>4</sub> Production by a Hyperthermophilic Methanogen under High-Pressure Cultivation ». *Proceedings of the National Academy of Sciences* 105 (31): 10949-54. <https://doi.org/10/crqvsn>.

- Tamm, C., M. E. Hodes, et E. Chargaff. 1952. « The Formation Apurinic Acid from the Desoxyribonucleic Acid of Calf Thymus ». *The Journal of Biological Chemistry* 195 (1): 49-63.
- Weyrich, Laura S., Andrew G. Farrer, Raphael Eisenhofer, Luis A. Arriola, Jennifer Young, Caitlin A. Selway, Matilda Handsley-Davis, Christina J. Adler, James Breen, et Alan Cooper. 2019. « Laboratory Contamination over Time during Low-Biomass Sample Analysis ». *Molecular Ecology Resources* 19 (4): 982-96. <https://doi.org/10/ggvbjd>.

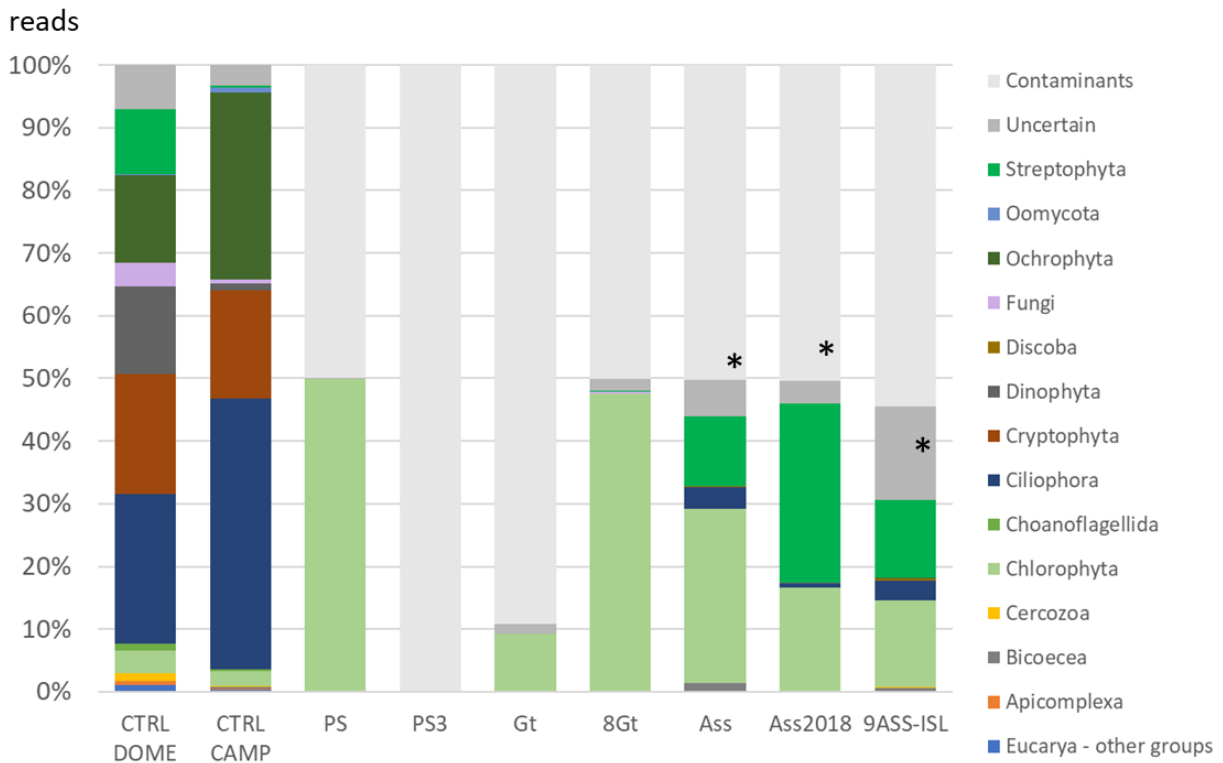
## 5.4 Supplementaries



**Supplementary Figure 1 | Bioaerosol collecting areas on Dallol dome.** **a**, Overview of the ancient hydrothermal chimneys area close to the tourist path that was chosen for filters 1 and 2. **b**, Filters 1 and 2 were put at the top on chimneys as shown in this picture, to avoid attracting curiosity of tourists. **c**, filter n°2 in position. **d**, The active gas chimney field that was chosen for filter 3. **e**, Placing of filter 3. **f**, Placing of filter 4, ~30m N-E of filter n°3, between salt boulders. **g**, The “chocolate” formation that was chosen for filters 5 and 6. **h**, Filter 5. **i**, Filter 6, few meters away from filter 5.

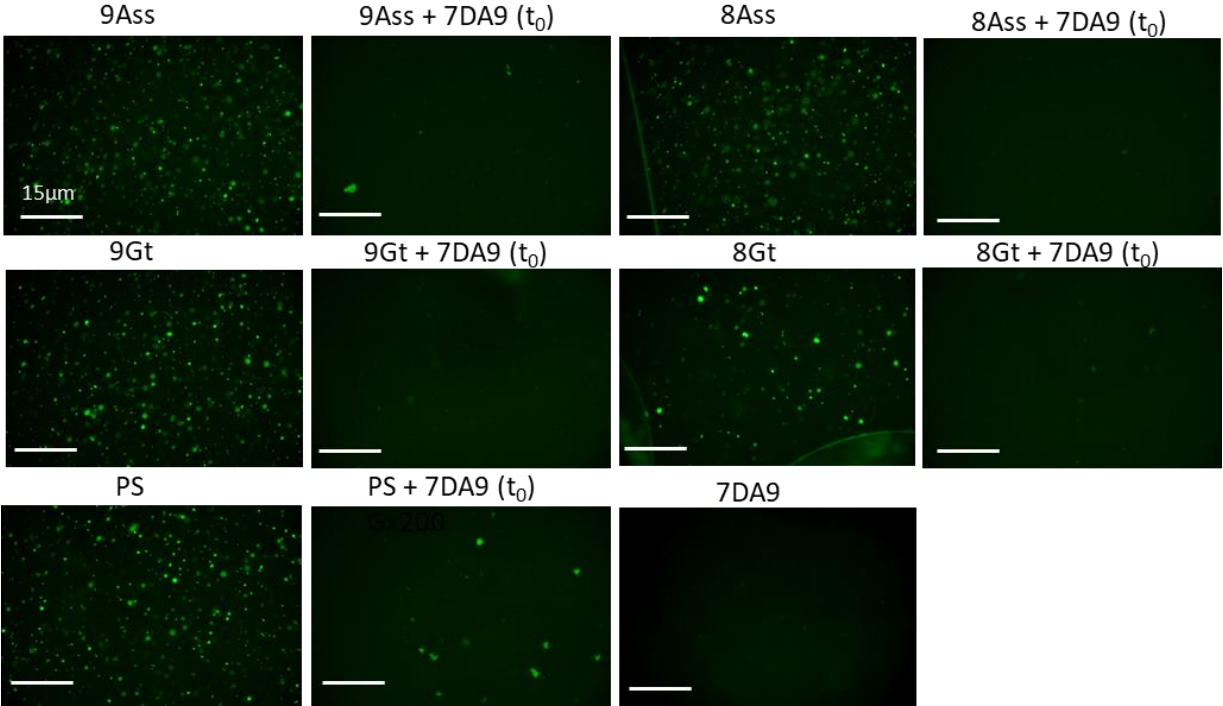


Supplementary Figure 2 | Same figure as Figure 22 with more detailed Proteobacteria groups.

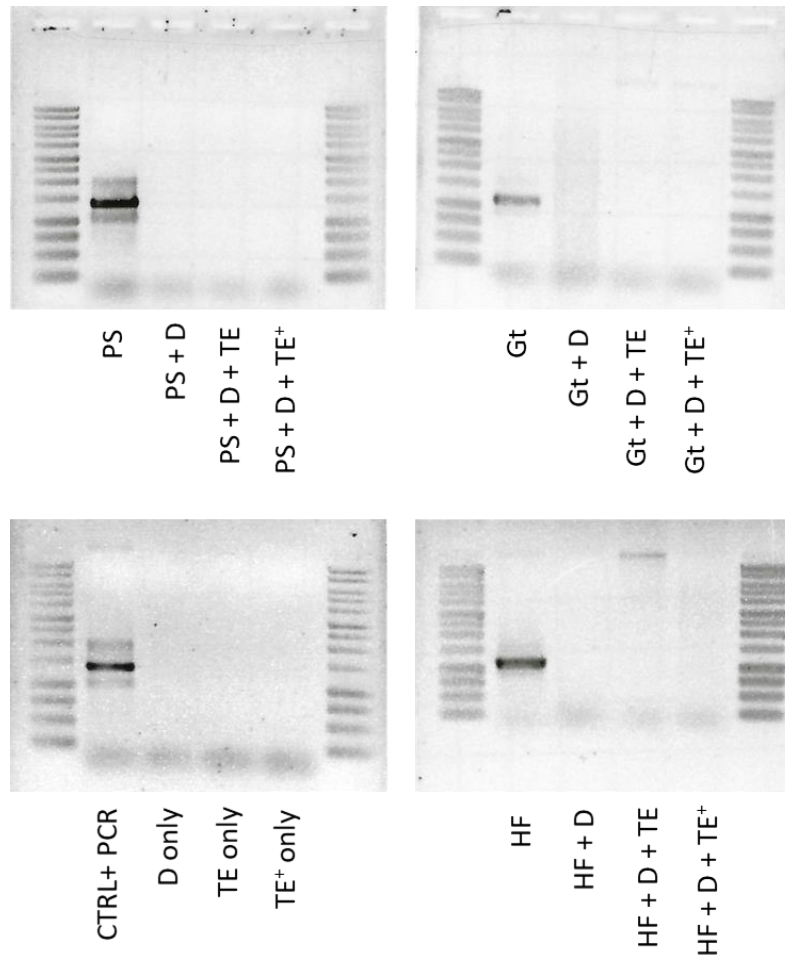


Supplementary Figure 3 | Eukaryotic presence, diversity and relative abundances in bioaerosols in comparison with Lake Assale/Karum, the salt plain and the cave reservoir. \* The "Streptophyta"

sequences found in Lake Karum correspond to unknown micro-eukaryotes according to the SYLVA database and may be Chlorophyta, when BLASTed against nt NCBI database.



**Supplementary Figure 4 | SYTO9 induced DNA epifluorescence of different samples before and after contact (t<sub>0</sub>) with 7DA9. The scale is similar on all images.**



**Supplementary Figure 5 | 16S rRNA gene amplifying test on cell pellets.** From left to right in one gel: positive control (cell pellet only), cell pellet in contact with acidified (pH~0) hypersaline medium (D), cell pellet in contact with D but the acidity have been neutralized with TE or TE<sup>+</sup> solutions (see Materials and Methods). Contact with D only last an instant (for vortex and centrifugation). All supernatant has been removed and pellets diluted in DNA buffer before PCR. CTRL+PCR: PCR positive control. HF: *Haloferax* culture.



***The Western Canyons Lakes***  
***© DEEM Team***

**ARTICLE 3**

## 6. The missing link of the Dallol ecosystems: the Western Canyons Lakes – a permanent, mildly acidic and hypersaline series of ponds

### 6.1 Context and objectives

After we addressed the limits of life along Dallol physicochemical gradients in the previous chapters, we were interested in refining them. The physicochemical conditions between the less polyextreme ecosystems (the salt plain, Lake Karum and the cave reservoir) and the most polyextreme sterile environments (the Dallol ponds, Lake Gaet'ale and the Black Lake) are drastically different, and there are little intermediates with the exception of the unique PS3 sample (an ephemeral hydrothermally influenced water channel in the salt desert). To better define the limits of life in the Dallol area, it would be necessary to fill the gap of the previously studied gradients with samples steadier than PS3 but with similar physicochemical conditions.

Located at the western side of the Dallol dome close to an elevation called the Round Mountain, are bubbling, orange-coloured lakes that resemble Lake Gaet'ale. The salinity of these Western Canyons Lakes is between 34 to 41 % (w/v, total solids) and their pH is around 4.9, fitting the wanted intermediate values of the salinity-acidity gradients. They have been observed from satellites since at least 2003 (see article in progress section 5.3 and Supplementary Figure 6) and were already mentioned by Holwerda and Hutchinson (1968), but to our knowledge had never been investigated. These characteristics make them a much steadier environment to study than the PS3 ephemeral brine that could only be observed once. Their physicochemical conditions and consistency make them good representatives to study potential ecosystems between the less and the most polyextreme environments from our previous study.

We thus established the following objectives to better determine the limits of life in the Dallol surroundings:

1. **Prospect the microbial diversity from five of the Western Canyons Lakes (WCL samples) from plankton filters prepared *in situ*.** After DNA extraction, we PCR-amplified 16S/18S rRNA genes from the microbial communities and used either Sanger or Illumina sequencing on amplicons depending on the primers used and amplicons size. We compared the microbial communities of WCL samples with less polyextreme environments already investigated, which are Lake Karum, the cave reservoir and the salt plain (PS, PS3). New (2019) samples of Lake Karum and the cave were also acquired for this study. Last, we built an archaeal phylogenetic tree with the sequences from all environments harbouring local extremophiles to compare their phylogenetic distribution.

2. **Analyse the physical parameters and the chemistry of the Western Canyons Lakes.**

We added the *in-situ* probe data and the ion chromatography/TXRF data of the WCL and other 2019 brine samples (from Lake Karum, the Cave reservoir, the Dallol hydrothermal ponds and the Black Lake and Lake Gaet'ale) to previous years data to carry out a Principal Component Analysis (PCA) to visualize the chemical variation present in the sample dataset with the elemental variables i.e. how samples cluster together in the PCA depending on their chemical similarities. Another PCA also merging all these samples focused on potentially life-limiting parameters such as temperature, pH, salinity (total solids) and water activity.

3. **Complete the microbial and chemical investigation with SEM observations** of 2019 samples filters (WCL samples, Lake Karum, the cave brine) in order to identify and characterize potential cells, biomorphs and inorganic features with the help of chemical maps/spectra to discriminate them.

The PCA (Figure 28) shows that the chemistry of the Western Canyons Lakes brine is NaCl-dominated as in Lake Karum, the cave and the salt plain (which they cluster with), the sample WCL3 being richest in Ca/Mg salts of WCL samples. From a physicochemical point of view, because they have higher salt concentration, lower pH and water activity than Lake Karum and the cave reservoir, the WCL samples cluster together closer to the limits of life previously established (Belilla et al. 2019).

When normalized and compared with other samples, the proportion of Archaea seems higher in the WCL samples than in less polyextreme samples and PS3 (Figure 28). Within Archaea, phyla composition is very similar within all studied environments: most reads belong to the Halobacteria phylum, followed by Nanohaloarchaeota. However, the Nanohaloarchaeota seem in higher proportion in the WCL samples. A higher proportion of Halobacteria and Nanohaloarchaeota has already been correlated with the increase of salinity in alkaline environments (Ventosa et al. 2015; Menéndez-Serra et al. 2020). Little is known about the effect of acidity gradients on both phyla, but we hypothesize that acidity may also play a role in the changes of phyla proportions. These dynamics may indicate a higher specialization of the Nanohaloarchaeota to the most extreme saline conditions compared to a more versatile behaviour of Halobacteria as suggested by Menéndez-Serra et al. (2020). We suspect the potential symbiotic (Hamm et al. 2019; Cono et al. 2019) or parasitic (section 5.3) lifestyle of Nanohaloarchaeota plays a role in these dynamics.

## 6.2 Results

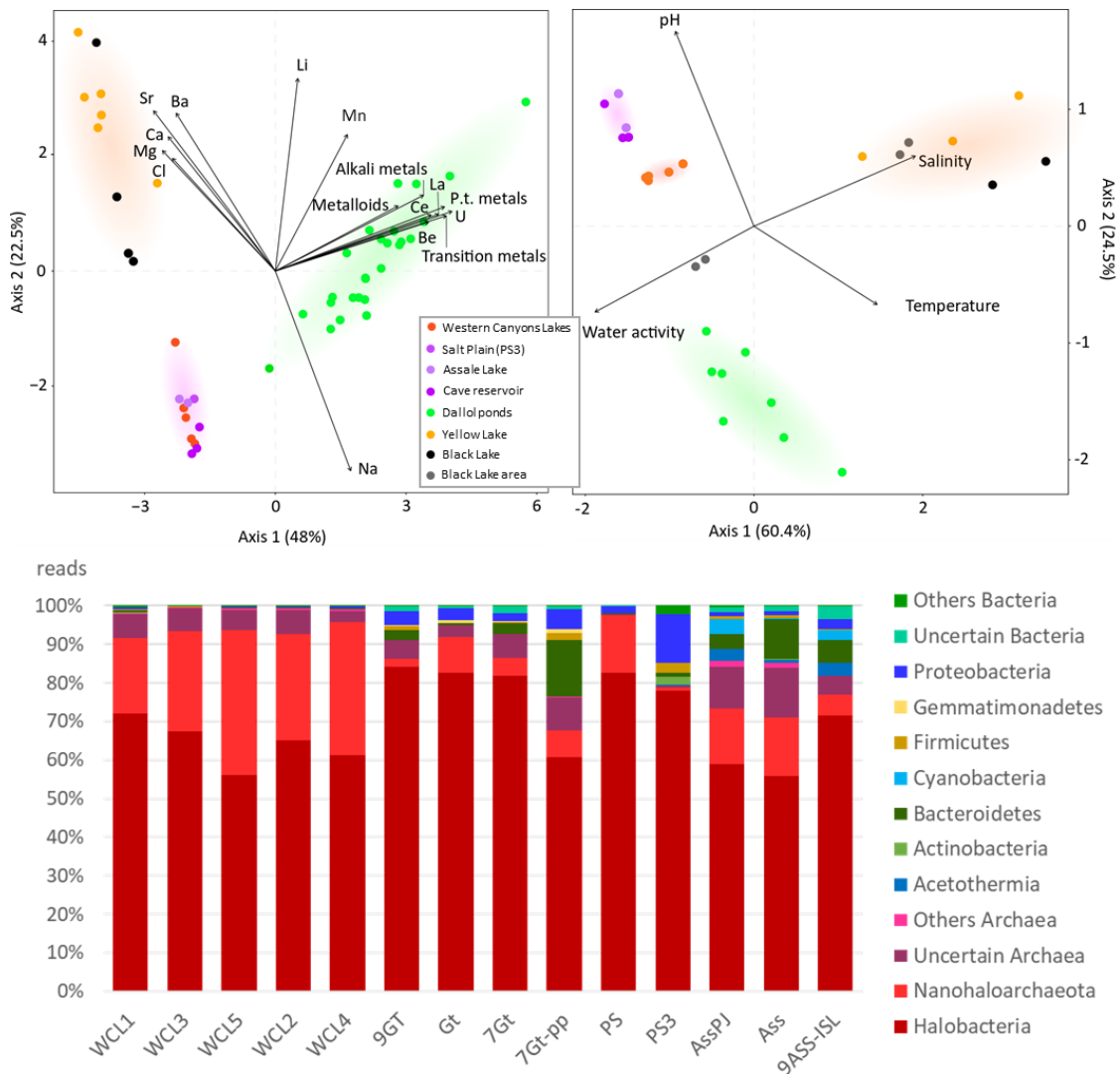


**Figure 28 | Principal component analyses of the chemistry and the physicochemical parameters of the Dallol geothermal system and its surroundings (upper panel) and histogram of the presence/absence and relative proportion of archaea and bacteria in the less polyextreme environments based on 16S rRNA gene metabarcoding (bottom panel).** For samples names' details, see Table 7.

The above results confirm that the WCL samples are closer to the limits of life than the previously studied samples and that their microbial communities structure are substantially different from those of less extreme environments (Lake Karum, the cave reservoir and the salt plain) and PS3. Finding more environments like the Western Canyons Lakes or PS3 would increase the statistical value of these results, and analysing samples closing further the gap between the WCL samples and the limits of life would be important to better delineate those limits. Whole metagenomics study would also help to understand the mechanisms behind the population dynamics along the salinity/acidity gradients.

## 6.3 Manuscript of article

*Article status: in progress*

### **Provisional title:**

- Microbial diversity in the hypersaline and acidic Western Canyons Lakes of the Dallol hydrothermal systems

**Authors:** Jodie Belilla<sup>1</sup>, David Moreira<sup>1</sup>, Karim Benzerara<sup>2</sup>, Guillaume Reboul<sup>1</sup>, Purificación López-García<sup>1</sup>

1. Ecologie Systématique Evolution, CNRS, Université Paris-Sud, Université Paris-Saclay, AgroParisTech, Orsay, France.

2. Institut de Minéralogie, de Physique des Matériaux et de Cosmochimie, CNRS, Sorbonne Université, Muséum National d'Histoire Naturelle, Paris, France.

### **Abstract**

The protovolcanic Dallol dome area (Afar region, Ethiopia) exhibits a unique collection of hydrothermal manifestations in a hypersaline context, with a wide array of combined extreme physicochemical settings, from neutral hypersaline water to acidic hot brine with different salt compositions. Along these gradients, we had previously identified a very large diversity of Halobacteria and Nanohaloarchaeota only in the less polyextreme places (30% salinity and  $\text{pH} \sim 6$ , with the exception of one ephemeral site at  $\text{pH} 4.2$ ), while no trace of endemic life was discovered in the most polyextreme sites (either because of their high chaotropicity/water activity, and/or  $\text{pH} < 0$  combined with high salinity). Nevertheless, the lack of stable sites with intermediate conditions between the less and most polyextreme environments of the Dallol area was an issue to discern with precision the limits of life. Recently, we accessed a series of lakes at the western side of the Dallol dome (the Western Canyons Lakes) with the required intermediate parameters ( $\text{pH} \sim 5$  and NaCl-dominated salinity 34-41%). We show in this study that these lakes host a diverse microbial life mostly dominated by Archaea, with a higher proportion of Nanohaloarchaeota than in the previously studied Dallol ecosystems. These results suggest an unsuspected correlation between the Nanohaloarchaeota and increasing acidity in hypersaline systems, that may be linked with their symbiotic lifestyle.

### 6.3.1 Introduction

Environments displaying a combination of low pH and high salinity are scarce around the world, limiting the investigation of the microbial communities potentially inhabiting them. Western Australia hosts a series of lakes that display pH values as low as 1.5 and salinity concentrations as high as 32% with high seasonal variability (flooding, evapoconcentration, desiccation). Some metabarcoding studies describing the microbial diversity of those lakes focused on sediments or solid samples, which seemed to be dominated by Bacteria (Johnson

et al. 2015); other used only bacterial-specific 16S rRNA gene primers (Mormile, Hong, and Benison 2009). Whole metagenomic shotgun analysis of one of these lakes (Lake Magic, pH 1.7) surprisingly did not reveal Archaea in the lake water and only a small proportion in the groundwater around it. The most dominant domain was Eucarya, followed by Bacteria (Zaikova et al. 2018). The results were unexpected since in (hyper)saline or (hyper)acidic situations, the best-adapted microorganisms are usually Archaea (see section 1.2.1). In the arid Central Andean high plateau of Chile, the salt flats of Gorbea and Ignorado display strongly acidic brines (pH 1-4.7) (Escudero et al. 2013). Their chemical composition shows high concentrations of sodium (up to 2479 mM), magnesium (up to 1549 mM) and chlorine (up to 4291 mM). The microbial diversity found in these salt flats was very low during the several years of survey. Eukaryotes were not investigated but both Archaea and Bacteria were detected although their relative proportions were not determined. Within Archaea, Halobacteria (especially *Halococcus*) and Thermoplasmata were the dominant phyla, while within Bacteria the phyla Firmicutes and Betaproteobacteria were predominant.

In the salt desert of the Danakil depression (Afar region, Ethiopia), the Dallol geothermal dome and its surroundings encompass a wide array of polyextreme lakes and hydrothermal ponds, exhibiting rare combinations of hypersalinity (20 to >50%), low pH (<1 to 6.0) and high temperature (up to 110 °C). In the less polyextreme environments, including transitory active ponds in the salt plain, Lake Karum and the salt canyons' cave reservoir, we previously identified a very wide diversity of Archaea, mainly composed of Halobacteria and Nanohaloarchaeota (Belilla et al. 2019). In contrast, no trace of life was discovered in the most polyextreme places such as the Dallol hydrothermal ponds, Lake Gaet'ale and the Black Lake, likely because their chemistry is not compatible with microbial life (high chaotropicity, potential presence of sterilizing chemical compounds) and/or because there is no organism adapted to the combination of extreme salinity and extreme acidity (Belilla et al. 2019). This is consistent with the fact that microorganisms thriving at conditions of both very low pH (<1) and high salinity (>20%) have never been cultured (Harrison et al. 2013). Nevertheless, the significant gap of physicochemical parameter values between the less and the most polyextreme samples made it difficult to set a precise limit of life. Only one ephemeral hydrothermally-influenced water pond (PS3) in the salt desert showed intermediate values (35% salinity and pH 4.2) and was also largely dominated by Archaea (Belilla et al. 2019). To better pinpoint the limits of life in these hypersaline acidic sites, additional stable environments with intermediate physicochemical values need to be studied.

In our last expedition (January 2019) we sampled a series of small lakes that we named the Western Canyons Lakes (WCL) due to their location close to little salt canyons (from the Round Mountain) at the west side of Dallol. These lakes have pH values <5 and a salinity between 30 and 45%. They show a hydrothermal activity with intense constant gas bubbling. They were already mentioned by Holwerda and Hutchinson in 1968 and can be observed in satellite images since at least 2003, indicating that they are stable systems (Supplementary Figure 6). The WCL have higher salinity and acidity than the most extreme places where we previously detected life in Dallol (Belilla et al. 2019). Therefore, these lakes are ideal systems

to test if life has adapted to more saline and acidic conditions, and what kind of microorganisms we can expect. Here, we applied environmental 16S/18S rRNA gene metabarcoding and scanning electron microscopy (SEM) combined with chemical analyses to explore these systems.

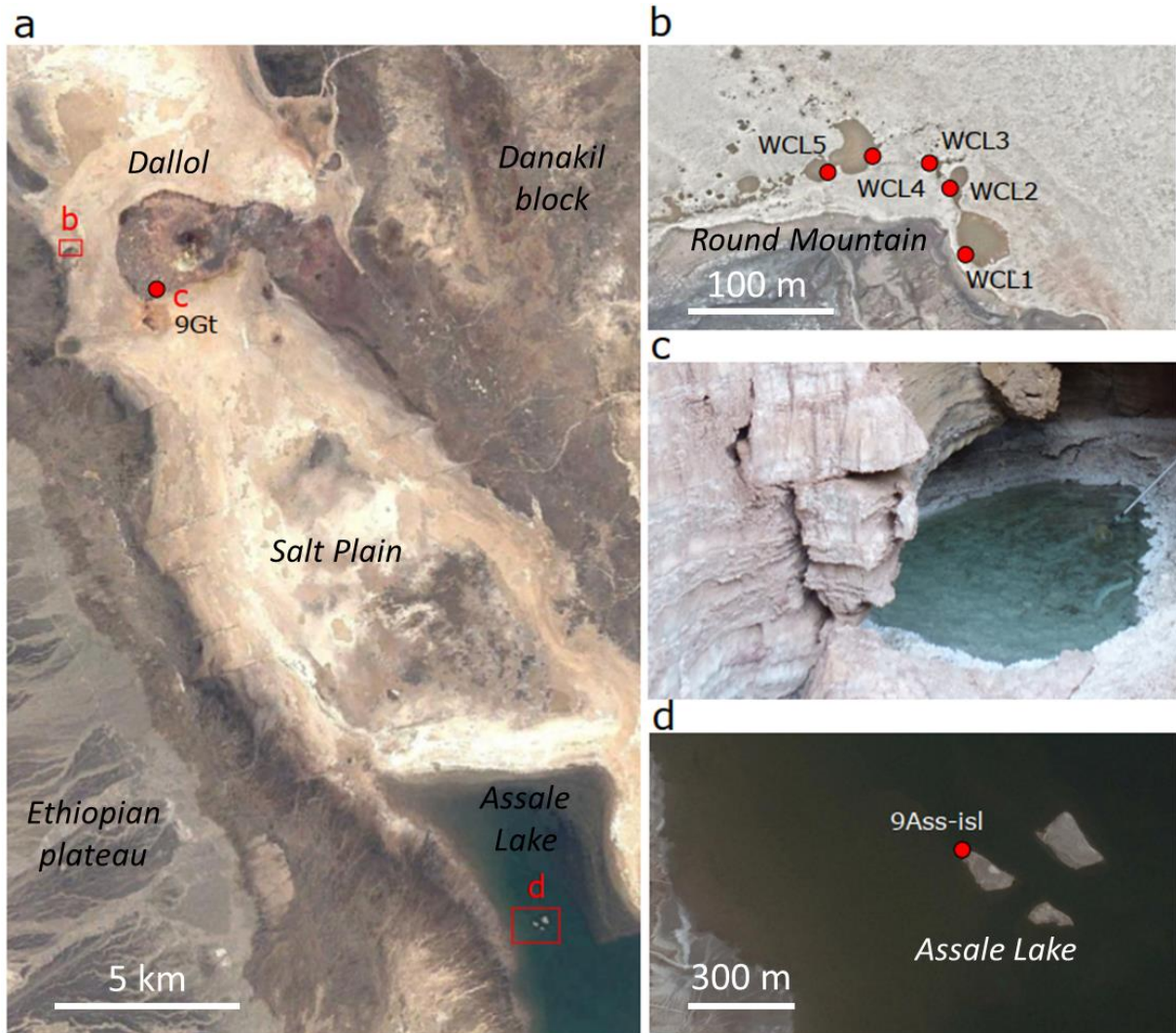


**Figure 29 | Localisation of the sampling sites of this study.** **a**, Position of the three sampling areas in the Danakil depression. **b**, Detail of the Western Canyons Lakes sampling sites. **c**, The cave reservoir (with the sampling pole for scale). **d**, The islands in the middle of Lake Karum. The dots indicate the localisation of each sample and their name. Satellite pictures from CNES and distributed by Google Earth. North always face the top of satellite pictures.

**Table 7 : Samples from the Dallol area analysed in this study and type of analyses performed. Refractometry-derived salinity refers to the percentage (w/v) of salt measured in situ. Salinity was also measured by weighting the total solids after water evaporation (dry weight measured in triplicates). TS: total solids, SD: standard deviation, n.d: not determined.**

	Coordinates	Collection date	Brief description	Color	Temp (°C)	pH	ORP (mV)	Physicochemical parameters		
								Refractometry Inferred salinity (%)	Salinity - TS (g/l) ± SD	Water activity
<b>Western Canyons Lake</b>										
WC11	14°14'29.44"N 40°16'1.99"E				29.33	4.85	165.43	30	404.133 ± 20.16	0.719
WC12	14°14'30.89"N 40°16'4.71"E				29.2	5.07	164.6	35	338.67 ± 35.46	0.716
WC13	14°14'31.70"N 40°16'4.27"E	18.01.2019	Hypersaline hydrothermal (bubbling) lakes close to the western part of the salt canyons		30.50	4.93	130	n.d	412.53 ± 18.29	0.69
WC14	14°14'32.00"N 40°16'2.89"E				29.1	4.97	132.4	35	346.03 ± 4.20	0.726
WC15	14°14'31.60"N 40°16'1.79"E				29.30	5.1	119.8	32	337.83 ± 11.69	0.725
<b>Assale/Karum lake</b>										
9A52	14° 3'13.13"N 40°22'51.97"E	23.01.2019	Water from Lake Assale (Karum), island in the middle-west of the lake		30.60	6.70	184.30	29.00	302.27 ± 4.76	0.771
<b>Salt canyon's cave brine</b>										
9G1	14.239704N 40.289952E	13-16.01.2019	Cave hypersaline water reservoir at the salt canyons, West Dallol dome		25.50	5.94	240.30	30.00	335.27 ± 5.46	0.725
<b>Dallol dome</b>										
DAL4-5	14.23916N 40.297059E	17.01.2016	Yellow salt crust from inside the closest pond of a chimney hydrated with sterile milliq. water in the lab		n.d	n.d	n.d	n.d	n.d	n.d
7DA13-W2	14.235495N 40.298135E	11.01.2017	Brine from the closest pond to a grey hydrothermal chimney		50.2	0.43	323.8	35	n.d	n.d
9DA1B	14°14'13.94"N 40°17'53.57"E		Large cool pond		27.7	-0.79	386.4	38	n.d	n.d
9DA2B	14°14'14.04"N 40°17'49.05"E		Hydrothermal fluid collected directly from the chimney		109.1	n.d	n.d	n.d	n.d	n.d
9DA2C			Hydrothermal fluid collected directly from the chimney		108.6	n.d	n.d	n.d	n.d	n.d
9DA3A			Brine from the closest pond to a field of hydrothermal chimneys		53.5	-0.28	236.2	39	n.d	n.d
9DA3B		14.01.2019	Pond a bit below 9DA3A and further from the chimneys		30.1	-0.54	247.6	39	n.d	n.d
9DA3C	14°14'20.69"N 40°17'47.75"E		Pond a bit below 9DA3B and further from the chimneys		29.9	-0.56	358.2	39	n.d	n.d
9DA3D			Pond a bit below 9DA3C and further from the chimneys		29.4	-0.65	386.2	42	n.d	n.d
9DA3E			Pond a bit below 9DA3D and further from the chimneys		30	-0.91	400.3	45	n.d	n.d
9DA3G			Brine from a green-blue pond under salt crust		34.4	-0.43	219	35	n.d	n.d
<b>Yellow Lake</b>										
9YL	14.213574N 40.31228E	17.01.2019	The Lake seems to shallow with years. Brine from surface.		n.d	n.d	n.d	n.d	n.d	n.d
<b>Black Lake</b>										
9BL	14.22182N 40.286208E	17.01.2019	Black lake bischofite-rich brine (surface)		74.4	2.7	n.d	n.d	n.d	n.d

### 6.3.2 Results and Discussion

The western part of the Dallol dome is composed of anhydrite-covered halite salt canyons. Further to the west, the Round Mountain constitutes a small relief on the Salt Plain that has the same geological structure as the Dallol dome salt canyons (López-García et al. 2020). During a recent expedition in January 2019, we explored a series of small lakes on the north of the Round Mountain, which we named the “Western Canyon Lakes” (WCL) (Figure 29-a,b, Supplementary Figure 7-a-d). They showed intense hydrothermal activity, in the form of numerous chimneys with constant bubbling of gas, likely CO<sub>2</sub> (Holwerda and Hutchinson 1968). We sampled 5 of these lakes (WCL1 to WCL5) and measured *in situ* pH values ~5 and salinity values from 30 to 45% (Table 7). We filtered water from the five lakes through 0.2 μm filters and also collected water samples for chemical analyses. We also collected additional samples from the Lake Karum (9Ass, collected for the first time from the middle of the lake, Figure 29-a,d; Supplementary Figure 7-e,f) and the cave reservoir of the salt canyons (9Gt) (Figure 29-a-c). Despite the absence of life in these places (Belilla et al. 2019), we also collected several brine samples from hydrothermal chimneys and ponds of the Dallol dome, Lake Gaet’ale and the Black Lake to generate additional chemistry data (Supplementary Figure 7-g-l). The complete list of samples from this study is given in Table 7 and information about samples from previous years can be found in Belilla et al. (2019).

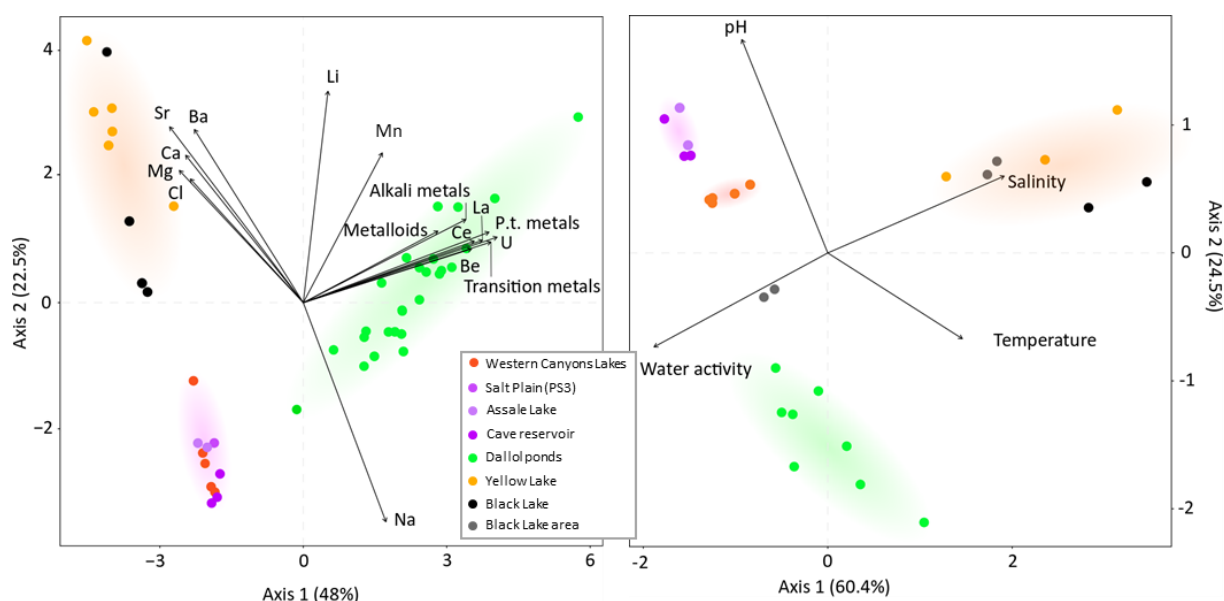


**Figure 30 | Principal component analyses of liquid samples.** Analysis of 46 samples according to their chemical composition (left); analysis of 27 samples according to potentially life-limiting physicochemical parameters (right). Coloured zones in the PCA analyses highlight the groups of related samples. A detailed PCA with sample names and unmerged variables is given in Supplementary Figure 8.

Principal component analysis (PCA) of the chemical data shows that samples clustered in three major groups according to their elemental composition (Figure 30 and Supplementary Figure 8). The NaCl-saturated, iron and other heavy metal-rich Dallol ponds clustered together

as previously seen (Belilla et al. 2019). These Dallol samples were organized along a linear repartition from younger ponds, with more diluted salts and unoxidized, to older ones, more evaporated and with a higher concentration of oxidized iron and other heavy metals (Belilla et al. 2019; Kotopoulou et al. 2019). The Black Lake and Lake Gaet'ale are also clustered together because of their high concentration of  $Mg^{2+}$  and  $Ca^{2+}$  salts (>50%) which are responsible for their high chaotropicity, ionic strength and low water activity, thought to be limiting factors for life (Hallsworth et al. 2007; Stevenson et al. 2015 and 2017; Belilla et al. 2019). Even though the Western Canyons Lakes' yellowish colour resembled the one of Lake Gaet'ale, the chemical analysis showed that they are NaCl-dominated and more closely similar to the less polyextreme sites. Only the WCL3 sample, which comes from the most evaporated lake of the series, showed higher  $Mg^{2+}$  and  $Ca^{2+}$  concentrations. In the PCA based on physicochemical data (temperature, pH, salinity and water activity) (Figure 30), the clusters were similar except this time the WCL samples were clearly separated from the other less polyextreme samples (Lake Karum and the cave reservoir) and were positioned closer to the Dallol, Lake Gaet'ale and Black Lake clusters. This is explained by their higher salt concentrations, more acidic pH and slightly lower water activity.

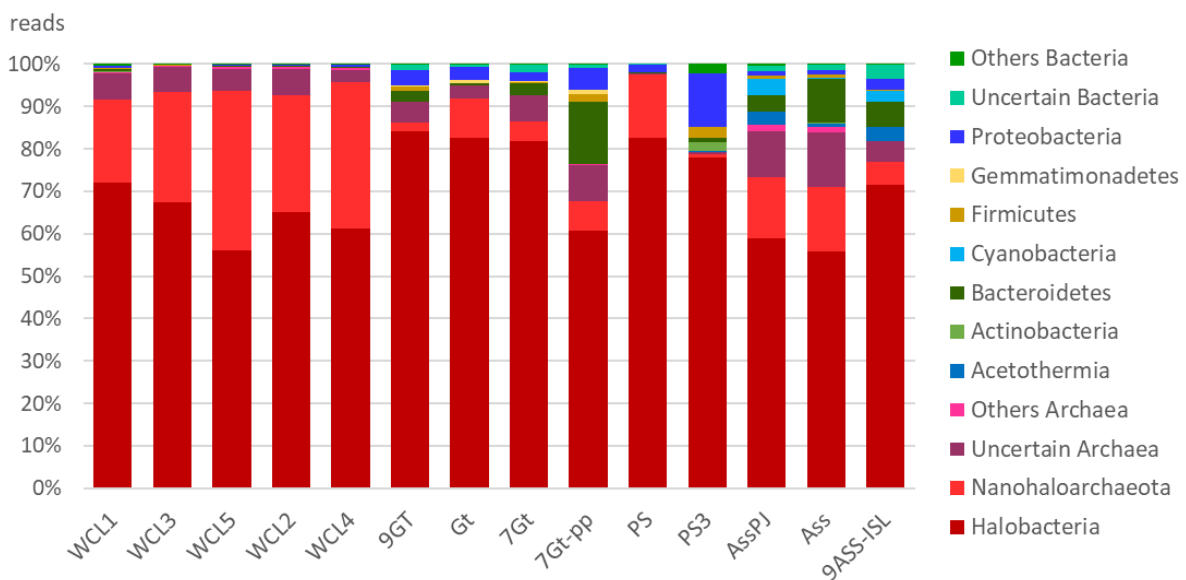


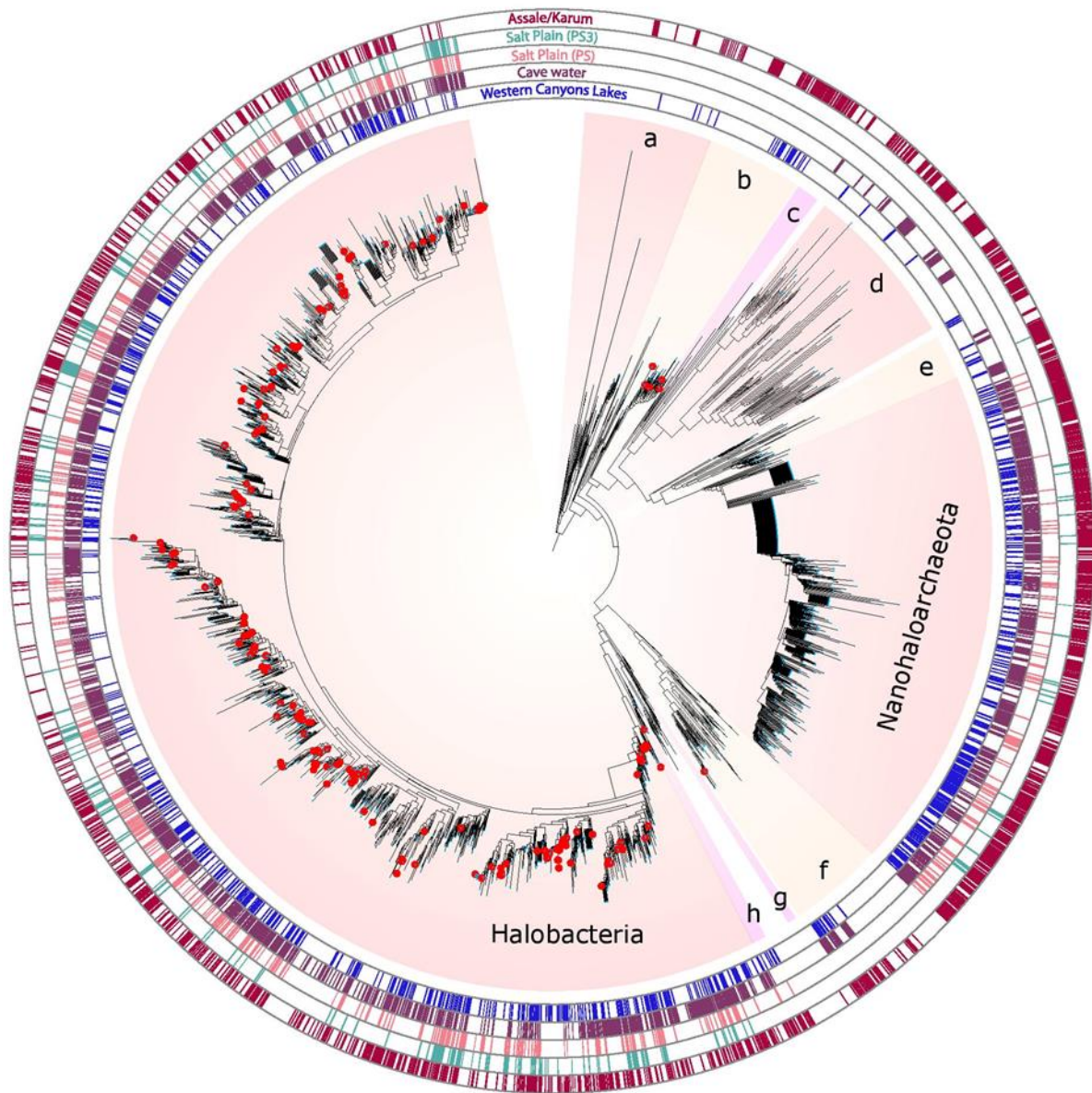
**Figure 31 | Presence/absence and relative proportion of archaea and bacteria in the Western Canyons Lakes, the cave brine, the salt plain and Lake Assale/Karum based on 16S rRNA gene metabarcoding.**

To describe the potential microbial diversity present in these physicochemically intermediate lakes, we filtered water through 0.2  $\mu m$  filters and purified DNA to carry out 16S/18S rRNA gene-based studies by high-throughput short-amplicon sequencing (metabarcoding approach). We also applied this procedure to new samples from the Lake Karum/Assale (9Ass) and the Western Canyons cave reservoir (9Gt). We also amplified and Sanger-sequenced almost full-length 16S/18S rRNA genes from clone libraries to obtain longer reference sequences for more accurate phylogenetic analyses. For comparison, we also

included sequences from our previous study of the Lake Karum, cave reservoir and Salt Plain (Belilla et al. 2019). All samples, including the WCL ones, were dominated by Archaea, with Halobacteria being the most abundant phylum, followed by Nanohaloarchaeota. This was particularly remarkable in the WCL lakes, almost completely dominated by Archaea ( $99.1\pm 0.5\%$  of reads abundance), compared with the other ecosystems ( $88.8\pm 8.4\%$  for the cave reservoir,  $84.2\pm 2\%$  for Lake Karum and  $79.3\%$  for the hydrothermally influenced salt plain PS3) and even richer than the community from a diluted evaporite from the salt plain (PS,  $97.9\%$ ). Another important difference was that the WCL showed a greater proportion of Nanohaloarchaeota ( $29.3\pm 7.1\%$  of total prokaryotic reads versus 1-15% for the others). Higher proportions of Archaea, including Nanohaloarchaeota, have been correlated with increasing salinity in soda lakes (Ventosa et al. 2015; Menéndez-Serra et al. 2020). Little is known about the effect of the acidity gradient on Halobacteria and Nanohaloarchaeota, but we suggest acidity may also accentuate the microbial communities' change observed. A higher preference of the Nanohaloarchaeota for the most extreme saline conditions compared to the more versatile Halobacteria, was suggested by Menéndez-Serra (2020). We suggest that it is because of the possible symbiotic lifestyle of Nanohaloarchaeota. Indeed, studies have suggested that the Nanohaloarchaeota are not free-living organisms but potential mutualistic symbionts (Hamm et al. 2019; Cono et al. 2019) or parasites (section 5.3) of Halobacteria. In the case of a mutualistic lifestyle, the higher proportion of Nanohaloarchaeota at the most extreme conditions may suggest that the association of both partners (haloarchaea and nanohaloarchaea) is more resistant than the host alone. In the case of a parasitic lifestyle, it would be possible that the rise of acidity and salinity may weaken the host and increase the parasite prevalence. Future metagenomic and metaproteomic studies and, ideally, cultivation of these organisms will help to understand their biological interactions and their adaptations to these polyextreme conditions.

In addition to the dominant Halobacteria and Nanohaloarchaeota, the diversity found in our samples virtually spans all along the archaeal tree as in our previous study (Belilla et al. 2019). Notably, we found lineages typically present in hypersaline environments (e.g., Methanonatronoarchaeia and Candidate Division MSBL1) but also lineages not specifically associated with hypersaline systems, including Thermoplasmata, Woesearchaeota, Archaeoglobi, Aenigmarchaeota, Altiarchaeales, Thaumarchaeota and Crenarchaeota (Figure 32). As in our previous study, Lake Karum contained the greatest archaeal diversity of all ecosystems. The Western Canyons cave reservoir also hosted a rich diversity of archaea, in contrast with the two Salt Plain samples, PS and PS3, with much-reduced diversity, especially in the case of PS3 (an ephemeral hydrothermally-influenced water pool) that contained the lowest diversity of all areas. This reduced diversity could be related to the abrupt changes of physicochemical conditions that the salt plain undergoes by recurrent flooding, desiccation and temporary hydrothermal influence, which may select only the most versatile organisms. The WCL hosted very diverse archaea, quite different from those in the salt plain and the cave reservoir, especially regarding phyla apart from the Halobacteria and Nanohaloarchaeota.

Interestingly, all WCL OTUs are branched within phyla that are also present in Lake Karum (Figure 4). In fact, 83% of WCL OTUs are shared with Lake Karum. This suggests that these OTUs might be able to thrive in the two different physicochemical conditions. The differences between the Dallol area ecosystems may be better explained by the relative abundance of reads rather than their OTU distributions.



- |                             |                          |
|-----------------------------|--------------------------|
| a. Proteoarchaeota          | e. Aenigmarchaeota       |
| b. Candidate division MSBL1 | f. Thermoplasmata        |
| c. Altiarchaeales           | g. Archaeoglobi          |
| d. Woesearchaeota           | h. Methanonatronarchaeia |

**Figure 32 | Phylogenetic tree of archaeal 16S rRNA gene sequences showing the phylogenetic placement of archaeal OTUs identified in the different samples.** Concentric circles around the tree indicate the presence/absence of the corresponding OTUs in the different sampling sites. Longer sequences derived from cloning and Sanger sequencing of environmental samples, cultures and FACS-sorted cells are labelled with red dots.

Eukaryotic 18S rRNA gene amplicons could only be obtained from WCL2 and WCL4, using semi-nested PCR, and from 9Ass, using direct PCR. No amplicons could be obtained from 9Gt and the other WCL samples. Some of the eukaryotic sequences retrieved most likely corresponded to airborne or human contamination (e.g. land plants/fungi, and human's associated microbes). The remaining, likely autochthonous eukaryotic microorganisms were dominated by primary producers, such as the halophilic *Dunaliella* (Chlorophyta) (Supplementary Figure 9). Halophilic ciliates (possibly *Fabrea*) and bicosoecids (*Halocafeteria*) could also be found in smaller proportions, though the latter was absent from the more extreme WCL samples.

In addition to metabarcoding analysis, we further explored the biotic and abiotic features present in the WCL samples using scanning electron microscopy (SEM, see Figure 33). One of the most common objects observed were cocci-like aggregates, which we infer to be abiotic biomorphs because of both their small size ( $\leq 100$  nm, too small for a cell) and their inorganic chemical composition, mostly silicates (Figure 33-d,g), sometimes enriched with iron, which may play a role in the orange colour of the WCL brines. We also observed numerous almond-shaped calcium carbonate ( $\text{CaCO}_3$ ) particles that appear to be composed of aragonite (Figure 33-a,b,i) (Blue et al. 2017; González-López, Fernández-González, and Jiménez 2018). Some gypsum fragments were also visible (Figure 33-h). Although gypsum may come from the erosion of the gypsum deposits of the Round Mountain (López-García et al. 2020), gypsum precipitation has been reported in some saline acidic lakes (Escudero et al. 2013; Zaikova et al. 2018), but not aragonite which, in principle, should be inhibited by the acidic pH of the WCL lakes. Aragonite precipitates, though, along with gypsum under hypersaline alkaline conditions such as in the Dead Sea (Golan et al. 2017), which is at the origin of the Danakil salt plain. It is possible that the aragonite and part of the gypsum observed in our samples come from the underneath lacustrine deposits of the ancient Lake Afrera that covered the Danakil depression (López-García et al. 2020), which may have been partially dissolved by the acidic hydrothermal fluids that emerge in many places of the depression. It is even possible that the dissolution of calcium carbonate makes the brine less acidified than it would be without contact with the underneath bedrock. The dissolution reaction may participate to the  $\text{CO}_2$  venting already suspected by Holwerda and Hutchinson (1968), in agreement with the chromatography results that revealed a very intense peak at 1.43 mins of retention time with  $m/z$  44 (that could correspond to  $\text{CO}_2$  or another gas of the same weight (not included in this manuscript, but may be available in the final version of this article). We cannot exclude that other (bio)geochemical processes intervene (including microbial activity) and favour local precipitation of aragonite and/or gypsum. In addition to these diverse mineral precipitates, we also observed small to ultrasmall cocci ( $\sim 0.5$   $\mu\text{m}$ ), either solitary or grouped, which most likely correspond to Nanohaloarchaeota, particularly abundant in the WCL lakes (Figure 33-a-c,e-f). Cells of similar shape and size had already been observed in the cave reservoir and the salt plain (Belilla et al. 2019).

This work has shown that the WCL have physicochemical conditions in-between the previously described less polyextreme, life-harboring ecosystems (Lake Karum, the salt plain and the cave reservoir) and most polyextreme, lifeless sites (Dallol hydrothermal ponds, Gaet'ale Lake and Karum Lake). Despite their more extreme characteristics, these WCL lakes are inhabited by a large variety of microorganisms, almost completely dominated by very diverse archaea, which further extend the limits of life under polyextreme, saline and acidic, conditions of the Dallol area. New investigations of other even more extreme, environments, such as some known hypersaline acidic lakes in Chile and Australia and, potentially, many other lakes in the Danakil depression, will help to bridge the gap still existing between the WCL lakes and the most extreme sterile environments in Dallol. Metagenomic, metatranscriptomic and/or metaproteomic studies will also help understand how microorganisms adapt to these harsher polyextreme conditions.

### 6.3.3 Materials and methods

#### 6.3.3.1 Sample collection and *in-situ* physicochemical parameters measures

The samples listed in Table 7 were collected during a field trip to the Danakil depression in January 2019 (when air temperature rarely exceeded 40–45 °C). All sampling points and mapping data were georeferenced using a Trimble® handheldGPS (JunoSB series) equipped with Environmental Systems Research Institute software ArcPad® 10. Samples were collected from three major areas: 1) the Western Canyons Lakes (WCL samples); 2) the salt canyons cave reservoir (9Gt samples); and 3) the Lake Assale/Karum (9Ass samples) island that we accessed by helicopter. Water samples (5 to 14 litres for Lake Karum and the Western Canyons Lakes, and 25 litres for the cave reservoir) were prefiltered through 30-µm pore-diameter filters to remove large particles and sequentially filtered through 0.22-µm pore-diameter filters (Whatman). Filters retaining 0.2–30 µm particles were fixed in 2-ml cryotubes with absolute ethanol (>80% final concentration). Back in the laboratory, ethanol-fixed samples were stored at –20 °C until use. Brine samples for chemical analyses were collected in 50-ml glass bottles after prefiltration through 0.22-µm pore-diameter filters. Bottles were filled to the top and sealed with rubber stoppers to prevent the (further) oxidation of reduced fluids. A few additional liquid samples were collected for chemical analysis also from the Dallol hydrothermal ponds, Lake Gaet'ale and the Black Lake. Physicochemical parameters were measured *in situ* with a YSI Professional Series Plus multiparameter probe up to 70 °C and with a Hanna HI93530 temperature probe (working range –200/1,000 °C) and a Hanna HI991001 pH probe (working pH range –2.00/16.00) at higher temperatures. Salinity was measured *in situ* with a refractometer on 1/10 dilutions in MilliQ water.

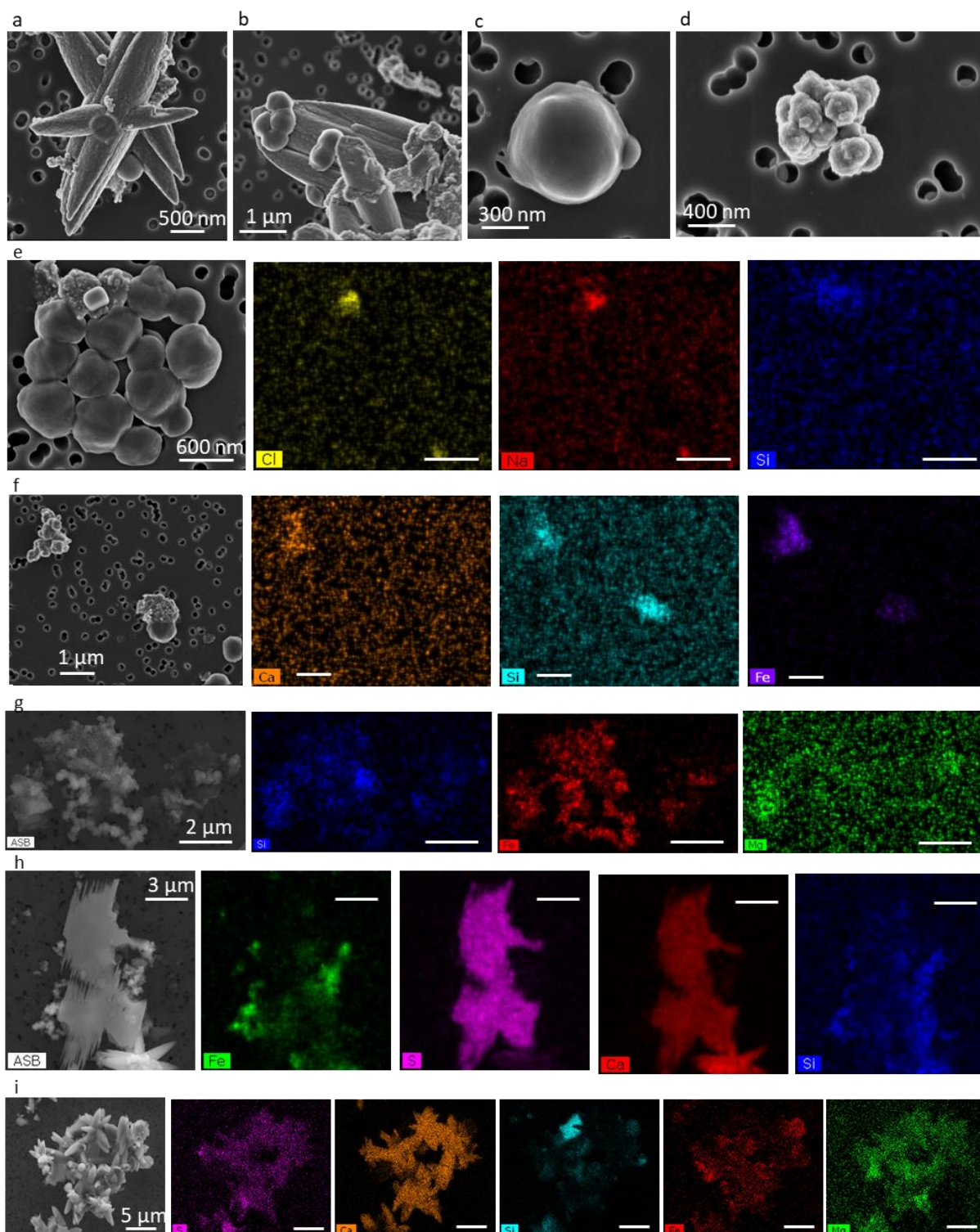


**Figure 33 | SEM pictures and chemical maps of cells and abiotic biomorphs identified in the Western Canyons Lakes brine. a-b,** Cells on minerals resembling aragonite that are common in WCL samples. **c,** Close picture of a solitary cell. **d,** Close picture of round-shaped silicate biomorphs that are also common in WCL. Pictures **e-i** present the area of interest on the left and associated chemical maps on the right. The brighter the colour on the chemical maps, the higher the concentration of the concerned element. **e,** A group of cells. **f,** Cells and biomorphs similar to (d). **g,** More of the round-shaped biomorphs. **h,** Gypsum fragments. **i,** Spiked calcium carbonate minerals (possibly aragonite).

### *6.3.3.2 Chemical analyses, water activity and salinity estimations*

The chemical composition of 0.2- $\mu\text{m}$  prefiltered brine samples was analysed at SIDI Service (Servicio Interdepartamental de Investigación, Universidad Autónoma de Madrid). Major and trace elements in liquid samples were analysed by total reflection X-ray fluorescence with a TXRF-8030c FEI spectrometer and inductively coupled plasma–mass spectrometry using a Perkin–Elmer NexION 300XX instrument. Ions were analysed using a Dionex DX-600 ion chromatography system. Organic molecules were characterized using a Varian HPLC–diode array detector/FL/LS liquid chromatograph. Salinity (weight/volume, expressed in percentage throughout the manuscript) and water activity were measured as described in (Belilla et al. 2019). We used R-software (R Development Core Team 2017) packages FactoMineR (Lê, Josse and Husson, 2008) and factoextra (Kassambara and Mundt 2017) to carry out principal component analyses of samples.

### *6.3.3.3 DNA purification and 16S/18S rRNA gene amplification, sequencing and analysis*

DNA purification from filters, concentration measurement and PCR reactions were performed as previously described (Belilla et al. 2019). No nested PCRs were needed to obtain 16S rRNA gene amplicons. Amplicons were sequenced with Illumina MiSeq (2x300 bp). The raw reads obtained were pooled with reads previously obtained from 2016-2017 samples of Lake Karum, the salt canyons cave reservoir and the salt plain prior to be assembled and clustered into OTUs at 95% identity. In parallel, we tried to amplify near-complete 16S/18S rRNA gene fragments (~1,400–1,500 bp) using combinations of archaea-specific primers as previously described. Phylogenetic tree construction and visualisation were processed as previously described (Belilla et al. 2019).

### *6.3.3.4 Scanning electron microscopy (SEM) and elemental mapping*

SEM analyses were carried out on liquid brine samples that were deposited onto 0.1  $\mu\text{m}$  pore-diameter filters (Whatman) coupled with a vacuum aspiration regime and briefly rinsed with 0.1- $\mu\text{m}$  filtered and autoclaved MilliQ water under the same vacuum regime. Filters were vacuum-dried briefly and stocked within dry atmosphere until they were sputtered with carbon for SEM observations. SEM observations occurred as described in (Belilla et al. 2019)

## **Acknowledgements**

We are grateful to Olivier Grunewald for co-organizing the Dallol expeditions, documenting field research and providing drone images and Frederic Paulsen for funding the 2019 field trip. We thank Luigi Cantamessa for the *in situ* logistics. We acknowledge Dr. Makonen Tafari (Mekelle University), Abdul Ahmed Aliyu and the Afar authorities for local

assistance as well as the Afar police for providing security. We thank Jacques Barthélémy for help during the field trip. We thank Paola Bertolino; Jonathan Huc and Ulysse Tuquoi for punctual help with the experiments and Maria Ciobanu for technical advice. We thank Guillaume Reboul, Ana Gutierrez and Fabian van Beveren for punctual help with the sequence treatment.

## References

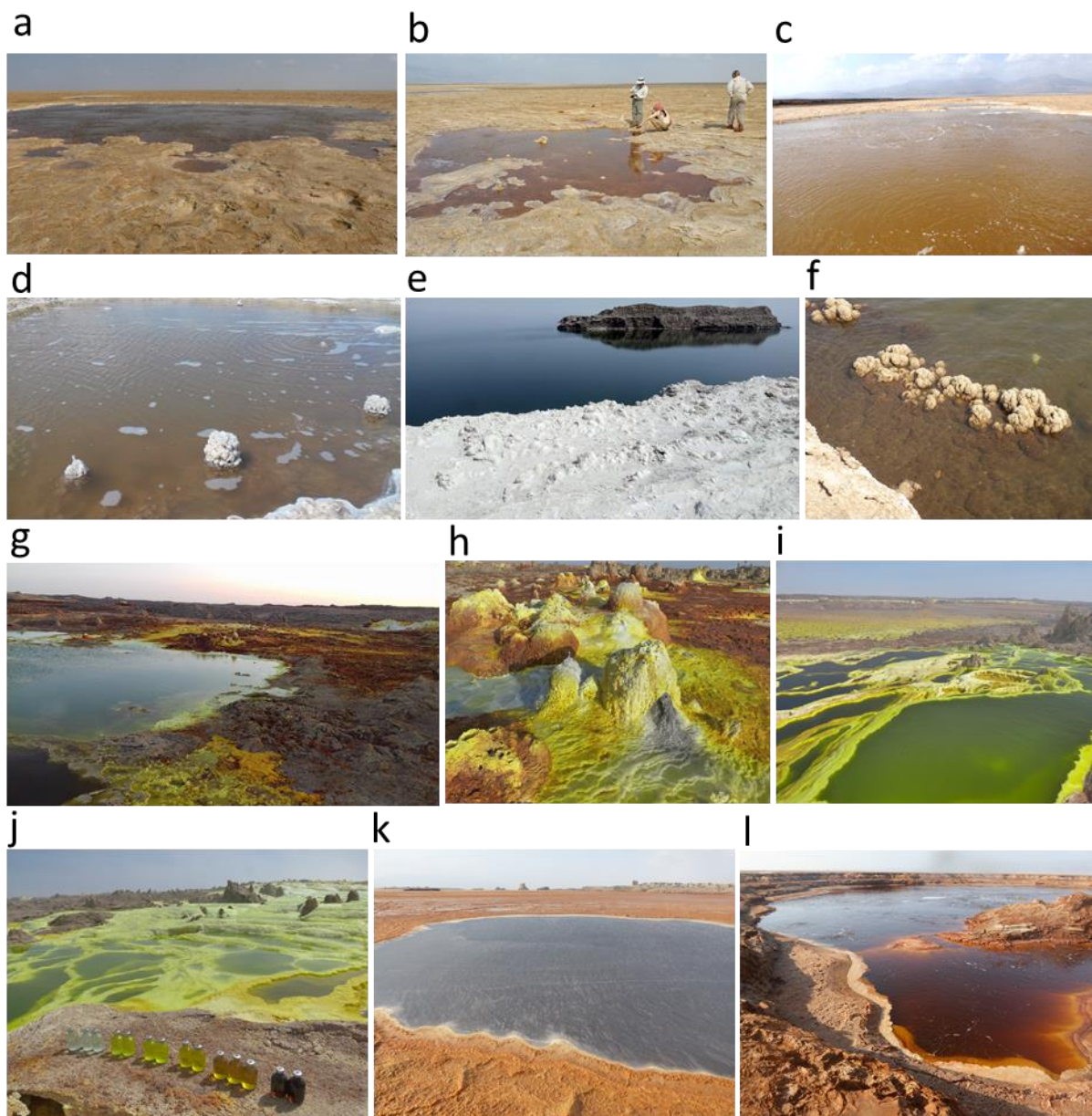
- Belilla, Jodie, David Moreira, Ludwig Jardillier, Guillaume Reboul, Karim Benzerara, José M. López-García, Paola Bertolino, Ana I. López-Archilla, and Purificación López-García. 2019. 'Hyperdiverse Archaea near Life Limits at the Polyextreme Geothermal Dallol Area'. *Nature Ecology & Evolution* 3 (11): 1552–61. <https://doi.org/10/ggr3sj>.
- Blue, C. R., A. Giuffre, S. Mergelsberg, N. Han, J. J. De Yoreo, and P. M. Dove. 2017. 'Chemical and Physical Controls on the Transformation of Amorphous Calcium Carbonate into Crystalline CaCO<sub>3</sub> Polymorphs'. *Geochimica et Cosmochimica Acta* 196 (January): 179–96. <https://doi.org/10/f9jt8n>.
- Cono, Violetta La, Enzo Messina, Manfred Rohde, Erika Arcadi, Sergio Ciordia, Francesca Crisafi, Renata Denaro, et al. 2019. 'Differential Polysaccharide Utilization Is the Basis for a Nanohaloarchaeon: Haloarchaeon Symbiosis'. *BioRxiv*, October, 794461. <https://doi.org/10/ghdpj5>.
- Escudero, L., J. Bijman, G. Chong, J. J. Pueyo, and C. Demergasso. 2013. 'Geochemistry and Microbiology in an Acidic, High Altitude (4,000 m) Salt Flat — High Andes, Northern Chile'. <https://doi.org/10/ghdcg7>.
- Golan, Rotem, Boaz Lazar, Eyal Wurgaft, Nadav Lensky, Jiwchar Ganor, and Ittai Gavrieli. 2017. 'Continuous CO<sub>2</sub> Escape from the Hypersaline Dead Sea Caused by Aragonite Precipitation'. *Geochimica et Cosmochimica Acta* 207 (June): 43–56. <https://doi.org/10/gbjq73>.
- González-López, Jorge, Ángeles Fernández-González, and Amalia Jiménez. 2018. 'Precipitation Behaviour in the System Ca<sup>2+</sup>-Co<sup>2+</sup>-CO<sub>3</sub><sup>2-</sup>-H<sub>2</sub>O at Ambient Conditions — Amorphous Phases and CaCO<sub>3</sub> Polymorphs | Elsevier Enhanced Reader'. *Chemical Geology* 482: 91–100. <https://doi.org/10.1016/j.chemgeo.2018.02.003>.
- Hallsworth, John E., Michail M. Yakimov, Peter N. Golyshin, Jenny L. M. Gillion, Giuseppe D'Auria, Flavia De Lima Alves, Violetta La Cono, et al. 2007. 'Limits of Life in MgCl<sub>2</sub>-Containing Environments: Chaotropicity Defines the Window'. *Environmental Microbiology* 9 (3): 801–13. <https://doi.org/10/fktqwc>.
- Hamm, Joshua, Susanne Erdmann, Emiley Eloë-Fadrosh, Allegra Angeloni, Ling Zhong, Christopher Brownlee, Timothy Williams, et al. 2019. 'Unexpected Host Dependency of Antarctic Nanohaloarchaeota'. *Proceedings of the National Academy of Sciences* 116 (June). <https://doi.org/10/gf4ggj>.
- Harrison, Jesse P., Nicolas Gheeraert, Dmitry Tsigelnitskiy, and Charles S. Cockell. 2013. 'The Limits for Life under Multiple Extremes'. *Trends in Microbiology* 21 (4): 204–12. <https://doi.org/10/f4wgwh>.
- Holwerda, James G., and Richard W. Hutchinson. 1968. 'Potash-Bearing Evaporites in the Danakil Area, Ethiopia'. *Economic Geology* 63 (2): 124–50. <https://doi.org/10/dppvm6>.

- Johnson, Sarah Stewart, Marc Gerard Chevrette, Bethany L. Ehlmann, and Kathleen Counter Benison. 2015. 'Insights from the Metagenome of an Acid Salt Lake: The Role of Biology in an Extreme Depositional Environment'. *PLOS ONE* 10 (4): e0122869. <https://doi.org/10/f7j2jj>.
- Kassambara, A. & Mundt, F. factoextra: extract and visualize the results of multivariate data analyses. <https://CRAN.R-project.org/package=factoextra> (2017)
- Kotopoulou, Electra, Antonio Delgado Huertas, Juan Manuel Garcia-Ruiz, Jose M. Dominguez-Vera, Jose Maria Lopez-Garcia, Isabel Guerra-Tschuschke, and Fernando Rull. 2019. 'A Polyextreme Hydrothermal System Controlled by Iron: The Case of Dallol at the Afar Triangle'. *ACS Earth & Space Chemistry* 3 (1): 90–99. <https://doi.org/10/ghdcr4>.
- Lê, S., Josse, J. & Husson, F. FactoMineR: an R package for multivariate analysis. *J. Stat. Softw.* 25, 1–18 (2008)
- López-García, José M., David Moreira, Karim Benzerara, Olivier Grunewald, and Purificación López-García. 2020. 'Origin and Evolution of the Halo-Volcanic Complex of Dallol: Proto-Volcanism in Northern Afar (Ethiopia)'. *Frontiers in Earth Science* 7. <https://doi.org/10/ggsr6x>.
- Menéndez-Serra, M, Vj Ontiveros, X Triadó-Margarit, D Alonso, and Eo Casamayor. 2020. 'Dynamics and Ecological Distributions of the Archaea Microbiome from Inland Saline Lakes (Monegros Desert, Spain)'. *FEMS Microbiology Ecology* 96 (3). <https://doi.org/10/ghdpsf>.
- Mormile, Melanie R., Bo-Young Hong, and Kathleen C. Benison. 2009. 'Molecular Analysis of the Microbial Communities of Mars Analog Lakes in Western Australia'. *Astrobiology* 9 (10): 919–30. <https://doi.org/10/d7jdsm>.
- Stevenson, Andrew, Jonathan A Cray, Jim P Williams, Ricardo Santos, Richa Sahay, Nils Neuenkirchen, Colin D McClure, et al. 2015. 'Is There a Common Water-Activity Limit for the Three Domains of Life?' *The ISME Journal* 9 (6): 1333–51. <https://doi.org/10/f7cm86>.
- Stevenson, Andrew, Philip G. Hamill, Callum J. O’Kane, Gerhard Kminek, John D. Rummel, Mary A. Voytek, Jan Dijksterhuis, and John E. Hallsworth. 2017. 'Aspergillus Penicillioides Differentiation and Cell Division at 0.585 Water Activity'. *Environmental Microbiology* 19 (2): 687–97. <https://doi.org/10/f9n7kk>.
- Ventosa, Antonio, Rafael R. de la Haba, Cristina Sánchez-Porro, and R. Thane Papke. 2015. 'Microbial Diversity of Hypersaline Environments: A Metagenomic Approach'. *Current Opinion in Microbiology* 25 (June): 80–87. <https://doi.org/10/ghdbwb>.
- Zaikova, Elena, Kathleen C. Benison, Melanie R. Mormile, and Sarah Stewart Johnson. 2018. 'Microbial Communities and Their Predicted Metabolic Functions in a Desiccating Acid Salt Lake'. *Extremophiles: Life Under Extreme Conditions* 22 (3): 367–79. <https://doi.org/10/gc9w84>.
- R Development Core Team R: A Language and Environment for Statistical Computing (R Foundation for Statistical Computing, 2017)

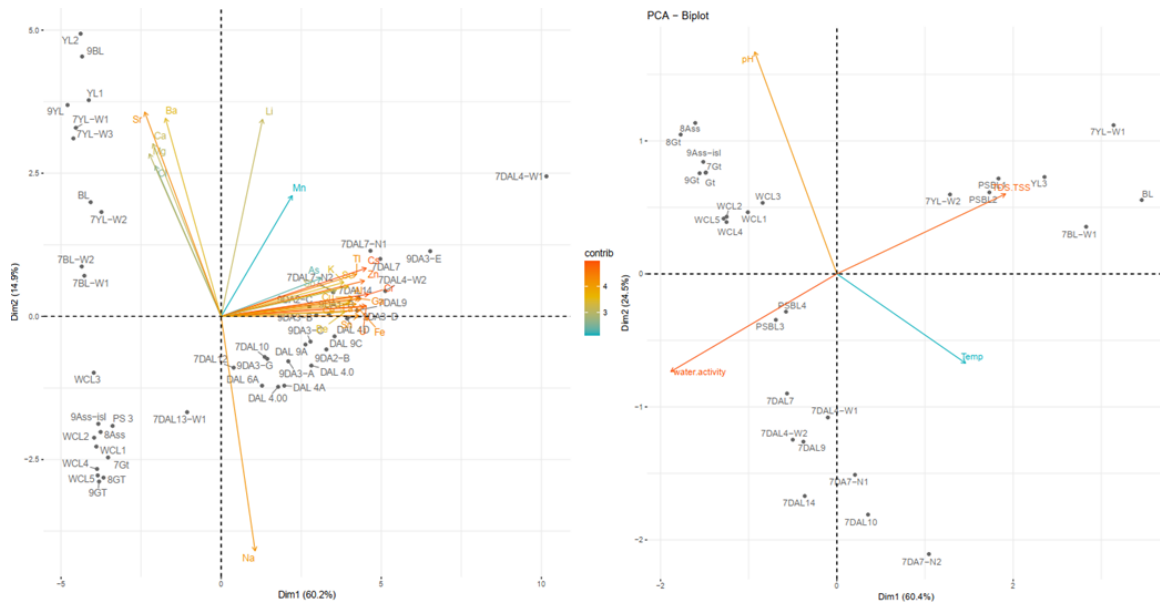
### 6.3.4 Supplementaries



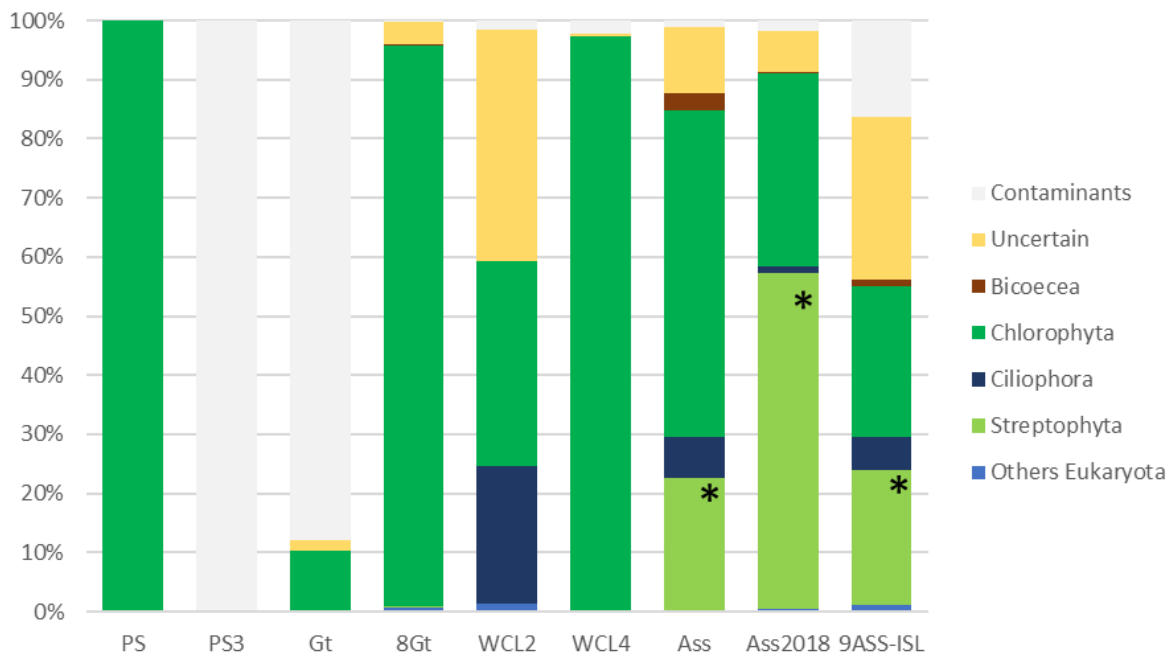
**Supplementary Figure 6 | Evolution of the Western Canyons Lakes between 2003 and 2018. Pictures from CNES/Airbus satellites and distributed by Google Earth.**



**Supplementary Figure 7 | Pictures of the different sites from this study. a, WCL1. WCL2 is barely visible behind it. b, WCL3. c, Bubbling surface of WCL4 and WCL5 in the back. d, Salt chimneys in WCL4. e, View from the top of the island where 9Ass-isl was sampled. f, Area of sampling of 9Ass-isl, where gypsum formation evocating stromatolites can be seen. g, The Dallol dome 9DA1B site. h, Hydrothermal chimneys where 9DA2B and 9DA2C (little grey exit) were sampled. i-j, Overview of the 9DA3-series sampling site, with brine samples shown on (j). k, The Black Lake. l, Lake Gaet'ale.**



**Supplementary Figure 8 | Detailed principal component Analyses (PCA) of Dallol area sampling sites as a function of physicochemical parameters.** 46 samples from the Dallol area according to their chemical composition and (left) 27 samples according to potentially life-limiting physicochemical parameters in the Dallol area. The colour gradient shows the contribution value of each variable and is redundant with the information given by the arrows' length (right).



**Supplementary Figure 9 | Histogram showing the phylogenetic affiliation and abundance of 18S rRNA gene amplicon reads of eukaryotes obtained with universal eukaryotic primers.** Only a few samples yielded amplicons. Sequences corresponding to terrestrial plants and fungi (probably derived from pollen or spores) were considered as contaminants (light grey). The phylogenetic affiliation of dominant eukaryotic groups is colour-coded. \*The "Streptophyta" sequences (identified with SILVA database) found in Lake Karum correspond to unknown micro-eukaryotes that may be Chlorophyta, according to nt NCBI database.





*The Assale Lake south shore*  
© DEEM Team

DISCUSSION

## 7. Discussion

Before our survey in 2016, little was known about the polyextremophiles of hypersaline ( $\geq 20\%$  w/v salt), hyperacidic ( $\text{pH} \leq 1$ ) and eventually hot (up to  $118^\circ\text{C}$ ) brines: can life prosper in such conditions or are they limiting for life? If there is life, what kind of organisms are present? We also didn't know well how the increase of both salinity and acidity (eventually temperature) would shape the microbial communities until the potential limits of life are reached. Replying to these questions could lead to major advances in our understanding of present or past ecosystems and could have consequences in applied microbiology (e.g. biotechnologies) and well as astrobiology (e.g. widen or narrow the habitability concept).

Providing clear answers to these questions is difficult, mainly because environments presenting a combination of hypersalinity and (hyper)acidity are rare. Environments with acidic brines were reported in Central Andean high plateau of Chile ( $\text{pH}$  1-4.7 with up to 2479 mM Na, 1549 mM Mg, 4291 mM Cl) (Escudero et al. 2013) and Western Australia ( $\text{pH}$  down to 1.5 and salinity up to 32% w/v with high seasonal variability) (Mormile, Hong, and Benison 2009; Johnson et al. 2015; Zaikova et al. 2018). However, either only sediments were studied (Escudero et al. 2013; Johnson et al. 2015), either the focus was on the bacterial fraction of the total diversity (Mormile, Hong, and Benison 2009), or the results were against expectations: the acidic hypersaline Lake Magic in Australia is dominated by eukaryotes without traces of archaea, while archaea are normally the most abundant organisms in hypersaline or hyperacidic settings (Zaikova et al. 2018). Hence, these few studies only give partial replies to the above-mentioned questions, some even raise more (see section 1.2.3 for more details).

The Dallol geothermal system and its surroundings is a key set of environments to answer those questions, as it shows gradients of the extreme conditions of interest: hypersalinity (20% to  $>50\%$ , with different salt composition), different levels of acidity ( $\text{pH}$  range between -1.5 to 6), with some hydrothermal systems displaying very high temperature ( $>110^\circ\text{C}$ ). Despite the immense potential of the Dallol area for studying extremophiles, no study aiming to ascertain the microbial presence and diversity along those gradients had been carried out before our first field trip in 2016. In total between 2016 and 2020, we collected 235 samples from 95 sampling sites, some of which had also been little inspected by geologists or geochemists before. Using a panel of multidisciplinary techniques, we investigated the presence/absence of life along the polyextreme gradients of Dallol and its surroundings and attempted to characterize it. The results were correlated, when possible, with chemical analyses of the brines or sediments.

While further work is needed to complete the analyses shown in chapters 5 and 6 (e.g. construction of bacterial 16S rRNA tree), we will now discuss the major outcomes that have emerged from those results and their implications.

7.1 The microbial communities in hypersaline, mildly acidic environments are dominated by a surprisingly wide diversity of Archaea. The closer the physicochemical conditions of an environment are to the limits of life, the higher the proportion of Archaea (especially Nanohaloarchaeota) among prokaryotes.

Our work presented the first study of the microbial communities of Lake Karum, the salt plain, the cave reservoir and the Western Canyons Lakes, with a four years survey for Lake Karum and the cave reservoir (January 2016-2019). Although extreme environments are usually low-diversity systems (Sharp et al. 2014), 16S/18S rRNA gene metabarcoding analysis revealed impressively diverse microbial communities in those hypersaline ( $\geq 30\%$  w/v), mildly acidic (pH 3.5-6) environments of the Dallol area with a total of 2414 archaeal OTUs, 1267 bacterial OTUs and 1357 eukaryotic OTUs, clustered at 95% identity. Lake Karum contains the greatest archaeal richness of all the ecosystems we studied. In contrast, the two salt plain samples, PS and PS3, contain the lowest archaeal richness (especially PS3). This reduced diversity could be related to the abrupt changes of physicochemical conditions that the salt plain undergoes by recurrent flooding, desiccation and occasional hydrothermal influence. Those phenomena may select only the most adapted organisms. A wide majority of the OTUs found in the less polyextreme environments belonged to phyla or genera usually found in hypersaline settings (e.g. Halobacteria and Nanohaloarchaeota phyla for archaea, *Salinibacter* for bacteria and *Dunaliella* and *Halocafeteria* for eukaryotes) (Belilla et al. 2019, section 6.3). Prokaryotic 16S rRNA gene amplicons were obtained through direct PCR, whereas eukaryotic 18S rRNA gene amplicons could only be obtained from some samples (WCL2, WCL4, Gt, 8Gt, the salt plain and Lake Karum samples) using semi-nested PCR (except for PS and Lake Karum samples for which direct PCR was enough), suggesting little eukaryotic presence in most of the samples. Our chemical analyses showed that all samples in which life was detected, are NaCl-dominated (Belilla et al. 2019)(section 6.3). The unexpected wide microbial diversity of those environments may be consistent with suggestions that NaCl-dominated brines are not as extreme as previously thought. This may be linked to the fact that NaCl is not a chaotropic salt (Lee et al. 2018; Cray et al. 2013). The mixing of meteoric and geothermal fluids may also lead to hyperdiverse communities (Colman, Lindsay, and Boyd 2019). Despite this great diversity, the biomass remains very low in the Dallol area, probably because of the extreme conditions, as it is suggested by the very low cell counts estimated by FACS for the cave ( $\sim 3.1 \times 10^4$  cells/ml) and PS sample ( $\sim 5.3 \times 10^4$  cells/ml) (Belilla et al. 2019) and by the size of the endemic cells, which is usually under 1  $\mu\text{m}$  and maximum around 5  $\mu\text{m}$  (the biggest cells have been found in PS) (Belilla et al. 2019, section 6.3). For most samples, DNA concentrations were below the detection limit and for the others, only a few ng/ $\mu\text{L}$  were measured (Belilla et al. 2019, section 6.3).

The prokaryotic sequence abundance is at least 80% dominated by Archaea (mainly being Halobacteria and Nanohaloarchaeota) in all those environments (Belilla et al. 2019,

section 6.3). This was particularly remarkable in the WCL samples, almost completely dominated by Archaea ( $99.1\pm 0.5\%$  of reads abundance), in comparison with the other ecosystems ( $88.8\pm 8.4\%$  for the cave reservoir,  $84.2\pm 2\%$  for Lake Karum and  $79.3\%$  for the Salt Plain PS3) and even richer than the community from a diluted evaporite from the salt plain (PS,  $97.9\%$ ). Another important difference resides in the greater proportion of Nanohaloarchaeota in the WCL lakes ( $29.3\pm 7.1\%$  of total prokaryotic reads versus 1-15% in the other environments) (section 6.3). Higher proportions of Archaea, including Nanohaloarchaeota, have been correlated with increasing salinity (Ventosa et al. 2015; Menéndez-Serra et al. 2020). Since the Western Canyons Lakes are so far the most polyextreme environments harbouring life from the Dallol area (section 6.3), it seems that when the salinity and acidity of an environment increase, getting closer to the limits of life, the proportion of Archaea increases (and among them, the proportion of Nanohaloarchaeota too). A higher preference of Nanohaloarchaeota for the most extreme saline conditions compared to the more versatile Halobacteria, was suggested by Menéndez-Serra et al. (2020). Little is known about the effect of the acidity gradient on haloarchaea and nanohaloarchaea, but we suggest that acidity may also accentuate the observed changes in the microbial community composition. Other studies also suggest that the Nanohaloarchaeota are not free-living organisms but potential mutualistic symbionts (Hamm et al. 2019; Cono et al. 2019). Given the co-occurrence and relative proportions of Halobacteria and Nanohaloarchaeota in our samples plus the FISH observations that revealed very small cells associated with bigger ones (more or less depleted in DNA), our study supports the dependency of nanohaloarchaea on haloarchaeal hosts and suggest that it may be a parasitic interaction. We suggest that this symbiotic interaction may be one of the mechanism behind the changes observed. In the case of a potential mutualistic lifestyle, the association of both partners (halobacteria and nanohaloarchaea) may be more resistant than the host alone, explaining the higher proportion of Nanohaloarchaeota. In the case of a parasitic lifestyle, the rise of acidity and salinity may weaken the host and increase the parasite prevalence.

Besides this suspected host-parasite interaction, some small cells forming groups surrounded by what seemed to be extracellular polymeric substances (EPSs), were observed in PS. Depending on the ecosystem, EPSs may have a protective role against abrupt environment changes in terms of pH, salinity or desiccation, metal concentrations. It may also preserve the cohesion of symbiotic relationships (Poli et al. 2011). The presence of EPSs, of cytoplasmic bridges and/or potential cell fusions, suggest that they might be archaeal colonies as these structures have been observed in archaeal halophiles (Naor and Gophna 2013). Packs of cells have also been observed in the Western Canyons Lakes. This colonial behaviour of the polyextreme microbial communities found in the Dallol area may also play a role in their versatility.

Similar archaeal and bacterial phyla have been found in the acidic brines of Chile and the less polyextreme environments of the Dallol area, though only part of the microbial diversity from Chile was published and the relative proportion of archaea is not known

(Escudero et al. 2013). On the other hand, our results seem at odds with the results from the hypersaline and acidic Lake Magic in Australia, where no Archaea were found (Zaikova et al. 2018). It would be interesting to study whether this contrast is due to the seasonal fluctuations of the Lake Magic, which may periodically be much less acidic and saline when flooded, and to estimate the influence of bioaerosols falling into the lake to the final microbial diversity measured.

To expand the findings of our study and settle more precisely where the physicochemical boundaries of life are, it would be necessary to perform a meta-analysis of the hypersaline-acidic environments with a similar methodology for each site if possible. These environments could be from the Dallol area, the Chile salt flats' acidic brine and the acidic salt lakes of Western Australia, or other yet to be discovered ecosystems with fitting criteria. Additionally, a seasonal survey of the Dallol ecosystems would be necessary to know if the physicochemical conditions changes over the year and how the microbial composition fluctuates along with them. To complete our metabarcoding analyses, whole metagenome profiling, metatranscriptomics and metaproteomics would allow us to assess the molecular strategies involved behind the resistance of both hypersalinity and mildly acidic conditions. We anticipate that it would also significantly improve our understanding of how different organisms interact under such conditions (e.g. the relationship between Nanohaloarchaeota and Halobacteria and the colonial behaviour mentioned above). Our team has already started assembling metagenomes from Lake Karum, the cave reservoir and the Western Canyons Lakes for this purpose and have already obtained promising near-complete metagenome-assembled genomes (MAGs) of Nanohaloarchaeota (unpublished data).

To determine whether our OTUs might correspond to thermophilic species, we plotted the GC content of the 16S rRNA gene region used for metabarcoding analyses of a selection of 88 described archaeal species with optimal growth temperatures ranging from 15 to 103 °C. These included representatives of all Halobacteria genera because they are often characterized by high GC content. A regression analysis confirmed the positive correlation between GC content and optimal growth temperature (Wang, Xia, and Hickey 2006) for this shorter 16S rRNA gene amplified region. Plotting the GC content of our archaeal OTUs on the same graph we could assess that around 27% and 6% of archaeal OTUs from the less polyextreme sites were inferred to correspond to thermophilic and hyperthermophilic organisms, respectively (Belilla et al. 2019) (the more recent 2019 field expedition samples have not yet been added to the calculation). Life under high salt conditions requires extensive molecular adaptations (Oren 1999; 2013; Gunde-Cimerman, Plemenitaš, and Oren 2018), which might seem at odds with the several independent adaptations to extreme salinity across archaea that we have inferred from our phylogenetic analyses. Among those adaptations, the intracellular accumulation of K<sup>+</sup> ('salt-in' strategy), together with the corresponding adaptation of intracellular proteins to function under those conditions, has been crucial. Based on the observation that the deepest archaeal branches correspond to (hyper)thermophilic lineages (Giulio 2003; López-García et al. 2015) and that non-halophilic

hyperthermophilic archaea also accumulate high intracellular K<sup>+</sup> (1.1–3 M) for protein thermoprotection (Hensel and König 1988; Shima, Thauer, and Ermler 2004) (thermoacidophiles also need K<sup>+</sup> for pH homeostasis (Buetti-Dinh et al. 2016)), we hypothesize that intracellular K<sup>+</sup> accumulation is an ancestral archaeal trait linked to thermophilic adaptation that has been independently exapted in different taxa for adaptation to hypersaline habitats.

7.2 Two physicochemical barriers are limiting for life in the presence of water in the Dallol area: the combination of hyperacidity and hypersalinity (and possibly some sterilizing chemical compounds) and the chaotropicity/water activity/ionic strength values.

Despite extensive sampling and relatively large volumes filtered, no 16S/18S rRNA gene amplicons could be amplified through direct PCR from samples from the Dallol dome itself, the Black Lake, Lake Gaet'ale and associated ponds, suggesting little to no DNA presence in the most polyextreme (salinity 20% to >50% and pH up to 3.5) sites of the Danakil depression. Seminested PCR reactions (using the 16S rRNA gene amplicons of the first PCR as templates, including the first PCR negative controls) produced amplicons in all samples including in the first PCR controls, the second PCR controls remaining negative. Those semi-nested amplicons revealed a dominance of non-extremophilic bacteria, in sharp contrast with the archaea-dominated communities found in the moderately acidic hypersaline systems around Dallol described above. Most of them were related to well-known molecular biology kit and laboratory contaminants (Weyrich et al. 2019; Sheik et al. 2018), while others were human-related bacteria probably introduced during the intensive Afars and tourists daily visits to the site. A few halophile archaeal sequences were present in all samples and in the controls too, probably a result from aerosol cross-contamination despite extensive laboratory precautions. After the removal of contaminant sequences from the controls in all samples, most of the remaining reads from the Dallol ponds, the Black Lake and Lake Gaet'ale samples were from halophilic archaea, including Nanohaloarchaeota, similar to the ones that can be found in the less polyextreme sites of the Danakil depression. The difficulty to amplify 16S rRNA genes from the most polyextreme samples and, after contamination check, their similarity with sequences from the surrounding area (e.g. the salt plain) suggest they are not autochthonous, but dispersal forms transported by the strong wind of the Danakil depression. The absence of microorganisms in the most polyextreme samples is supported by cross-analyses of microscope observations (optical, SEM, confocal), multiparametric analyses on the flow cytometer showing the absence of DNA, and the inability to obtain enrichment cultures from these environments despite the use of various growth media and culture conditions. This conclusion is consistent with the inference of Kotopoulou et al. (2019) that life, if present, is not involved in the iron cycling and iron mineral precipitation occurring at the Dallol dome. Recently, another group of researchers have investigated the Dallol dome region, and their

results so far revealed no evidence of life in what they call the outcrop zone (the dome itself) and the volcanic base region (the Black Lake and Lake Gaet'ale) due to the extreme conditions of the brines, supporting our findings (Moors et al. 2020). Similar to our study, they reported the presence of halophiles from the Halobacteria archaeal phyla and the *Salinibacter* bacterial genus in the distant south area, close to Lake Karum.

We identified two major barriers limiting life in the most polyextreme environments of the Dallol area. In line with previous studies, one barrier is imposed by the life-limiting values of high chaotropicity (Hallsworth et al. 2007), ionic strength (Fox-Powell et al. 2016) and low water activity (Stevenson et al. 2015; 2017) in the Black Lake and Lake Gaet'ale areas, which are associated with their high  $Mg^{2+}$  and  $Ca^{2+}$  salt concentration (Belilla et al. 2019). On the other hand, due to the dominance of NaCl salts, the chaotropicity, ionic strength and water activity values of Dallol ponds are not limiting for life, except for one very concentrated pond with high iron salts concentration. The barrier limiting life in the Dallol dome hydrothermal system seems to be imposed by the hyperacid–hypersaline conditions (pH 0.5 to -1.5, salinity 20 to 45%), regardless of temperature. This suggests that molecular adaptations to simultaneous low pH and high salt are incompatible at these extreme values. In principle, more acidic proteins, intracellular  $K^+$  accumulation ('salt-in' strategy) or internal positive membrane potential generated by cations or  $H^+$ /cation antiporters serve both acidophilic and halophilic adaptations (Slonczewski et al. 2009; Buetti-Dinh et al. 2016; Gunde-Cimerman, Plemenitaš, and Oren 2018). However, the properties of the cell membrane necessary for extreme acidophiles (e.g. impermeability to maintain neutral pH, reduced pores...) may not have evolved in halophiles or may not be compatible with their adaptations. Besides, since the salt-in strategy involves  $Cl^-$  pumps that transport  $Cl^-$  from the environment into the cytoplasm (Oren 1999), the positive anomalies in  $Cl^-$  observed in Dallol fluids (Kotopoulou et al. 2019; Belilla et al. 2019) may induce a massive import of  $H^+$  and cations ( $K^+/Na^+$ ) that could potentially disrupt the membrane bioenergetics (Buetti-Dinh et al. 2016). While those suggestions could explain the absence of life in the Dallol hydrothermal system, we cannot exclude other explanations such as: 1) the effect of hyperacidity alone which in some ponds is below the known record of tolerance (Schleper et al. 1996); 2) the role of several other stressors, such as high metal content or the potential presence of sterilizing molecules forming in the pond such as perchlorate (Carrier and Kounaves 2015). Future metagenomics, metatranscriptomics or metaproteomics studies on less polyextreme environments should help to identify the molecular barriers limiting the adaptation of life towards this combination of extremes.

7.3 The absence of life in the Dallol dome hydrothermal ponds, the Black Lake and Lake Gaet'ale makes them especially sensitive to biocontamination, though their physicochemical properties may get rid of most of it.

While we interpreted it as local contamination, the detection of one Nanohaloarchaeota OTU in one of Dallol's ponds has led several authors to claim that polyextremophiles were proliferating in Dallol's brine (Gómez et al. 2019). To test further the local contamination hypothesis, during our last field trip we collected bioaerosols from the Dallol dome top and base and showed that a wide diversity of microorganisms was actively transported by the wind. Most of the bioaerosols were composed of non-halophilic eukaryotes (including plants, most likely in the form of pollen) and bacteria that probably originate from the escarpments limiting the depression or the touristic activity, but we could also detect halophilic archaea, including Halobacteria and Nanohaloarchaeota. Unfortunately, we were unable to compare them with the rest of the metabarcoding data of Gomez et al. (2019) since they did not provide it. The nanohaloarchaea found in the Dallol pool by these authors was very similar to the ones that we found in the less extreme places around the dome (Lake Karum, the cave reservoir, the salt plain). Using the same FISH protocol as Gomez et al. (2019), we showed that the signal they observed in hybridization experiments with a Nanohaloarchaeota-specific probe could not be differentiated from the background noise. Moreover, the objects that they observed with SEM strongly resemble certain nanominerals that precipitate abundantly in the Dallol hyperacidic pools, such as jarosite (Kotopoulou et al. 2019) and silicate spherules (Belilla et al. 2019, section 5.3). These biomorphs were different from actual cells such as the ones that we observed in the PS sample (Belilla et al. 2019, section 5.3), which do present the size, morphology, and close association to larger cells that have been described for the Nanohaloarchaeota (Narasingarao et al. 2012; Hamm et al. 2019). In fact, there is growing evidence that nanohaloarchaea depend on other organisms for their growth (Hamm et al. 2019; Cono et al. 2019). In that sense, it is also surprising that Gomez et al. only reported a nanohaloarchaeal OTU but not any suitable host. Those results privilege the local contamination hypothesis and refute the claim about the presence of life in the hyperacidic hypersaline brines of Dallol. Our study underlines the importance of studying a site in its entirety, considering the surrounding environments with which it is likely to interact. The lower the endemic biomass, the easier it can be impacted by exogenous import or laboratory contaminants (Weyrich et al. 2019; Sheik et al. 2018). Thus, the discrimination between autochthonous and exogenous organisms is crucial to draw the right conclusions on the microbial diversity of some very extreme environments. The comparison of metabarcoding data with controls or known kit contaminants and the study of field bioaerosols can substantially increase the reliability of the results. We also underlined the importance of always using positive and negative controls even during microscope observations to avoid interpretation bias. The most polyextreme sites of the Dallol area are not the only ones where biocontamination may be a major issue in the interpretation of results. One example is the Don Juan Pond, a  $\text{CaCl}_2$ -rich brine in Antarctica where the presence of planktonic microbial life is debated since different authors have reinterpreted previous culture experiments and in situ  $\text{N}_2\text{O}$  fluxes as airborne contamination (Cameron, Morelli, and Randall 1972) and abiotic degassing (Samarkin et al. 2010), respectively. Another controversial example is the Discovery deep brine (Red Sea), where the  $\text{MgCl}_2$  concentration increases with

depth to near saturation and DNA traces are detectable almost all along this gradient, whereas RNA traces become undetectable after a certain depth and  $\text{MgCl}_2$  concentration (2.3 M) (Hallsworth et al. 2007). Based on experiments showing that DNA is better preserved than RNA in  $\text{MgCl}_2$  and that no cultivation was successful at more than 2.3 M  $\text{MgCl}_2$  without chaotropic salt compensation, Hallsworth et al. (2007) argued that there is no active life after this concentration limit and that the DNA detected comes from dead cells from upper levels. The preservation of DNA from dead cells in some salts may also be an overlooked issue when studying (poly)extreme sites with high salinity concentration.

The local biocontamination hypothesis may seem paradoxical because, while the bioaerosols-transported biomass should be continuously falling onto the Dallol dome and its surroundings, it was difficult to obtain amplicons from the most polyextreme brine pools (nested PCRs were necessary). To explain this paradox, we hypothesize that a very active DNA destruction process occurs in the Dallol hydrothermal ponds (and possibly the Black Lake and Lake Gaet'ale), limiting the detection of the aerosol-transported biomass. Our experiments confirmed this hypothesis as we measured an almost instantaneous disappearance of DNA from the salt plain's cells incubated in Dallol brine. As the salinity of the salt plain and the Dallol sample are similar, we suggest that the additional hyperacidity of the dome's brine is the main factor leading to DNA destruction. Indeed, depurination of DNA under acidic conditions has been known for a long time (Tamm, Hodes, and Chargaff 1952; Hevesi et al. 1972), though most likely it had never been studied under the extremely low pH values (<0) typical of the Dallol brines. Likewise, we observed a dramatic instantaneous ( $t \leq 2$  mins) decrease of the salt plain DNA concentration by a factor of two to six immediately after contact with the Dallol brine, with final concentrations always  $\leq 5$  ng/ $\mu\text{L}$ , close to the detection limit of our instrument. We were also unable to obtain direct-PCR amplicons from cells pellets of the cave reservoir, Lake Karum, the salt plain and a culture of *Haloferax* after contact with a hypersaline, hyperacidic solution mimicking the physicochemical conditions of Dallol brines, even when trying to rapidly neutralize the acidity with basic solutions. Nevertheless, the high salinity and the complex and poorly-known chemistry of the Dallol brines possibly also play a role, for example through the abundant presence of chaotropic salts (e.g.,  $\text{FeCl}_2$ ,  $\text{FeCl}_3$ ,  $\text{MgSO}_4$ ) (Belilla et al. 2019; Kotopoulou et al. 2019) that can disrupt cell membranes and facilitate acid attack on DNA. It has recently been shown that another chaotropic salt, sodium perchlorate, is formed under high UV irradiation of  $\text{NaCl}$  in presence of silica (Carrier and Kounaves 2015), conditions which are prevalent in Dallol. The very high chaotropicity of Lake Gaet'ale and the Black Lake area may also be a major driver of the DNA degradation in those brines. Environmental DNA degrades faster in environments with either high temperature, exposed to strong UV irradiation, and acidic pH than other physicochemical settings (Strickler, Fremier, and Goldberg 2015), conditions which are reunited in Dallol and their surroundings.

## 7.4 Implications of our work in other research fields such as astrobiology and the study of the origin and evolution of life

An important issue regarding the search for traces of life in extreme environments, the fossil record and other terrestrial bodies is the interpretation of biomorphs. Biomorphs are organic or inorganic structures whose shape resembles that of living organisms, in our case microorganisms. The contrasting conclusions of Gomez et al (2019) and ours about the nature of silicate nanospheres of the Dallol dome illustrate how biomorph observations can be confusing. We assume that this interpretation bias can be reduced by thoughtful cross-analyses to assess the presence of life and its nature, including positive control observations with similarly expected cells, paying attention to the mineralogy of the geological area and by checking the confounding abiotic biomorphs. This may also apply to astrobiology. Biocontamination is also one of the major issues in the search of life beyond Earth, which is why Planetary Protection rules impose very strict sterilization procedures for rovers destined to land on planets of astrobiological interest such as Mars (National Research Council 2006). We expect that developing robust protocols for interpreting the microbial composition of extreme environments on Earth can potentially help the search for life on other planets.

I will conclude by quoting a common idea: “[...]in the past few decades we have come to realize that where there is liquid water on Earth, virtually no matter what the physical conditions, there is life” (Rothschild and Mancinelli 2001). This “where is water there is life” adage is widespread especially in the astrobiology field, along with the “follow the water” one (Pohorille and Pratt 2012). While it is true that water is a *necessary* condition for life (Ball 2008; Bergethon 2010) our study of the Dallol hydrothermal ponds, Lake Gaet’ale and Black Lake argues that it is not a *sufficient* condition for life. The known physicochemical limits of life should be considered to maximise the chances to find life beyond Earth.

### Reference:

- Ball, Philip. 2008. ‘Water as an Active Constituent in Cell Biology’. *Chemical Reviews* 108 (1): 74–108. <https://doi.org/10/c42mx6>.
- Belilla, Jodie, David Moreira, Ludwig Jardillier, Guillaume Reboul, Karim Benzerara, José M. López-García, Paola Bertolino, Ana I. López-Archilla, and Purificación López-García. 2019. ‘Hyperdiverse Archaea near Life Limits at the Polyextreme Geothermal Dallol Area’. *Nature Ecology & Evolution* 3 (11): 1552–61. <https://doi.org/10/ggr3sj>.
- Bergethon, Peter R. 2010. ‘Water: A Unique Solvent and Vital Component of Life’. In *The Physical Basis of Biochemistry: The Foundations of Molecular Biophysics*, edited by Peter R. Bergethon, 389–408. New York, NY: Springer. [https://doi.org/10.1007/978-1-4419-6324-6\\_14](https://doi.org/10.1007/978-1-4419-6324-6_14).
- Buetti-Dinh, Antoine, Olga Dethlefsen, Ran Friedman, and Mark Dopson. 2016. ‘Transcriptomic Analysis Reveals How a Lack of Potassium Ions Increases Sulfolobus

- Acidocaldarius Sensitivity to PH Changes'. *Microbiology (Reading, England)* 162 (8): 1422–34. <https://doi.org/10/f3rw6d>.
- Cameron, R.E, F.A Morelli, and L.P Randall. 1972. 'Aerial, Aquatic, and Soil Microbiology of Don Juan Pond, Antarctica'. *Antarctic Journal of the United States* 7 (6): 254–58.
- Carrier, Brandi L., and Samuel P. Kounaves. 2015. 'The Origins of Perchlorate in the Martian Soil'. *Geophysical Research Letters* 42 (10): 3739–45. <https://doi.org/10/f7hpcn>.
- Colman, Daniel R., Melody R. Lindsay, and Eric S. Boyd. 2019. 'Mixing of Meteoric and Geothermal Fluids Supports Hyperdiverse Chemosynthetic Hydrothermal Communities'. *Nature Communications* 10 (1): 681. <https://doi.org/10/gg7kc9>.
- Cono, Violetta La, Enzo Messina, Manfred Rohde, Erika Arcadi, Sergio Ciordia, Francesca Crisafi, Renata Denaro, et al. 2019. 'Differential Polysaccharide Utilization Is the Basis for a Nanohaloarchaeon: Haloarchaeon Symbiosis'. *BioRxiv*, October, 794461. <https://doi.org/10/ghdpj5>.
- Cray, Jonathan A., John T. Russell, David J. Timson, Rekha S. Singhal, and John E. Hallsworth. 2013. 'A Universal Measure of Chaotropicity and Kosmotropicity'. *Environmental Microbiology* 15 (1): 287–96. <https://doi.org/10/ggddmj>.
- Escudero, L., J. Bijman, G. Chong, J. J. Pueyo, and C. Demergasso. 2013. 'Geochemistry and Microbiology in an Acidic, High Altitude (4,000 m) Salt Flat — High Andes, Northern Chile'. <https://doi.org/10/ghdcg7>.
- Fox-Powell, Mark G., John E. Hallsworth, Claire R. Cousins, and Charles S. Cockell. 2016. 'Ionic Strength Is a Barrier to the Habitability of Mars'. *Astrobiology* 16 (6): 427–42. <https://doi.org/10/f8qjhr>.
- Giulio, MASSIMO DI. 2003. 'The Universal Ancestor Was a Thermophile or a Hyperthermophile: Tests and Further Evidence'. *Journal of Theoretical Biology* 221 (3): 425–36. <https://doi.org/10/cn8863>.
- Gómez, Felipe, Barbara Cavalazzi, Nuria Rodríguez, Ricardo Amils, Gian Gabriele Ori, Karen Olsson-Francis, Cristina Escudero, Jose M. Martínez, and Hagos Miruts. 2019. 'Ultra-Small Microorganisms in the Polyextreme Conditions of the Dallol Volcano, Northern Afar, Ethiopia'. *Scientific Reports* 9 (1): 1–9. <https://doi.org/10/gf2756>.
- Gunde-Cimerman, Nina, Ana Plemenitaš, and Aharon Oren. 2018. 'Strategies of Adaptation of Microorganisms of the Three Domains of Life to High Salt Concentrations'. *FEMS Microbiology Reviews* 42 (3): 353–75. <https://doi.org/10/gc577v>.
- Hallsworth, John E., Michail M. Yakimov, Peter N. Golyshin, Jenny L. M. Gillion, Giuseppe D'Auria, Flavia De Lima Alves, Violetta La Cono, et al. 2007. 'Limits of Life in MgCl<sub>2</sub>-Containing Environments: Chaotropicity Defines the Window'. *Environmental Microbiology* 9 (3): 801–13. <https://doi.org/10/fktqwc>.
- Hamm, Joshua, Susanne Erdmann, Emiley Eloë-Fadrosch, Allegra Angeloni, Ling Zhong, Christopher Brownlee, Timothy Williams, et al. 2019. 'Unexpected Host Dependency of Antarctic Nanohaloarchaeota'. *Proceedings of the National Academy of Sciences* 116 (June). <https://doi.org/10/gf4ggj>.
- Hensel, Reinhard, and Helmut König. 1988. 'Thermoadaptation of Methanogenic Bacteria by Intracellular Ion Concentration'. *FEMS Microbiology Letters* 49 (1): 75–79. <https://doi.org/10/fjwnj5>.
- Hevesi, L., E. Wolfson-Davidson, J. B. Nagy, O. B. Nagy, and A. Bruylants. 1972. 'Contribution to the Mechanism of the Acid-Catalyzed Hydrolysis of Purine Nucleosides'. *Journal of the American Chemical Society* 94 (13): 4715–20. <https://doi.org/10/cwwqd3>.

- Johnson, Sarah Stewart, Marc Gerard Chevrette, Bethany L. Ehlmann, and Kathleen Counter Benison. 2015. 'Insights from the Metagenome of an Acid Salt Lake: The Role of Biology in an Extreme Depositional Environment'. *PLOS ONE* 10 (4): e0122869. <https://doi.org/10/f7j2jj>.
- Kotopoulou, Electra, Antonio Delgado Huertas, Juan Manuel Garcia-Ruiz, Jose M. Dominguez-Vera, Jose Maria Lopez-Garcia, Isabel Guerra-Tschuschke, and Fernando Rull. 2019. 'A Polyextreme Hydrothermal System Controlled by Iron: The Case of Dallol at the Afar Triangle'. *ACS Earth & Space Chemistry* 3 (1): 90–99. <https://doi.org/10/ghdcr4>.
- Lee, Callum J. D., Phillip E. McMullan, Callum J. O'Kane, Andrew Stevenson, Inês C. Santos, Chayan Roy, Wriddhiman Ghosh, et al. 2018. 'NaCl-Saturated Brines Are Thermodynamically Moderate, Rather than Extreme, Microbial Habitats'. *FEMS Microbiology Reviews* 42 (5): 672–93. <https://doi.org/10/gdpmx3>.
- López-García, Purificación, Yvan Zivanovic, Philippe Deschamps, and David Moreira. 2015. 'Bacterial Gene Import and Mesophilic Adaptation in Archaea'. *Nature Reviews Microbiology* 13 (7): 447–56. <https://doi.org/10/gfb6fm>.
- Menéndez-Serra, M, Vj Ontiveros, X Triadó-Margarit, D Alonso, and Eo Casamayor. 2020. 'Dynamics and Ecological Distributions of the Archaea Microbiome from Inland Saline Lakes (Monegros Desert, Spain)'. *FEMS Microbiology Ecology* 96 (3). <https://doi.org/10/ghdpsf>.
- Moors, Hugo, Miroslav Honty, Carla Smolders, Ann Provoost, Mieke De Craen, and Natalie Leys. 2020. 'The Waterbodies of the Dallol Volcano: A Physico-Chemical and Geo-Microbial Survey - NASA/ADS'. In . <https://ui.adsabs.harvard.edu/abs/2020EGUGA..22.1581M/abstract>.
- Mormile, Melanie R., Bo-Young Hong, and Kathleen C. Benison. 2009. 'Molecular Analysis of the Microbial Communities of Mars Analog Lakes in Western Australia'. *Astrobiology* 9 (10): 919–30. <https://doi.org/10/d7jdsd>.
- Naor, Adit, and Uri Gophna. 2013. 'Cell Fusion and Hybrids in Archaea'. *Bioengineered* 4 (3): 126–29. <https://doi.org/10/ghdpw7>.
- Narasingarao, Priya, Sheila Podell, Juan A. Ugalde, Céline Brochier-Armanet, Joanne B. Emerson, Jochen J. Brocks, Karla B. Heidelberg, Jillian F. Banfield, and Eric E. Allen. 2012. 'De Novo Metagenomic Assembly Reveals Abundant Novel Major Lineage of Archaea in Hypersaline Microbial Communities'. *The ISME Journal* 6 (1): 81–93. <https://doi.org/10/bmkzrz>.
- National Research Council. 2006. 'Preventing the Forward Contamination of Mars'. Washington, DC: The National Academies Press. <https://www.nap.edu/catalog/11381/preventing-the-forward-contamination-of-mars>.
- Oren, Aharon. 1999. 'Bioenergetic Aspects of Halophilism'. *Microbiology and Molecular Biology Reviews* 63 (2): 334–48.
- . 2013. 'Life at High Salt Concentrations, Intracellular KCl Concentrations, and Acidic Proteomes'. *Frontiers in Microbiology* 4 (November): 315. <https://doi.org/10/ghdpw8>.
- Pohorille, A., and L. R. Pratt. 2012. 'Is Water the Universal Solvent for Life?' *Origins of Life and Evolution of Biospheres* 42 (5): 405–9. <https://doi.org/10/gfx2rn>.
- Poli, Annarita, Paola Di Donato, Gennaro Roberto Abbamondi, and Barbara Nicolaus. 2011. 'Synthesis, Production, and Biotechnological Applications of Exopolysaccharides and Polyhydroxyalkanoates by Archaea'. Edited by Alessandra Morana. *Archaea* 2011 (October): 693253. <https://doi.org/10/dpdqw5>.

- Rothschild, L. J., and R. L. Mancinelli. 2001. 'Life in Extreme Environments'. *Nature* 409 (6823): 1092–1101. <https://doi.org/10/fn7zhp>.
- Samarkin, Vladimir A., Michael T. Madigan, Marshall W. Bowles, Karen L. Casciotti, John C. Priscu, Christopher P. McKay, and Samantha B. Joye. 2010. 'Abiotic Nitrous Oxide Emission from the Hypersaline Don Juan Pond in Antarctica'. *Nature Geoscience* 3 (5): 341–44. <https://doi.org/10/bchns8>.
- Schleper, Christa, Gabriela Puhler, Hans- Peter Klenk, and Wolfram Zillig. 1996. 'Picrophilus Oshimae and Picrophilus Tomdus Fam. Nov., Gen. Nov., Sp. Nov., Two Species of Hyperacidophilic, Thermophilic, Heterotrophic, Aerobic Archaea', *International Journal of Systematic Bacteriology*, 46 (3): 814–16. <https://doi.org/10.1099/00207713-46-3-814>.
- Sharp, Christine E., Allyson L. Brady, Glen H. Sharp, Stephen E. Grasby, Matthew B. Stott, and Peter F. Dunfield. 2014. 'Humboldt's Spa: Microbial Diversity Is Controlled by Temperature in Geothermal Environments'. *The ISME Journal* 8 (6): 1166–74. <https://doi.org/10/f56c26>.
- Sheik, Cody S., Brandi Kiel Reese, Katrina I. Twing, Jason B. Sylvan, Sharon L. Grim, Matthew O. Schrenk, Mitchell L. Sogin, and Frederick S. Colwell. 2018. 'Identification and Removal of Contaminant Sequences From Ribosomal Gene Databases: Lessons From the Census of Deep Life'. *Frontiers in Microbiology* 9: 840. <https://doi.org/10/gdkk9b>.
- Shima, S., R. K. Thauer, and U. Ermler. 2004. 'Hyperthermophilic and Salt-Dependent Formyltransferase from Methanopyrus Kandleri'. *Biochemical Society Transactions* 32 (Pt 2): 269–72. <https://doi.org/10/cqt4nh>.
- Slonczewski, Joan L., Makoto Fujisawa, Mark Dopson, and Terry A. Krulwich. 2009. 'Cytoplasmic PH Measurement and Homeostasis in Bacteria and Archaea'. *Advances in Microbial Physiology* 55: 1–79, 317. <https://doi.org/10/c7h3v6>.
- Stevenson, Andrew, Jonathan A. Cray, Jim P. Williams, Ricardo Santos, Richa Sahay, Nils Neuenkirchen, Colin D. McClure, et al. 2015. 'Is There a Common Water-Activity Limit for the Three Domains of Life?' *The ISME Journal* 9 (6): 1333–51. <https://doi.org/10/f7cm86>.
- Stevenson, Andrew, Philip G. Hamill, Callum J. O'Kane, Gerhard Kminek, John D. Rummel, Mary A. Voytek, Jan Dijksterhuis, and John E. Hallsworth. 2017. 'Aspergillus Penicillioides Differentiation and Cell Division at 0.585 Water Activity'. *Environmental Microbiology* 19 (2): 687–97. <https://doi.org/10/f9n7kk>.
- Strickler, Katherine M., Alexander K. Fremier, and Caren S. Goldberg. 2015. 'Quantifying Effects of UV-B, Temperature, and PH on EDNA Degradation in Aquatic Microcosms'. *Biological Conservation*, Special Issue: Environmental DNA: A powerful new tool for biological conservation, 183 (March): 85–92. <https://doi.org/10/f63rhr>.
- Tamm, C., M. E. Hodes, and E. Chargaff. 1952. 'The Formation Apurinic Acid from the Desoxyribonucleic Acid of Calf Thymus'. *The Journal of Biological Chemistry* 195 (1): 49–63.
- Ventosa, Antonio, Rafael R. de la Haba, Cristina Sánchez-Porro, and R. Thane Papke. 2015. 'Microbial Diversity of Hypersaline Environments: A Metagenomic Approach'. *Current Opinion in Microbiology* 25 (June): 80–87. <https://doi.org/10/ghdbwb>.
- Wang, Huai-Chun, Xuhua Xia, and Donal Hickey. 2006. 'Thermal Adaptation of the Small Subunit Ribosomal RNA Gene: A Comparative Study'. *Journal of Molecular Evolution* 63 (1): 120–26. <https://doi.org/10/dgwdmw>.

- Weyrich, Laura S., Andrew G. Farrer, Raphael Eisenhofer, Luis A. Arriola, Jennifer Young, Caitlin A. Selway, Matilda Handsley-Davis, Christina J. Adler, James Breen, and Alan Cooper. 2019. 'Laboratory Contamination over Time during Low-Biomass Sample Analysis'. *Molecular Ecology Resources* 19 (4): 982–96. <https://doi.org/10/ggvbjd>.
- Zaikova, Elena, Kathleen C. Benison, Melanie R. Mormile, and Sarah Stewart Johnson. 2018. 'Microbial Communities and Their Predicted Metabolic Functions in a Desiccating Acid Salt Lake'. *Extremophiles: Life Under Extreme Conditions* 22 (3): 367–79. <https://doi.org/10/gc9w84>.



*A nice "wave" of salt in the salt canyons*

© DEEM Team

CONCLUSION

## 8. Conclusion

Before this study, there were several doubts regarding the possibility for microorganisms to thrive in a combination of hypersaline, hyperacidic (and eventually high temperature) conditions. There were also only a few studies attempting to describe the composition of microbial communities along the salinity-acidity gradient. My PhD project centred on the prospection of microorganisms in the polyextreme environments of Dallol and its surroundings in the Danakil depression of Ethiopia, which display within a radius of few kilometres range a wide array of polyextreme hypersaline-acidic-hot conditions.

The major outcomes of our work are listed below:

1. The microbial communities in hypersaline ( $\geq 30\%$ ), mildly acidic (pH 4.2 to 6) environments are dominated by a surprisingly wide diversity of Archaea when the dominant salt is NaCl (the Lake Karum, the salt plain, the cave reservoir, the Western Canyons Lakes). The higher the salinity and the acidity, the greater the proportion of archaea (especially nanohaloarchaea) among prokaryotes.
2. Based on their co-occurrence and microscope observations, our study supports the dependency of nanohaloarchaea cells to a haloarchaea host and suggest it may be a parasitic interaction.
3. Regardless of temperature, little or no DNA could be amplified from the samples from the most polyextreme sites of the Danakil depression (salinity 20% to  $>50\%$  with a high concentration of  $\text{Fe}^{2+}/\text{Fe}^{3+}$  or  $\text{Ca}^{2+}/\text{Mg}^{2+}$  salts and pH -1.5 to 3.5).
4. Two physicochemical barriers limiting for life are identified in the presence of water in the Dallol area: 1) the combination of hyperacidity and hypersalinity (possibly combined with the high heavy metal concentration and some sterilizing chemical components) for the Dallol dome itself, and the chaotropicity/water activity/ionic strength values for Lake Gaet'ale and the Black Lake.
5. The absence of life in the Dallol dome hydrothermal ponds, Lake Gaet'ale and the Black Lake makes them especially sensitive to biocontamination (through the bioaerosols on-site and during laboratory experiments) for the interpretation of results, though their physicochemical properties may get rid of most of it.
6. We propose, through our different studies (section 4.3, 5.3, 6.3) a rigorous protocol to discriminate endogenous and exogenous DNA, as well as cells and biomorphs.



*A Dallol dome active grey chimney*  
© DEEM Team

SUMMARIES

# L'exploration des communautés microbiennes le long des gradients physicochimiques poly-extrêmes de Dallol et de ses environs

*Résumé de thèse en français*

## Introduction

Bien que les microorganismes soient les plus petites formes de vie existantes, collectivement ils représentent au moins la seconde plus grande source de biomasse sur Terre (Bar-On, Phillips, and Milo 2018). Leur présence n'a pourtant été révélée qu'au XVII<sup>ème</sup> siècle grâce à des observations au microscope (Leeuwenhoek 1705; Hooke 1665; Lane 2015). Leur découverte a aussitôt ouvert la question de leur nature, à une époque où les êtres vivants étaient classifiés essentiellement sur des critères morphologiques. Ce n'est qu'à partir du XX<sup>ème</sup> siècle que les progrès scientifiques et techniques ouvrent la possibilité de faire des phylogénies à partir de marqueurs moléculaires, permettant de révéler que les organismes seraient séparés en trois grands domaines : les eucaryotes, les bactéries et les archées (Woese and Fox 1977; Woese, Kandler, and Wheelis 1990).

Le domaine des archées a longtemps été perçu comme étant constitué essentiellement d'extrémophiles, c'est-à-dire d'organismes vivant dans des conditions physicochimiques se rapprochant des limites connues de la vie. On sait aujourd'hui que les archées sont également présentes dans les environnements non-extrêmes, néanmoins elles sont surreprésentées dans les environnements extrêmes et dominent dans nombres d'entre eux (Schmid, Allers, and DiRuggiero 2020), dont :

- Les environnements hypersalés (>5% de sel), où vivent des organismes dits halophiles
- Les environnements acides (pH 3-5) et hyperacides (pH<3), où vivent des organismes dits acidophiles.
- Les environnements chauds (>60 °C) où vivent des organismes dits thermophiles

Parmi les nombreuses motivations derrière l'étude des extrémophiles, on peut citer des applications biotechnologiques de certaines biomolécules découvertes chez ces organismes (Saiki et al. 1988). De par la nature extrême des environnements pollués, certains extrémophiles intéressent également les secteurs de bioremédiation (dépollution) (Sara Parwin Banu et al. 2003; Kang et al. 2015). Les premiers fossiles microbiens, des stromatolites, dateraient d'environ 3.5 milliards d'années, même si la biogénicité des traces les plus anciennes reste à prouver (Walter, Buick, and Dunlop 1980; Schopf and Packer 1987; Brasier et al. 2002). A cette époque, l'activité volcanique et l'hydrothermalisme étaient plus présents qu'aujourd'hui et les océans étaient supposés être environ trois fois plus salés et potentiellement plus riches en certains métaux (Knauth 2005; Oremland et al. 2009; Albareda et al. 2020). Etudier les extrémophiles peut donc apporter des clés pour mieux comprendre les conditions d'émergence de la vie et certains paléoenvironnements. Enfin, les limites de la vie sur Terre et ses conditions d'apparition intéressent fortement des domaines comme

l'exobiologie afin de mieux guider la recherche de planètes susceptibles de renfermer ou d'avoir pu renfermer la vie (Merino et al. 2019).

Malgré l'importance des extrémophiles et le progrès des connaissances à leur sujet ces dernières décennies, certaines incertitudes persistent, en particulier concernant les polyextrémophiles (organismes adaptés à plusieurs paramètres physicochimiques extrêmes). On sait en effet peu de choses sur la composition des communautés microbiennes dans les milieux hypersalés le long du gradient de pH jusqu'à 1.5 (Mormile, Hong, and Benison 2009; Escudero et al. 2013; Harrison et al. 2013; Zaikova et al. 2018; Johnson et al. 2015), et l'on ignore tout de la viabilité d'environnements à  $\text{pH} < 1.5$  et à saturation de sel. A noter qu'on ignore également l'impact sur ces gradients de la température.

C'est dans ce contexte qu'interviennent les sites de nos études. Le désert de sel de la dépression de Danakil en Ethiopie se situe à la confluence de trois plaques tectoniques dans le rift Est Africain (López-García et al. 2020). Au milieu de cette zone géologiquement active, le dôme géothermal de Dallol et ses environs offrent une rare combinaison de paramètres physicochimiques, alliant forts taux de sels (20 à 78%, riches en  $\text{Mg}^{2+}/\text{Ca}^{2+}$  ou en  $\text{Na}^{+}/\text{Fe}^{2+}/\text{Fe}^{3+}$ ) et des pH neutres à négatifs (~6 à -1.5) (Tableau 1). Par conséquent, l'ensemble de ces sites constituent un bon modèle pour étudier les limites de la vie et les différentes communautés microbiennes potentielles le long de ces gradients de conditions et ses explorer ses limites (

**Tableau 2)** le long de ces gradients de salinité, température et acidité rares et uniques. Au moment de la première expédition de notre équipe (janvier 2016), il y avait peu de littérature sur la composition chimique de ces différents sites et aucune étude microbienne n'avait encore été effectuée.

**Tableau 1 | Température, pH et salinité moyennes et écarts-type des principaux sites de Dallol et de ses environs**

	Température (°C)	pH	Salinité (%)
Dôme de Dallol	52,13 ± 31,00	-0,53 ± 0,32	38 ± 9
Yellow Lake (Gaet'ale)	39,20 ± 1,60	1,80 ± 0,20	>50
Black Lake	68,13 ± 7,13	2,92 ± 0,50	76
Western Canyons Lakes	29,56 ± 0,64	4,96 ± 0,10	32 ± 3
La grotte des canyons de sels	25,50 ± 3,50	6,25 ± 0,30	30
La plaine de sel active	29,3	4,21	20
Le Lac Assalé (Karum)	27,18 ± 3,95	6,65 ± 0,08	25 ± 6

**Tableau 2 | Limites de la vie actuellement connues susceptibles d'être rencontrées dans les environnements de Dallol et ses environs.**

	<i>Plage d'habitabilité</i>	<i>Références</i>
<i>Température</i>	-15°C ↔ 122°C	(Mykytczuk et al. 2013; Takai et al. 2008)
<i>pH</i>	~0 ↔ 11,4	(Schleper et al. 1996; Sturr, Guffanti, and Krulwich 1994)
<i>Salinité (NaCl)</i>	≤350 (g/L)	(Bodaker et al. 2010; Antón et al. 2000)
<i>Activité de l'eau</i>	≥0,585	(Stevenson et al. 2017; 2015)
<i>Chaotropicité</i>	≤87,3 (kJ/kg)	(Hallsworth et al. 2007)
<i>Force ionique</i>	≤12,141	(Fox-Powell et al. 2016)

## Objectifs

Ma thèse était motivée par le questionnement suivant :

Quelles sont les communautés microbiennes de ces environnements hypersalés, (hyper)acides et éventuellement chauds ? Y a-t-il de la vie en-deçà de la limite de pH 1.5 pour les environnements saturés en sel ?

## Matériel et méthodes

Au total, trois expéditions sur le terrain entre 2016 à 2019 ont permis de collecter 235 échantillons (liquides, solides, filtres) à partir de 95 points d'échantillonnage provenant de 6 sites majeurs et de leurs environs : le dôme de Dallol, le lac Gaet'ale (aussi nommé Yellow Lake, YL), le Black Lake (BL), la grotte (Gt) des canyons de sels, la plaine de sel (PS), le lac Karum (aussi nommé lac Assalé, Ass) et les Western Canyons Lakes (WCL). Ces échantillons ont passé une série d'analyses pour caractériser leur environnement d'origine, déterminer la présence ou absence de vie et la diversité microbienne associée. Ces analyses sont résumées dans la Figure 1.

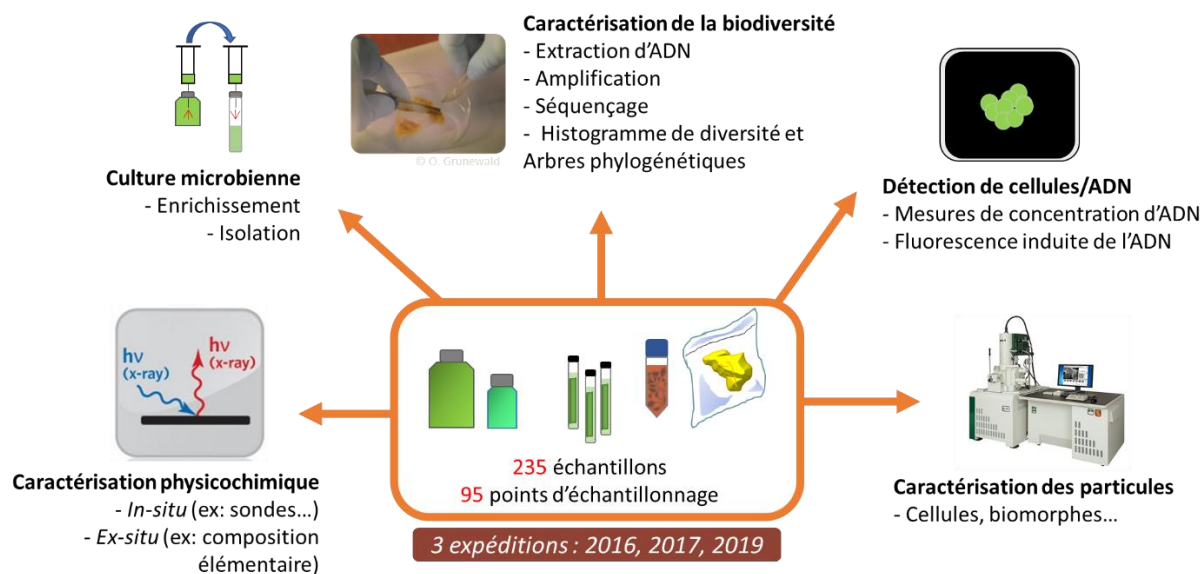


**Figure 1 | Schéma résumant les différentes analyses appliquées aux échantillons de Dallol et de ses environs au cours de cette thèse**

## Les communautés microbiennes de Dallol et de ses environs

Notre première étude concernait les campagnes d'échantillonnage exploratoires de 2016 et de 2017. Les échantillons proviennent de l'ensemble des sites présentés plus tôt à l'exception des Western Canyons Lakes, qui n'ont été échantillonnés qu'en 2019. Comme évoqué plus haut, ces échantillons présentent une chimie très variée avec des gradients d'acidité, de température et de salinité extrêmement larges.

Ces échantillons étaient donc le support idéal pour se poser les questions suivantes :

- 1) Peut-on détecter la vie microbienne le long des gradients physicochimiques multi-extrêmes de Dallol et de ses environs ?
- 2) Si oui, quelles sont les communautés microbiennes que nous allons y trouver ?

Au total pour cette étude, 183 échantillons dans plus de 63 points d'échantillonnage ont été récoltés. Dans les sites les moins extrêmes (la plaine salée, le lac Karum et la grotte), une grande diversité de micro-organismes halophiles a été trouvée. Les archées étaient dominantes (90 %) par rapport aux bactéries (10 %). Au sein des archées, les principaux phyla étaient les Halobacteria (56-84% du total des séquences procaryotes) et les Nanohaloarchaeota (1-15% du total des séquences procaryotes). En revanche, les amplicons n'ont été obtenus qu'après une PCR semi-nichée pour les échantillons les plus multi-extrêmes (le dôme hydrothermal de Dallol, les Yellow et Black Lakes), ce qui atteste de la très faible concentration d'ADN dans ces échantillons. Après nettoyage des séquences contaminantes dans les amplicons de PCR semi-nichées, les séquences restantes ont été identifiées. Celles-ci étant identiques ou similaires à certaines OTUs trouvées dans les endroits les moins multi-

extrêmes, nous suspectons qu'il s'agit en fait d'organismes exogènes transportés des alentours jusqu'au dôme par le vent (bioaérosols). Ces résultats sont conformes aux observations au microscope et aux tentatives de détection d'ADN avec l'analyse multiparamétrique du cytomètre de flux. Les résultats de cette étude sont résumés dans le Tableau 3.

**Tableau 3 | Synthèse des résultats de chaque type d'analyse par zone d'échantillonnage.** Fond vert : détection d'une grande diversité d'halophiles. Fond jaune : contamination microbienne locale (dispersion) suspectée. Fond rouge : aucune trace de vie détectée.

	Plaine de sel Grotte Lac Karum (Assalé)	Sources hydrothermales de Dallol	Lac Gaet'ale (Yellow Lake)	Black Lake
Microscope (optique, MEB)	Cellules observées, parfois avec (bio?)minéralisation	Pas de cellules observées, présence de biomorphes	Pas de cellules observées, présence de biomorphes	Pas de cellules observées
Séquençage (Sanger, Illumina) and analyses	90% archées 10% bactéries	Concentration d'ADN faible, dispersion aérienne suspectée	Concentration d'ADN faible, dispersion aérienne suspectée	Rien après retrait des contaminants de laboratoire
Cytométrie en flux (Analyse multiparamétrique et tri)	ADN détecté et populations triées sur filtre	Pas d'ADN détecté, pas de cellules sur les filtres	Pas d'ADN détecté, pas de cellules sur les filtres	Non testé (viscosité trop élevée)
Cultures (enrichissement, isolation)	Enrichissements réussis ; 1 isolation réussie	Pas de croissance	Pas de croissance	Pas de croissance

L'analyse en composantes principales (Figure 2) montre que le Yellow Lake et le Black Lake sont caractérisés par une forte concentration en sels de magnésium et de calcium, ce qui entraîne leur faible activité de l'eau ainsi que leur forte chaotropie et force ionique. Nous avons estimé que l'absence de vie dans ces deux environnements est liée à leur composition et leur concentration en sels, causant des valeurs inhospitalières d'activité de l'eau (Stevenson et al. 2015; 2017), de chaotropie (Hallsworth, Heim, and Timmis 2003; Hallsworth et al. 2007; Cray et al. 2013) et de force ionique (Fox-Powell et al. 2016). Les sources hydrothermales du dôme de Dallol, au contraire, sont caractérisées par une forte concentration de sels de sodium (NaCl) qui sont kosmotropes. Malgré leur forte teneur en chlorure de fer ou chlorure ferreux, elles restent dans la fourchette des paramètres habitables (Table 2). Nous interprétons que la combinaison d'hypersalinité (40% en moyenne) et d'hyperacidité (pH négatif) constitue la principale barrière à la vie dans ces bassins, même si nous ne pouvons pas exclure que d'autres facteurs de la chimie locale (ex : la forte teneur en métaux lourds) jouent également un rôle dans leur stérilité.

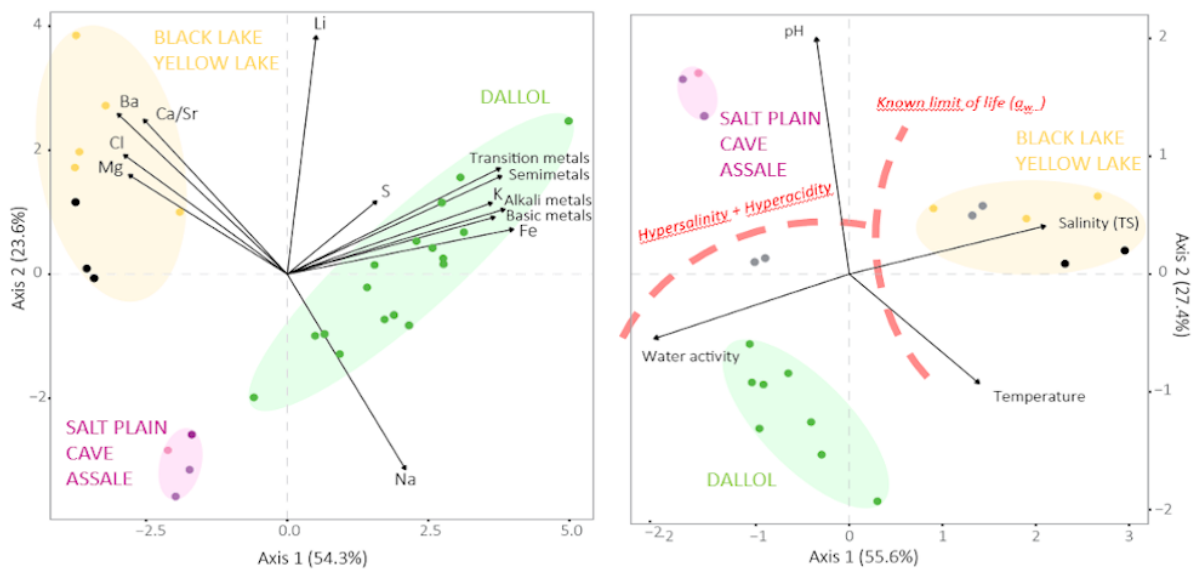


**Figure 2 | Analyses en composantes principales des échantillons liquides de la région de Dallol en fonction de leur composition chimique (à gauche) et de leurs paramètres physico-chimiques potentiellement limitant la durée de vie (à droite).** Les seuls échantillons où la vie a pu être détectée avec certitude sont la plaine salée, le réservoir de la grotte et le lac Assale/Karum. Les deux principales barrières de la vie identifiées sont représentées schématiquement pour les échantillons de Dallol et les échantillons des Yellow Lake (Gaet'ale) et Black Lake.

## Biocontamination et biomorphes : l'hypothèse de la contamination par les bioaérosols

Lors de notre seconde étude, nous nous sommes penchés davantage sur l'hypothèse de dispersion locale de microorganismes. Une source potentielle de contamination pourrait être les bioaérosols. Nous avons donc voulu répondre à deux questions :

- 1) Peut-on effectivement détecter des microorganismes dispersés par le vent sur le terrain.
- 2) Si oui, correspondent-ils aux microorganismes détectés à Dallol et au Yellow et Black Lake ?

Nous avons donc collecté lors de la campagne de 2019 des bioaérosols au niveau du dôme de Dallol et du camp de manière passive, avec des filtres exposés à l'air libre, et active avec une pompe manuelle. L'extraction de l'ADN de ces bioaérosols ont montré qu'ils contenaient une majorité de bactéries (99%) dont la plupart ne sont pas halophiles, et très peu d'archées (1%) dont des Halobacteria et Nanohaloarchaeota (Figure 3). Cette domination de la fraction bactérienne contraste avec les sites où la vie a été identifiée précédemment (où les archées halophiles sont dominantes) et rappelle fortement ce qui a été trouvé dans les contaminants de PCR de la première étude (Belilla et al. 2019). Les quelques séquences de haloarchées des bioaérosols sont très similaires aux OTUs de la plaine salée et du lac Assale, ce qui soutient l'idée qu'ils puissent être transportés depuis ces endroits par le vent. Au cours

de l'expérience FISH, aucune trace de cellule n'a été détectée sur les filtres de Dallol, tandis que des associations cellulaires qui pourraient correspondre à une interaction parasitaire entre nanohaloarchées (parasite) et haloarchées (hôte) ont été observées sur l'échantillon témoin (la plaine de sel).

Dans les endroits où les communautés microbiennes sont déjà établies, l'impact de l'apport exogène peut être négligeable, mais dans les endroits où la biomasse est très faible, inexistante ou inactive (comme c'est le cas dans certains environnements multi-extrêmes comme Dallol) son influence peut être plus importante et doit être prise en compte pour une meilleure interprétation des résultats.

Malgré l'apport exogène vraisemblablement non négligeable, il reste très difficile d'amplifier l'ADN dans les sites les plus extrêmes de la zone de Dallol. Nous montrons dans cette étude que l'ADN des cellules exogènes qui entrent en contact avec Dallol est presque instantanément totalement dégradé. Nous émettons l'hypothèse que la combinaison de salinité et d'acidité dans les sites les plus extrêmes (et/ou la forte chaotropie, pour le Yellow Lake et le Black Lake) sont à l'origine de la lyse de l'ADN, mais il est possible que certains constituants chimiques par exemple, des perchlorates qui pourraient être présents à Dallol (Wadsworth and Cockell 2017; Cavalazzi et al. 2019) jouent également un rôle stérilisateur.

Dans l'ensemble, ces résultats confirment les conclusions de notre étude précédente, à savoir l'absence de microorganismes endémiques dans les sources de Dallol, le Yellow Lake et le Black Lake, tout en attirant l'attention sur l'importance de contrôles approfondis pendant les expériences afin d'éviter les biais d'interprétation

## Les Western Canyons Lakes : plus proches des limites de la vie

Les conditions physicochimiques entre les écosystèmes les moins multi-extrêmes (la plaine de sel, le lac Assalé et la grotte) et les environnements stériles les plus multi-extrêmes (les sources de Dallol, le Yellow Lake et le Black Lake) sont radicalement différentes, et il y a peu d'intermédiaires, à l'exception de l'échantillon unique PS3 (un canal d'eau éphémère du désert de sel à l'odeur de sulfure d'hydrogène). Notre dernière étude souhaitait donc répondre aux questions suivantes :

- 1) Peut-on affiner les limites de la vie précédemment identifiées ?
- 2) Comment évoluent les communautés microbiennes lorsque l'on se rapproche davantage de ces limites ?

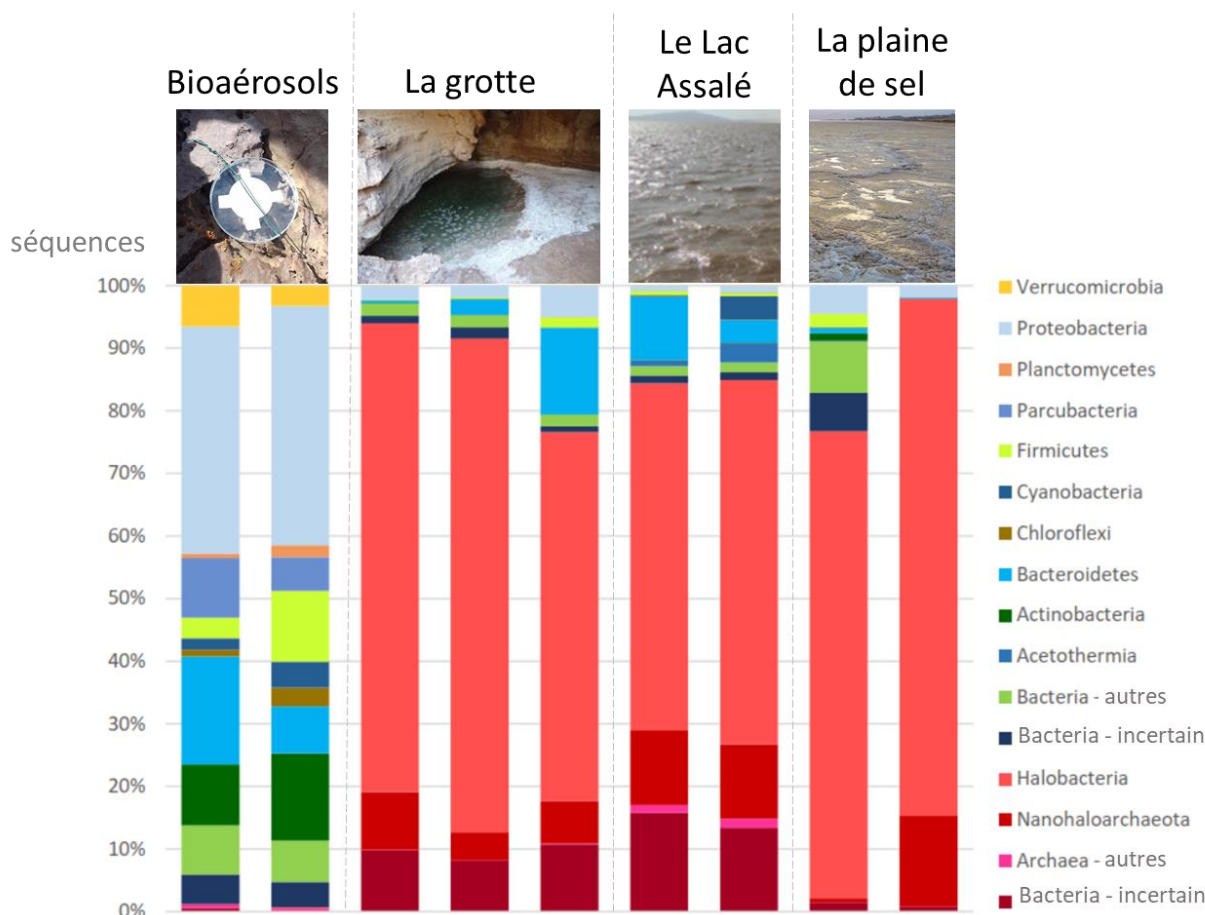


**Figure 3 | Histogramme comparant la présence/absence des phyla d'archées et de bactéries ainsi que leur abondance relative (en pourcentage de séquences/amplicons) des échantillons de bioaérosols de la zone de Dallol en comparaison avec les sites où la vie a été identifiée dans notre première étude.** Les phyla qui représentaient <1% du total des lectures ont été classés dans les catégories "autres". Les catégories "incertain" sont celles pour lesquels le premier hit dans les bases de données est  $\leq 90\%$  identique à l'OTU.

Non loin du versant ouest du dôme de Dallol, à proximité d'une élévation appelée la "Round Mountain", se trouvent des lacs dont la couleur jaune et le dégazage visible évoquent le Yellow Lake. Ces lacs, les Western Canyons Lakes (WCL), ont une salinité comprise entre 34 et 41 % (p/v) et leur pH est d'environ 4,9, ce qui correspond aux valeurs intermédiaires recherchées de salinité et d'acidité. Ils sont visibles par satellite depuis au moins 2003, et leur première mention dans la littérature scientifique date du siècle dernier (Holwerda and Hutchinson 1968). Leurs conditions physico-chimiques et leur persistance dans le temps en font de bons candidats au chaînon manquant des gradients précédemment étudiés.

L'ACP (Figure 4, gauche) montre que le sel dominant dans les Western Canyons Lakes est le chlorure de sodium, à l'instar du Lac Assalé, de la grotte et la plaine de sel (avec lesquels ils se regroupent). Seul l'échantillon de WCL3 est plus riche en sels de calcium et de magnésium que les autres échantillons de la même série. D'un point de vue physico-chimique, parce qu'ils ont un pH plus acide et une concentration en sel plus élevée que le Lac Assalé et

la grotte (et par conséquent une activité de l'eau plus faible), les échantillons WCL se regroupent plus proche des limites de la vie définies dans Belilla et al. (2019).

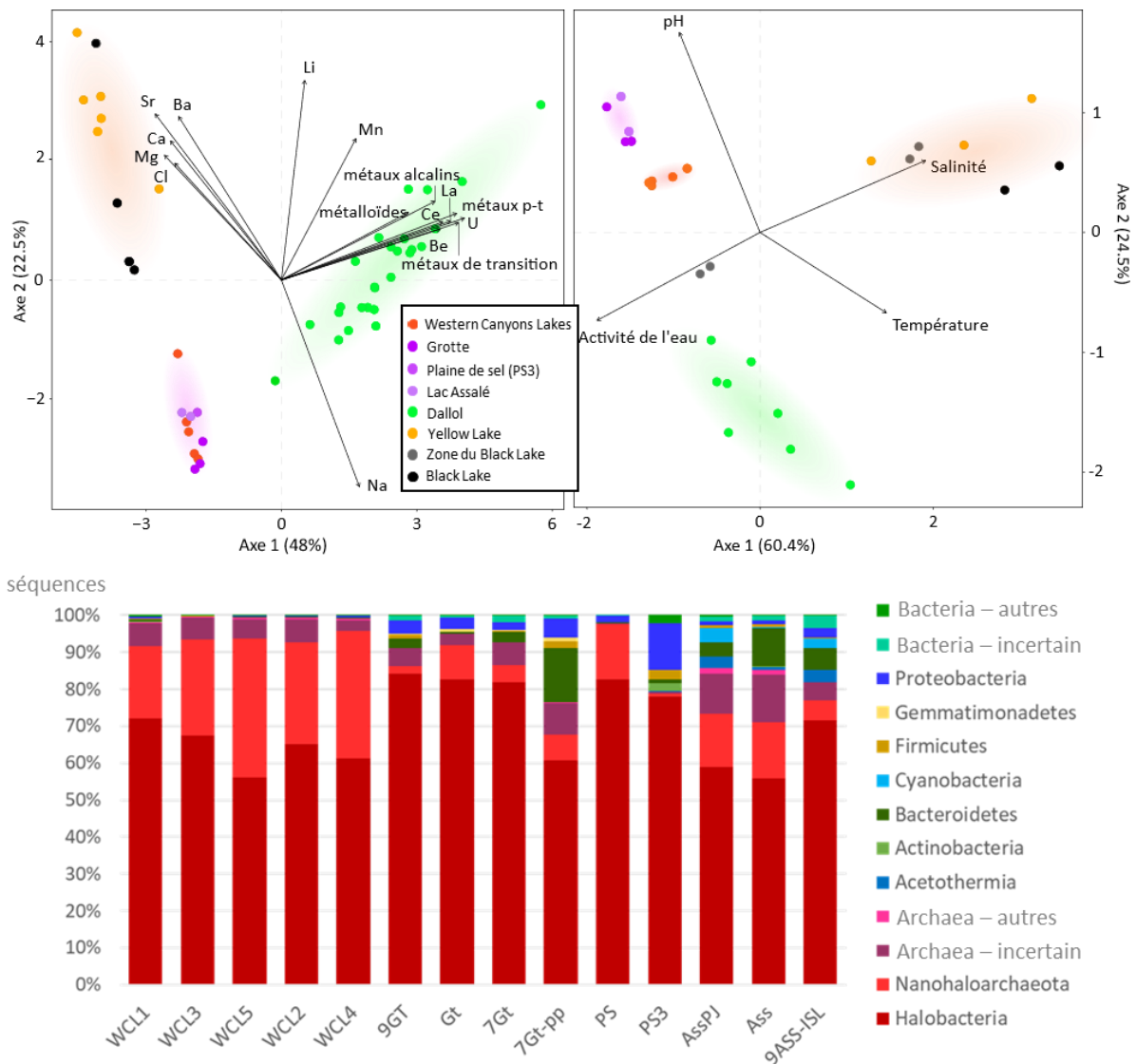


**Figure 4 | Analyses en composantes principales de la composition chimique et de paramètres physico-chimiques de Dallol et de ses environs (panneau supérieur) et histogramme de la présence/absence et de la proportion relative d'archées et de bactéries dans les environnements moins multi-extrêmes, basé sur les données de metabarcoding du gène ARNr 16S (panneau inférieur).** WCL : Western Canyons Lakes ; GT/Gt : grotte ; PS/PS3 : plaine de sel et plaine de sel active respectivement ; Ass/ASS : Lac Assalé.

Une fois normalisée et comparée à d'autres échantillons, la proportion d'archées semble plus élevée dans les échantillons WCL que dans les échantillons moins multi-extrêmes ou que la PS3 (Figure 4, bas). Au sein des archées, la composition des phyla est très similaire dans tous les environnements étudiés, avec une majorité des séquences appartenant aux Halobacteria, suivi les Nanohaloarchaeota. Toutefois, l'on observe une plus grande proportion de Nanohaloarchaeota dans les échantillons de WCL. Une proportion plus élevée d'archées (et en particulier de nanohaloarchées) a déjà été corrélée avec l'augmentation de la salinité

dans des milieux plus alcalins (Ventosa et al. 2015; Menéndez-Serra et al. 2020). On sait peu de choses sur l'effet des gradients d'acidité sur les deux phyla, mais nous supposons que l'acidité joue également un rôle dans les changements observés. Ces changements de proportion pourraient indiquer une plus grande spécialisation des nanohaloarchées aux conditions les plus hypersalées par rapport à un comportement plus polyvalent des haloarchées, comme le suggèrent Menéndez-Serra et al. (2020). Le potentiel mode de vie symbiotique (Hamm et al. 2019; Cono et al. 2019) ou parasitaire (section 5.3) des nanohaloarchées peut également jouer un rôle dans ces changements.

Les résultats ci-dessus confirment que les Western Canyons Lakes (pH ~5, salinité 34-41%) sont plus proches des limites de la vie que les autres sites présentant de la vie dans les environnements de Dallol et de ses environs. Ils suggèrent que plus on se rapproche des limites de salinité et d'acidité de la vie, plus la proportion d'archées (et en particulier de nanohaloarchées) augmente. Trouver des environnements aux paramètres similaires aux à ceux d'où proviennent les échantillons WCL/PS3 permettrait d'affiner d'avantage les limites de la vie. Des études de métagénomique, métatranscriptomique et/ou de métabotomique de ces environnements permettraient de mieux comprendre l'écologie des espèces présentes et leurs mécanismes d'adaptation aux conditions multi-extrêmes. Enfin, des co-cultures de haloarchées et des nanohaloarchées provenant des alentours de Dallol permettraient déterminer la réelle nature de leur association supposée.

## Conclusion

Avant cette étude, l'on savait peu de choses quant à la possibilité pour les micro-organismes de se développer dans une combinaison de conditions hypersalines, hyperacides (et éventuellement de température élevée). Seules quelques études ont tenté de décrire la composition des communautés microbiennes le long des gradients de salinité et d'acidité, sans répondre entièrement à la question. Mon projet de doctorat s'est concentré sur la prospection de micro-organismes dans les environnements multi-extrêmes de Dallol et de ses environs dans la dépression de Danakil en Éthiopie, qui présentent dans un rayon de quelques kilomètres un large éventail de gradients de salinité-acidité-température.

Les principaux résultats de notre travail sont énumérés ci-dessous :

1. Les communautés microbiennes dans les environnements hypersalés ( $\geq 30\%$ ) et légèrement acides (pH 4,2 à 6) sont dominées par une diversité étonnamment grande d'archées halophiles (Halobacteria, Nanohaloarchaeota) lorsque le sel dominant est le NaCl, comme c'est le cas pour le Lac Assalé, la plaine de sel, le réservoir de la grotte, les Western Canyons Lakes. Plus la salinité et l'acidité sont élevées, plus la proportion d'archées (en particulier de nanohaloarchées) parmi les procaryotes est importante.

2. Sur la base de leur co-occurrence et d'observations au microscope, nos études soutiennent l'hypothèse la dépendance des nanohaloarchées à des hôtes haloarchées et suggère qu'il pourrait s'agir d'une interaction parasitaire.
3. Indépendamment de la température, il n'y a pas ou peu d'ADN détectable dans les échantillons provenant des sites les plus polyextrêmes de la dépression de Danakil (salinité de 20% à >50% avec une forte concentration de sels  $\text{Fe}^{2+}/\text{Fe}^{3+}$  ou  $\text{Ca}^{2+}/\text{Mg}^{2+}$  et pH de -1,5 à 3,5).
4. Deux barrières physico-chimiques limitant la vie sont identifiées malgré la présence d'eau liquide (condition nécessaire à la vie) dans la région de Dallol : 1) la combinaison de l'hyperacidité et de l'hypersalinité (éventuellement associées à la forte concentration en métaux lourds et à certains composants chimiques stérilisants) pour le dôme de Dallol lui-même, et 2) les valeurs de chaotropicité, d'activité de l'eau et de force ionique pour le Yellow Lake et le Black Lake.
5. Cela montre que la présence d'eau, même si elle est une condition nécessaire à la vie, n'est pas une condition suffisante à sa présence.
6. L'absence de vie dans les bassins hydrothermaux les plus multi-extrême (dôme de Dallol et des Yellow et Black Lakes) les rend particulièrement sensibles à la biocontamination (par les bioaérosols sur place et lors des expériences en laboratoire) pour l'interprétation des résultats, bien que leurs propriétés physico-chimiques puissent en éliminer la plus grande partie.
7. Nous proposons, à travers nos différentes études, un protocole rigoureux pour discriminer l'ADN endogène et exogène, ainsi que les cellules et les biomorphes.

## Références

- Albarede, Francis, Fanny Thibon, Janne Blichert-Toft, and Harilaos Tsikos. 2020. 'Chemical Archeoceanography'. *Chemical Geology* 548 (August): 119625. <https://doi.org/10/ghdb8x>.
- Antón, Josefa, Ramón Rosselló-Mora, Francisco Rodríguez-Valera, and Rudolf Amann. 2000. 'Extremely Halophilic Bacteria in Crystallizer Ponds from Solar Salterns'. *Applied and Environmental Microbiology* 66 (7): 3052–57.
- Bar-On, Yinon M., Rob Phillips, and Ron Milo. 2018. 'The Biomass Distribution on Earth'. *Proceedings of the National Academy of Sciences* 115 (25): 6506–11. <https://doi.org/10/cp29>.
- Belilla, Jodie, David Moreira, Ludwig Jardillier, Guillaume Reboul, Karim Benzerara, José M. López-García, Paola Bertolino, Ana I. López-Archilla, and Purificación López-García. 2019. 'Hyperdiverse Archaea near Life Limits at the Polyextreme Geothermal Dallol Area'. *Nature Ecology & Evolution* 3 (11): 1552–61. <https://doi.org/10/ggr3sj>.

- Bodaker, Idan, Itai Sharon, Marcelino T. Suzuki, Roi Feingersch, Michael Shmoish, Ekaterina Andreishcheva, Mitchell L. Sogin, et al. 2010. 'Comparative Community Genomics in the Dead Sea: An Increasingly Extreme Environment'. *The ISME Journal* 4 (3): 399–407. <https://doi.org/10/fk6c34>.
- Brasier, Martin D., Owen R. Green, Andrew P. Jephcoat, Annette K. Kleppe, Martin J. Van Kranendonk, John F. Lindsay, Andrew Steele, and Nathalie V. Grassineau. 2002. 'Questioning the Evidence for Earth's Oldest Fossils'. *Nature* 416 (6876): 76–81. <https://doi.org/10/d39djh>.
- Cavalazzi, B., R. Barbieri, F. Gómez, B. Capaccioni, K. Olsson-Francis, M. Pondrelli, A. P. Rossi, et al. 2019. 'The Dallol Geothermal Area, Northern Afar (Ethiopia)-An Exceptional Planetary Field Analog on Earth'. *Astrobiology* 19 (4): 553–78. <https://doi.org/10/ggvk97>.
- Cono, Violetta La, Enzo Messina, Manfred Rohde, Erika Arcadi, Sergio Ciordia, Francesca Crisafi, Renata Denaro, et al. 2019. 'Differential Polysaccharide Utilization Is the Basis for a Nanohaloarchaeon: Haloarchaeon Symbiosis'. *BioRxiv*, October, 794461. <https://doi.org/10/ghdpj5>.
- Cray, Jonathan A., John T. Russell, David J. Timson, Rekha S. Singhal, and John E. Hallsworth. 2013. 'A Universal Measure of Chaotropicity and Kosmotropicity'. *Environmental Microbiology* 15 (1): 287–96. <https://doi.org/10/ggddmj>.
- Escudero, L., J. Bijman, G. Chong, J. J. Pueyo, and C. Demergasso. 2013. 'Geochemistry and Microbiology in an Acidic, High Altitude (4,000 m) Salt Flat — High Andes, Northern Chile'. <https://doi.org/10/ghdcg7>.
- Fox-Powell, Mark G., John E. Hallsworth, Claire R. Cousins, and Charles S. Cockell. 2016. 'Ionic Strength Is a Barrier to the Habitability of Mars'. *Astrobiology* 16 (6): 427–42. <https://doi.org/10/f8qjhr>.
- Hallsworth, John E., Sabina Heim, and Kenneth N. Timmis. 2003. 'Chaotropic Solutes Cause Water Stress in *Pseudomonas Putida*'. *Environmental Microbiology* 5 (12): 1270–80. <https://doi.org/10/db2s9s>.
- Hallsworth, John E., Michail M. Yakimov, Peter N. Golyshin, Jenny L. M. Gillion, Giuseppe D'Auria, Flavia De Lima Alves, Violetta La Cono, et al. 2007. 'Limits of Life in MgCl<sub>2</sub>-Containing Environments: Chaotropicity Defines the Window'. *Environmental Microbiology* 9 (3): 801–13. <https://doi.org/10/fktqwc>.
- Hamm, Joshua, Susanne Erdmann, Emiley Eloë-Fadrosh, Allegra Angeloni, Ling Zhong, Christopher Brownlee, Timothy Williams, et al. 2019. 'Unexpected Host Dependency of Antarctic Nanohaloarchaeota'. *Proceedings of the National Academy of Sciences* 116 (June). <https://doi.org/10/gf4ggj>.
- Harrison, Jesse P., Nicolas Gheeraert, Dmitry Tsigelnitskiy, and Charles S. Cockell. 2013. 'The Limits for Life under Multiple Extremes'. *Trends in Microbiology* 21 (4): 204–12. <https://doi.org/10/f4wgwh>.
- Holwerda, James G., and Richard W. Hutchinson. 1968. 'Potash-Bearing Evaporites in the Danakil Area, Ethiopia'. *Economic Geology* 63 (2): 124–50. <https://doi.org/10/dppvm6>.
- Hooke, Robert (1635-1703) Auteur du texte. 1665. *Micrographia or Some physiological descriptions of minutes bodies made by magnifying glasses : with observations and inquiries thereupon ([Reprod.]) / by R. Hooke,...* <https://gallica.bnf.fr/ark:/12148/bpt6k98770v>.
- Johnson, Sarah Stewart, Marc Gerard Chevrette, Bethany L. Ehlmann, and Kathleen Counter Benison. 2015. 'Insights from the Metagenome of an Acid Salt Lake: The Role of Biology

- in an Extreme Depositional Environment'. *PLOS ONE* 10 (4): e0122869. <https://doi.org/10/f7j2jj>.
- Kang, Chang-Ho, Soo Ji Oh, YuJin Shin, Sang-Hyun Han, In-Hyun Nam, and Jae-Seong So. 2015. 'Bioremediation of Lead by Ureolytic Bacteria Isolated from Soil at Abandoned Metal Mines in South Korea'. *Ecological Engineering* 74 (January): 402–7. <https://doi.org/10/f6wxqb>.
- Knauth, L. Paul. 2005. 'Temperature and Salinity History of the Precambrian Ocean: Implications for the Course of Microbial Evolution'. *Palaeogeography, Palaeoclimatology, Palaeoecology*, *Geobiology: Objectives, Concept, Perspectives*, 219 (1): 53–69. <https://doi.org/10/dncb4c>.
- Lane, Nick. 2015. 'The Unseen World: Reflections on Leeuwenhoek (1677) "Concerning Little Animals"'. *Philosophical Transactions of the Royal Society B: Biological Sciences* 370 (1666): 20140344. <https://doi.org/10/ghc9rd>.
- Leeuwenhoek, Antoni Van. 1705. 'I. A Letter to the Royal Society, from Mr. Anthony Van Leeuwenhoek, F. R. S. Concerning Animalcula on the Roots of Duck-Weed, &c'. *Philosophical Transactions of the Royal Society of London* 24 (295): 1784–93. <https://doi.org/10/bmmr48>.
- López-García, José M., David Moreira, Karim Benzerara, Olivier Grunewald, and Purificación López-García. 2020. 'Origin and Evolution of the Halo-Volcanic Complex of Dallol: Proto-Volcanism in Northern Afar (Ethiopia)'. *Frontiers in Earth Science* 7. <https://doi.org/10/ggsr6x>.
- Menéndez-Serra, M, Vj Ontiveros, X Triadó-Margarit, D Alonso, and Eo Casamayor. 2020. 'Dynamics and Ecological Distributions of the Archaea Microbiome from Inland Saline Lakes (Monegros Desert, Spain)'. *FEMS Microbiology Ecology* 96 (3). <https://doi.org/10/ghdpsf>.
- Merino, Nancy, Heidi S. Aronson, Diana P. Bojanova, Jayme Feyhl-Buska, Michael L. Wong, Shu Zhang, and Donato Giovannelli. 2019. 'Living at the Extremes: Extremophiles and the Limits of Life in a Planetary Context'. *Frontiers in Microbiology* 10. <https://doi.org/10/gfzhhb6>.
- Mormile, Melanie R., Bo-Young Hong, and Kathleen C. Benison. 2009. 'Molecular Analysis of the Microbial Communities of Mars Analog Lakes in Western Australia'. *Astrobiology* 9 (10): 919–30. <https://doi.org/10/d7jdsm>.
- Mykytczuk, Nadia C S, Simon J Foote, Chris R Omelon, Gordon Southam, Charles W Greer, and Lyle G Whyte. 2013. 'Bacterial Growth at –15 °C; Molecular Insights from the Permafrost Bacterium *Planococcus Halocryophilus* Or1'. *The ISME Journal* 7 (6): 1211–26. <https://doi.org/10/f463p7>.
- Oremland, Ronald S., Chad W. Saltikov, Felisa Wolfe-Simon, and John F. Stolz. 2009. 'Arsenic in the Evolution of Earth and Extraterrestrial Ecosystems'. *Geomicrobiology Journal* 26 (7): 522–36. <https://doi.org/10/cfkxdc>.
- Saiki, R. K., D. H. Gelfand, S. Stoffel, S. J. Scharf, R. Higuchi, G. T. Horn, K. B. Mullis, and H. A. Erlich. 1988. 'Primer-Directed Enzymatic Amplification of DNA with a Thermostable DNA Polymerase'. *Science* 239 (4839): 487–91. <https://doi.org/10/gfdb23>.
- Sara Parwin Banu, Kamaludeen, K Arunkumar, Avudainayagam Subramanian, and K Ramasamy. 2003. 'Bioremediation of Chromium Contaminated Environments'. *Indian Journal of Experimental Biology* 41 (October): 972–85.
- Schleper, Christa, Gabriela Puhler, Hans- Peter Klenk, and Wolfram Zillig. 1996. 'Picrophilus Oshimae and Picrophilus Tomdus Fam. Nov., Gen. Nov., Sp. Nov., Two Species of

- Hyperacidophilic, Thermophilic, Heterotrophic, Aerobic Archaea', *International Journal of Systematic Bacteriology*, 46 (3): 814–16. <https://doi.org/10.1099/00207713-46-3-814>.
- Schmid, Amy K., Thorsten Allers, and Jocelyne DiRuggiero. 2020. 'SnapShot: Microbial Extremophiles'. *Cell* 180 (4): 818-818.e1. <https://doi.org/10/gg37tx>.
- Schopf, J. W., and B. M. Packer. 1987. 'Early Archean (3.3-Billion to 3.5-Billion-Year-Old) Microfossils from Warrawoona Group, Australia'. *Science (New York, N.Y.)* 237 (July): 70–73. <https://doi.org/10/cnv8vd>.
- Stevenson, Andrew, Jonathan A Cray, Jim P Williams, Ricardo Santos, Richa Sahay, Nils Neuenkirchen, Colin D McClure, et al. 2015. 'Is There a Common Water-Activity Limit for the Three Domains of Life?' *The ISME Journal* 9 (6): 1333–51. <https://doi.org/10/f7cm86>.
- Stevenson, Andrew, Philip G. Hamill, Callum J. O'Kane, Gerhard Kminek, John D. Rummel, Mary A. Voytek, Jan Dijksterhuis, and John E. Hallsworth. 2017. 'Aspergillus Penicillioides Differentiation and Cell Division at 0.585 Water Activity'. *Environmental Microbiology* 19 (2): 687–97. <https://doi.org/10/f9n7kk>.
- Sturr, M G, A A Guffanti, and T A Krulwich. 1994. 'Growth and Bioenergetics of Alkaliphilic Bacillus Firmus OF4 in Continuous Culture at High PH.' *Journal of Bacteriology* 176 (11): 3111–16.
- Takai, Ken, Kentaro Nakamura, Tomohiro Toki, Urumu Tsunogai, Masayuki Miyazaki, Junichi Miyazaki, Hisako Hirayama, Satoshi Nakagawa, Takuro Nunoura, and Koki Horikoshi. 2008. 'Cell Proliferation at 122°C and Isotopically Heavy CH<sub>4</sub> Production by a Hyperthermophilic Methanogen under High-Pressure Cultivation'. *Proceedings of the National Academy of Sciences* 105 (31): 10949–54. <https://doi.org/10/crqvsn>.
- Ventosa, Antonio, Rafael R. de la Haba, Cristina Sánchez-Porro, and R. Thane Papke. 2015. 'Microbial Diversity of Hypersaline Environments: A Metagenomic Approach'. *Current Opinion in Microbiology* 25 (June): 80–87. <https://doi.org/10/ghdbwb>.
- Wadsworth, Jennifer, and Charles S. Cockell. 2017. 'Perchlorates on Mars Enhance the Bacteriocidal Effects of UV Light'. *Scientific Reports* 7 (1): 4662. <https://doi.org/10/gbnpsq>.
- Walter, M. R., R. Buick, and J. S. R. Dunlop. 1980. 'Stromatolites 3,400-3,500 Myr Old from the North Pole Area, Western Australia'. *Nature* 284 (5755): 443–45. <https://doi.org/10/dqqhk2>.
- Woese, C. R., O. Kandler, and M. L. Wheelis. 1990. 'Towards a Natural System of Organisms: Proposal for the Domains Archaea, Bacteria, and Eucarya'. *Proceedings of the National Academy of Sciences of the United States of America* 87 (12): 4576–79. <https://doi.org/10/b7s3gv>.
- Woese, Carl R., and George E. Fox. 1977. 'Phylogenetic Structure of the Prokaryotic Domain: The Primary Kingdoms'. *Proceedings of the National Academy of Sciences* 74 (11): 5088–90. <https://doi.org/10/ft974h>.
- Zaikova, Elena, Kathleen C. Benison, Melanie R. Mormile, and Sarah Stewart Johnson. 2018. 'Microbial Communities and Their Predicted Metabolic Functions in a Desiccating Acid Salt Lake'. *Extremophiles: Life Under Extreme Conditions* 22 (3): 367–79. <https://doi.org/10/gc9w84>.





*Sunrise, view from the campsite © DEEM Team*

**Titre :** Exploration des communautés microbiennes le long des gradients physicochimiques poly-extrêmes de Dallol et de ses environs (dépression de Danakil, région Afar, Ethiopie)

**Mots clés :** Polyextremophiles, microorganismes, Dallol, limites de la vie, metabarcoding

Parmi toute la diversité microbienne des trois domaines du vivant, une fraction des microorganismes (en particulier certaines Archées) s'est adaptée aux conditions les plus extrêmes. La plupart des environnements extrêmes se caractérisant par de multiples facteurs de stress, une partie des extrémophiles sont en réalité polyextrémophiles. Néanmoins, il n'y a pas de microorganismes connus adaptés simultanément à un pH très faible (<1.5) ainsi qu'une très forte salinité (et éventuellement une forte température). Soit il n'existe pas d'adaptations moléculaires capables de supporter certaines combinaisons de pH et de salinité, soit ces incertitudes sont liées au fait que les environnements hyperacides et hypersalés (et chauds) sont rares et inexplorés. Le désert de sel de la dépression de Danakil en Ethiopie se situe à la confluence de trois plaques tectoniques dans le rift Est Africain. Au milieu de cette zone géologiquement active, le dôme géothermal de Dallol et ses environs offrent une rare combinaison de paramètres physicochimiques, alliant forts taux de sels (20 à 78%, riches en  $Mg^{2+}/Ca^{2+}$  ou en  $Na^{+}/(Fe^{2+}/3^{+})$ ) et des pH neutres à négatifs (~6 à -1.5). Par conséquent, l'ensemble de ces sites constitue un bon modèle pour étudier les communautés microbiennes le long de ces gradients rares et uniques. Au cours des quatre dernières années, nous avons collecté 235 échantillons au niveau des différents sites de Dallol et ses alentours. Des mesures physicochimiques *in situ* et *ex situ* nous ont permis de caractériser chaque environnement et d'estimer son habitabilité théorique. Nous avons ensuite procédé à la purification d'ADN des échantillons, amplifié et séquençé les gènes d'ARNr 16S/18S afin de caractériser la diversité microbienne que nous avons comparée à des bases de données et classée phylogénétiquement. Nous avons également complété notre étude par des analyses/observations au cytomètre de flux au microscope (optique, électronique à balayage et confocal). Les environnements hypersalés (~30% de NaCl) et légèrement acides (pH 4-6) ont montré une diversité de microorganismes très élevée, dominée par les Archées (80% du total des séquences) en particulier des phyla Halobacteria et Nanohaloarchaeota, fréquemment associés dans les milieux hypersalés. Nous avons pu constater que l'augmentation de l'acidité et la salinité s'accompagnaient de l'augmentation de la proportion d'archées (en particulier de Nanohaloarchaeota). Une meilleure adaptation d'archées halophiles par rapport aux bactéries pourrait expliquer leur prévalence. Quant aux nanohaloarchées, leur augmentation pourrait être liée à leur rôle suspecté d'ectosymbiontes de haloarchées : dans le cas d'une relation mutualiste, ils pourraient favoriser l'adaptation de leur hôte aux conditions plus extrêmes ; dans le cas d'une relation parasitaire, des conditions environnementales plus difficiles pour l'hôte pourrait favoriser le parasitisme. Aucune trace de vie microbienne n'a été trouvée dans les environnements les plus polyextrêmes (salinité 20-78%, pH -1 à 3). Pour certains sites, nous interprétons que les valeurs de chaotricité, d'activité de l'eau et de force ionique liés à la composition et concentration de sels (minimum 50%, riches en  $Mg^{2+}/Ca^{2+}$ ) sont limitantes pour la vie microbienne. Pour d'autres, comme le dôme de Dallol, la combinaison d'hypersalinité et d'hyperacidité (pH~0) pourraient le rendre inhospitalier, sans exclure d'éventuels composés chimiques stérilisateurs. Les environnements avec une biomasse faible ou absente étant sensibles à la biocontamination, nous avons tâché d'estimer l'impact de cette biocontamination sur l'étude des sites multi-extrême de Dallol et de ses environs. Nous proposons ainsi un protocole rigoureux, basé sur l'utilisation d'analyses croisées et de témoins positifs/négatifs dans toutes nos expériences afin de séparer l'ADN endogène et exogène, et de distinguer les cellules des biomorphes abiotiques dans nos échantillons.

**Title :** Unveiling microbial communities along the polyextreme physicochemical gradients of Dallol and its surroundings (Danakil depression, Afar region, Ethiopia)

**Keywords :** Polyextremophiles, microorganisms, Dallol, limits of life, metabarcoding

From the vast microbial diversity of the three domains of life, a fraction of microorganisms (in particular some Archaea) have adapted to the most extreme conditions. Since extreme environments are usually characterised by multiple stressors (e.g. hot and acidic hydrothermal springs, saline and alkaline lakes, etc.), some extremophiles are in fact polyextremophiles. Nevertheless, there is no microorganism known to be adapted simultaneously to a very low pH (<1.5) and high salinity (and possibly high temperature). Either there are no molecular adaptations capable of withstanding certain combinations of pH and salinity, or this absence is related to the rarity of hyperacidic and hypersaline (and hot) environments, leaving them unexplored. The salt desert of the Danakil Depression (Afar region) in Ethiopia lies at the confluence of three tectonic plates in the East African Rift. In the middle of this geologically active zone, the Dallol geothermal dome and its surroundings offer a rare combination of physicochemical parameters, with high salt levels (20 to 78%, rich in  $Mg^{2+}/Ca^{2+}$  or  $Na^{+}/(Fe^{2+}/3^{+})$ ) and neutral to negative pH values (~6 to -1.5). Therefore, these sites provide a good model for studying microbial communities along these rare and unique gradients. Over the last four years, we have collected 235 samples (solids, liquids, plankton biomass) from the different sites on the Dallol dome and around it. *In situ* and *ex situ* physicochemical measurements enabled us to characterise each environment and estimate their theoretical habitability based on previously known life-limiting conditions. We proceeded to DNA purification of the samples and then amplified and sequenced 16S/18S rRNA genes in order to characterize the microbial diversity, which we compared with databases and classified phylogenetically. We also completed our study by using a flow cytometer (for multiparametric analysis), and microscope observations (optical, scanning electron and confocal laser scanning). Hypersaline (~30% salts, dominated by NaCl) and slightly acidic (pH 4-6) environments showed a very high diversity of microorganisms, dominated by Archaea (at least 80% of the total sequences) in particular Halobacteria and Nanohaloarchaeota, frequently associated in hypersaline environments. We observed that the increase in acidity and salinity was associated with an increase in the proportion of Archaea (especially Nanohaloarchaeota). A better adaptation of halophilic archaea compared to bacteria could explain their prevalence. Concerning nanohaloarchaea, their higher proportion could be linked to their suspected role as haloarchaea ectosymbionts: in the case of a mutualistic relationship, their association could favour the adaptation to more extreme conditions; in the case of a parasitic relationship, the rise of acidity and salinity may weaken the host and increase the parasite prevalence. No trace of microbial life has been found in the most polyextreme environments (salinity 20-78%, pH -1 to 3). For some sites, we interpret that the chaotricity, water activity and ionic strength values related to the composition and concentration of salts (minimum 50%, rich in  $Mg^{2+}/Ca^{2+}$ ) are limiting for microbial life. For others, such as the Dallol dome, it could be the combination of hypersalinity and hyperacidity (pH~0) that make it inhospitable, without excluding the possible presence of sterilising chemical compounds. As environments with low or absent biomass are sensitive to biocontamination (local or laboratory), we have also tried to estimate the impact of this biocontamination on the study of the multi-extreme sites of Dallol and its surroundings. We thus propose a rigorous protocol, based on the use of cross-analyses and positive/negative controls in all our experiments in order to separate endogenous and exogenous DNA, and to distinguish cells from abiotic mineral biomorphs in our samples.